UNIVERSITY OF Hull

School of Environmental Sciences

Thesis submitted for the Degree of Doctor of Philosophy

Molecular Level Biological Effects of Silver and Titania Nanoparticles on Zebrafish Embryos

By:

Zeinab H. Arabeyyat

Supervisors:
Prof. Jeanette M. Rotchell
Prof. Vesselin N. Paunov
Dr. Jinping Cheng

September, 2016

Abstract

Nanotechnology raises issues concerning the toxic impact of nanoparticles (NPs) in organisms and the environment. Nanoparticles have been defined as materials with dimensions that are equal to or less than 100 nm. It is important to develop early warning tools of NP-induced biological effects to be able to monitor and manage for any possible impacts. In the current study, two types of NPs have been selected based on their wide use: silver-NPs (AgNPs) and titanium dioxide-NPs (TiO_2NPs). Early zebrafish (*Danio rerio*) embryos exposed *in vitro* to 4-nm and 10-nm AgNPs, and to silver ions alone, and TiO_2NPs have been used to measure the expression level of selected target genes. A global transcriptomic approach employing Suppression Subtractive Hybridization (SSH) was used in parallel to identify novel genes that may be involved in the fish embryo response as a result of exposure to NPs. TiO_2NPs coated with different layers of anionic (PSS) and cationic (PAH) polyelectrolytes were also used to measure viability, morphology, and the expression level of selected target genes. The results indicate that pathways expressed in response to NP exposure differ among both AgNPs and TiO_2NPs, either due to the size, concentration, exposure time, exposure conditions, surface chemistry and surface charge of coatings of the NPs. The responses indicate that *D. rerio* embryos respond to NPs with not only an oxidative stress response, but with transcripts associated with fertility and metabolic functions such as membrane transport and mitochondrial metabolism. This information may be used to inform early warning biomarker development for environmental monitoring applications in future.

Dedication

I still remember how happy you were for me when I started this journey in my life. It was one of the best moments of my life. Your believing in me, and the endless encouragement you gave me, have helped me the most to continue.

To you, my great dad Hashem and my lovely mother Najla', I owe you my success.

Your little daughter,

Zeinab

Acknowledgements

First, I would like to express my deepest gratitude and appreciations to my main supervisor Professor Jeanette M. Rotchell for her invaluable and unconditional guidance, support and advices in both academic and life lessons. I have to say that Jeanette was not only my professor but she also became a successful module I want to follow. I would also like to thank my co-supervisor Professor Vesselin N. Paunov for his valuable guidance and suggestions, and I would like to thank my co-supervisor Dr. Jinping Cheng for supplying me with the silver nanoparticles and silver ion samples.

My special thanks go to Dr. Mark G. J. Hartl for serving as external examiner, and Professor Roland A. Ennos for serving as internal examiner on my thesis committee. Thank you for your brilliant comments, advices, and for letting my defence to be an unforgettable moment. I would like to thank Professor Roland A. Ennos again for his guidance and help in data analysis.

I am very grateful to Emma C. Chapman and Dr. Janine Wäge for all the technical support during the laboratory work, and for their amazing friendship which made my life easier in a foreign country.

A special thanks to Ann Lowry (University of Hull) for the help with obtaining scanning and transmission electron microscope images, and many thanks to Dr. Mohammed Al-Awady for preparing the titanium nanoparticles samples.

I would also like to extend my thanks to all my lovely family members (Diana, Arabiah, Talal, Khaled, Abdullah, and Saqer) and my close friends for their love, encouragement and supporting. Special thanks to my close friend Amber McCleerey for her amazing friendship, love, endless support and patience in the last two years, and special thanks to Graham Sellers; thank you for all the good conversations and laughs we shared over a cup of coffee. Thank you for being a good friend.Thank you all again for supporting me for everything.

Finally, this work was made possible through a financial support from the University of Jordan and the University of Hull.

Thank you all

Contents

Abstract iii

Dedication iv

Acknowledgements v

List of figures x

List of tables xvi

1. Chapter one: introduction & literature review 1

1.1 An introduction to Nanoparticles 1

1.1.1 Definition, properties and types of Nanoparticles 1

1.1.2 Applications of nanomaterials 2

1.2 Effects of nanomaterials in the environment 3

1.3 Effects of nanomaterials on aquatic organisms 5

1.4 Nanotoxicology and toxicity of nanomaterials 5

1.4.1 Mechanisms of toxicity of nanomaterials 6

1.5 *In vitro* toxicology research on nanomaterials 27

1.6 *In vivo* toxicology research on nanomaterials 29

1.7 Use of *D. rerio* in toxicology 29

1.8 Summary 30

Aims of the study 31

2. Chapter two: isolation and characterisation of nanoparticle-induced candidate genes 33

2.1 Introduction 33

2.2 Materials and Methods 33

2.2.1 Chemicals and characterization of AgNPs 33

2.2.2 Fish and exposure protocols 34

2.2.3 Total RNA isolation and purification from *D. rerio* embryos and adults tissue 34

2.2.4 Quantification and quality of RNA 35

2.2.5 First strand synthesis of cDNA for the Polymerase Chain Reaction (PCR) 36

2.2.6 Oligonucleotide primer design 36

2.2.7 Amplification of DNA by PCR 40

2.2.8 Agarose gel electrophoresis of DNA 40

2.2.9 Isolation of DNA fragments from agarose gel slices 41
2.2.10 Quantification of DNA 41
2.2.11 Sequencing 42
2.3 Results 42
2.3.1. RNA isolation 42
2.3.2 Quantification and quality of RNA 42
2.3.2 Candidate gene amplification using *D. rerio* cDNA template 43
2.3.5 Sequencing the DNA fragments 45
2.4 Discussion 53
3. Chapter Three: Quantitative PCR method development and validation for the quantification of candidate genes expression in *D. rerio* embryos 57
3.1 Introduction 57
3.2 Materials and Methods 58
3.2.1 *D. rerio* embryos 58
3.2.2 Total RNA isolation 58
3.2.3 First strand synthesis of cDNA for qPCR 58
3.2.4 Oligonucleotide primer design 58
3.2.5 Primer optimization 58
3.2.6 Assay performance 59
3.2.7 Evaluating reference mRNA transcript 59
3.2.8 Amplification using qPCR 59
3.2.9 Quantification and validation of the mRNA transcript method 60
3.2.10 Statistical analysis of qPCR data 60
3.2.11 Quantification of mRNA transcript in 10 nm AgNPs treated *D. rerio* embryos 60
3.3 Results 61
3.3.1 Oligonucleotide primer optimization 61
3.3.2 Standard curves for analysis of assay performance 62
3.3.3 Evaluating reference mRNA transcript 66
3.3.4 Quantitative PCR analysis of candidate genes mRNA in *D. rerio* embryos 67
3.3.5 Quantification of mRNA transcript in 10 nm AgNPs treated *D. rerio* embryos 68
3.4 Discussion 69

4. Chapter Four: Identification of differentially expressed genes in nanosilver-exposed *D. rerio* embryos using SSH 75

4.1 Introduction 75

4.2 Materials and Methods 76

4.2.1 *D. rerio* embryos 76

4.2.2 RNA isolation 76

4.2.3 RNA precipitation 76

4.2.3 First strand synthesis of cDNA 77

4.2.4 cDNA amplification by LD PCR 77

4.2.5 Column chromatography 78

4.2.6 *Rsa*1 restriction enzyme digestion 78

4.2.7 Purification of digested cDNA 79

4.2.8 Adaptor ligation 79

4.2.9 Ligation efficiency analysis 81

4.2.10 First hybridisation 82

4.2.11 Second hybridisation 82

4.2.12 PCR amplification 82

4.2.13 Cloning of PCR generated fragments 83

4.2.14 Sequencing of the subtracted cDNA clones 84

4.2.15 Bioinformatics analysis 85

4.2.16 qPCR validation 86

4.2.17 Statistical analysis 86

4.3 Results 86

4.3.1 SSH analysis 86

4.3.2 qPCR validation of the differentially expressed mRNA transcript levels 89

4.4 Discussion 89

5. Chapter Five: Nanotoxicity of polyelectrolyte-functionalized titania nanoparticles towards *D. rerio* embryos 94

5.1 Introduction 94

5.2 Materials and methods 96

5.2.1 Preparation and characterisation of TiO_2NPs 96

5.2.2 *D. rerio* embryos exposure to TiO_2NPs 97

5.2.3 *D. rerio* embryos viability after exposure to TiO_2NPs 97
5.2.4 Transmission Electron Microscopy (TEM) imaging 98
5.2.5 Quantitative PCR method 99
5.3 Results 100
5.3.1 Effect of TiO_2NP exposure on *D. rerio* embryo viability 100
5.3.2 Morphological analysis of *D. rerio* embryos after exposure to TiO_2NPs 102
5.3.3 QPCR analysis of target gene expression in *D. rerio* embryos following exposure to TiO_2NPs 110
5.4 Discussion 115
6. Chapter Six: Wider discussion, relevance and future work 120
Relevance and contribution to the research field 120
Summary and discussion of the main findings 121
Future work 127
General conclusion 129
6. References 131

List of figures

Chapter one: introduction & literature review

Figure 1.1 Schematic of NPs exposure pathways, affected organs, and related diseases in the human body from *in vivo* and *in vitro* epidemiological studies (Buzea et al., 2007). 4

Figure 1.2 Types of transporters in biological systems. (A) Transporters like a channel which can help diffusion through a transmembrane channel. (B) Transporters like a carrier coupled to chemiosmotic energy which needs a carrier-mediated process to be able to transport the substrate. (C) Primary active transporters directed by pyrophosphate hydrolysis where the solute (S) is bump into the membrane channel (M) by a receptor. (D) Multidomain transporters, phosphoryl transfer-driven group translocators, PEP-dependent and they modify the transported species throughout the transport. (Saier et al., 2002). 21

Chapter two: isolation and characterisation of NP-induced candidate genes

Figure 2.1 Ethidium bromide stained 1% agarose gel displaying total RNA samples from *D. rerio* embryos using an aliquot of the RNA samples as follows: 1-6 (untreated control samples), and 7-12 (1.925 mg Ag/L of 4 nm Ag (96 hpf)). 43

Figure 2.2 A 1% agarose gel, stained with gel red dye, displaying PCR amplification products from *D. rerio* embryos/tissues using various primer pairs. Lane 1: -ve control, lane 2: +ve control (*EF.1*), lane 3: *SOD2.1*, lane 4: *SOD2.2*, lane 5: *ATP.1*, lane 6: *ATPase.1*, lane 7: *HIF.4*, lane 8: *CRYaa*, lane 9: *HSP.2*, lane 10: *Cat.1*, lane 11*: Jupa.4*, lane 12: *Muc2.1*, lane 13: *Muc2.2*, lane 14: *Pxmp2.4*. 45

Figure 2.3 Multiple sequence alignment of the *SOD2.1* deduced amino acid sequence of *D. rerio* with *Ctenopharyngodon idella, Hypophthalmichthys molitrix,* and *Osmerus mordax*. Asterisks marks denote homology. 46

Figure 2.4 Multiple sequence alignment of the *SOD2.2* deduced amino acid sequence of *D. rerio* with *Hemibarbus mylodon, H. molitrix,* and *Megalobrama amblycephala*. Asterisks marks denote homology. 46

Figure 2.5 Multiple sequence alignment of the *ATP.1* deduced amino acid sequence of *D. rerio* with *Pongo abelii, M. musculus,* and *Sus scrofa.* Asterisks marks denote homology. 47

Figure 2.6 Multiple sequence alignment of the *HIF.4* deduced amino acid sequence of *D. rerio* with *M. musculus, Myxocyprinus asiaticus, and Spalax judaei*. Asterisks marks denote homology. 48

Figure 2.7 Multiple sequence alignment of the *CRYaa* deduced amino acid sequence of *D. rerio* with *Pimephales notatus*, *Cyprinodon variegates*, and *Notothenia angustata*. Asterisks marks denote homology. 49

Figure 2.8 Multiple sequence alignment of the *HSP.2* deduced amino acid sequence of *D. rerio* with *Oreochromis niloticus*, *C. auratus*, and *Ictalurus furcatus*. Asterisks marks denote homology. 49

Figure 2.9 Multiple sequence alignment of the *Cat.1* deduced amino acid sequence of *D. rerio* with *M. amblycephala, H. molitrix,* and *C. idella*. Asterisks marks denote homology. 50

Figure 2.10 Multiple sequence alignment of the *Jupa.4* deduced amino acid sequence of *D. rerio* with *Salmo salar, Xenopus laevis,* and *Ophiophagus hannah*. Asterisks marks denote homology. 51

Figure 2.11 Multiple sequence alignment of the *Muc2.2* deduced amino acid sequence of *D. rerio with M. amblycephala, H. sapiens, and Gallus gallus.* Asterisks marks denote homology. 53

Figure 2.12 Multiple sequence alignment of the *Pxmp2.4* deduced amino acid sequence of *D. rerio* with *H. sapiens, Rattus norvegicus,* and *X. laevis*. Asterisks marks denote homology. 53

Chapter Three: Quantitative PCR method development and validation for the quantification of candidate genes expression in *D. rerio* embryos

Figure 3.1 qPCR amplification and standard curves generated from amplification of each gene as following: A: *18S.1*, B: *18S.2*, C: *BT.2*, D: *EF.1*, E: *EF.2*, F: *SOD2.1*, G: *SOD2.2*, H: *ATP.1*, I: *ATPase.1*, J: *HIF.4*, K: *CRYaa*, L: *HSP.2*, M: *Cat.1*, N: *Jupa.4*, O: *Muc2.2*, and P: *Pxmp2.4* genes respectively. 66

Figure 3.2 Comprehensive gene stability investigation of the three candidate reference genes in control and treated *D. rerio* embryos samples. Geomean of ranking values (y-axis) of three reference genes with their ranking from least to most stable mRNA transcript (x-axis). Lower geomean values indicate more stable mRNA transcript. 67

Figure 3.3 qPCR expression analysis of target mRNA in controls, silver ion-treated and 4 nm range AgNPs-treated *D. rerio* embryos. Normalized average relative mRNA transcription ± standard error of the mean in *D. rerio* embryos for (A) *SOD2.1*, (B) *HIF.4*, (C) *Cat.1*, (D) *Muc2.2*, and (E) *Pxmp2.4* genes. 68

Figure 3.4 qPCR expression analysis of target mRNA in controls and 10 nm range AgNPs-treated *D. rerio* embryos. Normalized average relative mRNA transcription ± standard error of the mean in *D. rerio* embryos for (A) *SOD2.1*, (B) *HIF.4*, and (C) *Pxmp2.4* genes. 69

Chapter Four: Identification of differentially expressed genes in nanosilver-exposed *D. rerio* embryos using SSH

Figure 4.1 Schematic diagram for the preparation of adaptor-ligated tester cDNAs for hybridization and PCR. Each tester cDNA was ligated to the suitable adaptor. A. The forward subtraction which represents the control embryos. B. The reverse subtraction represents the treated embryos. C. A control subtraction was performed with skeletal muscle cDNA (Scheme modified based on the Select™ cDNA Subtraction Kit User Manual, Clontech. www.clontech.com). 80

Figure 4.2 Pie chart showing the proportion of down-regulated transcripts (in 4 nm size range AgNP- treated *D. rerio* embryos relative to healthy *D. rerio* embryos) that were identified with a similarity search using the GenBank database. 87

Figure 4.3 Pie chart showing the proportion of up-regulated transcripts (in 4 nm size range AgNP- treated *D. rerio* embryos relative to healthy *D. rerio* embryos) that were identified with a similarity search using the GenBank database. 87

Figure 4.4 Relative mRNA transcript expression levels, in *D. rerio* embryos, of *target* mRNAs previously identified as differentially regulated by the SSH approach. Data are expressed as normalized average relative mRNA transcript level +/- SEM in *D. rerio* embryos for (A) *Spata 2,* (B) *COXI,* (C) *actclb*, and (D) *SLC25A5* genes. N=20. *P*= < 0.05. 89

Chapter Five: Nanotoxicity of polyelectrolyte-functionalized titania nanoparticles towards *D. rerio* embryos

Figure 5.1 FDA stained *D. rerio* embryos of different types of TiO_2NPs samples using a total concentration of 500 and 1000 mg/L for each media under dark and visible light conditions. The viability was examined by using Olymbus BX51 fluorescence microscope attached to a DP70 digital camera and FITC fluorescence filter set. FDA is taken up by living cells and is hydrolysed to fluorescein, which fluoresces green, and thus determines which cells are living (green). (A-H) Embryos treated in dark condition. (I-P) Embryos treated in visible light condition. (A, E, I, and M) Control, untreated embryos for each batch; (B) Embryo treated with 500 mg/L bare TiO_2NPs; (C) Embryo treated with 500 mg/L TiO_2NPs/PSS; (D) Embryo treated with 500 mg/L TiO_2NPs/PSS/PAH; (F) Embryo treated with 1000 mg/L bare TiO_2NPs; (G) Embryo treated with 1000 mg/L TiO_2NPs/PSS; (H) Embryo treated with 1000 mg/L TiO_2NPs/PSS/PAH; (J) Embryo treated with 500 mg/L bare TiO_2NPs; (K) Embryo treated with 500 mg/L TiO_2NPs/PSS; (L) Embryo treated with 500 mg/L TiO_2NPs/PSS/PAH; (N) Embryo treated with 1000 mg/L bare TiO_2NPs; (O) Embryo treated with 1000 mg/L TiO_2NPs/PSS; (P) Embryo treated with 500 mg/L TiO_2NPs/PSS/PAH. 101

Figure 5.2 (A) Microscope image of control *D. rerio* embryos. (B) TEM image of control microtome-sectioned control *D. rerio* embryo. 103

Figure 5.3 TEM and EDS spectra images of control *D. rerio* embryo. (A) TEM image of microtome-sectioned *D. rerio* embryo. (B) EDS spectrum from microtome-sectioned *D. rerio* embryo. Table shows weight percent and atomic percent of the elements present in the sample. 104

Figure 5.4 TEM and EDS spectra images of *D. rerio* embryo after incubated for 3 hr with 500 mg/L of TiO_2NPs/PSS in dark. (A) TEM image of microtome-sectioned *D. rerio* embryo. (B) EDS spectrum from microtome-sectioned *D. rerio* embryo that included TiO_2NPs and other elements, the peaks on the EDS spectrum validated the presence of TiO_2NPs. Table shows weight percent and atomic percent of the elements present in the sample. 105

Figure 5.5 TEM and EDS spectra images of *D. rerio* embryo after incubated for 3 hr with 500 mg/L of TiO_2NPs/PSS in visible light. (A) TEM image of microtome-sectioned *D. rerio* embryo. (B) EDS spectrum from microtome-sectioned *D. rerio* embryo that included TiO_2NPs and other elements, the peaks on the EDS spectrum validated the presence of TiO_2NPs. Table shows weight percent and atomic percent of the elements present in the sample. 106

Figure 5.6 TEM and EDS spectra images of *D. rerio* embryo after incubated for 3 hr with 1000 mg/L of TiO_2NPs/PSS/PAH in dark. (A) TEM image of microtome-sectioned *D. rerio* embryo. (B) EDS spectrum from microtome-sectioned *D. rerio* embryo, no TiO_2NPs was detected in the analytical spectrum of EDS. Table shows weight percent and atomic percent of the elements present in the sample. 107

Figure 5.7 TEM and EDS spectra images of *D. rerio* embryo after incubated for 3 hr with 1000 mg/L of TiO_2NPs/PSS/PAH in visible light. (A) TEM image of microtome-sectioned *D. rerio* embryo. (B) EDS spectrum from microtome-sectioned *D. rerio* embryo, no TiO_2NPs was detected in the analytical spectrum of EDS. Table shows weight percent and atomic percent of the elements present in the sample. 108

Figure 5.8 TEM and EDS spectra images of *D. rerio* embryo after incubated for 3 hr with 1000 mg/L of TiO_2NPs/PSS/PAH in dark. (A) TEM image of microtome-sectioned *D. rerio* embryo. (B) EDS spectrum from microtome-sectioned *D. rerio* embryo that included TiO_2NPs and other elements, the peaks on the EDS spectrum validated the presence of TiO_2NPs. Table shows weight percent and atomic percent of the elements present in the sample. 109

Figure 5.9 Box-and-whisker plots of the gene expression levels of *SOD2.1* gene following exposure to TiO_2NPs with various coatings, concentration and exposure condition (p<0.05). The plots were generated using IBM SPSS Statistics 22 software. 112

Figure 5.10 Box-and-whisker plots of the gene expression levels of *HIF.4* gene following exposure to TiO_2NPs with various coatings, concentration and exposure condition (p<0.05). The plots were generated using IBM SPSS Statistics 22 software. 113

Figure 5.11 Box-and-whisker plots of the gene expression levels of *Pxmp2.4* gene following exposure to TiO_2NPs with various coatings, concentration and exposure condition (p<0.05). The plots were generated using IBM SPSS Statistics 22 software. 114

List of tables

Chapter one: introduction & literature review

Table 1.1 Summary of investigations selected publishing acute toxicity data (mortality and biological effects) for NMs in aquatic species 8

Table 1.2 Studies that investigate the mechanisms responsible for immunotoxicity after exposure to selected engineered NMs. 25

Chapter two: isolation and characterisation of nanoparticle-induced candidate genes

Table 2.1 Primer pairs used for the isolation of candidate and reference genes from *D. rerio*. 37

Table 2.2 The successful primer pairs and optimised annealing temperature used in PCR for each of the targeted genes. 43

Chapter Three: Quantitative PCR method development and validation for the quantification of candidate genes expression in *D. rerio* embryos

Table 3.1 Ct values of the qPCR amplifications using various primer concentrations. 61

Table 3.2 Ct values for each standard dilution and efficiency of references and candidate genes. 62

Chapter Four: Identification of differentially expressed genes in nanosilver-exposed *D. rerio* embryos using SSH

Table 4.1 The ligation analysis PCR components. 81

Table 4.2 Primer sequences used for expression analysis of selected differentially expressed target mRNAs in *D. rerio* embryos exposed to AgNPs and control samples. 85

Table 4.3 Differentially expressed (subtracted) mRNAs isolated from *D. rerio* embryos exposed to 4-nm range AgNPs (1.925 mg/L). 88

Chapter Five: Nanotoxicity of polyelectrolyte-functionalized titania nanoparticles towards *D. rerio* embryos

Table 5.1 Viability (%) determined using the FDA assay of *D. rerio* embryos after exposure to TiO_2NPs at 0, 500 and 1000 mg/L concentration for 3 hr exposure time kept in dark conditions and visible light. 102

Table 5.2 Summary of statistical analysis on the effect of TiO_2NPs, coated with different number of layers of anionic (PSS) and cationic (PAH) polyelectrolytes, on the mRNA expression level of *SOD2.*1, *HIF.*4, and *Pxmp2.*4 in *D. rerio* embryos. Exposures were conducted at three particle concentrations (0, 500 and 1000 mg/L) for 3 hr exposure time in either dark or visible light. 111

1. Chapter one: introduction & literature review

1.1 An introduction to Nanoparticles

1.1.1 Definition, properties and types of Nanoparticles

Nanomaterials (NMs) have been defined as materials with at least one dimension smaller than 100 nm (Liu and Sun, 2010; Aschberger et al., 2011; Hartl et al., 2015). While nanoparticles (NPs) are materials which measure as equal to or less than 100 nm (Buzea et al., 2007) and behave as a small object as a whole in terms of its porperties. These materials include produced NMs, such as diesel exhaust materials or airborne combustion by-products, as well as nanosized materials which occur in the environment, such as viruses or volcanic ash (U.S. EPA, 2007). In general, NMs offer relative surface areas bigger than the parallel common forms. Furthermore, the small size often leads to increased reactivity and change of surface properties of some consumer products such as paints, food, cosmetics, suntan lotions, medicines, and applications that directly release NMs into the environment, like remediation of polluted environments (Aitken et al., 2006).

NMs have been organized into four types according to the United States Environmental Protection Agency (U.S. EPA) in 2007. The first type is carbon-based materials, composed primarily of carbon and found in many forms like hollow spheres, ellipsoids or tubes. The fullerenes are spherical and ellipsoidal carbon NMs, and nanotubes are cylindrical carbon nanotubes. The second type includes metal-based materials, including quantum dots, nanogold, nanosilver and metal oxides such as titanium dioxide (TiO_2). The third type include dendrimer NMs, which are nanosized polymers consisting of branched units with a surface of numerous chain ends that can be tailored to perform specific chemical functions useful for catalysis. Finally, the last type is composites that combine NMs with other NMs or bulk-type large materials, such as nanosized clays used in packaging materials to enhance thermal, barrier and mechanical properties (U.S. EPA, 2007). In addition, there are also new types of NMs developing, these are known as the second generation and include targeted drug delivery systems, amplifiers and actuators (U.S. EPA, 2007). The third generation

involves robotics devices and the fourth generation is assumed to result in designing new atomic and molecular assemblies and self-assembly capabilities NMs (Roco, 2007). Unfortunately there are limited available data on those new NMs.

1.1.2 Applications of nanomaterials

According to the European Commission in 2012, there are globally uses of NMs. For example, in aerospace they are used to produce lightweight materials, resistant paints and coatings for aerodynamic surfaces (Klaine et al., 2008). In the automotive industry and transport they are used in scratch-resistant paints and coatings, plastics, lubricants, fluids, tyres. In agrifood they are used in sensors to optimize food production. In construction they are used in insulation, stronger building materials and self-cleaning windows. While in energy generation they are used in photovoltaics and storage like fuel cells and batteries. Furthermore, NMs can be used in the environment for soil and groundwater remediation. In cosmetics, they are used in sunscreens, toothpaste, and face creams, as well as in health, medicine and nanobiotechnology. For instance, a biodegradable NM has been developed from lignin to use as drug delivery vehicles and pharmaceutical formulations (Frangville et al., 2012). In information and communication technologies, electronics and photonics they are used in semiconductor chips, new storage devices and displays (European Commission, 2012). In security they are used in sensors to detect biological threats, and in textiles they are used in protective clothing, stronger, self-cleaning or fire resistant fibers (European Commission, 2012).

Focusing on carbon nanotubes, these NMs are used in shielding radio frequency interference (RFI) or electromagnetic interference (EMI) (Yang, 2007). They may also be used in flexible fibres and advanced polymers, owing to their mechanical properties (Avallone et al., 2006) and electrical energy and hydrogen storage (An et al., 2001). Carbon nanotubes may also be used in scanning probe microscopy (Rothschild et al., 1999).

NMs are therefore very useful to the life sciences, as well as environment and human health applications, used as sensors for environmental monitoring, nano-drug-delivery systems, biorobotics, nanoarrays, and nanoscale implants in medicine (Roco,

2003; Freitas, 2005). NMs are thus used in many applications and are a common element of daily life.

1.2 Effects of nanomaterials in the environment

NMs mainly occur in the environment associated with sediments and solids (Klaine et al., 2008). However, no accurate measurements of manufactured NMs in the environment have been developed to date because of the lack of analytical methods for measuring the concentrations of NMs (Gottschalk and Nowack, 2011). In addition, some of the NMs have been recommended as a capable, low cost and environmental friendly alternative to existing treatment materials either as resource conservation or environmental remediation (Friedrich et al., 1998; Dimitrov, 2006; Dastjerdi and Montazer, 2010). For example, iron oxide NMs are one of the promising NMs for industrial field wastewater treatment due to their low cost, high adsorption capacity, easy separation and high stability (Hu et al., 2005; Carabante et al., 2009; Fan et al., 2012). Magnetic NMs as nano zerovalent iron (nZVI), magnetite (Fe_3O_4) and maghemite (γ-Fe_2O_3) NMs have shown huge interest in studies related to engineering applications for treatment of polluted water or surface environments (Hu et al., 2005; Li et al., 2006a,b; Shen et al., 2009; Yantasee et al., 2007). Similarly, silver sulfide NMs are added in the final stage of sewage sludge treatment at municipal wastewater plants (Kim et al., 2010). If silver NMs are released into the environment in this way, then they represent a potential threat to the health of organisms living in the receiving environment (Xiu et al., 2011).

Various of the NMs may find their way into wastewater discharges and be transported to the aquatic environment (Liu, 2006). For instance, trace amounts of titanium have been reported in the magnetite materials of an uncultured freshwater magnetotactic Coccus (*Magnetococcus marinus*) sampled from a wastewater treatment ponds (Towe and Moench, 1981). It is therefore evident that there are potential sources of manufactured NMs contaminating the environment. Unfortunately, there is currently only limited information on the concentrations and physiochemical forms of such NMs in the environment because of the limitations in separation and analytical methodologies (Xu et al., 2012). Also, for carbon nanotubes, despite the fact that they are widely used, their environmental impacts, if any, are

largely unknown (Al-Shaeri et al., 2013). NMs may find their way into the human body through different pathways and affect different organs (Fig. 1.1). Furthermore, the route of exposure and subsequent risks posed to human health, as a result of atmospheric exposure for example, have only recently been investigated (Aschberger et al., 2010).

Nanotubes are emitted into the environment during manufacture, use and recycling. Carbon nanotubes can be released from textiles while tailoring, finishing and use (Koehler et al., 2008). While only a fraction of these materials will contaminate the environment, it is expected though that in the future the concentration of carbon nanotubes will increase in the environment especially when their prices fall and the applications of carbon nanotubes in consumer products becomes more widespread (Mueller and Nowack, 2008).

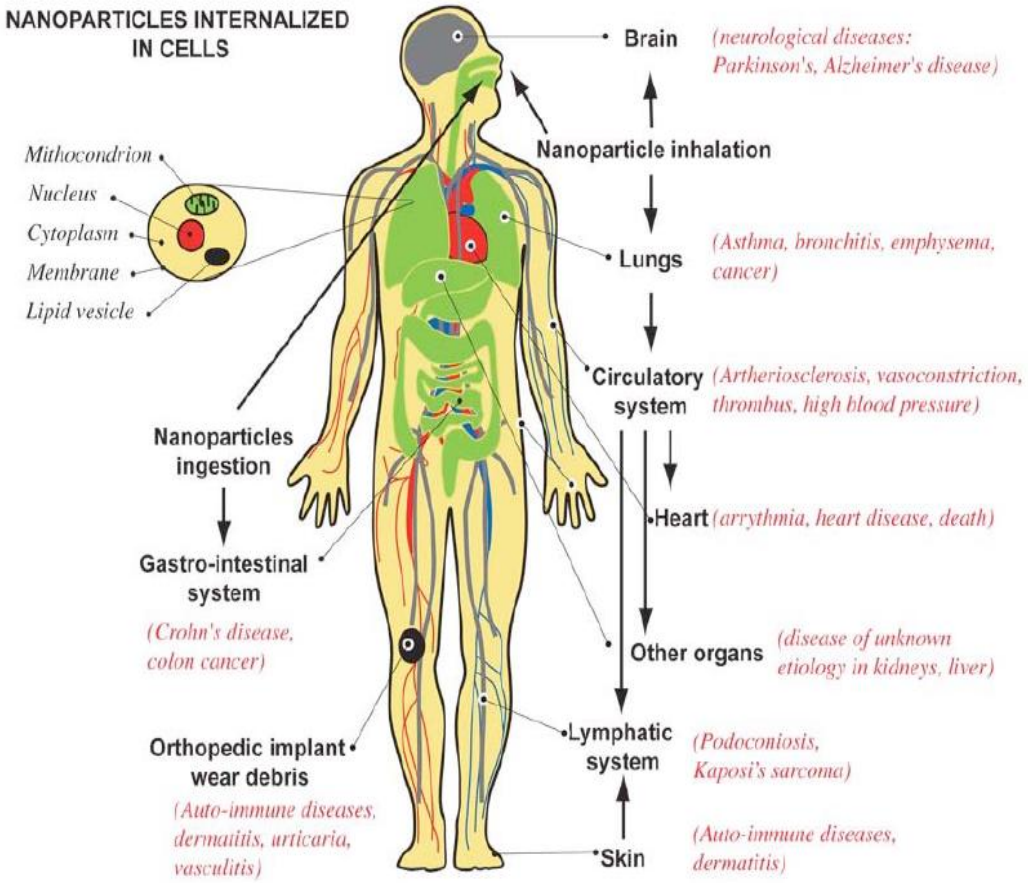

Figure 1.1. Schematic of NPs exposure pathways, affected organs, and related diseases in the human body from *in vivo* and *in vitro* epidemiological studies (Buzea et al., 2007).

Nowack's group (Mueller and Nowack, 2008; Gottschalk et al., 2009; Gottschalk et al., 2010) have suggested precautions on the flow of carbon NMs to different destinations (recycling, waste incineration, landfills, water treatment) based on limited available information. They released these NMs to different environmental areas (surface water, ground water, soil, sediment and atmosphere) and the results suggest that the main bulk of carbon nanotubes end up incinerated and released to the atmosphere or to a landfill (Gottschalk et al., 2010). However, more studies are required to evaluate the impacts that NMs may have in the environment, especially since the data known regarding interactions of NMs with the natural environment are as yet uncharacterized (Darlington et al., 2009).

1.3 Effects of nanomaterials on aquatic organisms

The increasing existence of NMs in aquatic systems may lead to impacts on aquatic organisms. For instance, in aquatic systems a safe concentration of carbon nanotubes is considered to be less than 2mg/L (Gusev et al., 2012). In marine mussels, SWCNT-induced DNA damage has been correlated with oxidative stress only in the absence of dissolved metals (Al-Shaeri et al., 2013). A number of metal contaminants related to raw single-wall carbon nanotubes (SWCNTs) may also have the ability to affect aquatic organisms when released into the aquatic environment, for instance by inhibiting the development of embryos (Cheng et al., 2007), or (in the case of rainbow trout (*Oncorhynchus mykiss*) brain exposed to SWCNTs), aneurisms or swellings (Smith et al., 2007). There is therefore a need to consider the biological impacts of NMs on organisms living in the receiving environment.

1.4 Nanotoxicology and toxicity of nanomaterials

Nanotoxicology is defined as "science of engineered nanodevices and nanostructures that deals with their effects in living organisms" (Oberdörster et al., 2005a); its aim is to provide safety evaluation and information about the possible harmful properties of engineered nanostructures and prevent possible detrimental biological effects (Oberdörster et al., 2005). The toxicity of certain NMs, such as carbon nanotubes, TiO_2 and silver NMs, is already known and documented (Wijnhoven et al., 2009), yet the toxicity of many others is largely unknown (Justo-Hanani and Dayan, 2014). Toxicity of NMs depends on several parameters such as size, shape, surface properties such as

charge, area, and reactivity (Ferreira et al., 2013). NMs are small enough to pass through biological membranes and reach more and different organs and tissues in the body.

Recently published work suggests that some types of NMs are toxic to fish and such impacts are similar to those of dissolved metals (Shaw et al., 2012). On the other hand, metal NMs could be dissolved to release metal ions by dissolution from the surface of the particles, leading to potential free ion toxicity (Shaw et al., 2012). Moreover, little data is known about the bioavailability of metal NMs and their accumulation effects in fishes (Shaw and Handy, 2011). In general, most of the studies concerned about the toxicity of NMs have focused on respiratory exposure in mammalian models and its participation in human health (Handy and Shaw, 2007). There is however a number of studies that investigate the toxic effects of NMs as summarized in Table 1.1 For example, fish exposure to fullerene aggregates reduced length and body weights (Zhu et al., 2008). The table below (Table 1.1) summarizes the current literature available for acute toxicity for NMs in aquatic species.

1.4.1 Mechanisms of toxicity of nanomaterials

There are many ways to investigate the measures of toxicity, yet studying the underlying cause and effect relationship is the main aim. To do this, studies typically involve on investigation at the sub-cellular molecular level. One approach to characterize how organisms or cells adapt to alterations in the external environment is to use mRNA transcription. Measuring mRNA transcription levels after exposure to a chemical can provide information about the mechanisms of action of toxicants and form a type of “genetic signature” (Lettieri, 2006). Although relatively little is known about the mechanisms of NM toxicity compared to other contaminant classes such as metals, some researchers have found evidence for NM induced damage via the production of reactive oxygen species (ROS) and generation of oxidative stress (Oberdörster, 2004; Pickering and Wiesner, 2005; Zhu et al., 2007). These include studies involving TiO_2 and carbonaceous NMs such as fullerenes, fullerols, and carbon nanotubes (Reeves et al., 2008; Xia et al., 2006).

1.4.1.1 Oxidative stress related mechanisms of nanomaterial-induced damage

To date, the most frequently reported mechanism of manufactured NM toxicity in vertebrates is oxidative stress, which causes inflammation via the activation of oxidative stress responsive transcription factors. Oxidative stress and inflammation are linked processes, since chronic inflammation is associated with elevated ROS levels (Terlecky et al., 2012). The oxidative stress and chronic inflammation caused by ongoing exposure may subsequently cause fibrosis, genotoxicity and cancer via fibre impacts or secondary mutation (Aschberger et al., 2011). It has been suggested that copper particles may induce oxidative stress in the gills, measured as both hypoxia-inducible factor (HIF-1) and heat shock protein 70 (HSP70) induction in fish (Van der Meer et al., 2005).

A common approach to estimate oxidative stress in biological systems includes the measurement of the increase or decrease in redox-sensitive molecules that respond to oxidative stress (Powers and Jackson, 2008). To protect biomolecules from oxidative stress, the cell produces different antioxidant molecules and enzymes (i.e. the antioxidant defence system). Key antioxidant enzymes include *superoxide dismutase* (*SOD*), *glutathione reductase* (*GR*), *glutathione peroxidase* (*GPx*), as well as *catalase* (*Cat*).

Table 1.1. Summary of investigations selected publishing acute toxicity data (mortality and biological effects) for NMs in aquatic species.

Nanomaterial	Size	Concentration (mg/L)	Exposure time	Species	Toxic effects observed	Reference
Chitosan NPs and normal chitosan	84.86 nm	100, 150, 200, 250, 300, 350 and 400 mg/L	96 and 120 hpf	*D. rerio* Zebrafish	The embryonic development of *D. rerio* was evaluated. The malformation, mortality and hatching rates of *D. rerio* embryo showed dose-dependent effects in both. The toxicity of chitosan nanoparticles to *D. rerio* was lower than normal chitosan particles.	Wang et al., 2016
Nanocopper, nanosilver and nano-TiO_2	26.7 ± 7.1 nm for nanocopper 26.6 ± 8.8 nm for nanosilver 20.5 ± 6.7 nm for nano-TiO_2	Nanocopper (1mg/L) Nanosilver (1 mg/L) TiO_2 (1 mg/L)	0, 2, 24, and 48 hr	*D. rerio* Zebrafish	Nanocopper and nanosilver increased metal content linked to gill tissue. Nanocopper increased gill filament width while nanosilver did not change gill filament width. Each NPs showed different biological effect by a	Griffitt et al., 2009

					different mechanism.	
Nanocopper	80 nm	Low nanocopper (0.25 mg/L), and high nanocopper (1.5 mg/L)	48 hr	*D. rerio* Zebrafish	Nanocopper caused inhibition of Na+/K+ ATPase (NPA) activity and caused proliferation of interlamellar cells. Nanocopper produced significant induction of HIF-1, HSP70, and copper transport regulatory protein (CTR). The toxicity appears to occur primarily at the gills.	Griffitt et al., 2007
Nanosilver, nanocopper, nanonickel, nanocobalt, nanoaluminum and nano-TiO_2	Nanosilver, 20–30 nm Nanocopper, 15–45 nm Nanonickel, 5–20 nm Nanocobalt, 10–20 nm Nanoaluminum, 51 nm	Nanosilver 7.2 mg/L. Nanocopper 0.94 mg/L. Nanonickel, nanocobalt, nanoalumin and nano-TiO_2 >10 mg/L.	48 hr	*D. rerio* Zebrafish	Nanosilver and nanocopper cuased toxicity with less than 10 mg/L. Nano-TiO_2 did not cause toxicity. NPs forms of metals were less toxic than soluble forms of metals.	Griffitt et al., 2008

	Nano-TiO_2, 30 nm					
(AgNPs) and $AgNO_3$	10–21 nm AgNPs	0–1000 µg /L	24 hr and 48 hr	*D. rerio* Zebrafish	Small differences in Ag toxicity were found between the different developmental stages of *D. rerio* and particulate and ionic Ag. The *D. rerio* stage with chorion accumulated more Ag compared to the later stages without chorion.	Böhme et al., 2015
Nanosilver	81 nm	0.084 mg/L	48 hr	*D. rerio* Zebrafish	Excess mucus (*Muc*) production in gill was recorded.	Bilberg et al., 2012
TiO_2NPs	21 nm	1 mg/L	14 d	*O. mykiss* Juvenile rainbow trout	TiO_2NPs caused some gill pathologies such as oedema and thickening of the lamellae. No haematological or blood disturbances were observed. TiO_2NPs decreased the Na^+K^+-ATPase activity in the intestine and gills, but a decrease of the enzyme activity in the brain was	Federici et al., 2007

					observed. TiO_2NPs caused increase in the total glutathione levels in the gills and depletion of hepatic glutathione. TiO_2NPs showed minor fatty changes, lipidosis, and some hepatocytes in liver cells.	
TiO_2NPs	10 nm	500 mg/L	96 hr	Pimephales Promelas Fathead minnow	TiO_2NPs were found more toxic to the tested invertebrate species.	Hall et al., 2009
AgNPs, Cu-TiO_2, and TiO_2NPs	20-30 nm AgNPs 20-70 nm Cu-TiO_2 < 15 nm TiO_2NPs	20 mg/L	2, 5, 8, 22, 27, 32, 48 and 72 hpf	*D. rerio* Zebrafish	Large number of genes was differently expressed after exposure to AgNPs, Cu-TiO_2, and TiO_2NPs. Most of these genes involved in apoptosis which may have other functions such as endocytosis and immune responses. AgNPs cause down-	Park and Yeo, 2013

					regulation in *HIF-1*.	
TiO_2 NPs ZnONPs	30 nm	0, 2, 5, 10, 30 and 50 mg/L for ZnONPs, and 0, 10, 50, 100, 150, 200 and 300 mg/L for TiO_2NPs	96 hr	*D. rerio* Zebrafish	ZnONPs caused oxidative stress in the gills but with no oxidative damage. TiO_2NP caused oxidative damage to gill tissue. Gut tissues showed oxidative effects after exposure to NPs.	Xiong et al., 2011
TiO_2 NPs	10, 20, 200 or > 200 nm anatase 200 nm rutile	10 mg/L	1-72 hr	Human bronchial epithelial cells BEAS-2B (ATCC CRL-9609)	10 and 20 nm anatase TiO2NPs showed increase in lipid peroxidation and levels of ROS which caused oxidative DNA damage. No oxidative stress result from > 200 nm anatase TiO2NPs.	Gurr et al., 2005
ZnO, TiO_2, Al_2O_3, C60, SWCNTs, and Multi-Walled Carbon Nanotubes (MWCNTs)		Different conc. For each particle suspensions.	48 h	*Daphnia magna* Water flea	The acute toxicities of all NMs tested are dose dependent. TiO_2, Al_2O_3, and carbon-based NMs were more toxic than their bulk counterparts. Moreover, *D.*	Zhu et al., (2009)

					magna were found to ingest NMs from the test solutions through feeding behaviours.	
SWCNTs and nanoTiO$_2$.	SWCNTs (diameter 1–2 nm) TiO2 had (diameter 32.4 nm)	30 mg/L	for 10 d at 15^{o}C, 8 hr light: 16 hr dark	*Arenicola marina* lugworm	No effects or uptake were observed after SWNTs exposure. NanoTiO$_2$ caused increase in cellular damage and DNA damage in coelomocytes.	Galloway et al., 2010
AgNPs	35 and 100 nm	1·25 mg/L for 35 nm particles 1·36 mg/L for 100 nm particles	96 hr	*P. promelas* (embryos) Fathead minnow	AgNPs caused larval abnormalities, mostly edema. Embryo toxicity increased after NPs solutions were sonicated more than when it stirred.	Laban et al., 2010
C60	10–100 nm	0·5 mg/L	48 hr	*P. promelas* (adults) Fathead minnow	THF-*n*C$_{60}$ caused 100% mortality in fish between 6-18 hr exposures. *n*C$_{60}$ caused increase in lipd peroxidation (LPO) in the gill and the brain. The CYP2	Zhu et al., 2006

					family isozymes increased in liver after exposure.	
C_{60} fullerenes	30–100 nm	0.5 or 1mg/L	48 hr	*Micropterus salmoides* (juveniles) Largemouth bass	Lipid peroxidation products increased in the brain and gill with the 0.5 mg/L concentration.	Oberdörster. 2004
*n*C60	100 nm	1·5 mg/L	96 hr	*D. rerio* Zebrafish (embryos)	*n*C_{60} at 1.5 mg/L caused pericardial edema, delayed embryo and larval development, it also decreased survival and hatching rates. Toxicity was decreased by adding an antioxidant (glutathione).	Zhu et al., 2007
C_{60} fullerenes	No sizes given	0-0.5 mg/L	24 hpf for 5 d	*D. rerio* Zebrafish (embryos)	Less mortality was observed after decreased light except for highest concentration (0.5 m/L) mortality happened.	Usenko et al., 2008
C_{60}, C_{70} and C_{60}	No sizes given	0.1–0.5 mg/L for	24 hpf	*D. rerio*	Embryos exposed to C_{60} and C_{70}	Usenko et

$(OH)_{24}$ fullerenes		C_{60} and C_{70}, 0.5–5 mg/L for $C_{60}(OH)_{24}$	until 96 hpf	Zebrafish (embryos)	showed developmental delays and abnormalities. Functionalized $C_{60}(OH)_{24}$ was less toxic compared to other fullerenes.	al., 2007
C_{60} fullerenes MWNT SWNT TiO_2NPs	5 and 200 nm	500 mg	6 weeks	*O. mykiss* juvenile Rainbow trout	NP agglomerates were cytotoxic at concentration > 3 mg/L, MWNT and SWNT produced ROS and cytotoxicity. Trace metals associated with NPs could be responsible for biological effects.	Thomas et al., 2011
C_{60} fullerenes	10–200 nm	0.5 mg/L	96 hr	*P. promelas* (adult males) Fathead minnow	Cytochrome P45o isozymes didn't change after exposure. The peroxisomal lipid transport protein (PMP70) was decreased in fathead minnow.	Oberdörster et al., 2006
SWCNTs	1–2 nm	0.1–0.5 mg/L	10 d	*O. mykiss* juveniles Rainbow trout	Brain and gill Zn or Cu changes were observed. SWCNT caused increases in Na^+ K^+ -ATPase	Smith et al., 2007

					activity in the intestine and gills, but not in the brain. SWCNT caused increases in the total glutathione levels in the gills and livers. SWCNT precipitated in the intestinal pathology and gut lumen. Aggressive behaviours cased mortality was also observed.	
Raw SWCNTs	11 nm	20, 40, 60, 120, 240, and 360 mg/L	4 to 96 hpf	*D. rerio* embryos Zebrafish	SWCNTs caused hatching delayes in embryos exposed at concentration > 120 mg/L.	Cheng et al., 2007
SWCNTs MWCNTs	SWCNTs: 2-nm average diameters MWCNTs: 10- to 20-nm diameters	800 mg of CNTs		*Hyalella azteca* *Amphipod crustacean* *Chironomus dilutus*	CNTs were observed in the gut and outer surface of the organism but no penetration through cell membranes were observed.	Mwangi et al., 2012

				Midge *Lumbriculus variegatus* Blackworm *Villosa iris* Rainbow mussel		
SWCNTs and MWCNTs	SWCNTs: 1-2 nm, and MWCNTs: 30-70 nm	^{14}C-SWNTs (0.03 or 0.003 mg/L) and MWNTs (0.37 or 0.037 mg/L)	28 d	*L. variegatus* Blackworm	The nanotubes observed in the organisms were connected with sediments remined in their guts and not being absorbed into cellular tissues.	Petersen et al., 2008
SWCNTs		30,000 mg/L		*Amphiascus tenuiremis* Copepods	SWNTs toxicity is size-dependent. The smallest size increased mortality and delayed copepod development.	Templeton et al., 2006
MWCNTs	20 nm	2 ng single dose	1 or 72 hpf	*D. rerio* Zebrafish	Toxic effects or developmental abnormalities were observed.	Cheng et al., 2009

		$2x10^{-6}$ mg		(embryos)		
Graphene oxide (GO) and MWNTs.	No sizes given	0, 3.4, 7.6, 12.5, 25 and 50 mg/L.	24 hpf	*D. rerio* Zebrafish	GO caused moderate toxicity and slight hatching delays. MWNTs caused serious morphological defects and strong inhibition of cell proliferation in developing embryos.	Chen et al., 2012
Purified MWCNTs	No sizes given	4 pg and 0.4 pg	48 hr	*D. rerio* Zebrafish *embryos*	MWCNTs caused severe developmental toxicity.	Cheng and Cheng, 2012
Purified SWCNTs	1.2 nm	0, 2.5, 5, 10, and 20 mg/L.	>24 hr	*D. magna* Water flea	Acute toxicity was only observed in the highest concentrations exposure.	Roberts et al., 2007
MWCNTs	No sizes given	0.025-0.25 mg/L	48 hr	*D. magna* Water flea	Acute toxicities SWCNTs toxicity > MWCNTs toxicity.	Petersen et al., 2011
Three MWCNTs samples.	MWCNTs outer diameters of <10 nm (MWCNTs 10),	(0, 5, 10, 20, 50, and 100 mg/L)	96 hr	*Chlorella sp.* Green algae	MWCNTs significantly inhibit algal growth.	Long et al., 2012

	20−40 nm (MWCNTs 40), and 60−100 nm (MWCNTs 100)					
Double-walled carbon nanotubes (DWNTs)	No sizes given	1; 10; 100; 125; 250; 500; 1000 mg/L	12 d	*Ambystoma mexicanum* *Mexican salamande*	CNTs showed no acutic toxicity or genotoxic effects to larvae at any CNTs concentration. CNTs were observed inside the gut.	Mouchet et al., 2007

Heat shock proteins (HSPs) are also induced by oxidative stress (Calabrese et al., 2000). GPx reduces hydroperoxides in the presence of GSH to protect cells from oxidative damage, including lipid peroxidation (Maiorino et al. 1995) whereas GR enzymes are involved in the ascorbate-GSH cycle, a pathway that allows the scavenging of superoxide radicals and Hydrogen Peroxide (H_2O_2) (Asada, 1999).

Peroxisomes are present in almost all eukaryotic cells as organelles enclosed by a single membrane, and are involved in different metabolic processes such as peroxisomal oxidation and respiration, fatty acid f3-oxidation, glyoxylate metabolism, cholesterol and dolichol metabolism, and ether lipid synthesis (Van den Bosch et al., 1992). Adrenoleukodystrophy protein (ALDP), PMP70, PMP70-related protein (P70R/PMP69), and ALDP-related protein (ALDRP) peroxisomal ABC transporters have been identified in mammalian peroxisomes (Imanaka et al., 1999).

There have been many studies involving an investigation of oxidative stress using these various antioxidant indicators as follows. In goldfish (*Carassius auratus*), exposed to anoxia conditions, increased *SOD* and *Cat* activities in liver have been observed (Lushchak et al., 2001). TiO_2 was also found to induce oxidative stress in mice after oral administration (Wang et al., 2007). In another study, it was observed that uncoated fullerenes could cause oxidative damage and depletion of GSH levels *in vivo* in Juvenile largemouth bass (*Micropterus salmoides*) (Oberdörster, 2004). Relevantly, Shvedova and colleagues (2003) also reported that SWCNTs exposure to human epidermal keratinocytes caused oxidative stress as accumulation of peroxidative products and decrease of intracellular levels of GSH. GSH reduction was also observed in gill cells of *O. mykiss* after treatment with coated manufactured silver NMs (Farkas et al., 2011). Oxidative stress is thus a well identified mechanism of NM-induced damage.

1.4.1.2 Receptor or membrane transporter protein blockage

Membrane transporters are essential for preserving a balance between the amounts of metal required for biological processes and those that could be toxic (Lin et al., 2009). Most of the molecules that enter or leave cells are aided by transport proteins. The four major types of transporters in biological systems that are based on the type,

transport direction and the energy mechanism (Saier et al., 2002) are shown in Figure 1.2.

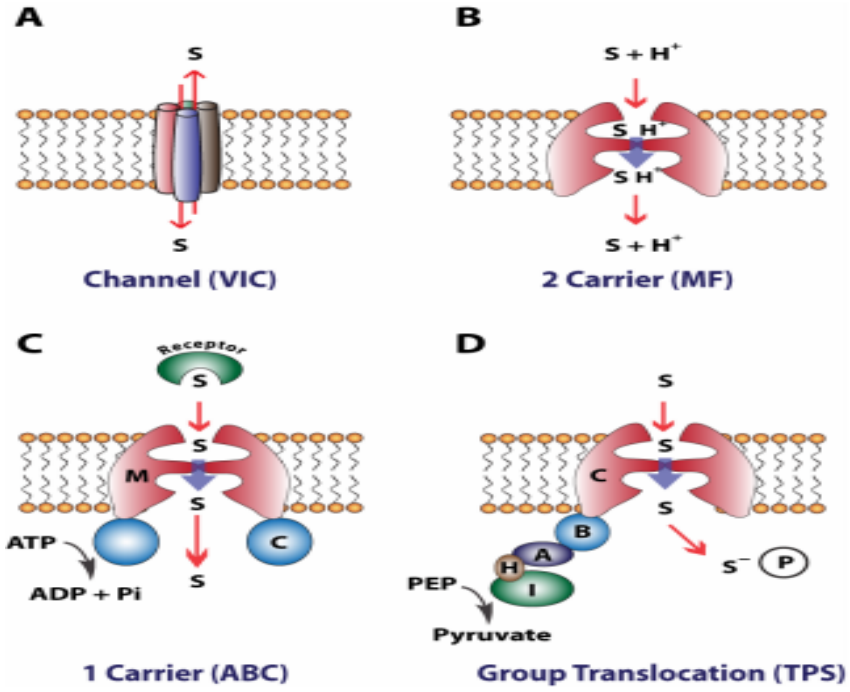

Figure 1.2. Types of transporters in biological systems. (A) Transporters like a channel which can help diffusion through a transmembrane channel. (B) Transporters like a carrier coupled to chemiosmotic energy which needs a carrier-mediated process to be able to transport the substrate. (C) Primary active transporters directed by pyrophosphate hydrolysis where the solute (S) is bump into the membrane channel (M) by a receptor. (D) Multidomain transporters, phosphoryl transfer-driven group translocators, PEP-dependent and they modify the transported species throughout the transport. (Saier et al., 2002).

Toxic chemicals induce cell injury through one of two general mechanisms (Kumar et al., 2005). In the first mechanism, some chemicals may act directly by combining with a critical molecular component or cellular organelle as in mercury chloride toxicity, mercury binds to the sulfhydryl groups of different cell membrane proteins causing inhibition of ATP-dependent transport and rise permeability of the membrane (Kumar et al., 2005). Cell damage may also induced by direct cytotoxic effects of many antineoplastic chemotherapeutic agents, and the biggest damage occurred with the cells that use, absorb, excrete or concentrate the compounds (Kumar et al., 2005). The second mechanism includes chemicals that first require conversion to reactive toxic

metabolites because as they are not biologically active and then these act on target cells (Kumar et al., 2005).

Many pollutants in the environment have been shown to apply toxic effects associated with oxidative stress and cause damage to membrane proteins (Gutteridge, 1995). For example, the physical interaction between ZnO and lipid membranes of E. coli induces leakage of pyridine through vesicle membranes (Zhang et al., 2010). In another study, C_{60} fullerenes have been found to down-regulate the expression of the PMP70 in the fathead minnow fish (*P. promelas*) (Oberdörster et al., 2006). There is therefore evidence that membrane components in fish may be susceptible to impact by selected NMs.

1.4.1.3 Mucosal inflammation

The vertebrate immune system consists of mucosal immune compartments (Esteban, 2012). According to the anatomical location, the mucosa-associated lymphoid tissue in teleost fish is subdivided into gut, skin, and gill associated lymphoid tissue (Esteban, 2012). Skin mucosa is the most important part of the fish immune system, serving as an anatomical and physiological barrier against external hazards (Esteban, 2012). Mucus secretion on the skin and gills of adult fish may trap NMs and get rid of it as a protective mechanism (Federici et al., 2007).

In mammals and fish, metals such as mercury can be taken up through adsorption via the gut mucosan or across the mucosal membrane into the cells (Foulkes, 2000). Once NMs enter the lymphatic system and capillaries they may then come into contact with the sub-mucosal tissue of mammals and reach other organs (Hoet et al., 2004). In a medical study, NMs that transferred through the human mucosal lining and epithelial barrier of the intestine quickly became associated with the GALT (gastroinstetinal associated lymphatic tissue) and circulatory system within an hour (Moghimi et al., 2001). With reference to fish, SWCNTs exposure in *O. mykiss* resulted in a dose-dependent increase in the ventilation rate, gill pathologies (such as oedema, altered mucocytes, hyperplasia), and mucus secretion (Smith et al., 2007).

The mucosal system is thus another potential cellular feature that may be impacted by NM exposure.

1.4.1.4 Epithelial cell damage

The innate immune response in fish is divided into the epithelial/mucosal barrier, the humoral response and the cellular response (Uribe et al., 2011). The most likely mechanism of gastrointestinal toxicity of metal poisoning in humans is damage to the epithelial cells, with resulting irritation (Saha et al., 1999). Human skin epithelial cells exposure to ZnO NMs showed severe cytotoxicity accompanied by oxidative stress and genotoxicity (Sharma et al., 2009). With regards to NMs, epithelial cells have been shown to be impacted in a number of species as follows. SWCNTs exposure results in a uniform thickening of epithelial cell numbers in *O. mykiss* (Smith et al., 2007). Epithelial cell injuries in the gill and the intestine has also been shown in *O. mykiss* following TiO_2 (Federici et al., 2007) and SWCNTs exposure (Smith et al., 2007). Silver NMs taken up into the gill cells of *O. mykiss* have also been observed to cause silver transport over cultured epithelial layers (Farkas et al., 2011). Other studies have tracked smaller NMs (in the range of 100-200 nm) and their apparent evasion of alveolar macrophage phagocytosis (Peters et al., 2006), demonstrating that they are capable of entering the pulmonary interstitial sites, and interacting with epithelial cells with ultimately access to the circulatory and lymphatic systems (Oberdörster et al., 2005a).

1.4.1.5 Immune response mechanisms

The immune system protects the host from foreign substances (Zolnik et al., 2010). The phagocytic cells of the immune system (such as macrophages) could interact with NMs and cause immunostimulation or immune suppression, which may increase inflammation or promote auto immune disorders (Zolnik et al., 2010). For instance, carbon nanotubes introduced into the abdominal cavity of mice have been observed to cause inflammation and the formation of lesions known as granulomas (Poland et al., 2008).

The fish immune system consists of a humoral and a cellular response plus organs tasked with immune defence (Jimeno, 2008). The most important immune competent

organs and tissue of fish include the kidney, thymus, spleen, liver, and mucosa-associated lymphoid tissues (Shoemarker et al., 2001). The aquatic environment surrounding fish may contain a variety of different contaminants such as pesticides, aromatic hydrocarbons, heavy metals and mycotoxins which are all capable of modulating the immune system, thus increasing the host susceptibility to infectious pathogens (Manning, 2010). *D. rerio* has been extensively used in biomedical research as a model, not only to study vertebrate development but also in the field of immunology (Novoa and Figueras, 2012). One component of the immune system is the stress proteins. Along with extrinsic chaperones, called HSPs, these are produced on exposure to stress (Welch, 1993). HSPs play many roles in relation to the immune system function (Roberts et al., 2010). In aquatic species, such as finfish and shrimp, HSPs play a major role in health and in the development of inflammation (Roberts et al., 2010).

Mucosal inflammation and epithelial cell damage have been mentioned above, yet there are other potential mechanisms of NM induced damage in other cells of the immune system (Table 1.2).

Table 1.2. Studies that investigate the mechanisms responsible for immunotoxicity after exposure to selected engineered NMs.

Engineered nanomaterial	Species	Concentration	Administration routes	Target immune cells	Immune effects	References
TiO_2	*Homo sapiens* and D*ark* Agouti rats (*Rattus rattus)*	For *H. sapiens*: 12 mg TiO_2/kg. For Dark Agouti rat: 1, 5, and 7.5 mg TiO_2 /kg. For 8 hr.	Oropharyngeal instillation	Neutrophils	Increase in numbers of neutrophils in BAL	(Gustafsson et al., 2011)
	Mice *(Mus musculus*)	2.5, 5, and 10 mg TiO_2/Kg for 90 days.	Intragastrical	Neutrophils	Decrease in numbers of neutrophils in the blood	(Sang et al., 2012)
	M. musculus	62.5, 125, and 250 mg TiO_2/Kg for 30 days.	Intragastrical	T cells	Decreased proliferation of both CD4+ and CD8+ T cells, as well as the ratio of CD4+ to CD8+ cells in the liver	(Duan et al., 2010)
	R. rattus	1, 5, and 7.5mg TiO2 /kg	Intratracheal	NK cells	Increase in numbers of NK	(Gustafsson

		at 1, 2, 8, 16, 30, and 90 days.	installation		cells in BAL as well as a transient increased expression of the NKR-P1A receptor on the NK cells	et al., 2011)
Carbon Nanotubes	*M. musculus*	50-100 µg/ml MWCNT at 24 h post treatment.	In vitro	Macrophages	MWCNTs induce COX-2 production through a MAPK-dependent mechanism and iNOS production through a MAPK-independent mechanism	(Lee et al., 2012)
	M. musculus	80 µg of SWCNT/mouse	In vitro	Macrophages	Coating of SWCNTs with SP-D enhanced the efficiency of their phagocytosis by murine RAW264.7 macrophage	(Kapralov et al., 2012)

1.5 *In vitro* toxicology research on nanomaterials

In vitro experiments are a rapid and inexpensive way to determine the potential toxicity of NMs (Oberdörster et al., 2005b). Such studies are conducted using parts of an isolated organism, such as individual tissues or cells. It allows a level of simplification by focusing on a small number of parts. In vitro studies also help address ethical issues raised by using whole animals. Approaches include using established cell lines and cells derived from target tissues to conduct nanotoxicological studies (Du et al., 2013). Using such approaches, the toxicity of carbon nanotubes on cells have consequently focused on cell apoptosis, toxic reactivity, ROS production, membrane perturbations and cell signalling (Hillegass et al., 2010). Studies have included a variety of cell lines. For example, human macrophage cell lines have been used to test carbon nanotubes toxicity. Impacts reported include inflammatory reactions, oxidative stress and cytotoxic response (Kagan et al., 2006). In addition, SWCNTs induced cytotoxicity in alveolar macrophages of the guinea pig (*Cavia porcellus*) with increasing dose of SWCNTs, and multi-walled carbon nanotubes (MWCNTs) also induced necrosis and degeneration in the alveolar macrophages of guinea pigs (Jia et al., 2005). When rat macrophages were exposed to MWCNTs, oxidative stress occurred by generating ROS (Pulskamp et al., 2007). In other studies, Cui and colleagues (2005) report that SWCNTs cause cell adhesion and cell proliferation in human embryonic kidney cells (Cui et al., 2005). MWCNTs can also cause toxic effects on human T cells in a concentration-dependent manner (Bottini et al., 2006). Additionally, refined SWCNTs toxicity on human fibroblast cells was found more toxic than that of unrefined counterparts (Tian et al., 2006).

In comparison, MWCNTs and oxidized MWCNTs have different effects on human T cells; oxidized MWCNTs cause more significant loss of cell viability via programmed cell death (Bottini et al., 2006). Moreover, mice lung cells have been exposed SWCNTs and reported lung fibroblast cell line lost the viability and was induced with DNA damage in a concentration and time dependent manner (Kisin et al., 2007). MWCNTs can also inhibit cell proliferation and cause cell death in human lung tumor cell lines (Simon-Deckers et al., 2008); and cause cytotoxic and genotoxic responses in Chinese hamster lung cells (Asakura et al., 2010). However, exposing

carcinoma A549 cells to high concentrations of SWCNTs led to inflammatory responses with oxidative stress and membrane damage (Choi et al., 2009). Thus, carbon nanotubes show toxicity in multiple mammalian cell lines.

Methods of nanotoxiclogical study may include comet assay and Ames test (bacterial reversion mutation test) to assess genotoxic potential of NMs. In 2011, Yu et al published a study on the impacts of geometry, porosity, and surface charge of SiO_2 on cellular toxicity and haemolytic activity. The haemolysis assay showed that the haemolytic activity was porosity and geometry dependent for bare SiO_2 and surface charge dependent for amine modified SiO_2 (Yu et al., 2011). The majority of the NMs tested *in vitro* and *in vivo* studies cause DNA strand breaks or oxidative DNA lesions (Karlsson, 2010). In addition, experiments were conducted to study the effects of carbon nanotubes using a variety of bacteria. For example, the ciliated protozoan *Tetrahymena thermophile* has been widely studied because of its role in the regulation of microbial populations by ingestion and digestion of bacteria and most importantly because it is an important organism in wastewater treatment and an indicator of sewage effluent quality (Dayeh et al., 2005). SWCNTs are also able to move up the food chain and impact the ingestion and digestion of bacteria by ciliated protozoa (Ghafari et al., 2008). The effect of SWCNTs on the developmental stages of biofilms has also been studied using *E.coli* as a model organism; the results show that SWCNTs induced toxic effects in the development of *E.coli* biofilm (Rodrigues and Elimelech, 2010). Another study demonstrated that contact with SWCNTs aggregates can cause cell membrane damage, leading to bacterial cell death (Kang et al., 2007).

Another factor affecting the impacts of SWCNTs on bacterial cytotoxicity are the different surface functionalization of SWCNTs. For example, the highly compact and narrowly distributed aggregate size of functionalized SWCNTs can reduce bacterial cytotoxicity (Pasquini et al., 2012). On the other hand, *Scenedesmus quadricauda* and *E. coli* show mechanical damage to the cell wall and membrane resulting in carbon nanotube cytotoxicity (Amarnath et al., 2012). Other NMs such as nano SiO_2, ZnO, Cu and Fe have varying toxic impacts in bacteria (Safekordi et al., 2012). For instance, *Vibrio fischeri* showed the highest toxicity to nano ZnO compared to SiO_2NPs (Safekordi et al., 2012).

1.6 *In vivo* toxicology research on nanomaterials

In vivo experiments use a whole, living organism as opposed to a cells or tissues, have also been used to investigate the effects of carbon nanotubes (and this is summarised in Table 1). Compared with *in vitro* methods, whole animal testing is relatively expensive and time-costly (European Commission, 2005). Yet, *in vivo* methods are used to determine toxicity of carbon nanotubes within a whole biological system, which is more complex than *in vitro* systems (Du et al., 2013). The first *in vivo* experiment exposure was conducted using rodents in 2001 and showed no measurable inflammations in the bronchoalveolar space following carbon nanotubes exposure (Huczko et al., 2001). In contrast, SWCNTs caused lung inflammatory response in mice (Lam et al., 2004). Carbon nanotubes can also cause inflammatory responses by dermal toxicity that increase dermal cell number, localized alopecia and thickened skin (Koyama et al., 2009). Inhalation of SWCNTs can cause inflammation and form granulomas in mice (Shvedova et al., 2005). On the other hand, some unpurified SWCNTs, when exposed to rabbits do not trigger skin irritation or allergic reactions (Huczko et al., 2001). Respiratory exposure to carbon nanotubes caused a series of lung toxicities as inflammation, lung injury and early signs of tumur formation (Muller et al., 2006). Inhalation of MWCNTs can cause histocytic and neutrophilic inflammation in Wister rats (Ma-Hock et al., 2009). A high dose of MWCNTs can lead to damage upper respiratory tract and lymph nodes (Pauluhn, 2010). Whereas the high dose SWCNTs caused 15% mortality of rats by instillation and the effect was dose independent (Warheit et al., 2004). Early whole organism exposure experiments therefore produced many, sometimes contrasting or contradictory, biological effects responses.

1.7 Use of *D. rerio* in toxicology

D. rerio has become widely recognized model laboratory animal for developmental, transgenic and toxicological studies due to many features. These include, low maintenance costs, low space requirements, rapid generation cycle (egg to mature adult in 2-3 months), rapid development (egg to hatching in 2-3 days), and large number of offspring, the embryos are well suited for experimental manipulation and microinjection, and the embryos are translucent (Lele and Krone, 1996). There are thus

an abundance of *in vivo* studies using rodents that can be used to predict biological effects in other organisms provided the organs tissues and exposure regime are similar, yet they do not represent aquatic organisms. The availability of the *D. rerio* genome has also enabled the design of a whole genome DNA microarray, which promotes *D. rerio* as a model for vertebrate in gene expression investigations (Hill et al., 2005), though is only available to those who can afford such methods.

Many types of toxicity studies have been conducted using *D. rerio* such as acute, chronic and subchronic toxicity studies. Toxicity studies using *D. rerio* included cardiotoxicity, carcinogenicity, endocrine disruption, reproductive, developmental, acute, neurotoxicity, neurobehavioral, vascular, and ocular toxicities (Hill et al., 2005). Following decades of use in developmental biology applications, *D. rerio* is recently increasingly utilized for testing of embryonic development, including measurements of differential regulation of gene expression, embryonic axis, formation of the peripheral and central nervous systems, cell lineage analysis, and determination muscle development (Lele and Krone, 1996). The advantages of the *D. rerio* system are the effects of both short and long-term exposure to a wide range of toxic compounds including carcinogenic agents that can be conducted with relative ease. *D. rerio* embryos have been proposed to serve as an economically feasible, medium throughput screening platform for assessment of NP toxicity (Bar-Ilan et al., 2009). *D. rerio* toxicity assays offer different compelling experimental advantages, such as the transparency of embryo and larva, easy manipulation, high throughput, low cost, small amount of compound required, short test period and direct compound delivery (Lieschke and Currie, 2007; McGrath and Li, 2008).

1.8 Summary

The toxicity of NMs and their specific biological effects separated from other classes of chemical contaminants found in the environment have not been fully characterised to date. A range of biological impacts have been observed in mammals such as respiratory damage, membrane interactions, immune system and general necrosis or cytotoxicity impacts. For fish there is less information available and observed impacts generally include embryo developmental abnormalities, gill damage and respiratory stress, oxidative stress indicators, oedema (swelling), mucosal changes and

osmoregulatory damage (all summarised in Table 1). All of these NM-induced impacts occur at the organism level of organisation and ideally a biomarker of biological effect would be available to detect changes at an earlier point before such impacts are observed.

Aims of the study

The increasing levels of NPs in the aquatic environment may lead to biological impacts in aquatic organisms. Of the investigations conducted to date, the most frequently reported mechanisms of manufactured NM toxicity in vertebrates have been oxidative stress, mucosal inflammation and epithelial cell irritation. Yet there may be other, as yet uncharacterised mechanisms of NP induced damage. Therefore, an investigation of the molecular level impacts, following exposure to specific NPs, may provide information about the mechanisms of action of toxicants. Therefore, the aims of this study are:

1. To identify, isolate and characterise possible early warning biological effects markers of NPs exposure in fish. The biological markers have been selected based on previous studies involving exposure fish to NPs reported in the literature.
2. To develop a quantitative qPCR-based assay using the candidate biomarkers characterised in Aim no.1
3. To utilise NP-injected *D. rerio* embryos to determine a profile of differentially expressed genes that respond to NP exposure. This will involve two methodological approaches: (a) employing the targeted genes isolated in Aim 1 and quantitative method developed in Aim 2, to investigate selected mRNA transcript, and (b) a global approach employing the Suppression Subtractive Hybridization (SSH) approach to identify novel genes not already identified in the scientific literature.
4. To expose *D. rerio* embryos to TiO_2NPs coated with different number of layers of anionic and cationic polyelectrolytes via an aqueous route upon illumination with visible light compared with that in dark conditions to measure cell viability, morphology and determine different expressed genes that respond to

the NPs exposure by employing the targeted genes isolated in Aim 1 and quantitative method developed in Aim 2.

The main hypothesis of this study is that: *D. rerio* embryos will show differential, and characteristic, mRNA transcript profiles following controlled experimental exposure to AgNPs and TiO_2NPs relative to control fish.

2. Chapter two: isolation and characterisation of nanoparticle-induced candidate genes

2.1 Introduction

As described in Chapter 1, NM usage is increasing (section 1.1.2) and this is possibly leading to an increase of their levels in the environment (section 1.2), including aquatic systems (section 1.3). According to the literature review, the precise toxicity of NMs and the biological effects have not been fully characterised to date. A range of biological impacts have been observed in animals such as oxidative stress (section 1.4.1), oedema (section 1.4.1.3), mucosal changes (section 1.4.1.3) and membrane interactions (section 1.4). All these NM-induced impacts occur at the organism level of organisation. Ideally, it would be desirable to detect such impacts earlier at the molecular level and then use such knowledge to design and validate biomarkers of biological effect before harmful impacts are observed.

The aim of this chapter was to isolate potential NM-induced genes from *D. rerio* based on the findings of literature review. In a gene targeting approach, degenerate primers based on the conserved domains of candidate genes available in closely related species were exploited to find such key genes. The candidate genes were selected according to the biological effects reported in the literature (see Table 1.1) and consideration of the potential toxicity mechanisms that may be occurring within the organism. The candidate genes selected were: *SOD*, *PMP*, *ATPase*, *HIF-1*, *HSP.2*, *junction plakoglobin*, *Muc*, and *Cat*. Once these candidate genes have been isolated it allows the development of a quantitative assay to measure changes in their mRNA transcript on exposure to NMs (described in Chapter 3).

2.2 Materials and Methods

2.2.1 Chemicals and characterization of AgNPs

Both AgNPs and $AgNO_3$ exposure media were prepared by Dr Jinping Cheng's research laboratory staff (in City University Hong Kong) and all *D. rerio* embryos were exposed to these media in the same laboratory. These samples were then shipped to the University of Hull for analyses as part of these PhD studies.

Powder form AgNPs were purchased from Suzhou ColdStones Technology Co., Ltd. (Suzhou, China). AgNPs had an approximate diameter of 4 nm, designated as S4 and coated with 10-13% fatty acid (oleic acid). Characterization of AgNPs was performed by TEM (Xin et al., 2015). AgNPs were dispersed in deionized water and sonicated at 40kHz for 20 min and a small drop of the suspension was placed on copper grids and air-dried at room temperature for TEM imaging. The z-average hydrodynamic diameter of AgNPs in a solution culture medium was determined by dynamic light scattering (DLS) using a Malvern Zetasizer Nano-ZS (Malvern Instruments Ltd, Malvern, UK). A crystalline powder silver nitrate $AgNO_3$ (CAS 7761-88-8) was purchased from Sigma-Aldrich (St. Louis, MO, USA), 99% purity (Xin et al., 2015).

2.2.2 Fish and exposure protocols

As described in the previous section, *D. rerio* tissue and embryos were supplied by Dr. Jinping Cheng (Co-supervisor) under ethical protocols at her own university (City University Hong Kong) and shipped to University of Hull. Healthy adult *D. rerio* tissues were dissected from skin, liver, and gill organs. In addition, healthy *D. rerio* embryos at 4 hours post-fertilization (hpf) were selected, washed with deionized water and transferred into 24-well cell culture plates containing 2 ml of control or test media per well at 28^{o}C. The dispersed AgNPs (4 nm) were prepared at 1.925 mg Ag/L, and silver ion alone at 0.018 mg/L. The exposure lasted from 4 to 96 hpf, and the samples were collected at 96 hpf.

2.2.3 Total RNA isolation and purification from *D. rerio* embryos and adults tissue

Total RNA was extracted from the tissue using the protocol and reagents supplied by Roche (Roche Diagnostics GmbH, Mannheim, Germany). For homogenization of the tissues, 400 µl of Lysis buffer [4.5 M guanidine-HCl, 100 mM sodium phosphate pH 6.6 (25^{o}C)] and approximately 20 mg of tissue were used. The adult tissue was homogenized using a rotor-stator homogenizer (Perkin Elmer, Massachusetts, USA) while the embryo tissues were homogenized using a plastic pestle. Lysate was then centrifuged for 2 min at maximum speed (13,000 x *g*) in a microcentrifuge and the supernatant used for subsequent steps. Approximately 200 µl of absolute ethanol was added to the lysate supernatant and mixed well. The 700 µl collection tube was

combined with high pure filter tube, the entire sample was pipetted into the upper reservoir and centrifuged at maximal speed (13,000 x *g*) for 30 sec in a microcentrifuge. The flow-through liquid was discarded after the filter tube was removed from the collection tube. In a new sterile 1.5 ml reaction tube, 90 µl DNase incubation buffer [1 M NaCl, 20 mM Tris-HCl, 10 mM $MnCl_2$, pH 7.0 (25^{o}C)] was pipetted and 10 µl DNase I working solution lyophilizate (10 kU DNase I) for digesting residual contaminating DNA was added for each isolate and mixed well. The solution was then pipetted to the upper reservoir of a new filter tube and incubated for 15 min at room temperature. Up to 500 µl wash buffer I [5 M guanidine-HCl, 20 mM Tris-HCl, pH 6.6 (25^{o}C), 20 ml absolute ethanol] was added to the upper reservoir of the filter tube and centrifuged at 8,000 x *g* for 15 sec. The filter tube was removed from the collection tube and the flow-through liquid was discarded. The filter tubes were combined with the used collection tube. A 500 µl wash buffer II [20 mM NaCl, 2 mM Tris-HCl, pH 7.5 (25^{o}C), 40 ml absolute ethanol] was added to the upper reservoir of the filter tube and centrifuged at 8,000 x g for 15 sec and the flow-through was discarded again. The filter tube was combined with the used collection tube. A further 300 µl of wash buffer II was added to the upper reservoir of the filter tube and centrifuged at full speed (approx 13,000 x *g*) for 2 min to remove residual ethanol. The column was removed and inserted into a nuclease free, sterile 1.5 ml microcentrifuge tube. 100 µl of elution buffer was added to the upper reservoir of the filter tube and centrifuged twice for 1 min at 8,000 x *g*. Then the microcentrifuge tube contains the eluted RNA and stored at -80^{o}C for later analysis.

2.2.4 Quantification and quality of RNA

To assess the integrity of total RNA, an aliquot of the RNA samples were analysed on a denaturing agarose gel. Each gel contained 1% agarose (Fisher Scientific, Loughborough, U.K.) in 1x gel running buffer (100 ml 10x FA gel running buffer, 20 ml 37% (12.3 M) formaldehyde, and 880 ml RNase-free water) and RNase-free water. All reagents were heated to melt the agarose and cooled to approximately 65^{o}C. Next, 1.8 ml of 37% (12.3 M) formaldehyde and 1.8 µl (10 mg/ml) ethidium bromide (Invitrogen™, Waltham, Massachusetts, USA) was added and the gel left to set. The gel was placed in a gel electrophoresis tank contain 1% FA gel running buffer for 30 min.

The gel was run at 90V for approximately 45 min and was analysed under a UV-transilluminator (Maker, Sebastopol, USA).

2.2.5 First strand synthesis of cDNA for the Polymerase Chain Reaction (PCR)

cDNA was prepared using SuperScript VILO cDNA Synthesis reagents and protocol (Life Technologies, Paisley, U.K.). In a 0.2 ml tube, the following reagents were added: 4 µl of 5X VILO™ Reaction Mix (includes random primers, $MgCl_2$, and dNTPs in a buffer formulation] 2 µl of 10X Superscript Enzyme Mix (includes SuperScript® III RT, RNaseOUT™ Recombinant Ribonuclease Inhibitor, and a proprietary helper protein) and 100 ng of RNA. All reagents were put in PCR tubes and reactions carried out using a TC-4000 Thermal Cycler (Techne, Cambridge, U.K.) equipped with a heated lid. All reactions were initially started at 25°C for 10 min, and then 60 min at 42°C followed by final step of 5 min at 85°C, ending with a holding step at 4°C. To degrade any remaining RNA in each sample, the following reagents were added later: 0.5 µl (5 units) of RNase H (which is an *E. coli* strain that carries the cloned RNase H gene (rnh) from *Escherichia coli* supplied in 100 mM KCl, 20 mM Tris-HCl (pH 7.5), 10 mM $MgCl_2$, 0.1 mM EDTA, 0.1 mM dithiothreitol and 50% glycerol) and 2 µl of 10X RNase H Reaction Buffer (includes 75 mM KCl, 50 mM Tris-HCl, 3 mM $MgCl_2$, 10 mM $MgCl_2$ in pH 8.3 at 25°C). All reagents were added into the previous PCR tubes and incubated at 37°C for 45 min and then stored at -20°C.

2.2.6 Oligonucleotide primer design

To design the oligonucleotide primers, an appropriate *D. rerio* gene nucleotide sequence was taken in FASTA format from GenBank (http://www.ncbi.nlm.nih.gov/genbank/) and blasted in order to find homologous sequences using the BLAST facility (http://www.ncbi.nlm.nih.gov/blast/). The nucleotide sequences were then aligned using a multiple sequence alignment program, Clustal Omega (http://www.ebi.ac.uk/Tools/msa/clustalo/) and the regions with greatest homology, indicating a possible conserved region, and highest GC content were used for the optimal primer design using the website (http://www.bioinformatics.nl/primer3plus). The primers used are shown in Table 2.1.

Table 2.1. Primer pairs used for the isolation of candidate and reference genes from *D. rerio*.

Gene name	Abbreviation	GenBank accession no.	Forward and reverse primers (5'-3')	Product length
18S small subunit ribosomal RNA (18S rRNA)	*18S.1*	FJ915075.1	F: TAGAGGGACAAGTGGCGTTC R: CCTCGTTGATGGGAAACAGT	195 bp
	18S.2		F: AGTTCCGACCGTAAACGATG R: GAGGTTTCCCGTGTTGAGTC	196 bp
Class I Beta tubulin (TUBB)	*BT.2*	AF528096.1	F: TGCTGAACGTCCAGAACAAG R: GCTCGGAGATACGCTTGAAC	162 bp
Elongation factor 1 alpha (Eef1a111)	*EF.1*	NM_131263.1	F: GATGCACCACGAGTCTCTGA R: TGATGACCTGAGCGTTGAAG	158 bp
	EF.2		F: TGGGTGTTGGACAAACTGAA R: AGCAACAATCAGCACAGCAC	180 bp

Superoxide dismutase 2, mitochondrial. (iron/manganese superoxide dismutase family) (SOD2)	*SOD2.1*	NM_199976.1	F: AGCGTGACTTTGGCTCATTT R: ATGAGACCTGTGGTCCCTTG	166 bp
	SOD2.2		F: AAGCGTGACTTTGGCTCATT R: ATGAGACCTGTGGTCCCTTG	167 bp
ATP-binding cassette, sub-family D (ALD), member 3a (68 kDa peroxisomal membrane protein) (abcd3a)	*ATP.1*	XM_005162843	F: GTATGTTGTTGCGGATGTCG R: AGGCACCAGTGTGAGCTTTT	194 bp
ATPase, H+ transporting , lysosomal, VI subunit C, isoform 1a (atp6v1c1a)	*ATPase.1*	NM_201322.1	F: GAACCTGCTGGCTAATGGAG R: GATGCTCGAGCTTTCAGGTC	156 bp
Hypoxia inducible factor 1 alpha-like protein (hif1al2)	*HIF.4*	AY835381.1	F: AGACTGCCACGGAAAAGCTA R: CCAGAGGCAGAAGAGCAGTT	161 bp
Heat shock protein. Crystalline, alpha A (CRYAA)	*CRYaa*	NM_152950.2	F: CCTGCACACTGTCTGCTGAT R: CCCACTCACACCTCCATACC	177 bp

Heat shock protein, alpha-crystallin-related, Mrna (hspb15)	*HSP.2*	NM_001098732.1	F: ACAAGCTTCCGGCTGACTTA R: GCAGGTAACCGTTTGTCCAT	154 bp
Catalase (Cat)	*Cat.1*	AF170069.1	F: GCGGATACCAGAGAGAGTCG R: ATCTGATGACCCAGCCTCAC	172 bp
Junction plakoglobin (Juba)	*Jupa.4*	NM_131177.1	F: GTCCTGTCCAACCTCACCTG R: CGTAATGCATTCGTACGGCG	202 bp
Mucin 2, oligomeric mucus/gel-forming, partial mRNA (Muc2)	*Muc2.1* *Muc2.2*	XM_002667544.3	F: TGGGATCGCAAAACCACTGT R: GTTGTGCATCAGGGCAAGTG F: CACCTGTGTTTCTCTCGCCT R: GCAAACACAGTGTTCGTCCC	187 bp 199 bp
Peroxisomal membrane protein 2, mRNA (pxmp2)	*Pxmp2.4*	NM_001004607.1	F: AGTTACTGGCCTGCGATGAA R: CACTGCAGTAAGGCACAACC	157 bp

2.2.7 Amplification of DNA by PCR

All the reactions were carefully prepared using DNAse/RNAse free-sterile disposable plastic tubes in order to avoid contamination. All reagents were aliquoted upon arrival and stored as such to prevent degradation by repetitive thawing/freezing cycles. Oligonucleotide primers employed in the reaction were synthesized by Integrated DNA Technologies (IDT, Leuven, Belgium) and supplied in a lyophilised form. Primers were resuspended in molecular grade deionised water to a concentration of 100 µM.

The standard PCRs were conducted using reagents supplied by Fisher (Fisher Scientific, Loughborough, U.K.). Reactions were carried out in a final volume of 25 µl consisting of (0.5 µl) 10 mM dNTPs, 5 µl amplification buffer (deoxynucleotide mix of ultrapure dATP, dCTP, dGTP, and dTTP), 0.5 µl of 0.5-4.5 mM $MgCl_2$, 0.5 µl of 1.5 µM for each sense and antisense primers and 0.25 µl (1.25 units) of Herculase II fusion DNA polymerase (Agilent Technologies, Santa Clara, U.S.A.).

Amplifications were carried out using TC-4000 Thermal Cycler (Techne, Staffordshire, U.K.) equipped with a heated lid. All reactions were initially denatured at 94^{o}C for 30 sec then 30 sec at 94^{o}C denaturation, 30 sec at 50/55/60^{o}C annealing and 30 sec at 72^{o}C elongation step. The last three steps were repeated 35 times followed by final extension step of 2 min at 72^{o}C. Positive and negative controls were set up alongside each set of PCR reactions. Negative controls consisted of all components of the PCR reaction excluding the template DNA, while the positive control was for the abundantly expressed *EF.1* gene, which was already available for *D. rerio*. Each amplification was optimized in order to create the right conditions for the amplification of the targeted fragment. The oligonucleotide primers, thermal cycling strategy of denaturation, annealing and extension were accordingly varied until PCR products of the correct size were obtained (Fig. 2.2).

2.2.8 Agarose gel electrophoresis of DNA

The PCR products were separated and visualised by agarose gel electrophoresis. Each gel contained 1% agarose (Fisher Scientific, Loughborough, U.K.) in TBE buffer (Tris base, boric acid, and EDTA)(Fisher Scientific, Loughborough, UK) and 1 µl gel stain SYBR Safe DNA gel stain (Life Technologies, Paisley, U.K.). The gel was placed in a gel

electrophoresis tank and the comb removed. Prior to loading on the gel, 10 µl of the sample was mixed with 2 µl loading dye (New England Biolabs, U.K.). To be able to determine the size of the of the DNA fragments a 100 bp DNA Ladder (New England Biolabs, U.K.) diluted 1/20 was loaded in a well next to the samples. The gel was run at 70V for approximately one hour and was analysed under UV- transilluminator (Maker, Sebastopol, USA).

2.2.9 Isolation of DNA fragments from agarose gel slices

Gel areas containing a DNA fragment of the correct size were excised on a UV transilluminator with a scalpel. The gel slices were purified with the NucleoSpin® Gel and PCR Clean-up reagents and protocol supplied by the manufacturer (Macherey Nagel, Düren, Germany). After the weight of the gel slice was determined, an appropriate amount of NTI buffer (contains guanidinium thiocyanate 30–60 %) was added as per the manufacturer's instructions. The gel was dissolved for 5-10 min at 50°C and vortexed every 2-3 min. Next, the melted gel was placed into a collection tube (2 ml) and centrifuged for 30 sec at 11,000 x g. The flow-through was discarded and 700 µl of ethanolic NT3 buffer was added and centrifuged for 30 sec at 11,000 x g. The flow-through was discarded and the washing step was repeated again. In order to remove NT3 buffer completely, the column was centrifuged for 1 min at 11,000 x g and then placed in a clean 1.5 ml microcentrifuge tube. Finally, 30 µl of elution buffer NE (5 mM Tris/HCl at pH 8.5) was added and incubated at room temperature for 1 min, then centrifuged for 1 min at 11,000 x g. The samples were stored at -20°C until further processing.

2.2.10 Quantification of DNA

The DNA concentration of the samples was measured with a Qubit-iT™ (Invitrogen™, Paisley, U.K.). First the Qubit® fluorometer was calibrated using two standard solutions made by preparing master mix of working solution containing 200 µl of dsDNA BR buffer and 1 µl dye (dsDNA BR reagent *200x concentrate in DMSO) per tube. The first standard solution required 190 µl of the working solution master mix and 10 µl of standard 1 (stored in fridge), and the second standard required 190 µl of the working solution master mix and 10 µl of standard 1 (stored in fridge). The DNA concentrations in the samples were measured by mixing 199 µl of the working solution and 1 µl of PCR

product sample. Each tube was allowed to incubate at room temperature for 2 min before taking the reading.

To calculate the DNA concentration of each sample from Qubit® fluorometer reading, the following equation was used:

Concentration of sample = QF value x 200/x

Where:

QF value= the value given by the Qubit® fluorometer

X= the number of microliters of sample added to the assay tube

2.2.11 Sequencing

The DNA concentration of the samples was measured with the QubitTM fluorometer (Invitrogen Detection Technologies) to obtain the desired amount of sample needed for sequencing. Together with the forward primer, a sample with a total volume of 10 µl (containing 50-100 ng DNA, 0.25 µl of 1.5 µM forward primer,) was sent to the commercial sequencing company Macrogen (Amsterdam, Netherlands).

2.3 Results

2.3.1. RNA isolation

Typical RNA isolations from gill and skin tissue yielded approximately 20 ng/µl, liver tissue ~30 ng/µl, while RNA isolations from embryos yielded ~20 ng/µl of total RNA.

2.3.2 Quantification and quality of RNA

To assess the quality of total RNA, an aliquot of selected RNA samples were analysed on a denaturing agarose gel (Fig. 2.1). Intact total RNA showed clear 28S and 18S rRNA bands where the 28S rRNA band had approximately twice as intense as the 18S rRNA band, confirming the integrity of the RNA prepared.

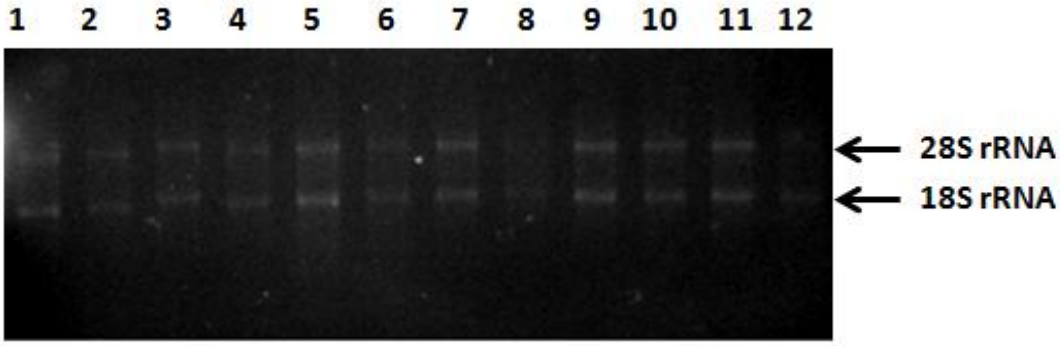

Figure 2.1. Ethidium bromide stained 1% agarose gel displaying total RNA samples from *D. rerio* embryos using an aliquot of the RNA samples as follows: 1-6 (untreated control samples), and 7-12 (1.925 mg Ag/L of 4 nm Ag (96 hpf)).

2.3.2 Candidate gene amplification using *D. rerio* cDNA template

Several amplifications were conducted in order to isolate the candidate genes for *SOD2.1*, *SOD2.2*, *ATP.1*, *ATPase.1*, *HIF.4*, *CRYaa*, *HSP.2*, *Cat.1*, *Jupa.4*, *Muc2.1*, *Muc2.2*, and *Pxmp2.4* from *D. rerio* using the optimal annealing temperature in PCR (Table 2.2).

Table 2.2. The successful primer pairs and optimised annealing temperature used in PCR for each of the targeted genes.

Gene name	Forward and reverse primers (5'-3')	Annealing temperature (°C)
SOD2.1	F: AGCGTGACTTTGGCTCATTT R: ATGAGACCTGTGGTCCCTTG	60
SOD2.2	F: AAGCGTGACTTTGGCTCATT R: ATGAGACCTGTGGTCCCTTG	60
ATP.1	F: GTATGTTGTTGCGGATGTCG R: AGGCACCAGTGTGAGCTTTT	60
ATPase.1	F: GAACCTGCTGGCTAATGGAG	55

	R: GATGCTCGAGCTTTCAGGTC	
HIF.4	F: AGACTGCCACGGAAAAGCTA R: CCAGAGGCAGAAGAGCAGTT	50
CRYaa	F: CCTGCACACTGTCTGCTGAT R: CCCACTCACACCTCCATACC	60
HSP.2	F: ACAAGCTTCCGGCTGACTTA R: GCAGGTAACCGTTTGTCCAT	47
Cat.1	F: GCGGATACCAGAGAGAGTCG R: ATCTGATGACCCAGCCTCAC	60
Jupa.4	F: GTCCTGTCCAACCTCACCTG R: CGTAATGCATTCGTACGGCG	60
Muc2.1	F: TGGGATCGCAAAACCACTGT R: GTTGTGCATCAGGGCAAGTG	60
Muc2.2	F: CACCTGTGTTTCTCTCGCCT R: GCAAACACAGTGTTCGTCCC	60
Pxmp2.4	F: AGTTACTGGCCTGCGATGAA R: CACTGCAGTAAGGCACAACC	60

For each target gene, the PCR amplifications were optimised to eventually yield one product of the correct size as shown in Figure 2.2.

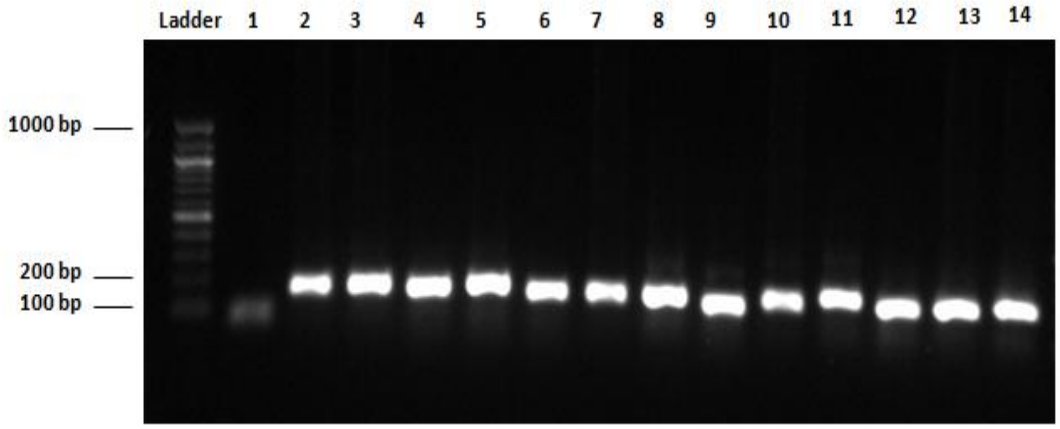

Figure 2.2. A 1% agarose gel, stained with gel red dye, displaying PCR amplification products from *D. rerio* embryos/tissues using various primer pairs. Lane 1: -ve control, lane 2: +ve control (*EF.1*), lane 3: *SOD2.1*, lane 4: *SOD2.2*, lane 5: *ATP.1*, lane 6: *ATPase.1*, lane 7: *HIF.4*, lane 8: *CRYaa*, lane 9: *HSP.2*, lane 10: *Cat.1*, lane 11: *Jupa.4*, lane 12: *Muc2.1*, lane 13: *Muc2.2*, lane 14: *Pxmp2.4*.

2.3.5 Sequencing the DNA fragments

The sequencing results showed high identity between the isolated fragments obtained using the *D. rerio* tissues and the candidate genes of other species, confirming their identity. The following figures show the alignment of the deduced amino acid sequence of each *D. rerio* candidate gene with a selection of other species, the sequence motifs in the gray boxes represent the conserved domains within each sequence (Fig. 2.3 - 2.12).

Copper/zinc *SOD* domain

```
O.mordax        MVLKAVCVLKGTGEVTGTVFFEQEGDNGPVKLTGEISGLTPGEHGFHVHAFGDNTNGCIS
D.rerio         MVNKAVCVLKGTGEVTGTVYFNQEGEKKPVKVTGEITGLTPGKHGFHVHAFGDNTNGCIS
C.idella        MVNKAVCVLKGDGQVTGTVYFEQEGEKSPVTLSGEITGLTAGKHGFHVHAFGDNTNGCIS
H.molitrix      MVNKAVCVLKGDGQVTGTVYFEQEAEKSPVKLSGEITGLTAGKHGFHVHAFGDNTNGCIS
                 ** ******** *:*****:*:**.:: **.::***:****:*****************

O.mordax        AGPHFNPHSKTHGGPTDDVRHVGDLGNVTAGQDNVAKISIQDKHLTLNGVHSIIGRTMVI
D.rerio         AGPHFNPHDKTHGGPTDSVRHVGDLGNVTADASGVAKIEIEDAMLTLSGQHSIIGRTMVI
C.idella        AGPHFNPYSKNHGGPTDSERHVGDLGNVIAGENGVAKIDIVDKMLTLSGPDSIIGRTMVI
H.molitrix      AGPHFNPYSKNHGGPTDSERHVGDLGNVTAGENGVAKIDIVDKMLTLSGPDSIIGRTMVI
               *******:.*.******. ********* *  . ****.* *  ***.* .*********

O.mordax          HEKADDLGKGGNEESLKTGNAGGRLACGVIGITQ
D.rerio           HEKEDDLGKGGNEESLKTGNAGGRLACGVIGITQ
```

```
C.idella          HEKEDDLGKGGNEESLKTGNAGGRLACGVIGITQ
H.molitrix        HEKEDDLGKGNNEESLKTGNAGGRLACGVIGIAQ
                  *** ****** **********************:*
```

Figure 2.3. Multiple sequence alignment of the *SOD2.1* deduced amino acid sequence of *D. rerio* with *Ctenopharyngodon idella, Hypophthalmichthys molitrix,* and *Osmerus mordax*. Asterisks marks denote homology.

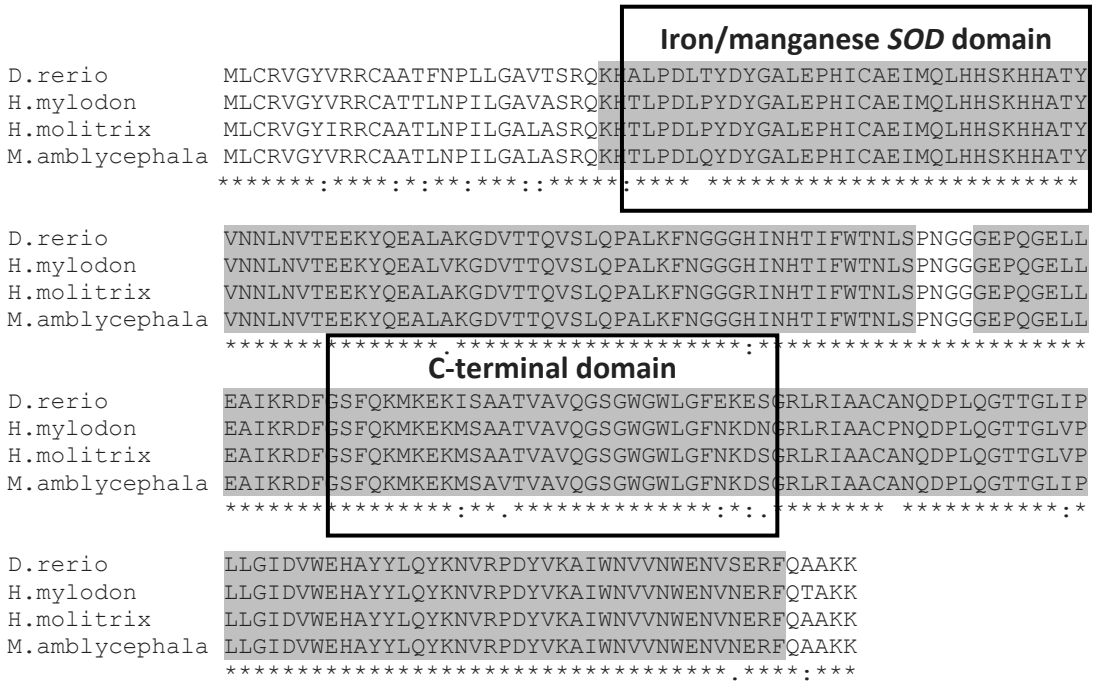

Figure 2.4. Multiple sequence alignment of the *SOD2.2* deduced amino acid sequence of *D. rerio* with *Hemibarbus mylodon, H. molitrix,* and *Megalobrama amblycephala*. Asterisks marks denote homology.

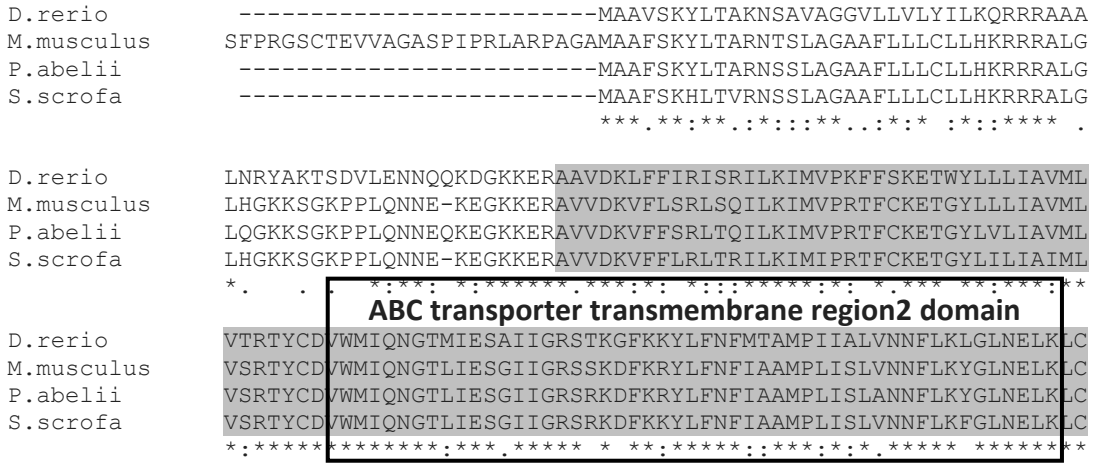

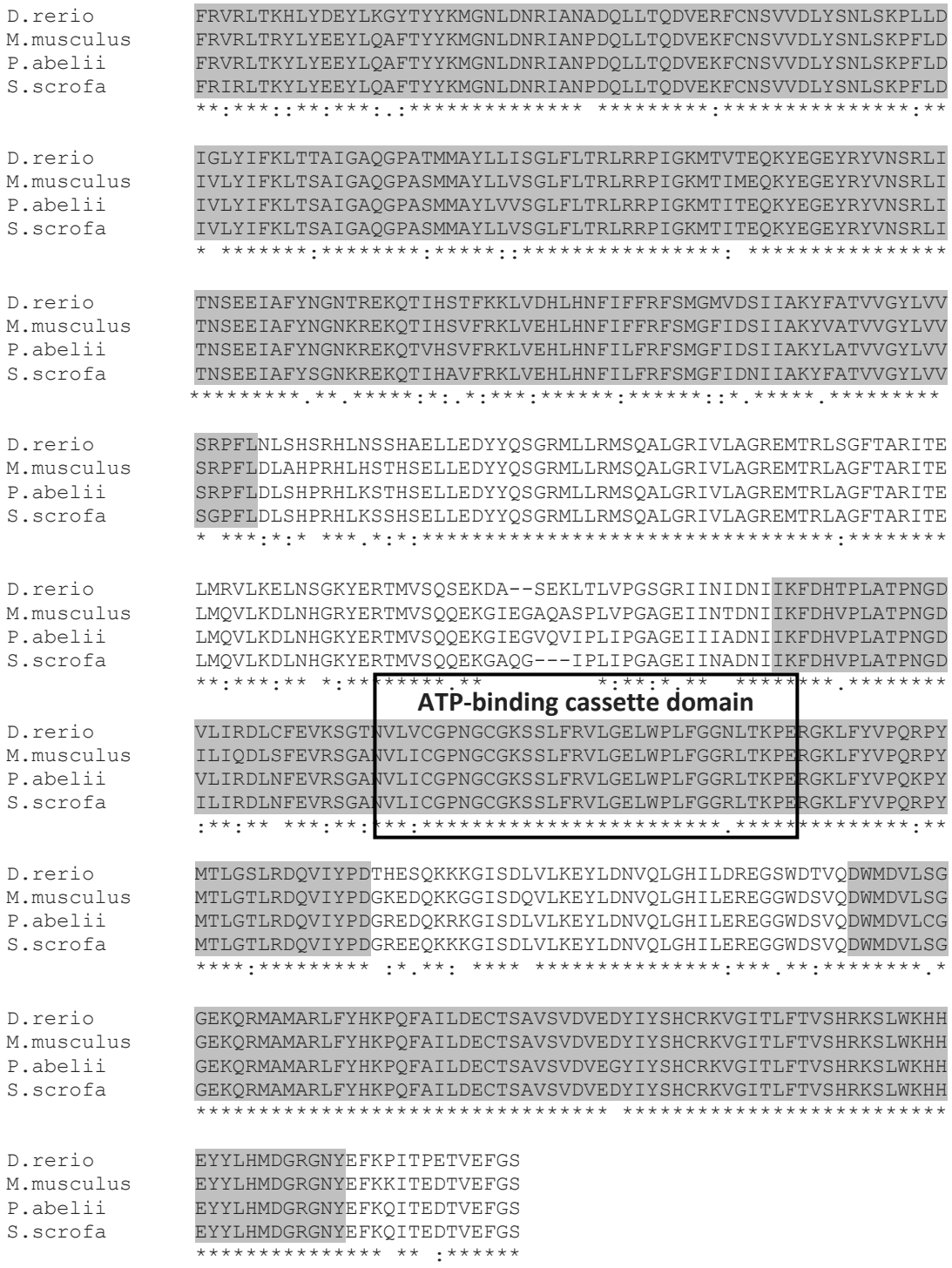

Figure 2.5. Multiple sequence alignment of the *ATP.1* deduced amino acid sequence of *D. rerio* with *Pongo abelii, M. musculus,* and *Sus scrofa.* Asterisks marks denote homology.

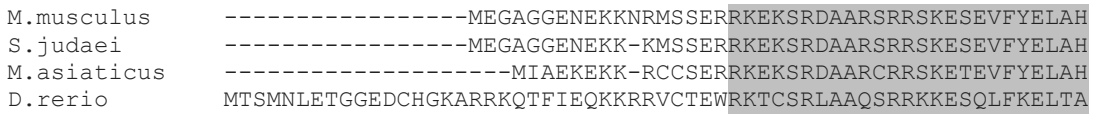

```
                                        ::** : .:* **  ** **:.**.**:::* **:

M.musculus      QLPLPHNVSSHLDKASVMRLTISYLRVRKLLDAGGLDSED-----EMKAQMDCFYLKALD
S.judaei        QLPLPHNVSSHLDKASVMRLTISYLRVRKLLDAGDLDIED-----EMKAQMNCFYLKALD
M.asiaticus     QLPLPQSISSHLDKASIMRLAISFLHTRKLLTSDCVTATETT---EVDRLMDTWYVKSLG
D.rerio         LLPLDLSMDGQRDKASVIRLTIAYLHLRGLLDTTDSLMKRPSPGVSDKSHERELLDSALG
                 ***  .:..: ****::**:*::*: * ** :            . .        .:*.

M.musculus      GFVMVLTDDGDMVYISDNVNKYMGLTQFELTGHSVFDFTHPCDHEEMREMLTHRNGPVRK
S.judaei        GFVMVLTDDGDMIYISDNVNKYMGLTQFELTGHSVFDFTHPCDHEEMREMLTHRNGPVKE
M.asiaticus     GFITVVTSDGDMIFLSENINKFMGLAQVELTGHSIFDFTHPCDHEEIRENLSFKTGMGKK
D.rerio         GFVVLLSLNGKVIFATKGLTTHTGINQMDLIGRSLLEFLHPCDQMEVKDILTRLIG----
                **: ::: :*.::: :..:... *: *.:* *:*:::* ****: *::: *:   *

M.musculus      GKELNTQRSFFLRMKCTLTSRGRTMNIKSATWKVLHCTGHIHVYDTNSNQPQCGYKKPPM
S.judaei        GKEQNTQRSFFLRMKCTLTSRGRTMNIKSATWKVLHCTGRIHVYDTNSNQPQCGYKKPPM
M.asiaticus     VKDLNTERDFFMRMKCTVTNRGRTVNLKSASWKVLHCTGQLKVYNGCPAHVLCGFKEPPL
D.rerio         -NQEPQKCEVFLRIK-------KAMNTKLTGWKIIQCSGKKRSSAT-----------PGS
                 ::   : ..*:*:*       :::* * : **:::*:*: :               *

M.musculus      TCLVLIC--EPIPHPSNIEIPLDSKTFLSRHSLDMKFSYCDERITELMGYEPEELLGRSI
S.judaei        TCLVLIC--EPIPHPSNIEIPLDSKTFLSRHSLDMKFSYCDERITELMGYEPEELLGRSI
M.asiaticus     TCVVMMC--EPIPHPSNIDTPLDSKTFLSRHSMDMKFTYCDDRVTELMGYNPEDLLGRSA
D.rerio         SCLVLECRVLPIQEITEVDEALNACTFMSVHSPDMTFTYCHSRVVKLIGFRDTDLLGQSV
                :*:*: *   ** . :::: .*:: **:* ** **.*:**..*:.:*:*:.  :***:*

M.musculus      YEYYHALDSDHLTKTHHDMFTKGQVTTGQYRMLAKRGGYVWVETQATVIYNTKNSQPQCI
S.judaei        YEYYHALDSDHLTKTHHDMFTKGQVTTGQYRMLAKRGGYVWVETQATVIYNTKNSQPQCI
M.asiaticus     YEFYHALDSDSVTKSHQNLCTKGQAVSGQYRMLAKHGGYVWVETQGTVIYNSRNSQPQCI
D.rerio         YQYYHPSDCQQIRKAHICLLSKGQVSTGKYRLLHRYGGYVWAETDASLVCNSQTGVPESV
                *::**. *.: : *:*  : :***. :*:**:* : *****.**:.::: *::.. *:.:

M.musculus      VCVNYVVSGIIQHDLIFSLQQTESVLKPVESSDMKMTQLFTKVESEDTSCLFDKLKKEPD
S.judaei        VCVNYVVSGIIQHDLIFSLQQTECVLKPVESSDMKMTQLFTKVESEDTSCLFDKLKKEPD
M.asiaticus     VCVNYVLSDIEEKSIIFSLDQTESLLKPQHLS-----SFFSPSKGLDSEELYNKLKEEPE
D.rerio         VCINYILSEVEQPNLPFLLEKTEQLLKPTSSS--------------------YCPETEPA
                **:**::* : : .: * *::** :***   *                     : **

M.musculus      ALTLLAPAAGDTIISLDFGSDDTETEDQQLEDVPLYNDVMFPSSN---------------
S.judaei        ALTMLAPAAGDTIISLDFGSDDTETEDQQLEDVPLYNDVMFPSSDDKLTSINLAMSPLPA
M.asiaticus     DLTQLAPTPGDTFISLNFGRPQYEEHPGYSEVSSIAPSVSHTIHDGHKPNYAADMPRMAS
D.rerio         PFPPSRGQEGEKDLKESNEHNSFITHLKQRDGDIQEVECTEIPHN---------------
                 :.      *:. :. .    .   .    :      .      :
```

Figure 2.6. Multiple sequence alignment of the *HIF.4* deduced amino acid sequence of *D. rerio* with *M. musculus, Myxocyprinus asiaticus, and Spalax judaei*. Asterisks marks denote homology.

```
                                Alpha crystalline A chain, N terminal domain
D.rerio         MDIAIQHPWFRRTLG--YPTRLFDQFFGEGLFDYDLFPFTTSTVSPYYRHSLFRNILDSS
P.notatus       MDIAIQHPWFKRNMG--YPTRLFDQFFGEGLFDYDLFPFAPSTISPYYRHSLFRNFLDSS
C.variegatus    MDIAIQHPWFRRALGSTYPARLFDQFFGEGIFDYDLFPITT-TISPYYRHSLFRNLLDSS
N.angustata     MEISIQHPWFRRAMGSVYPARLFDQFFGEGMFDYDFFPYTTSSISPYYRQSLFRSFLDSS
                *:*:*******:* :*  **:**********:****:** :. ::*****:*****.:****

D.rerio         NSGVSEVRSDREKFTVYLDVKHFSPDELSVKVTDDYVEIQGKHGERQDDHGYISREFHRR
P.notatus       NSGISEVRSDRDKFTVYLDVKHFSPEELNVKVTDDYVEIEGKHAERQDDHGYISREFHRR
C.variegatus    NSGISEVRSDRDKFTVYLDVKHFSPDELSVKVTDDYVEIQGKHGERQDDHGYISREFHRR
N.angustata     NSGTSEVRSDRDKYTLYLDVKHFSPEEISVKVTGDYVEIQGKHGERQDDHGYISREFHRR
                *** *******:*:*:*********:*:.****.*****:***.****************

D.rerio         YRLPSNVDQSAITCTLSADGLLTLCGPKTSG-IDAGRGDRTIPVTREDKSNSGSSS
```

```
P.notatus       YRLPSNVDQSAIHCSLTADGLLTLCGPKTGG-IDAGRGDRTIPVTREDKTNSGSSS
C.variegatus    YRLPSAVDQSAITCTLSADGLLTLTGPKVSGGSESGRGDRSIPVTRDDKTSAAPSS
N.angustata     YRLPSSVDQSAISCSLSADGLLTLSGPKVNGGTESGRSERSIPVTRDEKTNSAVSS
                ***** ****** *:*:******* ***..*  ::**.:*:*****::*:.:. **
```

Figure 2.7. Multiple sequence alignment of the *CRYaa* deduced amino acid sequence of *D. rerio* with *Pimephales notatus*, *Cyprinodon variegates*, and *Notothenia angustata*. Asterisks marks denote homology.

```
I.furcatus      MTERRIPFTFLRTPSWDPFRDWYQGSRIFDQAFGMPAVPEEMHVFPSTHWPGYMRPSIGA
O.niloticus     MAERRIPFTLLRTPSWDPFRDWHQSSRIFDQTFGMPALPEDIAAFPSTHWPGYLRPSI--
D.rerio         MAERRIPFSFMRTPSWDPFRDWYQGSRLLDQSFGMPALSEEMLTFPSTHWPGYMRPFGHP
C.auratus       MAERRIPFTFMHGQSWDPFRDWSQGSRLFDQTFGMPHFSEEMPTFPSTHWPGYFRPYGFP
                *:******::::  ******** *.**::**:**** ..*:: .*********:**
                                                     Alpha crystalline domain
I.furcatus      DMASLMHSAQVPPLTMPTPIVPHPAAYARALSRQLSTGLSEIKQTQDGWKVSLDVNHFAP
O.niloticus     -LAPELMTPHAP-LMYPTHMMAQ-QAQARALSRQLSSGISEIKQTQDSWKVSLDVNHFSP
D.rerio         DFAALMQGP----PVMPP---MMTPSYGRALSRQLSSGMSEVKQTGDSWKISLDVNHFSP
C.auratus       EMASLMQSPVAQMPMSPPASMMHPPTYSRALSRQMSSGMSEIKQTPDSWKISLDVNHFAP
                 :*. :  .       *.       : .******:*:*:**:*** *.**:*******:*

I.furcatus      EELTVKTKDGVVEITGKHEERKDEHGVISRSFTRKYTLPPGADAEKITSSLSPEGILTVE
O.niloticus     EELVVKTKDGVVEISGKHEERKDEHGFVSRSFTRKYTLPPSADVEKVNSALSPEGVLTVE
D.rerio         EELNVKTKDGVLEITGKHEERKDEHGFISRCFTRKYTLPPGVDSEKISSCLSPEGVLTVE
C.auratus       EELMVKTKDGVVEITGKHEERKDEHGFVSRCFTRKYTLPSGVDSEKITSSLSPEGVLTIE
                *** *******:**:***********.:**.********...* **:.*.*****:**:*

I.furcatus      APLPKPAIQSSEITIPVNTSS--SVVQKQDGAK
O.niloticus     APLIKPAIEHSETTIPVNVESKGGVVKK-----
D.rerio         APLPKPAIQAPEVNIPVNK---TTVSTTK----
C.auratus       ATLPKPAIQGPEVNIPINTGSAVTASSTKKP--
                *.* ****: .* .**:*      .  .
```

Figure 2.8. Multiple sequence alignment of the *HSP.2* deduced amino acid sequence of *D. rerio* with *Oreochromis niloticus*, *C. auratus*, and *Ictalurus furcatus*. Asterisks marks denote homology.

```
D.rerio         MADDREKSTDQMKLWKEGRGSQRPDVLTTGAGVPIGDKLNAMTAGPRGPLLVQDVVFTDE
C.idella        -MADREKATDQMKLWKEGRGSQRPDVLTTGAGVPVGDKLNLLTAGPRGPLLVQDVVFTDE
M.amblycephala -MADREKATDQMKLWKQGRGSQRPDVLTTGAGVPVGDKLNSMTAGPRGPLLVQDVVFTDE
H.molitrix      -MADREKATDQMKLWKESRGSQRPDVLTTGAGVPVGDKLNSMTAGPRGPLLVQDVVFTDE
                   ****:********:.***************:***** :******************

D.rerio         MAHFDRERIPERVVHAKGAGAFGYFEVTHDITRYSKAKVFEHVGKTTPIAVRFSTVAGEA
C.idella        MAHFDRERIPERVVHAKGAGAFGYFEVTHDITRYCKAKVFEHVGKTTPIAVRFSTVAGES
M.amblycephala MAHFDRERIPERVVHAKGAGAFGYFEVTHDITRYCKAKVFEHVGKTTPIAVRFSTVAGES
H.molitrix      MAHFDRERIPERVVHAKGAGAFGYFEVTHDITRYCKAKVFEHVGKTTPIAVRFSTVAGES
                **********************************.************************:

D.rerio         GSSDTVRDPRGFAVKFYTDEGNWDLTGNNTPIFFIRDTLLFPSFIHSQKRNPQTHLKDPD
C.idella        GSADTVRDPRGFAVKFYTDEGNWDLTGNNTPIFFIRDALLFPSFIHSQKRNPQTHLKDPD
M.amblycephala GSADTVRDPRGFAVKFYTDEGNWDLTGNNTPIFFIRDALLFPSFIHSQKRNPQTHLKDPD
H.molitrix      GSADTVRDPRGFAVKFYTDEGNWDLTGNNTPIFFIRDALLFPSFIHSQKRNPQTHLKDPD
                **:**********************************:**********************
```

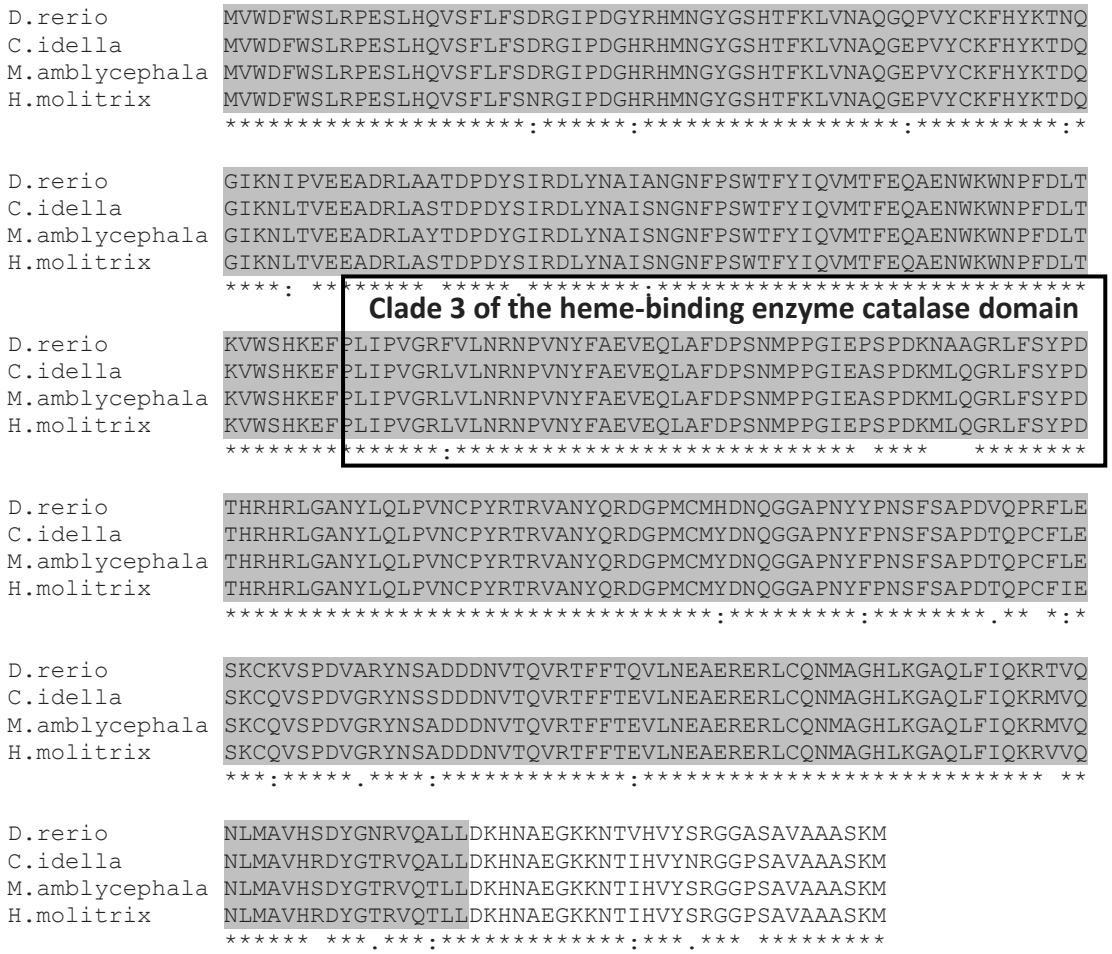

Figure 2.9. Multiple sequence alignment of the *Cat.1* deduced amino acid sequence of *D. rerio* with *M. amblycephala, H. molitrix,* and *C. idella*. Asterisks marks denote homology.

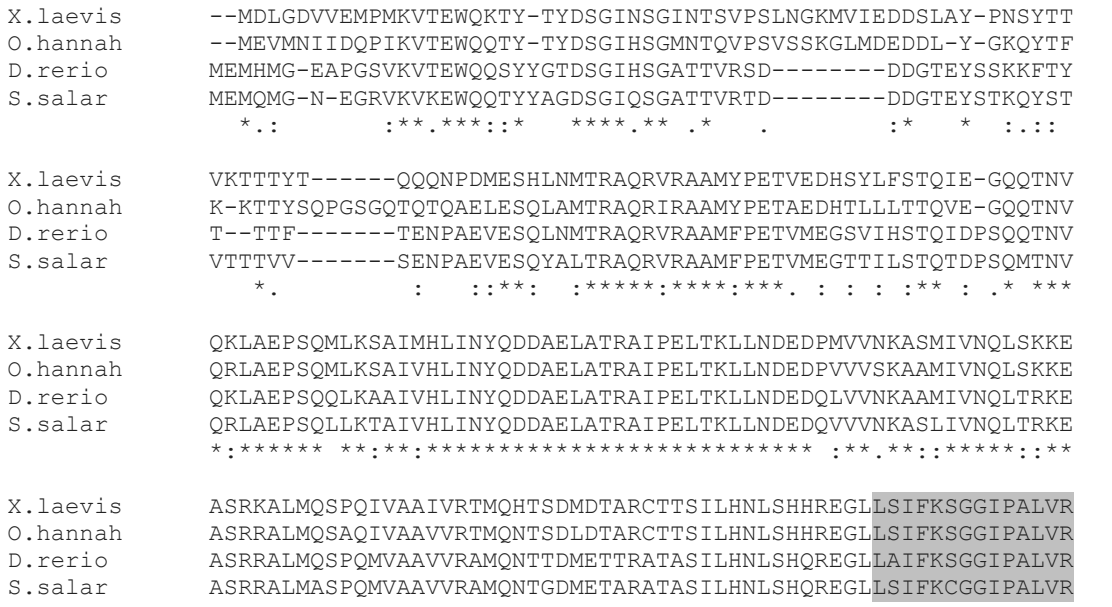

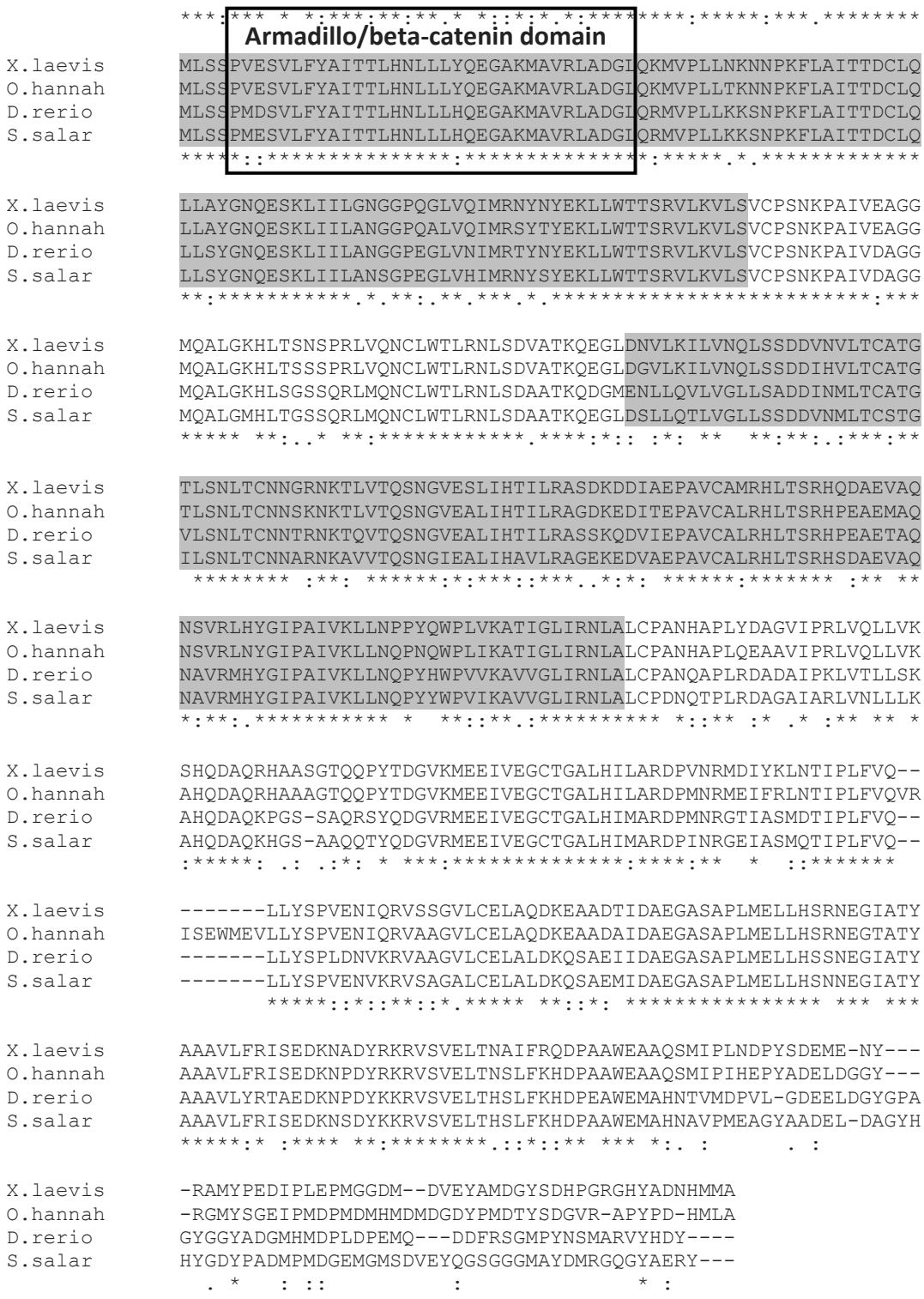

Figure 2.10. Multiple sequence alignment of the *Jupa.4* deduced amino acid sequence of *D. rerio* with *Salmo salar, Xenopus laevis,* and *Ophiophagus hannah*. Asterisks marks denote homology.

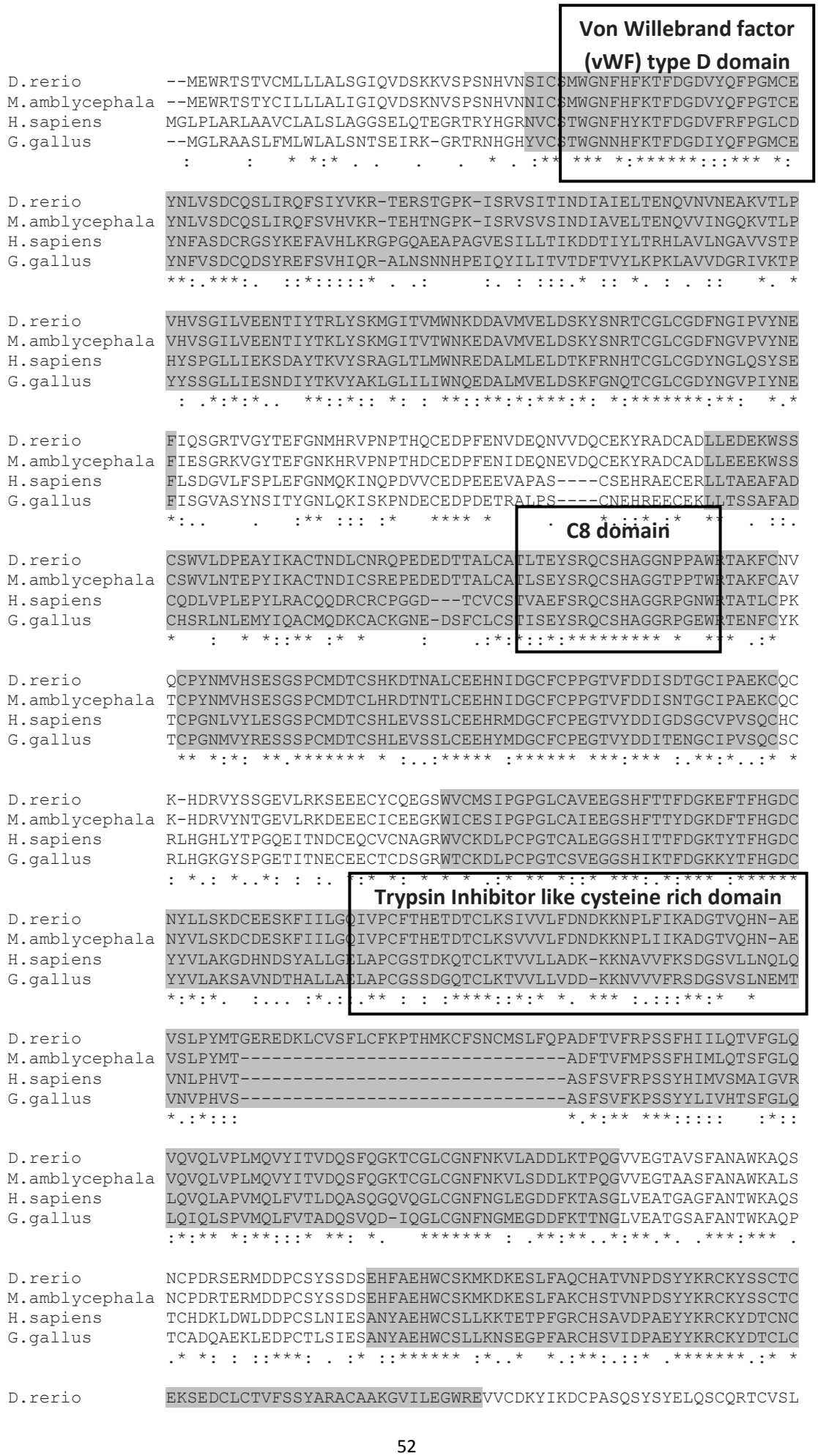
Von Willebrand factor (vWF) type D domain
C8 domain
Trypsin Inhibitor like cysteine rich domain

```
M.amblycephala EKSEDCLCTVFSSYARACAAKGIFLQGWRDIVCEKYTENCPASQKYSYQLQSCQRTCLSL
H.sapiens      QNNEDCLCAALSSYARACTAKGVMLWGWREHVCNKDVGSCPNSQVFLYNLTTCQQTCRSL
G.gallus       KDNEECLCAALSSYSRACAFKGIILGGWRQSVCSDEVSACPGNQVFLYNLTMCQQTCRSI
               :..*:***:.:***:***: **::* ***: **..    ** .* : *:*  **:** *:

D.rerio        ASERQSCNVDFVPVDGCACPDGLYQDENNLCVPMEKCPCYHNGQKIHPGKSLTIRDEHCV
M.amblycephala ASERQSCSIHFVPVDGCACPEGLYQDEN--------------------------------
H.sapiens      SEADSHCLEGFAPVDGCGCPDHTFLDEKGRCVPLAKCSCYHRGLYLEAGDVVVRQEERCV
G.gallus       ADGEKYCLQDFAPVDGCGCPDNTYLDNQDTCVPISKCPCYYKGSYLEPGEYVTKDGERCV
                    :.  . *   *.*****.**:  : *::
```

Figure 2.11. Multiple sequence alignment of the *Muc2.2* deduced amino acid sequence of *D. rerio with M. amblycephala, H. sapiens, and Gallus gallus*. Asterisks marks denote homology.

```
R.norvegicus   MAPAASRLRVESELRSLPKRALAQYLLFLKFYPVVTKAVSSGILSALGNLLAQMIEKKQ-
H.sapiens      MAPAASRLRAEAGLGALPRRALAQYLLFLRLYPVLTKAATSGILSALGNFLAQMIEKKR-
D.rerio        MPTQSVLVR-DPSLLAR---ALQQYLSLLKKYPIITKSVTSGILSALGNLLSQVLEYQKN
X.laevis       MPVASKPVPGSAPLHTV---LLLRYLQLLHSRPVLTKALTSAILSALGNILSQTIQKWR-
               *.  :  :  .. * :     * :** :*:  *::**: :*.*******:*:* ::  :

R.norvegicus   --KKD-SRSLEVSGLLRYLVYGLFVTGPLSHYLYLFMEYWVPPEVPWARVKRLLLDRLFF
H.sapiens      --KKENSRSLDVGGPLRYAVYGFFFTGPLSHFFYFFMEHWIPPEVPLAGLRRLLLDRLVF
D.rerio        VKENSPKKKISILGPVHFAIYGLFITGPVSHYFYHLLEVLLPTTVPYCLIKRLLLERLIF
X.laevis       -KEQKAPQNVDLRGPFRFAVYGLLFTGPLSHYFYLLLEQLVPSSAPLAGLQRLLIERLMI
                 ::.  :.:: * .. .**:: ***:**:.* ::*  :*  .*  .::***::**.:

               22-kDa peroxisomal membrane protein domain

R.norvegicus   APTFLLLFFFVMNLLEGKNISVFVAKMRSGFWPALQMNWRMWTPLQFININYVPLQFRVL
H.sapiens      APAFLMLFFLIMNFLEGKDASAFAAKMRGGFWPALRMNWRVWTPLQFININYVPLKFRVL
D.rerio        APAFLLLFYVVMNALEGKTLADVQNKLKTSYWPAMKMNWKVWTPFQFININYVPVQFRVL
X.laevis       APAFLLLFFLVMNLLEGKNLAKLNKKLKDHYWSALKLNWKVWTPFQFININYIPVQFRVL
               **:**:**:. ** **** : .  *::  :*.*:::**::***:*******:*::****

R.norvegicus   FANMAALFWYAYLASLGK
H.sapiens      FANLAALFWYAYLASLGK
D.rerio        FANMVALFWYAYLASVRK
X.laevis       FANLVAFFWYAYLASTRN
               ***:.*:********  :
```

Figure 2.12. Multiple sequence alignment of the *Pxmp2.4* deduced amino acid sequence of *D. rerio* with *H. sapiens, Rattus norvegicus,* and *X. laevis*. Asterisks marks denote homology.

2.4 Discussion

The aim of this chapter was to isolate and characterize the candidate genes for *SOD2.1*, *SOD2.2*, *ATP.1*, *HIF.4*, *CRYaa*, *Cat.1*, *Jupa.4*, *Muc2.2*, and *Pxmp2.4* from *D. rerio*. The deduced amino acid sequences of each of these genes showed a high level of sequence similarity to those for other species available in GenBank. Each shall be discussed in turn.

The SOD enzyme is involved in antioxidant defence system produced by cells to protect biomolelcules from oxidative stress. The *D. rerio SOD2.1* cDNA sequence amplified, encodes a putative 154 amino acid protein (**NP_571369.1**); that shares 86% similarity with *C. idella, H. molitrix,* and *O. mordax* (Fig. 2.3). The *SOD2.1* has a conserved domain (copper/zinc superoxide dismutase (*SOD*)) that catalyses the conversion of superoxide radicals to molecular oxygen (Maier et al., 2002). While *SOD2.2* amplified a fragment that encodes a putative 224 amino acid protein (**NM_199976.1**) which shares 93% similarity with *H. mylodon* , 94% similarity with *H. molitrix*, and 95% similarity with *M. amblycephala* (Fig. 2.4). The *SOD2.2* has two conserved domains, alpha-hairpin domain and iron/manganese superoxide dismutase, and c-terminal domain that catalyse the conversion of superoxide radicals to H_2O_2 and molecular oxygen (Maier et al., 2002). These are highlighted on the *D. rerio* sequence (Fig. 2.4).

The *ATP.1* amplified product encodes a putative 658 amino acid protein (**NM_213482.1**) which shares 81% similarity with *P. abeli*, *M. musculus*, and *S. scrofa* (Fig. 2.5). The *ATP.1* has two putative conserved domains: the first is an ABC transporter transmembrane region2. The mutations in this domain in human PMP70 are believed responsible for Zellweger Syndrome 2 (Gärtner et al., 1992). The second domain is an ATP-binding cassette domain of peroxisomal transporter; subfamily D. It shows a gap from 526-565 (Fig. 2.5). It is involved in the import of very long chain fatty acids (VLCFA) into the peroxisomes (Morita and Imanaka, 2012).

The *HIF.4* primers amplified a fragment encoding a putative 663 amino acid protein (**XM_005161350.2**) which shares 83% similarity with *M. musculus,* and *S. judaei*, and 35% similarity with *M. asiaticus* (Fig. 2.6). The deduced *HIF.4* has multiple putative conserved domains, helix-loop-helix domain found in specific DNA-binding proteins that work as transcription factors (Murre et al., 1994), and other PAS domains that have been found to sense oxygen, redox potential, light, and other motifs in signal transduction (Taylor and Zhulin, 1999).

The *CRYaa* primers amplified a fragment encoding a putative 173 amino acid protein (**AY035778.1**) which shares 90% similarity with *P. notatus*, 86% similarity with

C. variegates, and 77% similarity with *N. angustata* (Fig. 2.7). The *CRYaa* has one putative conserved domain (Alpha crystalline A chain, N terminal) which has the ability to increase cellular tolerance to stress (Augusteyn, 2004).

The *HSP.2* was amplified to generate a fragment that encoded a putative 199 amino acid protein (**BC097148.1**) which shares 70% similarity with *O. niloticus*, 78% similarity with *C. auratus*, and 72% similarity with *I. furcatus* (Fig. 2.8). The *HSP.2* has a putative conserved domain, Alpha crystalline domain (ACD), which has different functions such as, protection from oxidative stress through modulating GSH levels (Dubińska-Magiera et al., 2014).

The *Cat.1* fragment consisted of a 526 amino acid sequence (**NM_130912.1**) that showed 93% similarity with *M. amblycephala and C. idella*, and 92% similarity with *H. molitrix* (Fig. 2.9). The *Cat.1* deduced sequence has a putative conserved domain (clade 3 of the heme-binding enzyme catalase), which protects cells from the toxic effects of peroxides (Carpena et al., 2003). It catalyses the conversion of H_2O_2 to water and molecular oxygen, it also utilizes H_2O_2 to oxidise different substrates such as alcohol or phenols (Zámocký and Koller, 1999).

The *Jupa.4* primers amplified a fragment encoding a putative 729 amino acid protein (**NM_131177.**1) that shares 84% similarity with *S. salar* and 74% similarity with *X. laevis* and *O. hannah* (Fig. 2.10). The *Jupa.4* deduced sequence has two putative conserved domains of Armadillo/beta-catenin-like repeats which have a structural role in cell junctions and participate in Wnt signalling (Martin et al., 2009).

The *Muc2.2* amplified a product encoding a putative 1,548 amino acid protein (**XM_009303625.1**) which shares 82% similarity with *M. amblycephala*, 46% similarity with *H. sapiens* and *G. gallus* (Fig. 2.11). The *Muc2.2* deduced sequence has multiple putative conserved domains including a von Willebrand factor (vWF) type D domain, a C8 domain that is found in disease-related proteins (Mucin), and a trypsin inhibitor-like cysteine rich domain (Zhou et al., 2012).

Finally, the *Pxmp2.4* amplified a putative 194 amino acid protein (**NM_001004607.1**) which shares 59% similarity with *R. norvegicus*, 64% similarity with

X. laevis, and 56% similarity with *H. sapiens* (Fig. 2.12). The *Pxmp2.4* deduced sequence has a putative conserved domain, the 22-kDa peroxisomal membrane protein (PMP22), that is involved in pore forming activity and may lead to unspecific permeability of the organelle membrane (Brosius et al., 2002).

In summary, this chapter focused on the isolation and characterization of *SOD2.1*, *SOD2.2*, *ATP.1, HIF.4, CRYaa, HSP.2, Cat.1, Jupa.4, Muc2.2,* and *Pxmp2.4* from *D. rerio* and the designed primers were optimized for the expression analysis with the polymerase chain reaction (qPCR). The sequences will be subsequently used to develop assays of mRNA expression to examine their role in response to NMs which will be examined in the following chapter.

3. Chapter Three: Quantitative PCR method development and validation for the quantification of candidate genes expression in *D. rerio* embryos

3.1 Introduction

As discussed in Chapter 1, there are many ways to measure the biological effects of pollutants in the environment which can be at the molecular level or as high as the ecosystem level (section 1.4.1). The molecular level has the advantage that changes are found early before organisms die or population's crash (Robinson et al., 2000). Of the molecular techniques available, combining reverse transcription with the PCR is a powerful method to quantify mRNA transcript, the earliest response that can be measured (Murphy et al., 1990). qPCR is widely used in this respect (Wong and Medrano, 2005). It can distinguish between mRNAs with similar sequences and requires less amount of RNA template comparing to other methods of mRNA transcript analysis (Wong and Medrano, 2005).

The *D. rerio* embryos have shown to be suitable for the testing of NMs toxicity (Powers et al., 2011; Bilberg et al., 2012; Xin et al., 2015). For instance, the embryos are well suited for experimental manipulation and microinjection, and the embryos are translucent (Lele and Krone, 1996). The genotoxicity and developmental toxicity are viewable through the transparent embryo during development, and the complete genome sequence is also available (Hill et al., 2005). It is also convenient in time as it have been proposed to serve as an economically feasible, medium throughput screening platform for assessment of NP toxicity (Bar-Ilan et al., 2009). The qPCR method has, for example, been used to investigate the molecular responses to acidification in the gills and body of *D. rerio* (Tiedke et al., 2013). It has also been used to analyze the expression of genes related to toxicological response to xenobiotics in the the liver and gills of *O. mykiss* (Scown et al., 2010).

The aim of this chapter was to develop and validate an qPCR based assay for each of the candidate genes (*SOD2.1, SOD2.2, ATP.1, ATPase.1, HIF.4, CRYaa, HSP.2, Cat.1, Jupa.4, Muc2.1, Muc2.2,* and *Pxmp2.4*) isolated and described previously in Chapter 2, and the subsequent use for the expression analysis of early *D. rerio*

embryos (up to 96 hpf) that have been experimentally exposed to AgNPs and silver ions alone.

3.2 Materials and Methods

3.2.1 *D. rerio* embryos

All *D. rerio* embryos were collected and processed as described in section 2.2.2 and were kindly supplied by Dr Jinping Cheng. Twenty embryos that had been exposed to 1.925 mg Ag/L of 4 nm AgNPs were used as the exposed treatment group. Another 20 healthy embryos were used as a control reference group. In parallel, 20 embryos that had been exposed to 0.018 mg/L of silver ion alone were used as the metal ion alone exposed treatment group and another 20 healthy embryos were used as a second control reference group.

3.2.2 Total RNA isolation

The total RNA extraction from *D. rerio* embryos was carried out following the protocol described in section 2.2.2 and stored at -80^{o}C until further processing.

3.2.3 First strand synthesis of cDNA for qPCR

cDNA was synthesized using 100 ng RNA following the protocol described in section 2.2.5 and stored at -20^{o}C.

3.2.4 Oligonucleotide primer design

Target gene specific *primers for SOD2.1, SOD2.2, ATP.1, ATPase.1, HIF.4, HSP.2, Cat.1, Jupa.4, Muc2.2,* and *Pxmp2.4* genes, along with three potential reference genes (*18S.1/2, BT.2, EF1/2*) were designed following the protocol described in section 2.2.6.

3.2.5 Primer optimization

To examine the efficiency of the target templates, qPCR assays were optimized by evaluating different primer pair concentrations. To do that, five concentrations with equimolar amounts of each primer were tested: 100 nM, 200 nM, 300 nM, 400 nM, and 500 nM. An equal amount of 100 ng of template was used in all samples in the optimization experiments. All samples were run in duplicate. The best primer pair should yield the lowest average Ct value as well as presenting a dissociation curve that

shows a single product. The Ct or threshold cycle is the cycle number at which an amplification plot crosses the threshold fluorescence level.

3.2.6 Assay performance

To test the efficiency, accuracy, and sensitivity of the qPCR reaction, a standard curve was performed using a serial dilution of template starting with 1:10, 1:4, and 1:2 diluted cDNA. To obtain the standard curve, the Ct values of each dilution were plotted against the cDNA dilution.

3.2.7 Evaluating reference mRNA transcript

Transcription profiling was performed using qPCR assays with three candidate reference genes (*18S.1/2, BT.2,* and *EF.1/2*) and tested across untreated (controls, n=10) and treated (consisted of 1.925 mg Ag/L of 4 nm Ag, n=10) embryo samples to establish their stability. All genes were analyzed by direct comparison of their Ct and qPCR reactions were performed with equal quantity of cDNA template. Raw Ct data were analyzed to evaluate and screen each reference genes stability and then rank the best candidate. The method used different commercial computational programs (geNorm, Normfinder, BestKeeper, and the comparative Ct method). This approach uses the ranking from each program, specifying a suitable weight for each reference gene and calculates the geometric mean of their weights for the overall final ranking (http://www.leonxie.com/referencegene.php?type=reference).

3.2.8 Amplification using qPCR

The qPCRs were carried out using 20 µl reaction volumes consisting of 10 µl of the qPCR Master Mix (contains SYBR® Green I Dye, AmpliTaq Gold® DNA polymerase, dNTPs with dUTP, Passive Reference, and optimized buffer components), 7 µl of sterilised water, 1 µl of the cDNA template, and 2 µl of the ideal primer concentration from the primer concentrations prepared as described in section 3.2.5.

Amplifications were carried out using the CFX96™ qPCR system, C1000™ Thermal Cycler (Bio Rad, U.K.), and all samples were analysed in duplicate with two negative controls set up alongside each set of reactions, consisting of all components excluding the template. All reactions started with denaturation at 50^{o}C for 2 min, and then at 95^{o}C for 10 min followed by a three-step protocol of 40 cycles of denaturation

at 95°C for 10 sec and annealing at 60°C for 1 min then extension step at 72°C for 1 min. in order to measure the specificity of the primers, the products were slowly melted starting with 1 min at 95°C followed by 30 sec at 55°C and 30 sec at 95°C and the products were analysed in the melting or dissociation curve (plotting fluorescence versus temperature).

3.2.9 Quantification and validation of the mRNA transcript method

A relative quantitation method was used to determine changes in mRNA transcript of the target genes in the treatment group compared to untreated control samples. The target genes *SOD2.1, HIF.4, Cat.1, Muc2.2,* and *Pxmp2.4* were prioritised and selected for this work based on literature reviews of their established association with potential biological effects (see table 1.1). These five target genes were then used to determine changes in mRNA transcript in the *D. rerio* embryo samples. The results were normalized with the two most stable reference genes (*18S.1* and *EF.1*). The method used to measure the relative change values was the comparative ΔCt method using the formula $RQ=2^{-\Delta Ct}$ where $\Delta=Ct_{SOD2.1,\ HIF.4,\ Cat.1,\ Muc2.2 \text{ or } pxmp2.4} - Ct_{18S.1 \text{ or } EF.1}$ (RQ= relative quantitation) (Livak and Schmittgen, 2001).

3.2.10 Statistical analysis of qPCR data

Each gene was tested individually for significant differences in expression levels among controls and treatment groups. Outliers of values more than twice the standard deviation of the mean were identified and removed according to accepted methods in the literature (Bustin et al., 2009). All data were tested for homogeneity of variances using Levene's test in SPSS (Version 22, IBM corp. New York, U.S.A). Significance for relative mRNA transcript was tested using Mann-Whitney test in SPSS. A statistical significance value of $P<0.05$ was specified to be significant and values are presented as means $\pm$SE.

3.2.11 Quantification of mRNA transcript in 10 nm AgNPs treated *D. rerio* embryos

Additional work had been performed using *D. rerio* embryos kindly supplied by Dr. Jinping Cheng. Twenty embryos that had been exposed to 1.925 mg Ag/L of 10 nm AgNPs were used as the exposed treatment group, and another 20 healthy embryos were used as a control reference group. The qPCR was carried out as described in

section 3.2.8 and the changes in mRNA transcript of the target genes in the treatment samples compared to untreated samples were measured as descried in section 3.2.9. The target genes *SOD2.1, HIF.4,* and *Pxmp2.4* were preferably selected based on their significantly positive affects been obtained earlier in the current study with *D. rerio* embryos exposed to 1.925 mg Ag/L of 4 nm AgNPs.

3.3 Results

3.3.1 Oligonucleotide primer optimization

In order to determine the optimal primer concentration for the reference genes (*18S.1/2*, *BT.2*, and *EF.1/2*), and the targeted genes (*SOD2.1*, *SOD2.2*, *ATP.1*, *ATPase.1*, *HIF.4*, *CRYaa*, *HSP.2*, *Cat.1*, *Jupa.4*, *Muc2.2*, and *Pxmp2.4*), different concentrations of equimolar forward and reverse primers were used. The best Ct values for each gene were determined using the various primer concentrations, and are presented in Table 3.1.

Table 3.1. Ct values of the qPCR amplifications using various primer concentrations.

Gene name	Primer concentrations (nM)	Optimal Ct value
18S.1	300	7.83
18S.2	100	11.54
BT.2	100	23.49
EF.1	200	17.70
EF.2	200	19.62
SOD2.1	200	25.08
SOD2.2	400	24.58
ATP.1	200	31.69
ATPase.1	200	27.64

HIF.4	200	30.23
CRYaa	100	26.03
HSP.2	200	28.04
Cat.1	200	23.99
Jupa.4	200	24.84
Muc2.2	300	29.34
Pxmp2.4	300	28.70

3.3.2 Standard curves for analysis of assay performance

After amplification, a standard curve was generated for each gene and all the Ct values for each standard dilution (Table 3.2) were determined and plotted against the initial template dilution to evaluate the performance of the qPCR reaction. For example, the amplification of (*18S.1*) using a serial dilution (1:10) generated a standard curve with an efficiency of amplification of (87.92 %). The slope of the line of best fit determines the efficiency of a reaction using the equation $E=10^{(-1/slope)}-1$ (Fig. 15). The linearity of the assay, denoted by the R squared (RSq or R^2) was 0.9732. A value close to 1 implies a linear range and that the efficiency of the reaction is consistent at varying template concentrations (sensitivity) and indicates agreement between replicates (precision). The standard curves generated from amplification of each candidate and reference gene are presented in Figure 3.1.

Table 3.2. Ct values for each standard dilution and efficiency of references and candidate genes.

Gene	Dilutions (1/x)	Ct value for each standard dilution					Efficiency %
		(1/x)	$(1/x)^2$	$(1/x)^3$	$(1/x)^4$	$(1/x)^5$	
18S.1	1/10	8.02	11.11	14.66	18.50	22.59	87.82
18S.2	1/4	11.54	13.79	16.35	-	-	77.83
BT.2	1/10	25.59	28.04	32.25	36.18	-	89.64
EF.1	1/10	18.58	20.94	-	28.77	33.02	87.24
EF.2	1/10	19.32	22.32	26.61	-	-	88.08
SOD2.1	1/10	23.86	27.20	31.18	34.24	36.49	103.98

SOD2.2	1/10	25.59	28.75	32.72	-	-	90.77
ATP.1	1/10	26.07	29.34	33.27	-	-	89.57
ATPase.1	1/10	28.40	30.83	35.61	38.91	-	88.54
HIF.4	1/4	31.34	33.23	35.16	-	-	106.14
CRYaa	1/4	25.31	27.83	30.27	32.70	35.18	75.30
HSP.2	1/4	-	-	30.05	32.23	34.54	85.03
Cat.1	1/10	23.33	27.23	30.74	-	-	86.17
Juba.4	1/10	23.47	26.77	30.23	-	-	97.63
Muc2.2	1/2	29.63	29.77	31.36	34.49	-	90.01
pxmp2.4	1/4	28.50	30.04	32.72	34.19	-	101.26

Figure 3.1

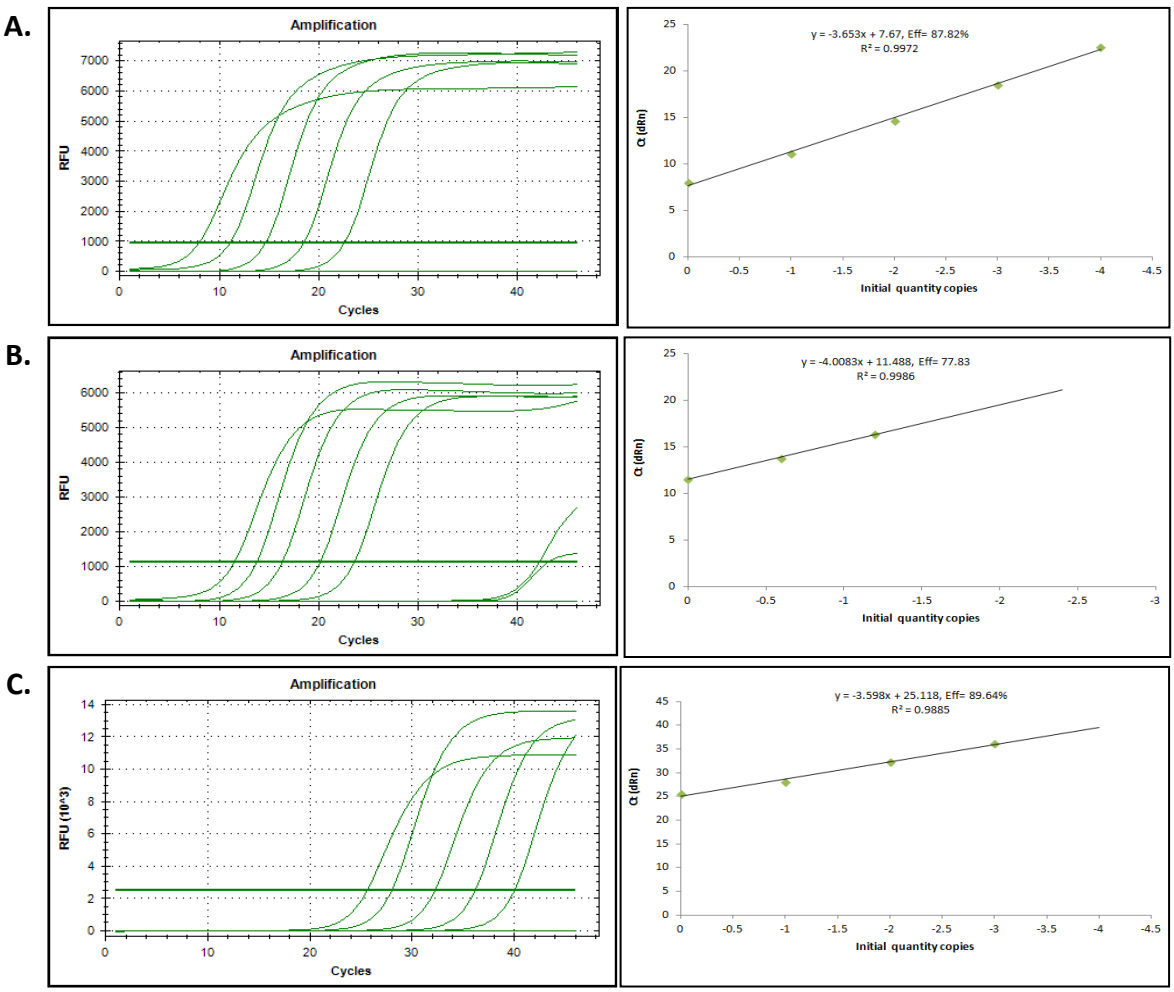

D.

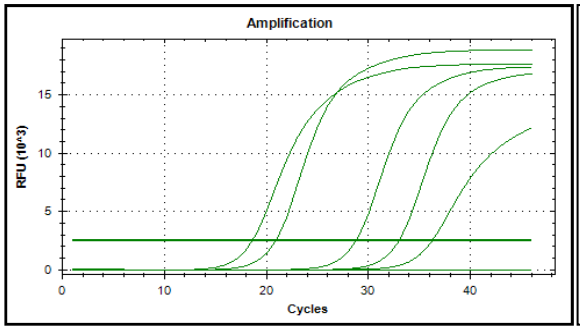
Amplification
RFU (10^3)
Cycles

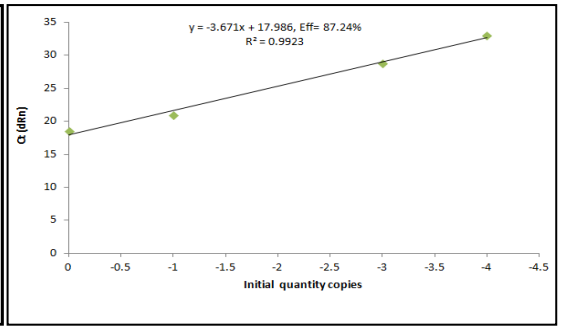
y = -3.671x + 17.986, Eff= 87.24%
R² = 0.9923
Ct (dRn)
Initial quantity copies

E.

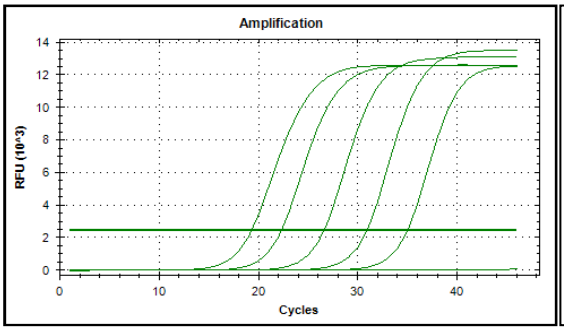
Amplification
RFU (10^3)
Cycles

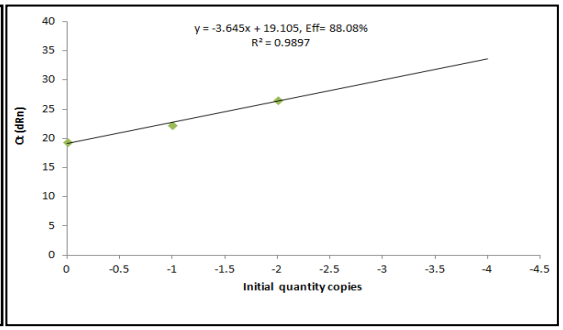
y = -3.645x + 19.105, Eff= 88.08%
R² = 0.9897
Ct (dRn)
Initial quantity copies

F.

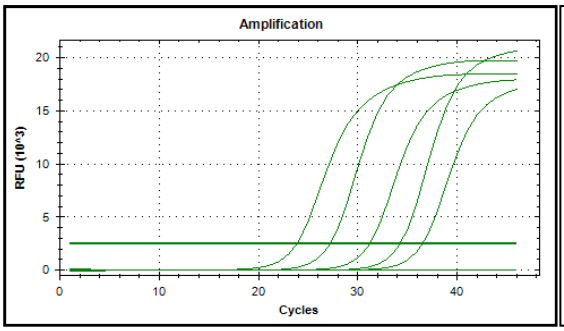
Amplification
RFU (10^3)
Cycles

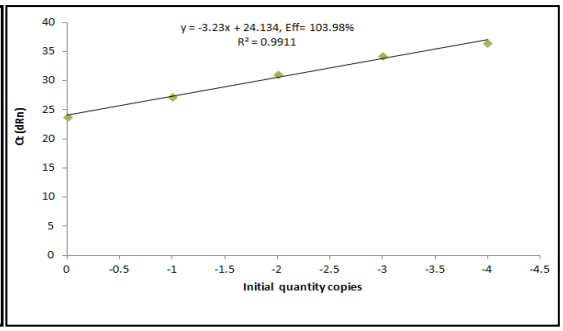
y = -3.23x + 24.134, Eff= 103.98%
R² = 0.9911
Ct (dRn)
Initial quantity copies

G.

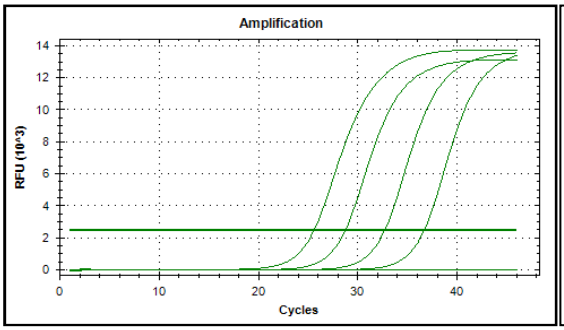
Amplification
RFU (10^3)
Cycles

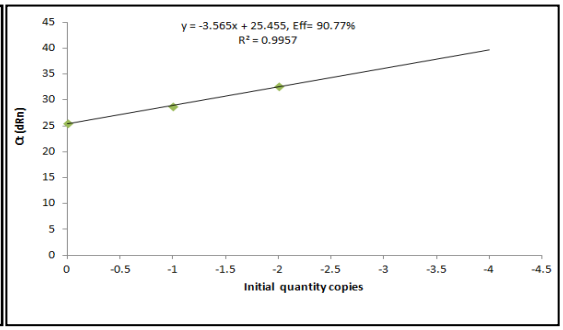
y = -3.565x + 25.455, Eff= 90.77%
R² = 0.9957
Ct (dRn)
Initial quantity copies

H.

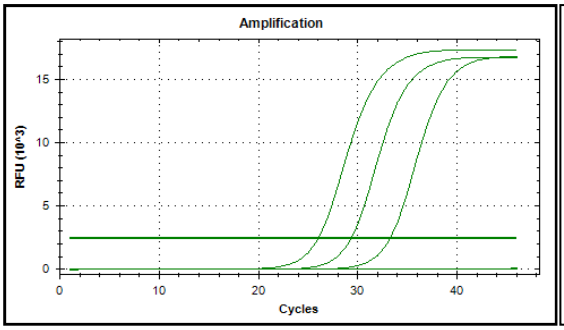
Amplification
RFU (10^3)
Cycles

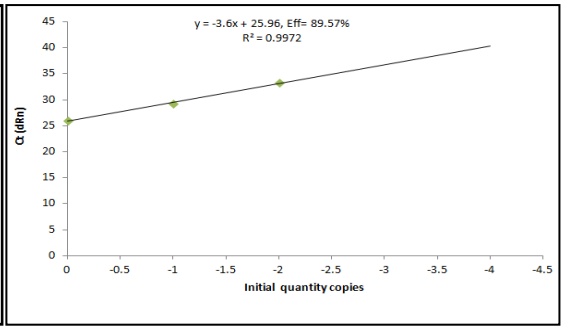
y = -3.6x + 25.96, Eff= 89.57%
R² = 0.9972
Ct (dRn)
Initial quantity copies

I.

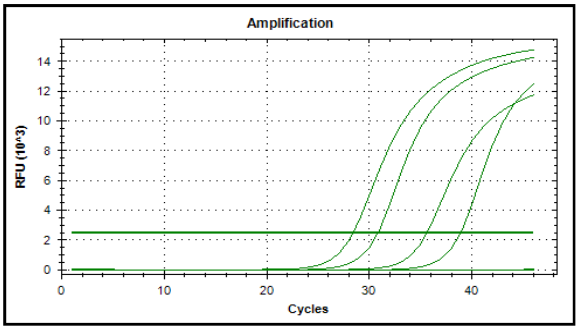
Amplification
RFU (10^3)
Cycles

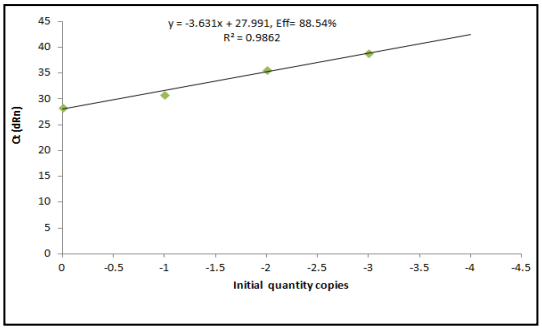
y = -3.631x + 27.991, Eff= 88.54%
R² = 0.9862
Ct (dRn)
Initial quantity copies

J.

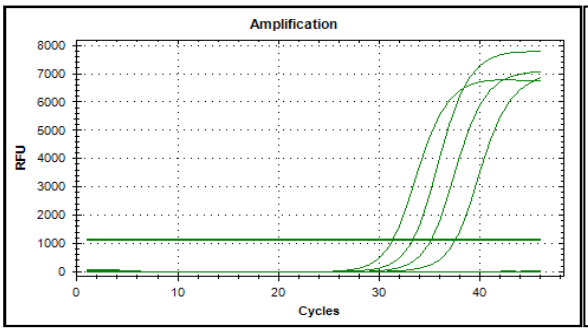
Amplification
RFU
Cycles

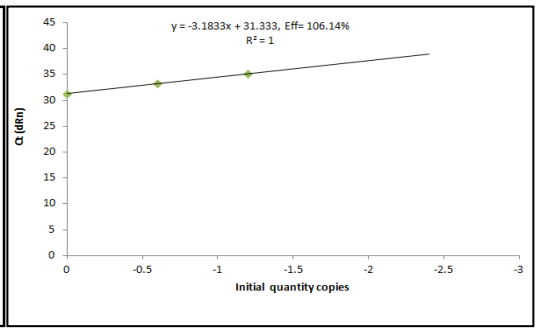
y = -3.1833x + 31.333, Eff= 106.14%
R² = 1
Ct (dRn)
Initial quantity copies

K.

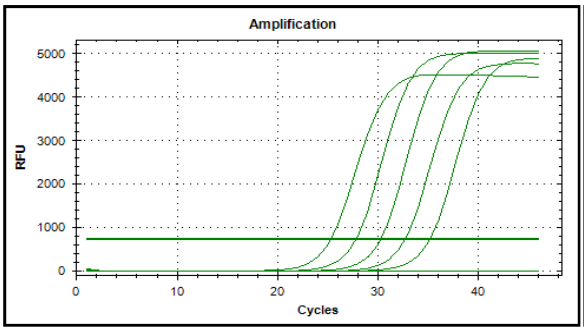
Amplification
RFU
Cycles

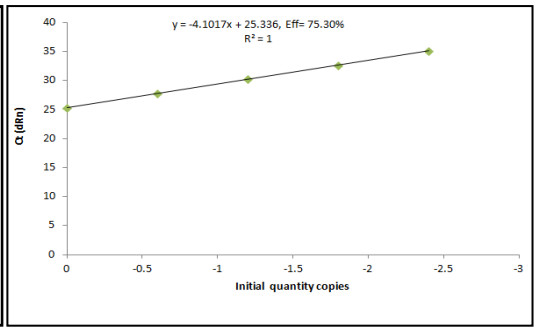
y = -4.1017x + 25.336, Eff= 75.30%
R² = 1
Ct (dRn)
Initial quantity copies

L.

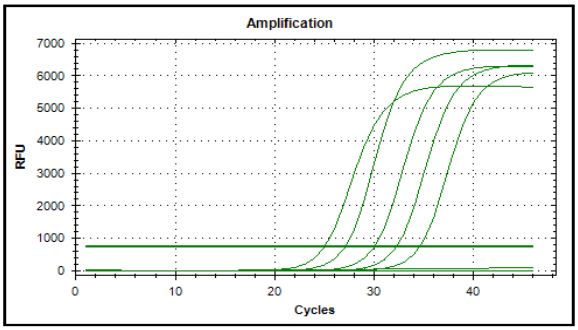
Amplification
RFU
Cycles

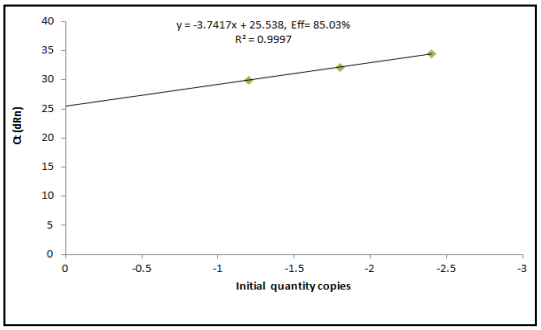
y = -3.7417x + 25.538, Eff= 85.03%
R² = 0.9997
Ct (dRn)
Initial quantity copies

M.

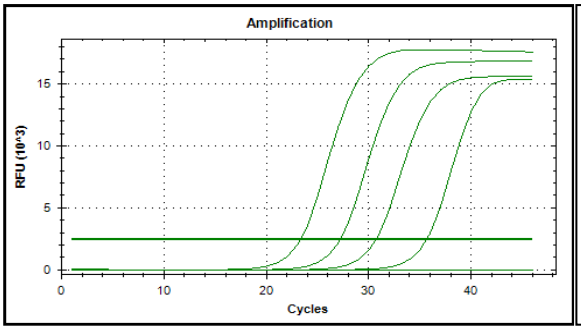
Amplification
RFU (10^3)
Cycles

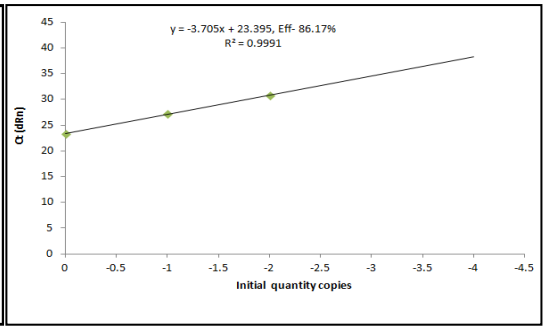
y = -3.705x + 23.395, Eff= 86.17%
R² = 0.9991
Ct (dRn)
Initial quantity copies

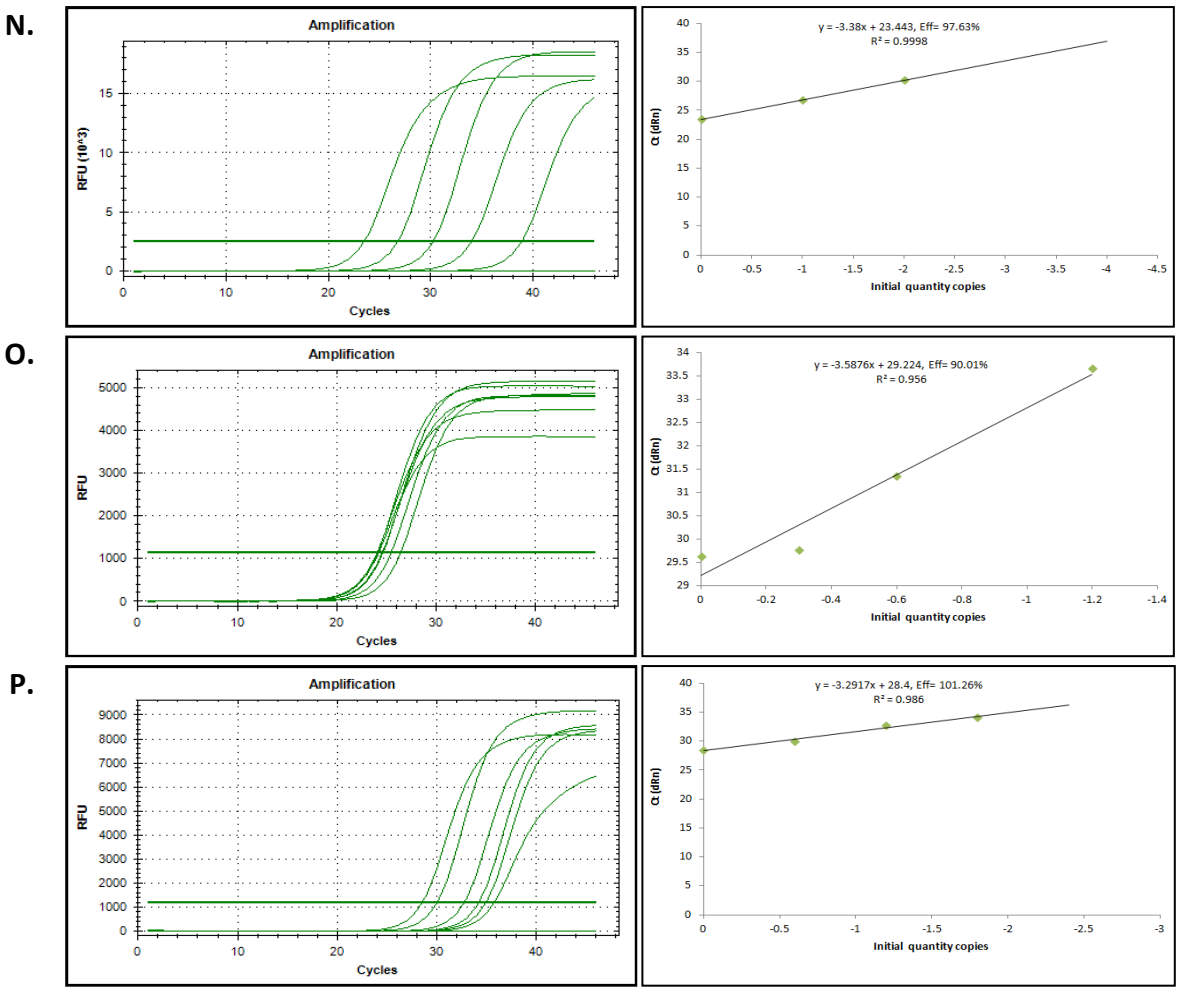

Figure 3.1. qPCR amplification and standard curves generated from amplification of each gene as following: A: *18S.1*, B: *18S.2*, C: *BT.2*, D: *EF.1*, E: *EF.2*, F: *SOD2.1*, G: *SOD2.2*, H: *ATP.1*, I: *ATPase.1*, J: *HIF.4*, K: *CRYaa*, L: *HSP.2*, M: *Cat.1*, N: *Jupa.4*, O: *Muc2.2*, and P: *Pxmp2.4* genes respectively.

3.3.3 Evaluating reference mRNA transcript

To compare mRNA transcript stability and rank the candidate reference genes, geNorm, Normfinder, BestKeeper, and the comparative Ct methods were used as described in 3.2.7. Rank orders of gene stability values from the most stable to least stable ones were calculated using each algorithm (Fig. 3.2). Accordingly the ranking order for the most stable reference gene was: *EF.1*, *18S.1*, and then *BT.2*.

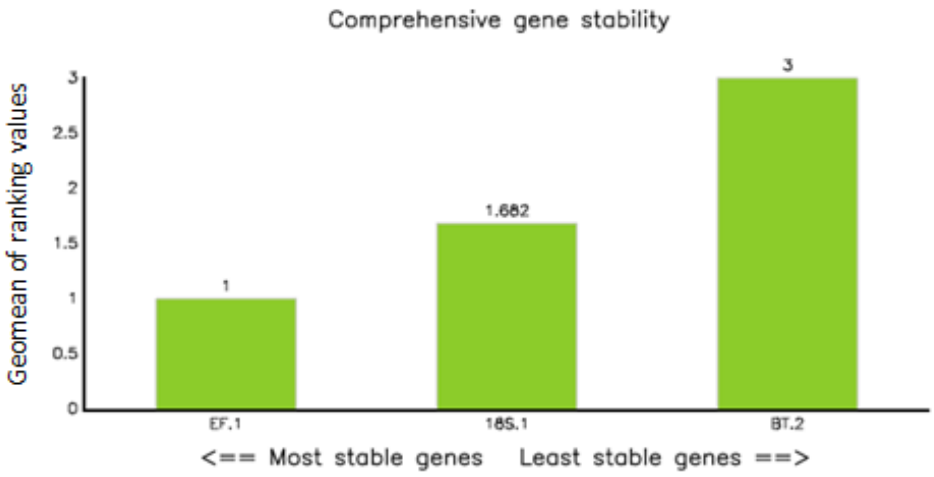

Figure 3.2. Comprehensive gene stability investigation of the three candidate reference genes in control and treated *D. rerio* embryos samples. Geomean of ranking values (y-axis) of three reference genes with their ranking from least to most stable mRNA transcript (x-axis). Lower geomean values indicate more stable mRNA transcript.

3.3.4 Quantitative PCR analysis of candidate genes mRNA in *D. rerio* embryos

The expression level of each target mRNA was analysed in controls, silver ion treated (0.018 mg/L), and 4 nm range AgNPs treated (1.925 mg/L), *D. rerio* embryos using the optimised qPCR method and the results are presented in Figure 3.3. *HIF.4* (p= 0.004, U= 89.000) and *Pxmp2.4* (p= 0.031, U= 100.000) mRNA expression was significantly up-regulated in *D. rerio* embryos following treatment with 1.925 mg/L of 4 nm AgNPs relative to control embryos (Fig. 3.3B, E). *SOD2.1* mRNA expression showed a trend towards up-regulation (P= 0.192, U= 151.500), though not statistically significant (Fig. 3.3A). *Cat.1* (P= 0.640, U= 182.000) and *Muc2.2* (P= 0.749, U= 178.500) mRNA expression levels showed no significant changes in AgNPs-treated embryos compared with corresponding control embryo samples (Fig. 3.3C, and D). No significant differences in any of the mRNA transcript levels were observed following 0.018 mg/L of silver ion exposure alone (*SOD2.1* p= 0.740, U= 168.000; *HIF.4* p= 0.166, U= 140.000; *Cat.1* p= 0.931, U= 177.000; *Muc2.2* p= 0.354, U= 148.000; *Pxmp2.4* p= 0.607, U= 171.000) (Fig. 3.3A-E).

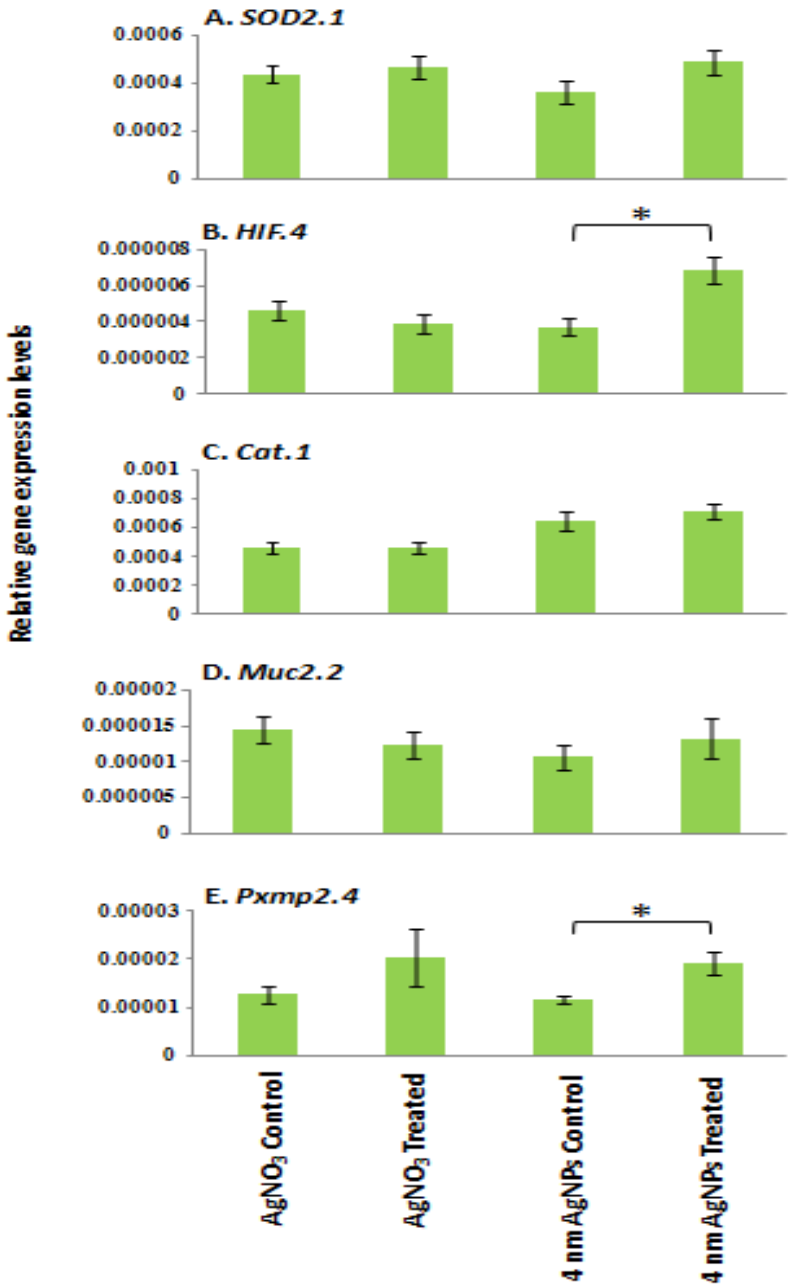

Figure 3.3. qPCR expression analysis of target mRNA in controls, silver ion-treated and 4 nm range AgNPs-treated *D. rerio* embryos. Normalized average relative mRNA transcription ± standard error of the mean in *D. rerio* embryos for (A) *SOD2.1*, (B) *HIF.4*, (C) *Cat.1*, (D) *Muc2.2*, and (E) *Pxmp2.4* genes.

3.3.5 Quantification of mRNA transcript in 10 nm AgNPs treated *D. rerio* embryos

The expression level of each target mRNA was analysed in controls and 10 nm range AgNPs treated (1.925 mg/L) *D. rerio* embryos using the optimised qPCR method and the results are presented in Figure 3.4. The *SOD2*.1 mRNA expression was significantly down-regulated (*P*= 0.023, U= 103.000) in *D. rerio* embryos (Fig. 3.4A). While no

significant differences in the mRNA transcript of *HIF.4* (*p*= 0.391, U= 142.500), and *Pxmp2.4* (p= 0.325, U= 146.000) was observed (Fig. 3.4A, B).

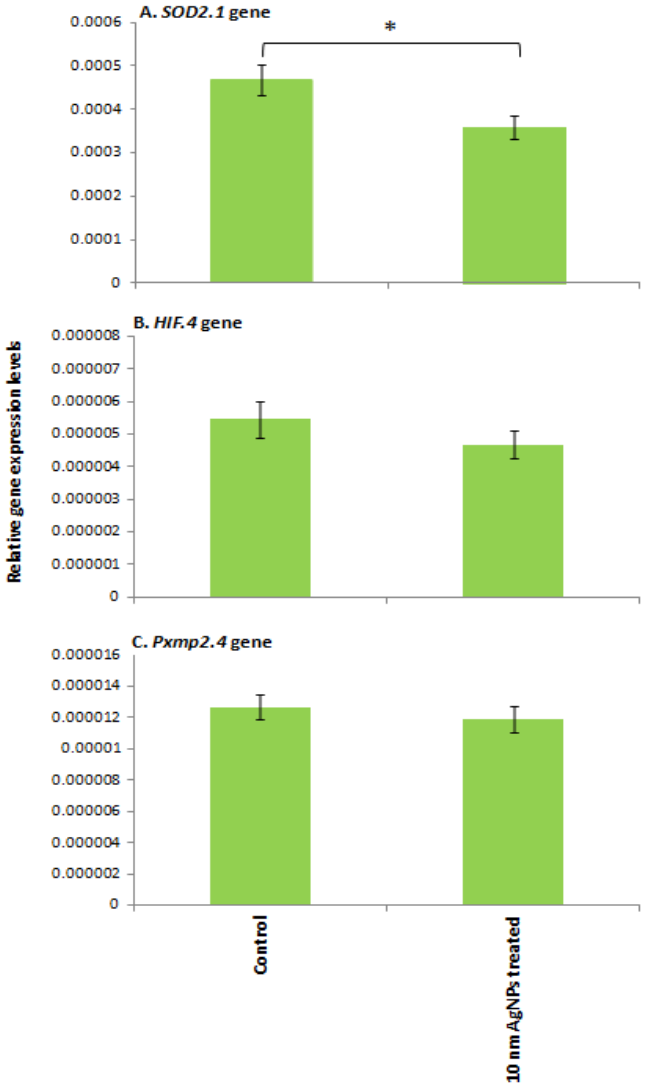

Figure 3.4. qPCR expression analysis of target mRNA in controls and 10 nm range AgNPs-treated *D. rerio* embryos. Normalized average relative mRNA transcription ± standard error of the mean in *D. rerio* embryos for (A) *SOD2.1*, (B) *HIF.4*, and (C) *Pxmp2.4* genes.

3.4 Discussion

The candidate genes selected for potential study were selected according to the biological effects reported in the literature and regarding the potential toxicity mechanisms that may be occurring within the organism as discussed in Chapter 1. Of the shortlist of candidate genes discussed in Chapters 1 and 2, five genes were then

prioritised for development and qPCR analysis: *SOD2.1*, *HIF.4*, *Cat.1*, *Muc2.2*, and *Pxmp2.4.* The remaining genes were left for future work if given further time and funds. The aim of this chapter was to develop and validate an qPCR based assay for these selected candidate genes to determine the expression levels in early *D. rerio* embryos up to 96 hpf exposed to 1.925 mg/L of 4 and 10 nm AgNPs, and to 0.018 mg/L of silver ion alone, relative to the corresponding control embryos.

The current study showed a significant up-regulation in expression of *HIF.4* and *Pxmp2.4* after exposure to 4 nm AgNPs relative to controls (Fig. 3.3B, E). An increased trend in up-regulation of *SOD2.1* mRNA expression was also observed (Fig. 3.3A), while, *Cat.1* and *Muc2.2* expressions remained unchanged (Fig. 3.3C, D). A down-regulation of *SOD2.1* mRNA expression was also observed after exposure to 10 nm AgNPs (Fig. 3.4A), and no significant differences in the mRNA transcript of *HIF.4,* and *Pxmp2.4* was observed (Fig. 3.4A, B). No significant differences were observed within the mRNA transcript levels upon exposure to silver ion alone (Fig.3.3A, B, C, D, and E).

According to the wider literature, NP size and surface charge has been shown to have great impact on their interaction with biological membranes and their toxicity (Al-Awady et al., 2015). In this study, the smaller sized AgNPs of 4 and 10 nm have been used. Previous studies have shown the AgNPs toxicity is somewhat size dependent at different concentrations and time points (Bar-llan et al., 2009). AgNPs of 5-20 nm diameters were detected inside 48h *D. rerio* embryos (Asharani et al., 2008). The availability of AgNPs could also depend on the coating media (Olasagasti et al., 2014). In this study the fatty acid coating (oleic acid) was used and according to previous studies using different free fatty acids including oleic acid, this coating does not contribute to toxicity (Jebali et al., 2014).

SODs are required for the conversion of $O_2^{-\bullet}$ to O_2 and H_2O_2, therefore the down-regulation of *SOD* would increase oxidative stress (Scott et al., 2010). The increasing up-regulation trend in *SOD2.1* expression levels following 4 nm AgNPs exposure (Fig. 3.3A) and the down-regulation in expression in *SOD2.1* following 10 nm AgNPs is indicative of oxidative stress (Fig. 3.4A). In order to protect tissues against oxidants, peroxisomes contain enzymes that scavenge ROS such as *SOD*, *Cat*, and some

peroxisome-specific integral membrane proteins (peroxisomal membrane protein 2) (Antonenkov et al., 2010). The *SOD* is an enzyme that catalyses the dismutation of the reactive superoxide ion (O_2^-) to yield H_2O_2 and oxygen molecule during oxidative oxygen processes (Velkova-Jordanoska et al., 2008). *SOD* gene was also up regulated at day 7 post-instillation in rats liver treated with AgNPs (50 µg/rat), whilst at day 28 the mRNA transcript was within basal levels (Coccini et al., 2014). The up-regulation of *SOD* gene was suggested to be an adaptive process by hepatic cells that can contrast the action of ROS generated and initial cytotoxic effects caused by AgNPs (Coccini et al., 2014). Increased *SOD* activity has also been observed in medaka fish (*O.latipes*) embryos up to 72 hpf at high AgNP concentration >250 µg/L (Wu and Zhou., 2012). In contrast, *SOD* activities were found to be reduced in rat plasma after they received AgNPs at 5, 50, 250, and 500 mg/Kg/day for two weeks (Ranjbar et al., 2014). Yet in another study, no significant difference in *SOD* levels in *C. carpio* following different exposures of 25, 50, 100, and 200 µg/L of AgNPs after 48-96 h exposure was observed (Lee et al., 2012), and the expression of *SOD1* mRNA in liver tissues of adult *D. rerio* was not significantly affected by treatment with 30, 60, and 120 mg Ag/L of AgNPs (Choi et al., 2010). The *SOD* response following AgNP exposure is therefore variable in different species and at different size and concentration levels.

In this study, *HIF.4* mRNA was significantly up-regulated in only 4 nm AgNP treated embryos (Fig. 3.3B) which is indicative of a hypoxic cellular environment. *Hypoxia inducible factor 1-alpha* (*HIF-1α*) subunits are expressed in many tissues such as heart, brain, liver, kidney, and embryo (Wiesener et al., 2003). *HIF-2α* mRNA is only slightly expressed in lung and other tissues (Hu et al., 2003), in contrast to widely expressed *HIF-1α* (Wiesener et al., 2003). *HIF-1α* increased expression was also similarly observed in *P. promelas* after exposure to 61.4 µg/L of poly (N-vinylpyrrolidone) AgNPs (PVP-AgNPs) for 96 h with a water change at 48 h (Garcia-Reyero et al., 2014).

On the other hand, *Cat.1* showed no significant difference of either 4 nm AgNP or silver ion exposure samples (Fig. 3.3C). Catalase enzyme is one of the active antioxidant defence that known to be highly cooperative with *SOD* and other H_2O_2 products at high flow of H_2O_2 (Patnaik et al., 2013). Catalase along with GPs and *SOD*

prevent or repair the cellular damage caused by ROS (Weydert and Cullen, 2010). Likewise, no significant difference in *Cat* activity was recorded in common carp (*Cyprinus carpio*) after 48 h of AgNPs exposure, but after 96 hr of exposure; *Cat* activity was significantly reduced in the liver at 25 µg/L concentration (Lee et al., 2012). This may be because the water in that experiment was not changed during the test. Also, a higher levels of catalyse activity were detected in the liver of *C. carpio* than in the brain and gills of the previous experimental fish (Lee et al., 2012). *Cat* expression was also decreased in the liver of adult *D. rerio* after treatment with AgNPs at 60 and 120 mg Ag/L for 24 h (Choi et al., 2010). Furthermore, *Cat* activities were reduced in rat plasma after received AgNPs, 5, 50, 250, and 500 mg/Kg/day for two weeks (Ranjbar et al., 2014). In summary, catalase therefore shows a decrease in expression in different species after exposure to AgNPs at high level or a long exposure time.

Muc2.2 mRNA expression levels in embryos of both 4 nm AgNPs and silver ion exposure samples were not impacted (Fig. 3.3D). Mucus is very important in fish for protection from xenobiotics because it forms a physical barrier to protect gill, skin, and intestine from surrounding environment (Shephard, 1994). *D. rerio* mucins are the major gel-forming building blocks of the mucus barrier and they are detectable in the head and tail region of a developing embryo from 48 hpf (Jevtov et al., 2014). It seems that gills mucus precipitates the NPs to prevent them from direct exposure to the gill epithelium in adults (Johari et al., 2013). Yet at 24 h post silver exposure, fish produced a greater amount of mucus than the controls (Hawkins et al., 2014). The explanation offered by the authors is that mucus concentration reduction by 96 h could be due to the formation of a protective physical barrier over the gills which prevent continues xenobiotic uptake (Hawkins et al., 2014). On the other hand, AgNPs were acutely toxic to male *D. rerio* after 48 h of semestatic exposure to LC_{50} of 84 µg/L and LC_{10} of 57 µg/L at pH (5-8), where all fish in the two highest test concentrations were dead after 24 h of exposure, fish mucus was observed at the bottom of tanks exposed to at least 89 µg/L suggested a mucus secretion at that dose (Bilberg et al., 2012). Mucus secretion was also increased in *O. mykiss* gills after exposed to the (>1 mg/L) AgNPs, the 96h LC50s of AgNPs were also measured to be 0.25 mg/L for the eleutheroembryos, 0.71 mg/L for the larvae, and 2.16 mg/L for the juveniles (Johari et al., 203). Mucus

secretion is therefore perhaps more important in adults than in embryos when responding to AgNP exposures.

Interestingly, for the first time, this study showed an increased in *Pxmp2.4* mRNA expression in *D. rerio* embryos exposed to 4 nm AgNPs (Fig. 3.3). Peroxisomal enzymes are involved in conversion of lipids, reactive oxygen species, hydroxyl- and amino acids, and purines (Wanders and Waterham, 2006). *Pxmp2* was assumed to be playing a role in the transmembrane transport of solutes by selectivity of pore-forming proteins (Van et al., 1987) which was confirmed with recombinant protein expressed in mouse liver (Rokka et al., 2009). The *Pxmp2* channel has been estimated to have a diameter of 1.4 nm, as having weak cation selectivity, and running as a general diffusion pore in the membrane (Rokka et al., 2009). Using 5 nm and 28 nm silver NPs (PVP-coated) induced superoxide within mitochondrial membranes in primary human monocytes (Yang et al., 2012), and consideration was given by Yang and colleagues, 2012 to the possibility of cell membrane disturbance through direct invasion of 5 and 28 nm AgNPs into cells. No previous studies on *D. rerio* were found on mRNA transcript differences on peroxisomal membrane protein 2 (PMP2) after exposure to NMs.

Only a few studies have focused on embryonic toxicity of AgNPs (Cho et al., 2013) and differences in AgNPs toxicity between embryos and adult fish (Chae et al., 2009; Kashiwada et al., 2012; Kwok et al., 2012). A study to investigate the developmental toxicity of AgNPs following exposure of *O. latipes* embryos to 0.1-1 mg/L of homogeneously dispersed AgNPs for 14 days showed that AgNPs exposure causes significant developmental toxicity to embryos while toxicity levels were enhanced at certain developmental stages (Cho et al., 2013). Yet very little is known about the specific mechanisms of the AgNPs, and further studies are needed to identify specific toxicity of both AgNP and silver ion (Kashiwada et al., 2012).

In summary, this chapter focused on determining changes in mRNA transcript using a qPCR based assay for *SOD2.1*, *HIF.4*, *Cat.1*, *Muc2.2*, and *Pxmp2.4* genes. An increase in expression of *HIF.4* and *Pxmp2.4* mRNA and an increasing trend in *SOD2.*1 gene was observed after exposure to AgNPs of 4 nm size range at the higher concentration level of 1.925 mg/L were observed. These are correspondingly

associated with membrane transport and potentially also oxidative stress. Small size of AgNPs has large surface area to volume ratio which increases deliver its toxicity (Cho et al., 2013). Accordingly, in comparison with the wider literature, the results indicate that AgNPs of different size, concentration, or stabilisation agents perform different degrees of toxicity in different species under different exposure conditions and time. It is also possible to utilise these changes in mRNA transcript to detect AgNP exposure and impacts under the conditions employed.

4. Chapter Four: Identification of differentially expressed genes in nanosilver-exposed *D. rerio* embryos using SSH

4.1 Introduction

Suppression Subtractive Hybridization (SSH) is a technique to compare between two different populations of mRNA and genes that are expressed in different ways (Diatchenko et al., 1996). It has been used in many molecular genetics and cloning studies for the identification of differently expressed genes from various organisms such as *Emiliania huxleyi* (Nguyen et al., 2005), *Salvelinus fontinalis* (Bobe and Goetz, 2000), *Platynereis dumerilii* (Wäge et al., 2015), *Poecilia vivipara* (Mattos et al., 2010), *Salmo salar* (Tsoi et al., 2004), *Penaeus monodon* (Leelatanawit et al., 2008), *Pachytriton brevipes* (Jiang et al., 2014), and humans (Diatchenko et al., 1996). In the SSH approach mRNAs are converted into cDNA for two different samples, making two different cDNA populations. The treated sample (containing exposed tissue or diseased tissues for instance) contains one population of expressed transcripts and is referred to as the 'tester'. The non-exposed or healthy tissue sample used to generate another population of cDNA is referred to as the 'driver'. In the SSH approach, the tester and driver cDNAS are hybridized, the hybrid sequences are excluded and the remaining unhybridized cDNAs represent genes that are expressed in only one population (Diatchenko et al., 1996). SSH has thus been used to find and characterise differently expressed genes in *Enchytraeus albidus* (Oligochaeta) after metal and pesticide exposures (Novais et al., 2012), 41% were found matched to known proteins in GenBank, and 5.5% of the sequences were assigned to a metabolic pathway. SSH was also used to identify genes differently expressed in the liver of *P. vivipara* (Guppy) exposed to a 10% diesel fuel water accommodated fraction (WAF), 27 differentially expressed gene fragments were highlighted that were related to different metabolic functions such as biotransformation membrane transport, and immune response (Mattos et al., 2010). The SSH technique is therefore a method that can be used to compare two samples, exposed/controls or diseased/healthy, and to isolate the genes differentially expressed between them. Identifying such genes then provides basic information about cellular pathways that may be affected by the exposure/disease.

Previously, the literature has suggested that AgNPs induce toxicity *in vitro* and *in vivo* (Chapter 1, sections 1.5 and 1.6), but that the precise molecular mechanisms of AgNP toxicity has not been fully elucidated (Lee et al., 2011). The aim of this chapter was to utilise the SSH technique in order to isolate mRNA transcripts differentially expressed in treated *D. rerio* embryos exposed to 4 nm AgNPs (1.925 mg/L) compared with normal embryos. The approach will allow us to find and identify potentially novel molecular responses to AgNP exposure that can then be used as an early warning tool of exposure in future biomonitoring programmes in the aquatic environment.

4.2 Materials and Methods

4.2.1 *D. rerio* embryos

All *D. rerio* embryos were collected and processed as described in section 2.2.2 and kindly supplied by Dr Jinping Cheng. Twenty *D. rerio* embryos that had been exposed to 1.925 mg Ag/L of 4 nm-Ag at 96 hpf were used as the exposed treatment group (Tester) and 20 healthy *D. rerio* embryos were used as the control reference group (Driver).

4.2.2 RNA isolation

The total RNA extraction from *D. rerio* embryos was carried out following the protocol described in section 2.2.3 and stored at -80^{o}C until further processing. The RNA concentration was measured using a Qubit® Fluorometer (Invitrogen™, Paisley, UK). The integrity of the RNA was checked using the protocol described in section 2.2.4.

4.2.3 RNA precipitation

Eight samples (consisting of a total RNA concentration of 2.5 µg) were used from each treatment to make a pool of cDNA. The RNA was mixed with 1:10 of sodium acetate (NaOAc, 3 M, pH 5.3) and two volumes of cold (4^{o}C) ethanol (EtOH) absolute and incubated at -80^{o}C for 30 min. Then the RNA was centrifuged for 20 min at 14,000 rpm in a microcentrifuge. The supernatant from each tube was removed and the remaining pellet was then air-dried using an Eppendorf AG (Hamburg, Germany), so that the ethanol evaporated off. Afterwards 3.5 µl sterile H_2O was added and the RNA concentration of the samples was measured with a Qubit® Fluorometer (Invitrogen™, Paisley, U.K.). All RNA samples were stored at -20^{o}C until further processing.

4.2.3 First strand synthesis of cDNA

The SMARTerTM PCR cDNA synthesis kit reagents (Clontech, SaintGermain-en-Laye, France) were used to generate cDNAs. 3 µl (2.5 µg) of pooled RNA, 1 µl 3' SMART CDS Primer II A (12 µM), and 0.5 µl deionised H_2O were mixed gently, centrifuged and incubated at 72°C in a hot-lid thermal cycler for 3 min and 2 min at 42°C. After incubation, a Master Mix for each tube was prepared by mixing 2 µl 5X First-Strand buffer, 0.25 µl DTT (100 mM), 1 µl dNTP mix (10 mM), 1 µl SMARTer II A Oligonucelotide (12 µM), 0.25 µl RNAse Inhibitor, and 1 µl SMARTScribe Reverse Transcriptase (100 U/µl). Then the tubes were incubated at 42°C for 1 hr and 30 min followed by incubation at 70°C for 10 min to terminate the reaction. The first-strand reaction product was diluted by adding 40 µl of TE buffer (10 mM Tris [pH 8.0], 0.1 mM EDTA] and the tubes were stored at -20°C until further processing.

4.2.4 cDNA amplification by LD PCR

Long-Distance Polymerase Chain Reaction (LD PCR) was applied to generate double stranded cDNA from the first-strand cDNA amplification. Three tubes of 0.5 ml capacity were used. In each tube, 10 µl cDNA (prepared in section 4.2.3.) was mixed with 74 µl deionised H_2O, 10 µl 10X Advantage 2 PCR Buffer, 2 µl 50X dNTPs mix (10 mM), 2 µl 5' PCR primer II A (12 µM) and 2 µl 50X Advantage 2 Polymerase Mix (50% glycerol, 15 mM Tris-HCl [pH 8.0], 75 mM KCl, 0.05 mM EDTA). The PCR thermal cycler was preheated. For the PCR conditions, an initial denaturation at 95°C for 1 min was used, followed by a range of cycles of denaturation to define the optimal numbers of cycles (15, 18, 21, 24, 27, and 30 cycles) at 95°C for 15 sec, annealing at 65°C for 30 sec, and extension at 68°C for 3 min. After 15 cycles, 70 µl from the one tube was transferred into a clean 0.5 ml tube, and the other two tubes all were stored at 4°C. The 30 µl in the other tube was returned to the thermal cycler. Each cycle stages was counterchecked by an aliquot on a 1.2% agarose/EtBr gel in 1X TAE buffer in order to attain the optimal number of cycles. The best number of cycles for the generation of double stranded cDNA from treated embryos and control embryos was 26 cycles in each case.

4.2.5 Column chromatography

The cDNA was purified after the PCRs. The three reaction tubes of PCR product (collected after 15 cycles) were combined into a 1.5 ml tube. 7 µl of the raw PCR product was transferred to a clean a clean microcentrifuge and labelled as "Sample A" and stored at -20^{o}C for agarose/EtBr gel analysis. The PCR product was mixed with an equal volume of phenol:chloroform:isoamyl alcohol (25:24:1) and mixed then centrifuged at 14,000 rpm for 10 min to separate the phases. The top aqueous layer was removed and placed in a clean 1.5 ml tube. To concentrate the PCR product to a volume of 40-70 µl, 700 µl of n-butanol was added, mixed thoroughly, and then centrifuged at 14,000 rpm for 1 min. Then the upper (n-butanol organic) phase was removed. The top and bottom caps of each column were removed and placed into a 1.5 ml centrifuge tube. The buffer inside each column was discarded and 1.5 ml of 1 x TNE buffer (10 mM Tris-HCl [pH 8], 10 mM NaCl, 0.1 mM EDTA) was added and allowed to drain through the column by gravity until the surface of the gel beads in the column matrix were seen. The collected buffer was discarded. Each sample was applied to the centre of the gel bed's flat surface in the column followed by 25 µl of 1 x TNE buffer and allowed to completely drain out of the column. Another 150 µl of 1XTNE buffer was applied and allowed to completely drain out of the column. A clean 1.5 ml microcentrifuge tube was applied to the column and 320 µl of 1 x TNE buffer was applied and the eluate was collected as a purified ds cDNA fraction. 10 µl of this fraction was transferred to a clean microcentrifuge tube and labelled as "Sample B" and stored at -20^{o}C for agarose/EtBr gel analysis. A clean 1.5 ml microcentrifuge tube was applied to the column and 75 µl of 1XTNE buffer was applied and the eluate was also collected as a purified ds cDNA fraction. 10 µl of this fraction was transferred to a clean microcentrifuge tube and labelled as "Sample C" and stored at -20^{o}C for agarose/ETBr gel analysis. To confirm the presence of PCR product in the purified ds cDNA fraction, samples A, B, and C were performed on the agarose/EtBr gel.

4.2.6 *Rsa*1 restriction enzyme digestion

The *Rsa* I digestion is necessary to produce short and blunt-ended ds cDNA fragments for the adaptor ligation and subtraction process. 10 µl of purified ds cDNA was set aside in new tube for agarose/EtBr gel analysis to estimate the size range of the ds

cDNA products. The purified cDNA was mixed with 36 µl (10X *Rsa*I Restriction Buffer) and 1.5 µl *Rsa*I (10 U/µl) and incubated at 37°C for 3 hr. To terminate the reaction in the digested cDNA, 8 µl of 0.5 M EDTA was added and stored at -20°C until further processing. To confirm success of *Rsa*I digestion, 10 µl of uncut ds cDNA and 10 µl of *Rsa*I-digested cDNA was electrophoresed on a 1.2% agarose/EtBr gel in 1XTAE buffer.

4.2.7 Purification of digested cDNA

The digested cDNA was purified using the NucleoSpin® Gel and PCR Clean-up kit (Macherey Nagel, from Fisher Scientific, Loughbourgh, U.K.). 1 volume of cDNA was mixed with 2 volumes of Buffer NTI (contains chaotropic salts, exact composition is confidential), loaded into the NucleoSpin® Column and centrifuged at 11,000 rpm for 30 sec. 700 µl of Buffer NT3 (composition is confidential) were added and the column was centrifuged again for 30 sec at 11,000 rpm. The flow-through was discarded and the column was centrifuged at 11,000 rpm for 2 min to remove all Buffer NT3. The column was placed in a new 1.5 ml microcentrifuge tube and eluted with 15 µl Buffer NE (5 mM Tris/HCL, pH 8.5) and then incubated at room temperature for 1 min and finally was centrifuged at 11,000 rpm for 1 min. The cDNA concentration of the samples was measured with a Qubit® Fluorometer (Invitrogen™, Paisley, U.K.). All samples were stored at -20°C until further processing.

4.2.8 Adaptor ligation

Three separate ligations were conducted for the forward (control embryos), reverse (treated embryos) and control subtraction (skeletal muscle, provided with the kit reagents) (Fig. 4.1). The protocol of the PCR-Select™ cDNA Subtraction Kit (Clontech, Mountain View, U.S.A) was applied. Each cDNA was divided into two tubes and ligated with Adaptor1 (Tester 1-1, 2-1, and 3-1) and the second with Adaptor R2 (Tester 1-2, 2-2, and 3-2) (Fig. 4.1). To prepare the control skeletal muscle tester cDNA (0.2% Hae III-digested φX174 DNA), the φX174/Hae III control DNA was diluted with sterile H_2O to a final concentration of 150 ng/ml. The control skeletal muscle cDNA was mixed with 5 µl of the diluted φX174/Hae III control DNA. To ligate the tester cDNAs to adaptors, 2 µl diluted cDNA (1 µl cDNA with 5 µl H_2O) was mixed with 2 µl of Adaptor 1 or Adaptor 2R and 6 µl Master Mix containing 3 µl sterile H_2O, 2 µl 5X DNA ligation buffer (250

mM Tris-HCl [pH 7.8], 50 mM $MgCl_2$, 10 mM DTT, 0.25 mM BSA) and 1 µl T4 DNA Ligase (400 units/µl). In a new 0.5 ml microcentrifuge tube, 2 µl of each adaptor ligated testers (1-1, 1-2, 2-1, 2-2, 3-1, and 3-2) were combined and incubated at 16^{o}C overnight. Afterward, 1 µl of EDTA/Glycogen mix was added to stop ligation reaction and the samples were heated for 5 min at 72^{o}C to inactivate the ligase. 1 µl was taken from each unsubtracted tester control and diluted into 1 ml H_2O to be used for PCR. All samples were stored at -20^{o}C until further processing.

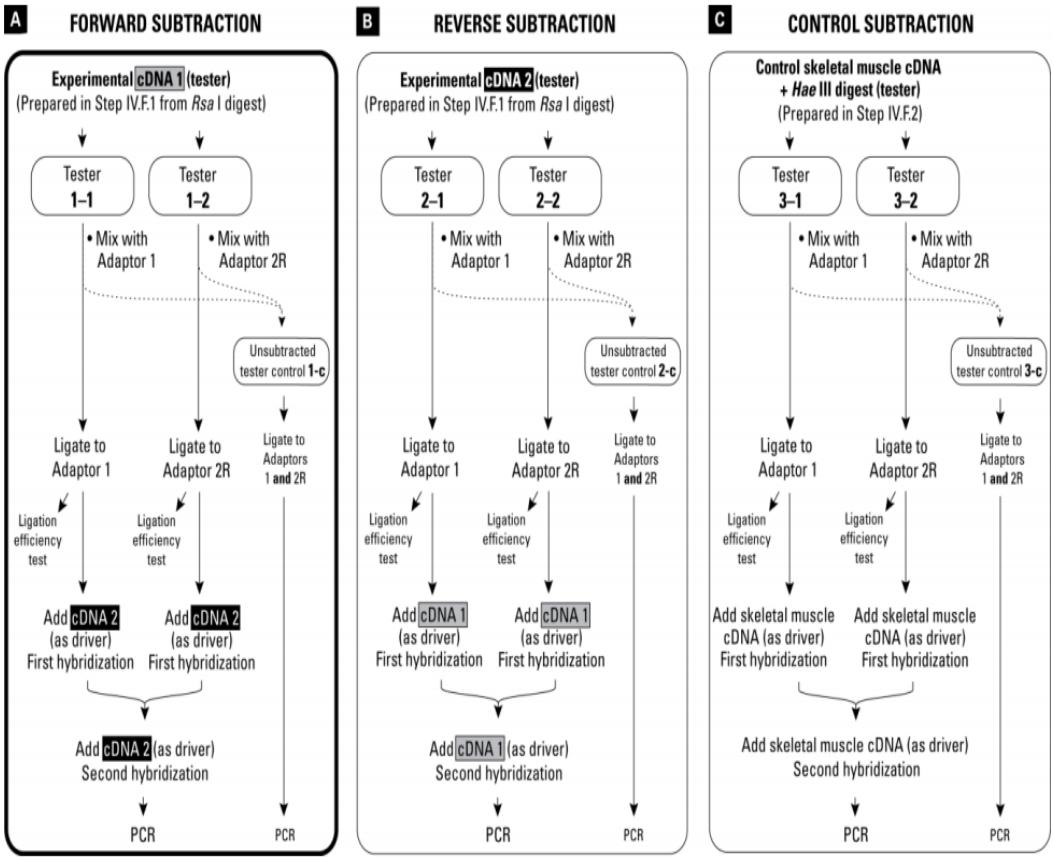

Figure 4.1. Schematic diagram for the preparation of adaptor-ligated tester cDNAs for hybridization and PCR. Each tester cDNA was ligated to the suitable adaptor. A. The forward subtraction which represents the control embryos. B. The reverse subtraction represents the treated embryos. C. A control subtraction was performed with skeletal muscle cDNA (Scheme modified based on the Select™ cDNA Subtraction Kit User Manual, Clontech. www.clontech.com).

4.2.9 Ligation efficiency analysis

To verify that at least 25% of the cDNAs have adaptors on both ends, 1 µl of each ligated cDNA (Testers 3-1 and 3-2) of the control DNA sample (Fig. 4.1C) was diluted into 200 µl of H_2O. The reagents in Table 4.2 were combined in four separate tubes and mixed with 22 µl of master mix that prepared by combining the following reagents: 18.5 µl sterile H_2O, 2.5 µl 10X PCR reaction buffer, 0.5 µl dNTP mix (10 mM), and 0.5 µl of 50X advantage cDNA polymerase mix. All reagents were mixed by vortexing and briefly centrifuged, and then 22 µl of master mix was aliquoted into each of the reactions (Table 4.1). The reaction mix was incubated at 75^{o}C for 5 min in a thermal cycler to extend the adaptors. All reactions were initially denatured at 94^{o}C for 30 sec, then 30 sec at 65^{o}C for annealing, and 2.5 min at 68^{o}C as an elongation step. The last three steps were repeated 20 times and 5 µl of each reaction were analyzed on a 2.0% agarose/EtBr gel run in 1 x TAE buffer.

Table 4.1. The ligation analysis PCR components.

Component	**Tube (µl)**			
	1	**2**	**3**	**4**
Tester 1-1* (ligated to Adaptor 1)	1	1	-	-
Tester 1-2* (ligated to Adaptor 2R)	-	-	1	1
G3PDH 3' Primer (10 µM)	1	1	1	1
G3PDH 5' (10 µM)	-	1	-	1
PCR Primer 1 (10 µM)	1	-	1	-
Ligation Analysis PCR Master Mix	22	22	22	22
Total volume	**25**	**25**	**25**	**25**

*Tester 1-1 and 1-2 are for embryo's experimental tester control cDNA and the same set-up was used for Tester 2-1 and 2-2 (the experimental tester treated cDNA, 3-1 and 3-2 (the control skeletal muscle cDNA).

4.2.10 First hybridisation

For each subtraction, 1.5 µl of *Rsa* I-digested Driver cDNA, 1.5 µl Adaptor 1-ligated Tester 1-1 or Adaptor 2R-ligated Tester 1-2, and 1 µl 4X Hybridization Buffer (200 mM HEPES-HCl [pH 8.0], 2 mM NaCl, 0.8 mM EDTA [pH 8.0]) were combined and incubated at 98^{o}C for 1.5 min followed by 68^{o}C for 12 hr. The same was applied to Tester 2-1 and 2-2, 3-1 and 3-2.

4.2.11 Second hybridisation

For the second hybridisation, the following reagents were added into a sterile tube: 1 µl of Driver cDNA, 1 µl of 4X Hybridisation buffer, and 2 µl of sterile H_2O and mixed well, then 1 µl of the mixture was placed in a 0.5 ml microcentrifuge tube and incubated at 98^{o}C for 1.5 min in a thermal cycler. The denatured driver sample is then simultaneously mixed with hybridization samples 1 and 2 followed by overnight incubation at 68^{o}C. Finally, 200 µl of dilution buffer (20 mM HEPES [pH 8.3], 50 mM NaCl, 0.2 mM EDTA [pH 8.0])) was added, and the mixture was heated for 7 min at 68^{o}C. All samples were stored at -20^{o}C until further processing.

4.2.12 PCR amplification

To prepare the PCR templates, 1 µl of each of the subtracted samples (section 4.2.11) and the unsustracted tester control (section 4.2.8) was diluted in 1 ml H_2O, and then 1 µl of the diluted cDNA was mixed with 19.5 µl sterile H_2O, 2.5 µl 10X PCR reaction buffer, 0.5 µl dNTPs (10 mM), 1 µl PCR Primer 1 (10 µM), and 0.5 µl 50X Advantage cDNA Polymerase Mix. The reaction mixture was incubated for 5 min at 75^{o}C in a thermal cycler to extend the adaptors. This was followed by an initial denaturation at 94^{o}C for 25 sec, and the 37 cycles of denaturation at 94^{o}C for 10 sec, annealing at 66^{o}C for 30 sec, and extension at 72^{o}C for 1.5 min. After 27, 32, and 37 cycles aliquot was analysed on 1.5% agarose/EtBr gel in 1X TAE buffer. For the second PCR reaction, 3 µl of each primary PCR product was diluted in 27 µl H_2O and 1 µl of the diluted PCR product was mixed with 18.5 µl sterile H_2O, 2.5 µl 10X PCR reaction buffer, 1 µl Nested PCR primer 1 (10 µM), 1 µl Nested PCR primer 2R (10µM), 0.5 µl dNTP mix (10 mM), and 0.5 µl 50X Advantage cDNA Polymerase Mix. The PCR was run for 12 cycles using 94^{o}C for 10 sec for a denaturation, an annealing at 68^{o}C for 30 sec, and an extension period at 72^{o}C for 1.5 min. An aliquot was analysed on a 1.5% agarose/EtBr gel in 1 x

TAE buffer. Gel areas containing the PCR product bands were excised on a UV transilluminator with a scalpel. The gel slices were purified using the protocol described in section 2.2.9. The eluted samples were stored at -20^{o}C until further processing.

4.2.13 Cloning of PCR generated fragments

Chemically competent *E. coli* cells were prepared under aseptic conditions; a Luria-Bertani (LB) agar plate containing 30 µg/ml streptomycin was streaked with MAX Efficiency® DH10B™ *E. coli* cells (Invitrogen, U.K) and incubated at 37^{o}C overnight. Two individual colonies were used to each inoculate at 5 ml aliquot of LB broth containing 10 µg/ml streptomycin that was then incubated at 37^{o}C overnight at a speed of 200 rpm. Both cultures were then added to 200 ml LB broth containing 10 µg/ml streptomycin pre-heated to 37^{o}C and were maintained at this temperature at a speed of 200 rpm to achieve an optical density (OD_{600}) approaching to obtain cells in the mid-log phase of growth. The culture was then chilled on ice for 5 min before being centrifuged in a pre-cooled centrifuge at 4^{o}C for 15 min at 3500 rpm. The supernatant was discarded and the cell pellet was re-suspended in 20 ml Transformation Buffer I (30 mM potassium acetate, 10 mM rubidium chloride, 50 mM manganese chloride, and 15% volume per volume glycerol) and incubated on ice for 10 min. Centrifugation was repeated using the previous parameters, the supernatant was discarded and the pellet was carefully re-suspended in 2 ml Transformation Buffer II (10 mM MOPs, 75 mM calcium chloride, 10 mM rubidium chloride, and 15% volume per volume glycerol) with minimal mechanical agitation of the cells and subsequently incubated on ice for 20 min. Aliquots of 50 µl were snap-frozen in liquid nitrogen and then stored at -80^{o}C until further processing. For the ligation reaction, 1.5 µl of the PCR product was mixed with 0.25 µl H_2O, 0.25 µl of 5X Ligation Buffer, 0.5 µl of pCR®2.1 vector (25 ng/µl) (LifeTechnologies, Paisley, U.K.), and 0.5 µl T4 DNA Ligase (4.0 Weiss units). The reaction mixture was incubated overnight at 14^{o}C. The samples were stored at -20^{o}C until use for transformation. To transform the ligated construct into competent DH10B *E. coli* cells, 2 µl of each ligation reaction was mixed gently with 50 µl of DH10B *E. coli* and incubated on ice for 30 min. The cells were heat shocked for 75 sec at 42^{o}C without shaking and then immediately transferred into ice. 250 µl of room

temperature LB broth was added and shaken horizontally at 37°C for 1 hr at 225 rpm in a shaking incubator. 50 µl from each transformation was spread on LB agar plates containing 100 µg/ml ampicillin and X-Gal (20 mg/ml DMSO), and incubated overnight at 37°C. White colonies, indicating a successfully transformed clone, were picked and cultured overnight in 5 ml LB broth containing 100 µg/ml ampicillin. The culture was then centrifuged, the pellet was mixed with 200 µl H_2O and heated at 100°C for 5 min. Samples were screened for inserts using the vector-based primers M13 (M13 Reverse: 5'CAGGAAACAGCTATGAC3' and M13 Forward 5'GTAAAACGACGGCCAG3') and was performed using the Thermal Cycler with a 105°C heated lid. All reactions were initially denatured at 94°C for 2 min, then followed with 35 cycles of denaturation at 94°C for 30 sec, 30 sec at 50°C for annealing, and 1 min at 72°C for an elongation step, followed by a final single extension step of 7 min at 72°C.

4.2.14 Sequencing of the subtracted cDNA clones

Samples containing inserts were purified using the Plasmid DNA purification kit (Macherey-Nagel, Germany). 5 ml of a saturated DH10B *E. coli* LB culture was pelleted for 30 sec at 11,000 rpm. The supernatant was discarded and the pellet was resuspended in 250 µl of Buffer A1 (composition is confidential). 250 µl of Buffer A2 (composition is confidential) was then added and mixed gently by inverting the tube 8 times, followed by incubation at room temperature for 5 min until the lysate appeared clear. 300 µl of Buffer A3 (composition is confidential) was added, mixed by inverting the tube 8 times, and centrifuged for 5 min at 11,000 rpm. The supernatant was transferred into a NucleoSpin® Plasmid/Plasmid (NoLid) Column and centrifuged at 11,000 rpm for 1 min to blind the DNA. The flow-through was discarded and 500 µl of Buffer AW (composition is confidential) was added into the column and centrifuged for 1 min at 11,000 rpm. To wash the silica membrane, 600 µl of Buffer A4 (composition is confidential) was added, the mixture was centrifuged for 1 min at 11,000 rpm, and the flow-through discarded. To dry the silica membrane, the mixture was centrifuge for an additional 2 min at 11,000 rpm. To elute the DNA, the Column was placed in a new 1.5 ml microcentrifuge tube and 50 µl of Buffer AE (composition is confidential) added. The mixture was then incubated for 1 min at room temperature and centrifuged at 11,000 rpm for 1 min. The DNA concentration of the samples was measured with the

QubitTM fluorometer (Invitrogen Detection Technologies) (as described in section 2.2.11) to obtain the desired amount of sample needed for sequencing. Together with the forward primer, a sample with a total volume of 10 µl (containing 50-100 ng DNA, 0.25 µl of 1.5 µ M M13 forward primer) was then sent to the commercial sequencing company Macrogen (Amsterdam, Netherlands).

4.2.15 Bioinformatics analysis

The SSH approach was used to construct the forward and reverse subtracted cDNA libraries, 63 positive (white, insert-containing) colonies (36 from the forward library and 27 from the reverse library) were selected and sequenced by a commercial sequencing company (Macrogen, Amsterdam, The Netherlands). BLAST searches (http://blast.ncbi.nlm.nih.gov/Blast.cgi) were then used to find similar sequences in the NCBI GenBank repository as a means of identifying the subtracted sequences. The sequences with an alignment of *E*-value < 10^{-3} (Table 4.3) were selected as a limit for identification of potential genes (Table 4.2).

Table 4.2. Primer sequences used for expression analysis of selected differentially expressed target mRNAs in *D. rerio* embryos exposed to AgNPs and control samples.

Gene name	Forward primer (5'-3')	Reverse primers (5'-3')
Spermatogenesis associated protein 2 (*spata 2*)	GGATATGGGGGACGACTTTT	CGCGAAGTTCTGTTCTTTCC
Cytochrome c oxidase subunit I (*COXI*)	TTGGCCACCCAGAAGTCTAC	GCTCGGGTGTCTACATCCAT
Actin alpha, cardiac muscle lb (*actclb*)	AAGGCCAACAGGGAGAAGAT	CTCATAGACGGGGACGTTGT
Solute carrier family 25, member 5 (*SLC 25A5*) mRNA	AAGCGACACCTCTCCAAGAA	GCAGTCCATAATGCCCTTGT

4.2.16 qPCR validation

Selected target mRNAs that had been identified using the SSH protocol above, were chosen for parallel validation using the qPCR technique. The subtracted libraries represented either up- or down-regulation of mRNA transcripts (representing possible genes) in response to AgNP exposure and had been derived from 2 pools of cDNA: AgNP-exposed embryos and control embryos (see section 4.2.4 above), and this pattern should therefore also be reflected in the qPCR analysis of individual embryo samples that have been subjected to the same exposure regime. All qPCR reactions were performed in duplicate following the protocol described in section 3.2.8 and using the primers contained in Table 4.2). The identity of each target gene was verified and the efficiency examined using the same protocol described in section 3.2.5. The Ct was detected for each target gene and normalized to the reference genes *18S.1* and *EF.1*.

4.2.17 Statistical analysis

The qPCR relative expression values were analysed for homogeneity of variances and significant differences between control and the AgNP treatment samples as described in section 3.2.10.

4.3 Results

4.3.1 SSH analysis

A total of sixty-three differentially expressed mRNA sequences were isolated, sequenced and then compared with sequences in the NCBI database using the blastn algorithms as described in section 4.2.15. Of these, 12.69% represented novel clones that could be identified. The remaining sequences showed no similarity with the sequences available in the GenBank database. In the reverse library there were 2 novel sequences 3.17% isolated (Figure 4.2), and in the forward library 6 novel sequences, representing 9.52% (Figure 4.3). The remaining sequences showed no significant similarity to sequences in the available public databases.

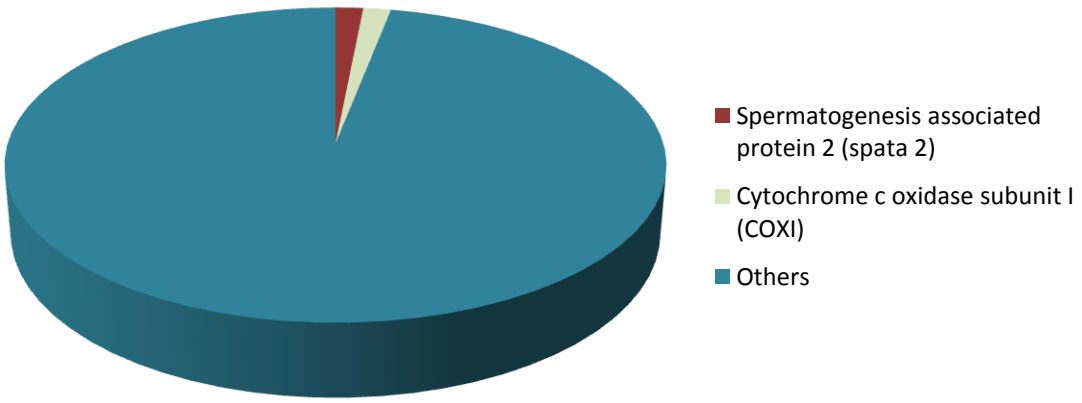

Figure 4.2. Pie chart showing the proportion of down-regulated transcripts (in 4 nm size range AgNP- treated *D. rerio* embryos relative to healthy *D. rerio* embryos) that were identified with a similarity search using the GenBank database.

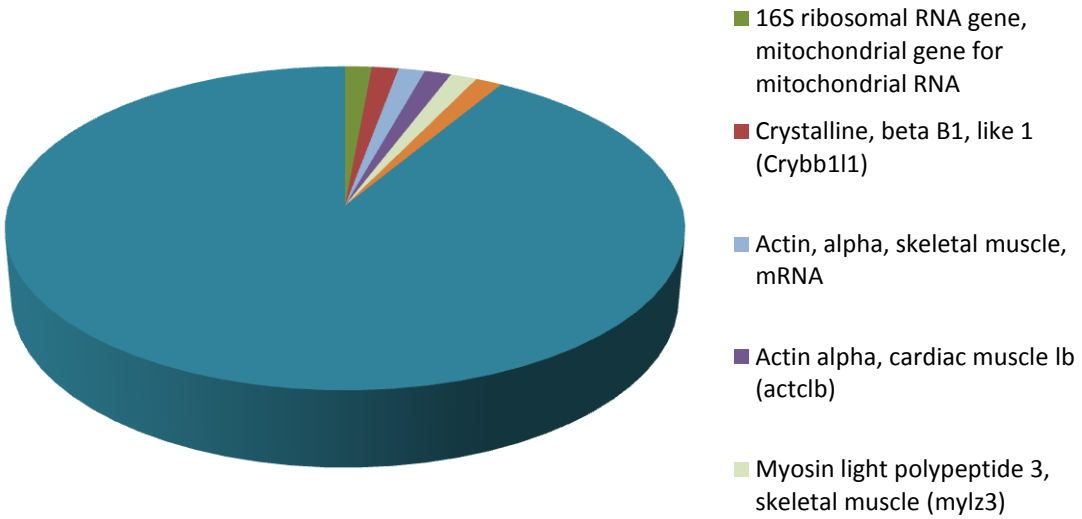

Figure 4.3. Pie chart showing the proportion of up-regulated transcripts (in 4 nm size range AgNP- treated *D. rerio* embryos relative to healthy *D. rerio* embryos) that were identified with a similarity search using the GenBank database.

Table 4.3. Differentially expressed (subtracted) mRNAs isolated from *D. rerio* embryos exposed to 4-nm range AgNPs (1.925 mg/L).

Gene identity	Number of sequences	GenBank accession no.	Homologous species	*E-value*	Size (bp)
Down-regulated in *D. rerio* embryos exposed to AgNP					
Spermatogenesis associated protein 2 (*spata 2*)	16	DQ869310.1	*D. rerio*	0.0	2936
Macoma balthica isolate W20 mitochondrion, partial genome (*Cytochrome c oxidase subunit I* (*COXI*))	1	KM373204.1	*M. balthica*	1e-08	15606
Up-regulated in *D. rerio* embryos exposed to AgNP					
16S ribosomal RNA gene, mitochondrial gene for mitochondrial RNA	21	AF036006.1	*D. rerio*	0.0	1623
Crystalline, beta B1, like 1 (*Crybb1l1*)	1	XM_005169625.2	*D. rerio*	0.0	2043
Actin, alpha, skeletal muscle, mRNA	1	BC161649.1	*D. rerio*	0.0	3107
Actin alpha, cardiac muscle lb (*actclb*)	5	NM_131591.1	*D. rerio*	0.0	1284
Myosin light polypeptide 3, skeletal muscle (*mylz3*)	3	NM_131619.2	*D. rerio*	0.0	986
Solute carrier family 25, member 5 (*SLC25A5*) mRNA	5	AY398420.1	*D. rerio*	0.0	1297

4.3.2 qPCR validation of the differentially expressed mRNA transcript levels

Four randomly selected target mRNAs were used to validate the SSH differential transcription results using qPCR (Figure 4.4). *Spata2* and *COXI* showed no regulation in 4 nm AgNP-treated *D. rerio* embryos compared with control *D. rerio* embryos (Figure 4.4 A and B), the results were not significant (t(14)=0.061; *p*=1.000 and t(14)=0.601; *p*=0.721). actclb was not significantly different (t(14)=-1.596; *p*=0.130) (Figure 4.4C), where *SLC25A*5 was significantly up-regulated (t(14)=-2.454; *p*=0.021) in 4 nm AgNPs treated *D. rerio* embryos compared with healthy *D. rerio* embryos (Figure 4.4D).

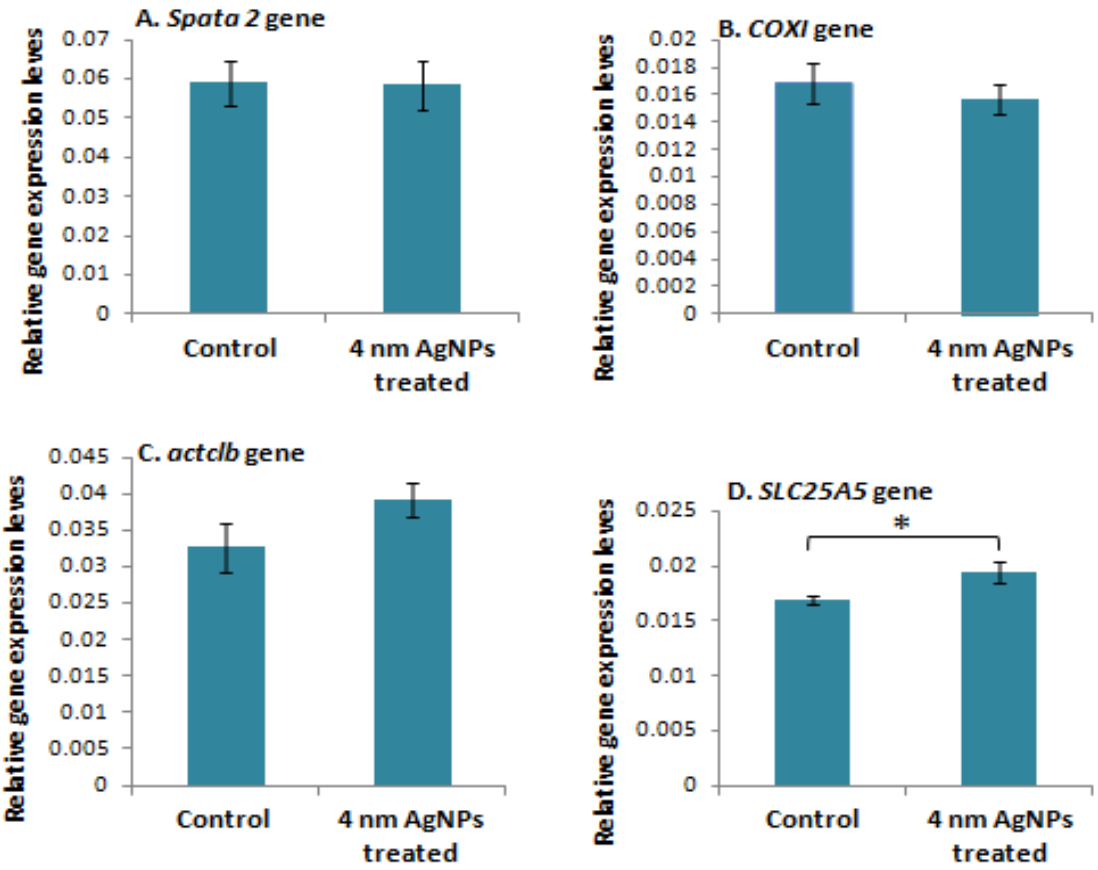

Figure 4.4. Relative mRNA transcript expression levels, in *D. rerio* embryos, of *target* mRNAs previously identified as differentially regulated by the SSH approach. Data are expressed as normalized average relative mRNA transcript level +/- SEM in *D. rerio* embryos for (A) *Spata 2,* (B) *COXI,* (C) *actclb*, and (D) *SLC25A5* genes. N=20. *P*= < 0.05.

4.4 Discussion

In this chapter, the main aim was to isolate novel genes that are impacted by AgNP exposure in *D. rerio* embryos. To do this the following steps were taken:

- Two SSH libraries enriched with genes that are differentially expressed as a result of exposure to 4 nm size range AgNP (1.925 mg/L), were made.
- cDNA inserts, representing the differentially regulated genes, were cloned, sequenced, and characterization according to their similarity to published sequences already available in the GenBank database.

As a result, 12.7% of novel clones were identified which is comparable to similar studies used the SSH to identified genes using vertebrates and invertebrates (6-53%, Gurskaya et al., 1996; Tsoi et al., 2004; Boutet et al., 2008; Leelatanawit et al., 2008; Craft et al., 2010; Mattos et al., 2010; Ciocan et al., 2011; Ciocan et al., 2012), and four targeted mRNA transcripts were used to validate the SSH results using qPCR. Using the SSH approach several genes were highlighted as differentially regulated upon AgNP exposure (Table 4.2). Only two genes were identifiable from the down-regulated cDNAs sequenced: *Spata* 2 and *COXI* (Table 4.2). While these transcripts showed no regulation in expression, the change in relative expression following AgNP exposure was not significant using the qPCR validation technique (perhaps for reasons that will be discussed later). Each of these genes will now be discussed in turn.

Spata2 relative expression was identified as not regulated in 4 nm AgNPs treated *D. rerio* embryos compared with control *D. rerio* embryos (Table 4.3). *D. rerio spata2* shares 37% identity with the human *spata2* which play a main role in regulating spermatogenesis (Maran et al., 2009). The highest expression of *spata2* have been detected in the brain of human and rodents while less abundant transcripts were found in skeletal muscle and kidneys (Onisto et al., 2001). At the same time, adult *D. rerio* was found to express high level of *spata2* mRNA which provided proof that this gene may have even more functions in *D. rerio* development (Moro et al., 2007). Spermatogenesis process is very sensitive to environmental toxicants (Pryor et al., 2000), the potential impacts of adverse environmental factors can affect not only the developing offspring, but also the male fertility by the decrease in the amount of sperm produced (Anway and Skinner, 2008; Boisen et al., 2001). Effects of Mo, Pb, Rb and As showed inhibition of spermatogenesis in Japanese eel (*Anguilla japonica*) testes (Yamaguchi et al., 2007). NPs are one of the toxicants of concern, and many studies suggested that these NPs are toxic to many organs including the testes (Li et al., 2009;

Yauk et al., 2008). NPs size impacted spermatogenesis, with 20 nm AgNP found to be more toxic than 200 nm (Gromadzka-Ostrowska et al., 2012). Different studies have also examined the effects of NPs on the male reproductive system as follows. MWCNTs reduced spermatogonia number in male mice (Bai et al., 2010). Human sperm motility and viability percentage were significantly reduced after treatment with up to 500 µM of AgNP (Terzuoli et al., 2011). A comparable study using male mice injected with high dose (500 mg/kg) of nanosized TiO_2NPs showed significantly reduced sperm density and motility (Guo et al., 2009), and a decreased in spermatogonia, spermatocytes, spermatids and mature sperm was observed in male infants of mice mothers treated with doses higher than 50 mg/kg of DMSA-coated magnetic NPs (Noori et al., 2011). These studies indicate that spermatogenesis reduced after exposure to different toxicants including NPs.

COXI is the subunit one of Cytochrome c oxidase that transfers electrons from reduced cytochorome c to oxygen and participates in maintaining the electrochemical gradient across the internal mitochondrial membrane (Baklouti-Gargouri et al., 2013). In the current study, no regulation of *COXI* in 4 nm AgNPs treated *D. rerio* embryos compared with healthy *D. rerio* embryos was observed (Table 4.3). On the other hand, 12 nm SiO_2 NPs (1-50µg/mL) decreased levels of cytochrome C oxidase subunit II and NADH dehydrogenase subunit 6 in Human U87 astrocytoma cells led to decreased mitochondrial energy production and decreased cell viability or proliferation signalling (Lai et al., 2010). Human lung cells also showed down-regulation of mitochondrial DNA-encoded genes involved in the maintenance of mitochondrial membrane potential after exposed to 45 nm nanosized PAMAM (polyamidoamine) dendrimers (Lee et al., 2009). In the freshwater bivalves (*Corbicula fluminea* and *Dreissena polymorpha*) and the marine bivalve (diploid or triploid *Crassostrea gigas*) *COXI* was down-regulated after exposure for 10 days to $ZnCl_2$ (15.3 µM Zn^{2+}) and $CdCl_2$ (0.13 µM Cd^{2+}) suggesting the metal component is toxic too (Achard-Joris et al., 2006). Furthermore, COX activity has been seen significantly decreased in the mitochondria of male Sprague Dawley rats after exposure to 250 mg/Kg AgNPs of 75nm-AgNPs once a week, during 1 month compared to control, while 10 nm AgNPs failed to cause damage to COX (Da silva, 2014). The reduced level of COX activity has been found to cause

functional reduction in Na^+-K^+- ATPase capacity, an important factor responsible for neuronal death in the mammalian brain (Greenamyre et al. 1999). Exposure to some toxic materials including NPs could decrease the COX activity and decrease expression of *COXI*.

On the other hand, this study showed up-regulation in *SLC25A*5 in 4 nm AgNPs treated *D. rerio* embryos compared with healthy *D. rerio* embryos (Figure 4.4D). Actins are considered as highly conserved proteins involved in cell mobility (Martins et al., 2013). There are three main groups of actin isoforms, alpha, beta, and gamma. The alpha actins are the major part of the contractile apparatus and found in muscle tissue (Martins et al., 2013). Exposure of 20 nm AgNP in primary rat cortical cell cultures led to an apparent loss of filamentous actin (F-actin) which is part of the actin (Xu et al., 2013). Changes in actin expression are therefore occasionally observed following AgNP exposure.

The solute carrier family 25 (SLC25) is known to have many different members known to transport molecules over the mitochondrial membrane (Haitina et al., 2006). *SLC25A5* is one of the SLC25 family members and is a highly conserved gene that is expressed in high levels in the cortex and hippocampus of human, and subsequently has been considered as a novel gene for non-syndromic intellectual disability human (Vandewalle et al., 2013). The function of the protein encoded by the *SLC25A5* on the X chromosome of humans is a counter-transporter for ADP/ATP exchange between the mitochondrial matrix and cytoplasm (Chevrollier et al., 2011; Ho et al., 2013). *SLC25A5* has been used as a target and growth marker for studies related to tumour cell growth (Chevrollier et al., 2011). No previous studies were found on the *SLC25A5* expression after exposure to environmental toxicants. However, *slc25a22* gene, a related homologue, was observed as up-regulated by two types of nanosilver, Ag nanocolloids (10 µg/L of 20-50 nm Ag NCs) and Ag nanotubes (1µg/L of 20-30 nm Ag NTs) adult *D. rerio* (Park and Yeo, 2014).

In summary, this chapter focused on isolating and characterising differentially regulated genes from *D. rerio* embryos exposed to 4 nm AgNPs. Of the sequences identified, transcripts associated with fertility, membrane transport, and cell mobility,

were highlighted as potentially impacted by exposure to 4 nm sized AgNPs (1.925 mg/L). These represent potential new biomarkers on AgNP exposure that could be used in future experiments concerned with early detection of impacts or with understanding the mechanisms of toxicity.

5. Chapter Five: Nanotoxicity of polyelectrolyte-functionalized titania nanoparticles towards *D. rerio* embryos

5.1 Introduction

One of the most widely used engineered NPs on a global scale are TiO_2NPs due to its photocatalytic properties (Rollerova et al., 2015). TiO_2NPs are used in sunscreens and cosmetic creams (Gelis et al., 2003) because of their ability to block UV light (Tsuji et al., 2006). They are also used in other consumer products such as toothpaste (Kaida et al., 2004), skin treatments (Wiesenthal et al., 2011), as well as having therapeutic uses such as photosensitizing agents for photodynamic therapy of endobronchial and esophageal cancers (Ackroyd et al., 2001), paints, pigments and food industry (Chen and Poon, 2009; Koivisto et al., 2012). They are also applied in wastewater treatment as a disinfectant (Cho et al., 2004), as well as in environmental decontamination of soil, air, and water (Esterkin et al., 2005; Choi et al., 2006).

The Australian government, Department of Health, Therapeutic Goods Administration (TGA) categorised the TiO_2NPs into different forms: rutile, anatase, and amorphous (TGA, 2013). Anatase TiO_2NPs are generally found to be more toxic than rutile TiO_2NPs (Al-Awady et al., 2015). TiO_2NPs can be toxic when released into the aquatic environment as it forms superoxide and hydroxyl radicals on exposure to sunlight and oxygen, which could then lead to damage of the cell contents (Dunford et al., 1997; Uchino et al., 2002). Several sunscreen products contain anatase TiO_2NPs, which were also found to cause ROS (Barker and Branch, 2008). The photoactivated TiO_2NPs can induce the generation of ROS which leads to biological damage (Dodd and Jha, 2011). In contrast, the potential of TiO_2NPs to produce oxidative damage to DNA without photoactivation is still unclear (Petersen et al., 2014). Thus, it is necessary to characterise the toxicity and potential biological effects posed by this type of NP.

In previous published work, these types of NP toxicity have shown to be size-dependent, with the smaller particles found to have higher mobility to move between biological sections (Hoshino et al., 2004). For example the 4 nm TiO_2NPs size can penetrate into the deeper layer of the epidermis (to the basal cell layer) (Wu et al., 2009). On the other hand, covering TiO_2NPs with coating agents (e.g., inert oxides of

silica, alumina, or zirconium) could help in reducing or eliminating ROS generating by TiO_2NPs following UV irradiation (Mills and Le Hunte, 1997). Coatings based on silicon dioxide were found to be very effective in reducing the oxidative activity of TiO_2NPs (Carlotti et al., 2009). Moreover, TiO_2NPs aggregation has also been considered as an important factor in understanding potential cytotoxicity (Baveye and Lada, 2008). TiO_2NPs for instance, are found in sunscreen as large aggregates or agglomerates after application onto skin (Schilling et al., 2010). Additionally, large TiO_2NPs aggregates (596 nm) have shown a larger effect on cell viability and gene expression of biomarkers focused on stress, inflammation, and cytotoxicity of a human acute monocytic leukemia and bronchial epithelial cell line when compared with the effect of small aggregates (166 nm), which suggests that particle size is related to cellular effects (Okuda-Shimazaki et al., 2010).

Overall, the increased use of TiO_2NPs and their ultimate release into the environment suggests an increasing need to evaluate their potential toxicity. The probability of human exposure to TiO_2NPs can occur by the use of TiO_2NPs products through inhalation and dermal applications. Therefore, studying the viability and morphology of *D. rerio* embryos after exposure to TiO_2NPs, alongside the characterization of possible early warning biological effects markers of exposure is particularly useful. *D. rerio* have been used as a model species in toxicological studies as described in section 1.7. In this study, *D. rerio* embryos were used to study the effect of TiO_2NPs coated with a different number of layers of anionic and cationic polyelectrolytes on embryo viability, and the level expression level of selected target genes. These targeted genes have been selected based on results obtained previously in section 3.3.4. *SOD2.*1, *HIF.*4, and *Pxmp2.*4 mRNA in *D. rerio* embryos were selected, washed with deionized water and exposed to control and test media (0, 500 and 1000 mg/L) for a 3 hr exposure duration in dark conditions and visible light. Embryo viability, morphology, and differential mRNA transcript following a controlled experimental exposure to TiO_2NPs relative to control embryos were thus investigated in this chapter.

5.2 Materials and methods

5.2.1 Preparation and characterisation of TiO_2NPs

The synthesis of TiO_2NPs was modified and prepared using a method described by Al-Awady et al. (2015) and carried out by research staff in the laboratory of Prof. Vessellin Paunov (Co-supervisor at University of Hull. This involved two different steps: (i) hydrolysis reaction of titanium isopropoxide (TTIP) by adding 1 M HNO_3 drop-wise to 250 ml of Milli-Q water to adjust the pH to 2 and 15 ml aliquot of isopropanol was added, and then 5 ml of TTIP was added drop-wise to the mixture with strong stirring until a white turbid dispersion was formed. (ii) The suspension of $Ti(OH)_4$ was heated at 70^{o}C for 20 hr to yield a yellow-white precipitate of titania, washed it with ethanol and dried it under vacuum (Gallenkamp vacuum oven) at 100^{o}C for 2 hr. The titania produced was annealed again at different temperautures (100-800^{o}C) for 2 hr to prepare different crystallite size of TiO_2NPs. The crystallite sizes of titania were characterised in solid state using Siemens D5000 X-Ray Diffractometer (XRD) using 0.15418 nm wavelength (CuKα-line). The crystallite size was measured using Scherrer's equation. The aqueous dispersions of TiO_2NPs were prepared by dispersing 4 mg of each titania sample in 10 ml aqueous of 20 mM aqueous solution of NaCl at pH 4 using digital sonicator (Branson 450, 5 mm tip, 400 W maximum power) at 40% of the maximum power for 10 min at 1 s ON/1 s OFF pulse time. Aqueous was then filtered using a syringe filter of pore size 0.22 µm. The characterization of the TiO_2NPs size distribution and zeta potential was done using a Zetasizer Nano ZL (Malvern, UK). pH was adjusted from 2-9 using 1 M HCl/1 M NaOH to test the pH effect on the particle hydrodynamic diameter and zeta potential.

The polyelectrolyte-coated TiO_2NPs was prepared using titania and annealed at 100^{o}C (anatase). 10 ml of 1500 µg/ml TiO_2NPs dispersion in Milli-Q water was added dropwise to 10 ml of 10 mg/ml of (sodium 4-styrene sulfonate) sodium salt (PSS) solution (M.W. ~70 kDa) dissolved in 1 mM NaCl solution and shaked for 20 min. The particles were centrifuged three times for 1 hr at 8000 rpm to wash the excess of PSS and finally dispersed in 10 ml of Milli-Q water. The PSS-coated TiO_2NPs were then mixed dropwise with 10 ml of 10 mg/ml of poly (allylamine hydrochloride) (PAH) (M.W. 15 kDa) dissolved in 1 mM NaCl solution, shaken for 20 min and then

centrifuged three times for 1 hr at 8000 rpm to produce TiO_2NPs/PSS/PAH. After each polyelectrolyte coat, the TiO_2NPs were characterised using Zetasizer Nano ZL to check their zeta potential and the particle aggregation.

Three different batches consisting of: bare titania NPs (TiO_2NPs), anionic NPs of TiO_2NPs/PSS, and the cationic NPs of TiO_2NPs/PSS/PAH, were kindly supplied by Prof. Vesselin Paunov. The layer-by-layer assembly technique was used to coat 25 nm anatase TiO_2NPs with alternating layers of alternating charge of PSS and PAH polyelectrolytes (Al-Awady et al., 2015).

5.2.2 *D. rerio* embryos exposure to TiO_2NPs

At the aquarium facilities of the University of Hull, twenty healthy *D. rerio* (1 male to 2 females approximately) were placed in 20 L water tank with dimensions (20 cm Width x 38.5 cm Length x 34 cm Height), with a water level of 30 cm, 25^{o}C and pH 8.1). In the bottom, egg catchers were placed. Egg catchers were cleaned three days prior collection and healthy *D. rerio* embryos at 0-72 hpf were collected and exposed to a treatment concentration of test media (bare TiO_2NPs, TiO_2NPs/PSS, or TiO_2NPs/PSS/PAH) and incubated for 3 hr in either dark conditions or illuminated with visible light (fluorescent light bulb, 220-240V, 23W), at particle concentrations (0, 500 or 1000 mg/L). The concentrations were selected based on Al-Awady et al, (2015) which stated a toxicity concentration threshold for TiO_2NPs for yeast cells in this range. Healthy *D. rerio* embryos were used as a control reference group in parallel. Embryos were expected to incubate under UV light over the same duration and concentration as normal light, yet a sudden drop in *D. rerio* egg-laying was observed and therefore the UV light exposure regime data was excluded from this study.

5.2.3 *D. rerio* embryos viability after exposure to TiO_2NPs

Ten embryos from each exposure regime (control, bare TiO_2NPs, TiO_2NPs/PSS, and TiO_2NPs/PSS/PAH) were isolated after the exposure and washed with molecular grade water (Fisher Scientific, Fair Lawn, New Jeresy, USA) three times, re-dispersed with 1 mL molecular grade water and incubated with a drop of 98% Fluorescein diacetate (FDA) (Fluka, U.K.) in acetone (0.5 mg/L) for 15 min. The embryos were then washed again with molecular grade water and the viability was examined by using Olymbus

BX51 fluorescence microscope attached to a DP70 digital camera and FITC fluorescence filter set. FDA is taken up by living cells and is hydrolysed to fluorescein, which fluoresces green, and thus determines which cells are living (green) (Oparka and Read, 1994). Assays were performed immediately after adding the FDA dye.

5.2.4 Transmission Electron Microscopy (TEM) imaging

The morphology of *D. rerio* embryos after 3 hr incubation with 0, 500 or 1000 mg/L of bare TiO_2NPs TiO_2NPs/PSS, or TiO_2NPs/PSS/PAH were examined with Transmission Electron Microscopy (TEM) using the following protocol. The embryos were washed with molecular grade water and fixed in 2.5% Glutaraldehyde (0.5 ml 25% Glutaraldehyde stock solution, 4.5 ml 0.1 M cacodylate buffer and glucose (20 mL 0.2 M cacodylate stock, 10 mL Mili-Q water, 0.216 g glucose, pH was dissolved with HCL to 7.3, and volume was made up to 40 mL) for 1 hr at room temperature. Next, cacodylate buffer was removed and embryos were fixed by 1% Osmium tetra-oxide in cacodylate buffer (2.5 mL 2% Osmium tetroxide, 2.5 mL 0.1 M cacodylate buffer and glucose 0.03M) at 4^{o}C overnight. After cacodylate buffer was removed, embryos were stained for 30 min with 1% uranyl acetate (2 ml 2.5% uranyl acetate stock, final volume 3 mL) and washed with solutions of ethanol of increasing concentration (30%, 50%, and 70% overnight). The embryos were washed again the next day with ethanol solutions of 90% and 100%. After standard dehydration, the embryos were embedded in fresh Epon/araldite at 60^{o}C for 48 hr. Embryos were removed from the oven and allowed to stand at room temperature for 48 hr, then sectioned using an ultramicrotome. An Oxford Instruments INCA Energy Dispersive Spectroscopy (EDS) was attached to the TEM and run at 120 KV to identify and semiquantitavely characterize the TiO_2NPs on *D. rerio* embryos. The sectioned samples were imaged using a JEOL 2010 TEM (Japan) operating at 80 kV and images were all captured with a Gatan Ultrascan 4000 digital camera and the corresponding software for imaging was the Digital Micrograph.

5.2.5 Quantitative PCR method

5.2.5.1 *D. rerio* embryos

Ten embryos that had been exposed to (bare TiO_2NPs, TiO_2NPs/PSS, or TiO_2NPs/PSS/PAH) at 500 or 1000 mg/L particle concentration for 3 hrs, in the dark or illuminated with visible light, were used as the exposed treatment groups. In parallel, 10 healthy, non-exposed embryos were used at each exposure as a control reference group.

5.2.5.2 Total RNA isolation

All the ten embryos collected from each exposure group were used to make a pooled sample. The total RNA extraction from each pooled sample were carried out following the protocol described in section 2.2.3 and stored at -80^{o}C until further processing.

5.2.5.3 First strand synthesis of cDNA for qPCR

100 ng of pooled RNA was used to generate cDNAs following the protocol described in section 2.2.5 and stored at -20^{o}C.

5.2.5.4 Oligonucleotide primer design, optimization and assay performance

Three target genes were selected (*SOD2.1, HIF.4,* and *Pxmp2.4* genes) for qPCR analysis using the exposed and control embryos samples. Primers were already designed as described in section 2.2.6, and optimized as described in section 3.2.5. Primer efficiency was determined in section 3.2.6.

5.2.5.5 Amplification using qPCR

The qPCRs analyses for each pooled cDNAs were carried out following the protocol described in section 3.2.8.

5.2.5.6 Quantification of mRNA transcript

The relative quantification method used to measure changes in mRNA transcript of each target gene, in the treatment group compared to control samples, is described in section 3.2.9.

5.2.5.7 Statistical analysis of qPCR data

Each target gene was tested individually for significant differences among controls and each treatment group. All data were tested for homogeneity of variances using Levene's test in SPSS. A non-parametric (Scheirer-Ray-Hare test) was used to assess the effect of anatase TiO_2NPs coating type (factor 1), TiO_2NPs concentration (factor 2) and the exposure condition (factor 3) and determine the interactions among them. Significance for relative gene expression, between TiO_2NPs different coatings, concentrations or conditions was tested individually using the Kruskal-Wallis non-parametric test for data that is distributed significantly different from normal. Differences were considered significant at $P<0.05$.

5.3 Results

5.3.1 Effect of TiO_2NP exposure on *D. rerio* embryo viability

Ten embryos were used for each concentration of different types of TiO_2NPs samples (bare TiO_2NPs, TiO_2NPs/PSS, or TiO_2NPs/PSS/PAH). A fixed amount of TiO_2NPs of each sample was incubated with *D. rerio* embryos in dark or illuminated with visible light for 3 hr. Control samples were used in parallel under the same condition for the same periods of time. The viable embryos stained with FDA, fluoresced under a fluorescence microscope (Fig. 5.1). All embryos showed no significant change in the embryo viability (Table 5.1). The percentage of embryo viability for controls and each treatment group are shown in Table 5.1.

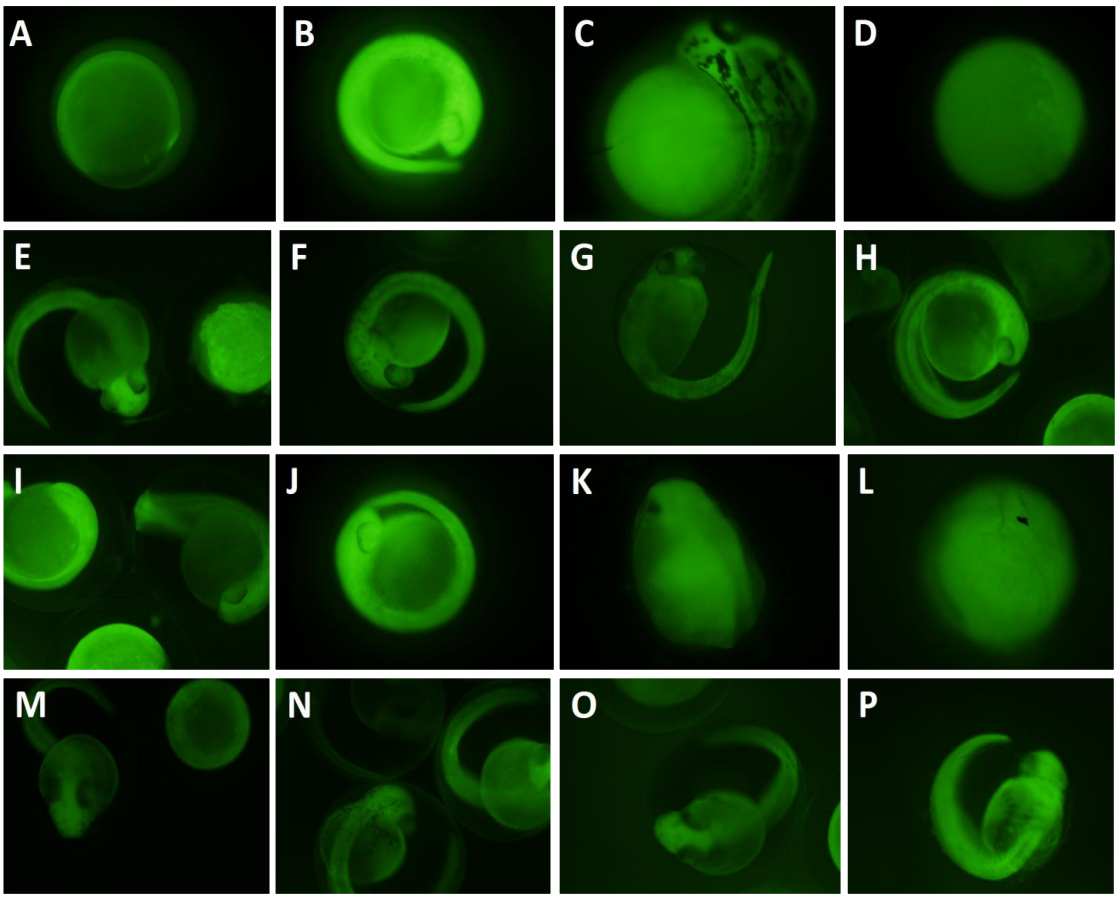

Figure 5.1. FDA stained *D. rerio* embryos of different types of TiO_2NPs samples using a total concentration of 500 and 1000 mg/L for each media under dark and visible light conditions. The viability was examined using Olymbus BX51 fluorescence microscope attached to a DP70 digital camera and FITC fluorescence filter set. FDA is taken up by living cells and is hydrolysed to fluorescein, which fluoresces green, and thus determines which cells are alive (green). (A-H) Embryos treated in dark condition. (I-P) Embryos treated in visible light condition. (A, E, I, and M) Control, untreated embryos for each batch; (B) Embryo treated with 500 mg/L bare TiO_2NPs; (C) Embryo treated with 500 mg/L TiO_2NPs/PSS; (D) Embryo treated with 500 mg/L TiO_2NPs/PSS/PAH; (F) Embryo treated with 1000 mg/L bare TiO_2NPs; (G) Embryo treated with 1000 mg/L TiO_2NPs/PSS; (H) Embryo treated with 1000 mg/L TiO_2NPs/PSS/PAH; (J) Embryo treated with 500 mg/L bare TiO_2NPs; (K) Embryo treated with 500 mg/L TiO_2NPs/PSS; (L) Embryo treated with 500 mg/L TiO_2NPs/PSS/PAH; (N) Embryo treated with 1000 mg/L bare TiO_2NPs; (O) Embryo treated with 1000 mg/L TiO_2NPs/PSS; (P) Embryo treated with 500 mg/L TiO_2NPs/PSS/PAH.

Table 5.1. Viability (%) determined using the FDA assay of *D. rerio* embryos after exposure to TiO_2NPs at 0, 500 and 1000 mg/L concentration for 3 hr exposure time kept in dark conditions and visible light.

		TiO_2NPs	Viability (%)*
Dark	**500 mg/L**	**Control**	100%
		Bare TiO_2NPs	100%
		TiO_2NPs/PSS	100%
		TiO_2NPs/PSS/PAH	100%
	1000 mg/L	**Control**	100%
		Bare TiO_2NPs	100%
		TiO_2NPs/PSS	100%
		TiO_2NPs/PSS/PAH	100%
Visible light	**500 mg/L**	**Control**	100%
		Bare TiO_2NPs	100%
		TiO_2NPs/PSS	100%
		TiO_2NPs/PSS/PAH	100%
	1000 mg/L	**Control**	100%
		Bare TiO_2NPs	100%
		TiO_2NPs/PSS	100%
		TiO_2NPs/PSS/PAH	100%

*%Viability = {number of viable embryos / total number of embryos (n=10)} x 100.

5.3.2 Morphological analysis of *D. rerio* embryos after exposure to TiO_2NPs

The composition of each coated TiO_2NPs was determined using EDS attached to TEM as described in section 5.2.4. A control *D. rerio* embryo was examined with TEM (Fig. 5.2). EDS attached to TEM was used to enable the detection of TiO_2NPs in *D. rerio* embryos exposed to different types of TiO_2NPs. EDS spectra confirmed the absence of TiO_2NPs in control *D. rerio* embryos (Fig. 5.3) and it confirmed the presence of TiO_2NPs on the outer surface of *D. rerio* embryo incubated with 500 mg/L of TiO_2NPs/PSS in both dark and visible light conditions (Fig. 5.4 and Fig. 5.5). No TiO_2NPs were detected in embryos incubated with 500 mg/L of TiO_2NPs/PSS/PAH in both dark and visible light

conditions (Fig. 5.6 and Fig. 5.7). Whereas TiO_2NPs were detected in embryos incubated with 1000 mg/L TiO_2NPs/PSS/PAH in the dark (Fig. 5.8). Other embryos were left for future work if given further funds.

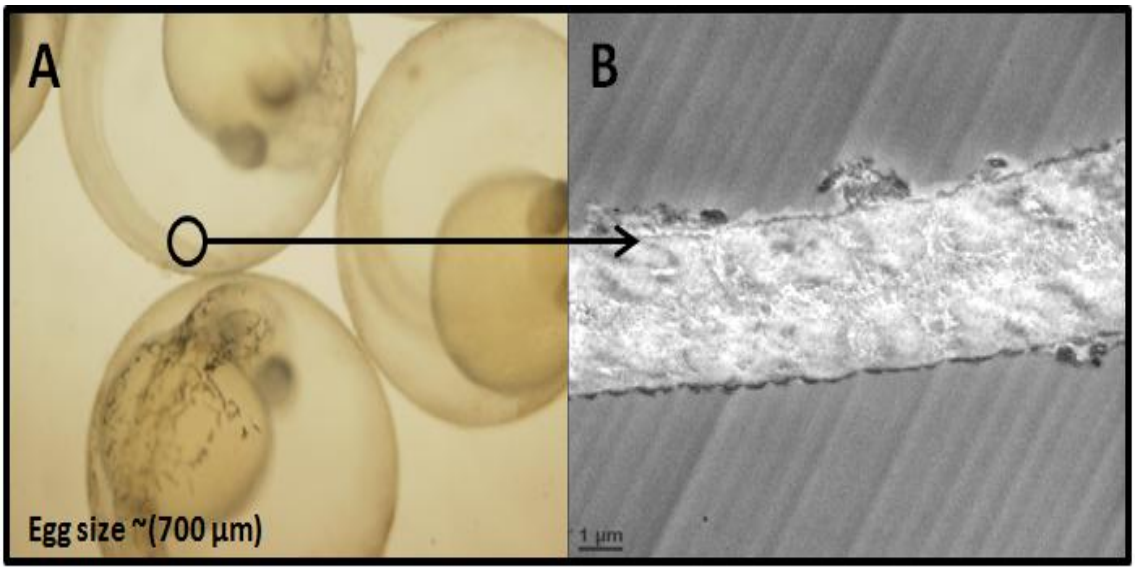

Figure 5.2. (A) Microscope image of control *D. rerio* embryos. (B) TEM image of control microtome-sectioned control *D. rerio* embryo.

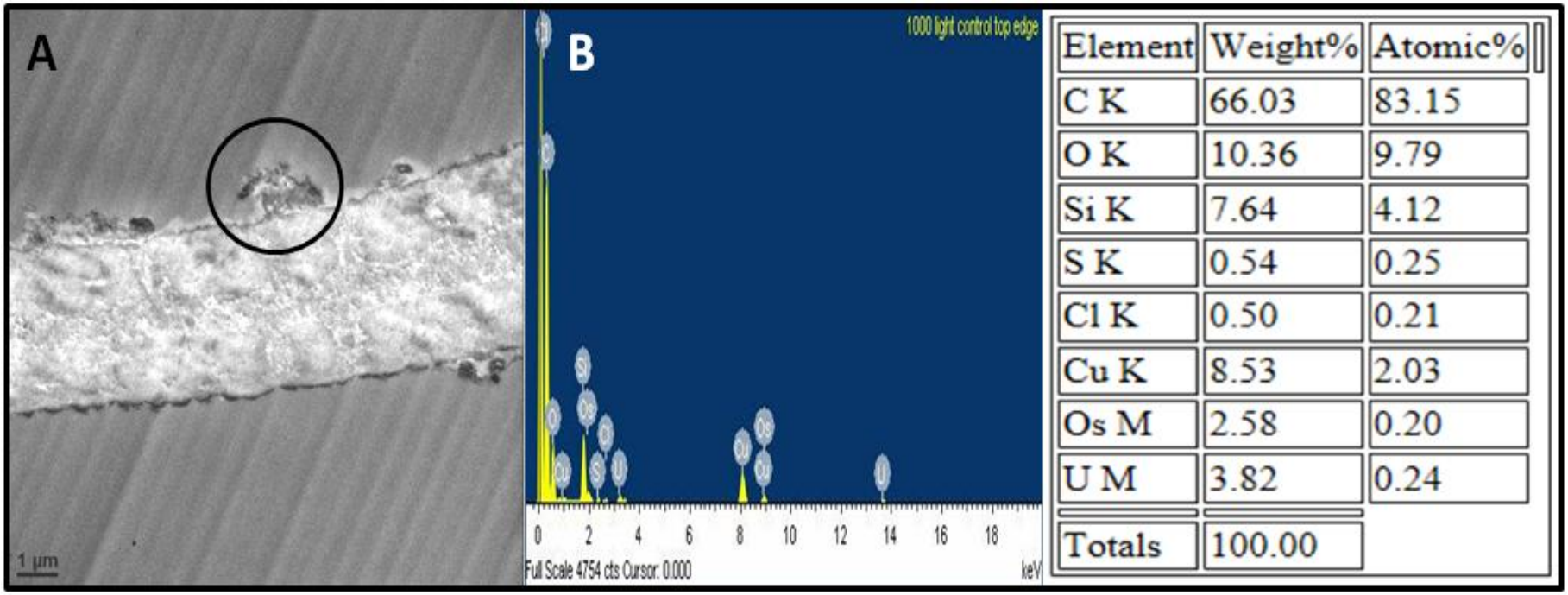

Element	Weight%	Atomic%
C K	66.03	83.15
O K	10.36	9.79
Si K	7.64	4.12
S K	0.54	0.25
Cl K	0.50	0.21
Cu K	8.53	2.03
Os M	2.58	0.20
U M	3.82	0.24
Totals	100.00	

Figure 5.3. TEM and EDS spectra images of control *D. rerio* embryo. (A) TEM image of microtome-sectioned *D. rerio* embryo. (B) EDS spectrum from microtome-sectioned *D. rerio* embryo. Table shows weight percent and atomic percent of the elements present in the sample.

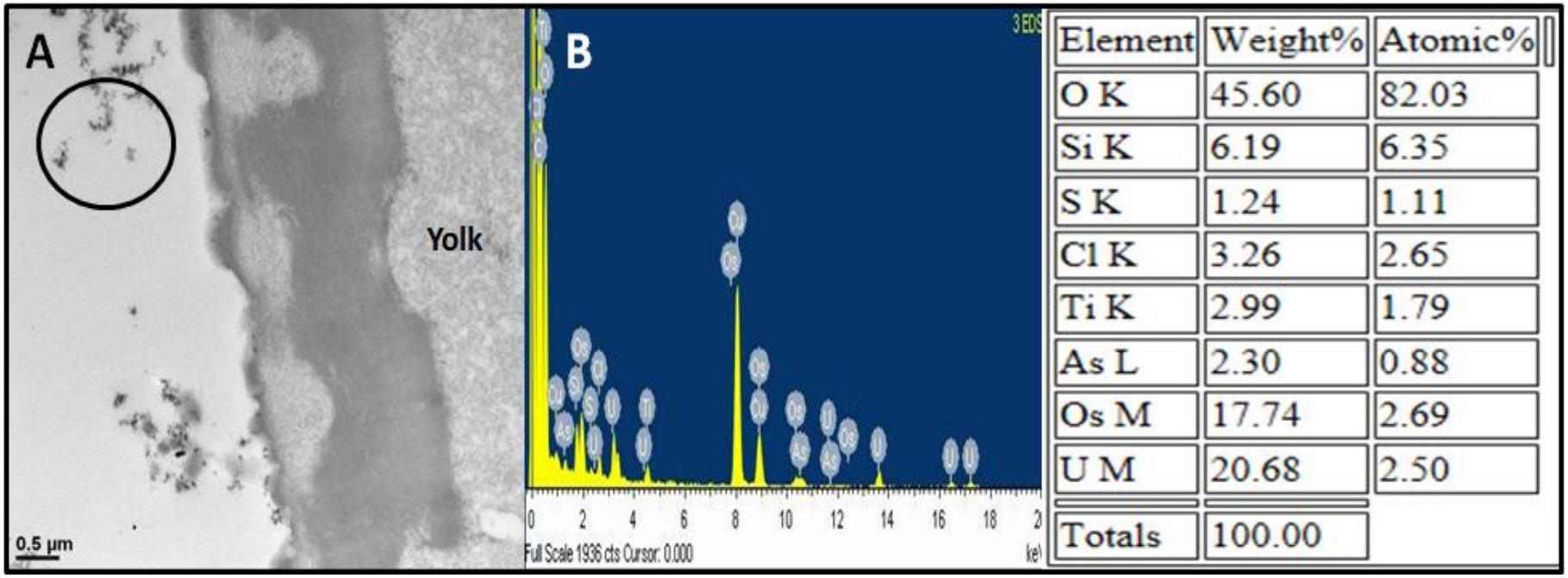

Element	Weight%	Atomic%
O K	45.60	82.03
Si K	6.19	6.35
S K	1.24	1.11
Cl K	3.26	2.65
Ti K	2.99	1.79
As L	2.30	0.88
Os M	17.74	2.69
U M	20.68	2.50
Totals	100.00	

Figure 5.4. TEM and EDS spectra images of *D. rerio* embryo after incubated for 3 hr with 500 mg/L of TiO_2NPs/PSS in dark. (A) TEM image of microtome-sectioned *D. rerio* embryo. (B) EDS spectrum from microtome-sectioned *D. rerio* embryo that included TiO_2NPs and other elements, the peaks on the EDS spectrum validated the presence of TiO_2NPs. Table shows weight percent and atomic percent of the elements present in the sample.

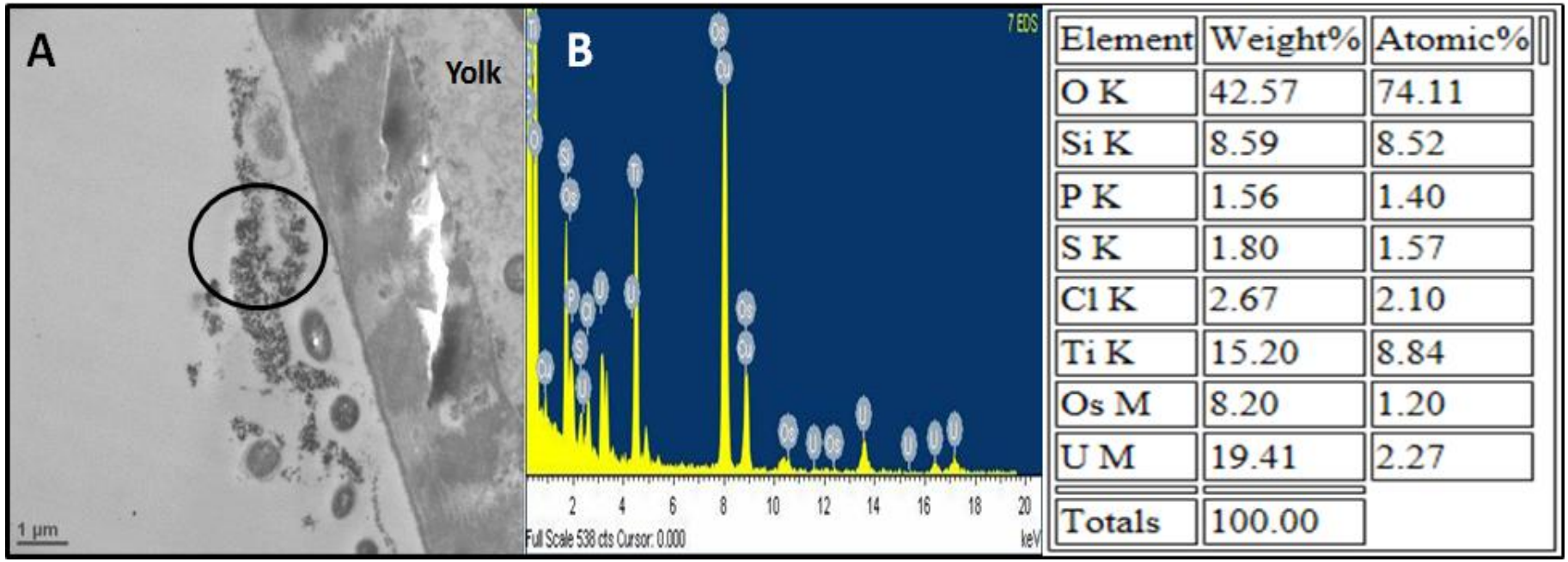

Element	Weight%	Atomic%
O K	42.57	74.11
Si K	8.59	8.52
P K	1.56	1.40
S K	1.80	1.57
Cl K	2.67	2.10
Ti K	15.20	8.84
Os M	8.20	1.20
U M	19.41	2.27
Totals	100.00	

Figure 5.5. TEM and EDS spectra images of *D. rerio* embryo after incubated for 3 hr with 500 mg/L of TiO_2NPs/PSS in visible light. (A) TEM image of microtome-sectioned *D. rerio* embryo. (B) EDS spectrum from microtome-sectioned *D. rerio* embryo that included TiO_2NPs and other elements, the peaks on the EDS spectrum validated the presence of TiO_2NPs. Table shows weight percent and atomic percent of the elements present in the sample.

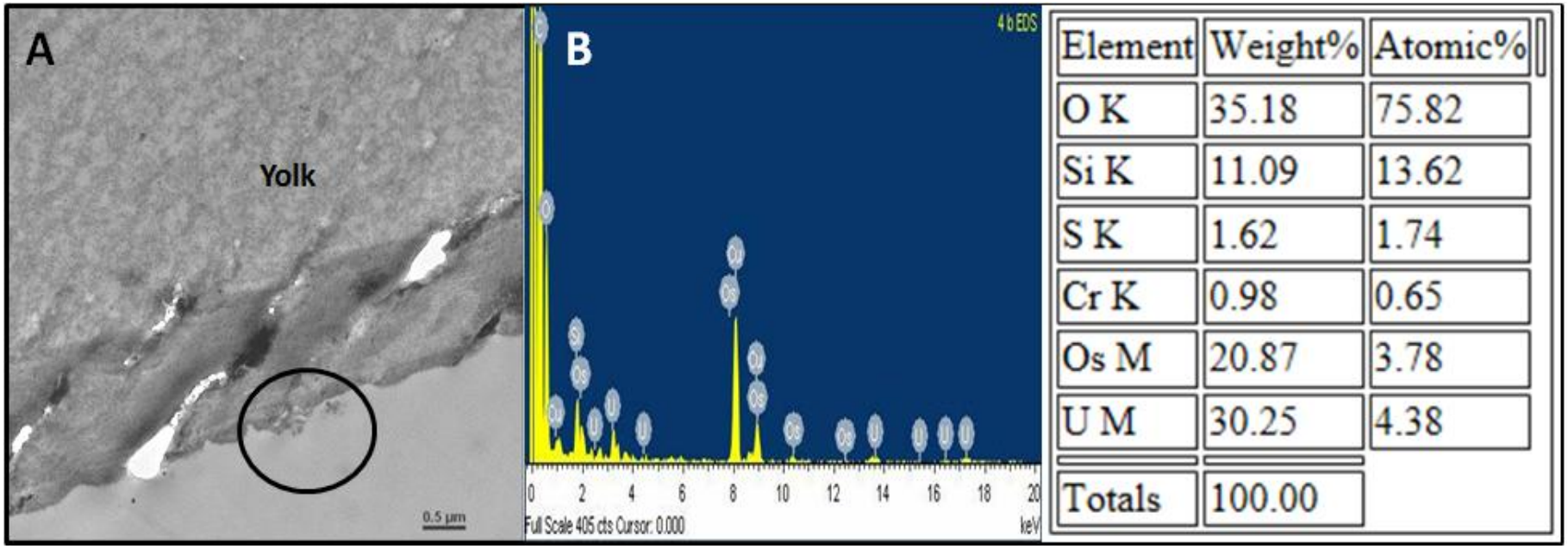

Element	Weight%	Atomic%
O K	35.18	75.82
Si K	11.09	13.62
S K	1.62	1.74
Cr K	0.98	0.65
Os M	20.87	3.78
U M	30.25	4.38
Totals	100.00	

Figure 5.6. TEM and EDS spectra images of *D. rerio* embryo after incubated for 3 hr with 1000 mg/L of TiO_2NPs/PSS/PAH in dark. (A) TEM image of microtome-sectioned *D. rerio* embryo. (B) EDS spectrum from microtome-sectioned *D. rerio* embryo, no TiO_2NPs was detected in the analytical spectrum of EDS. Table shows weight percent and atomic percent of the elements present in the sample.

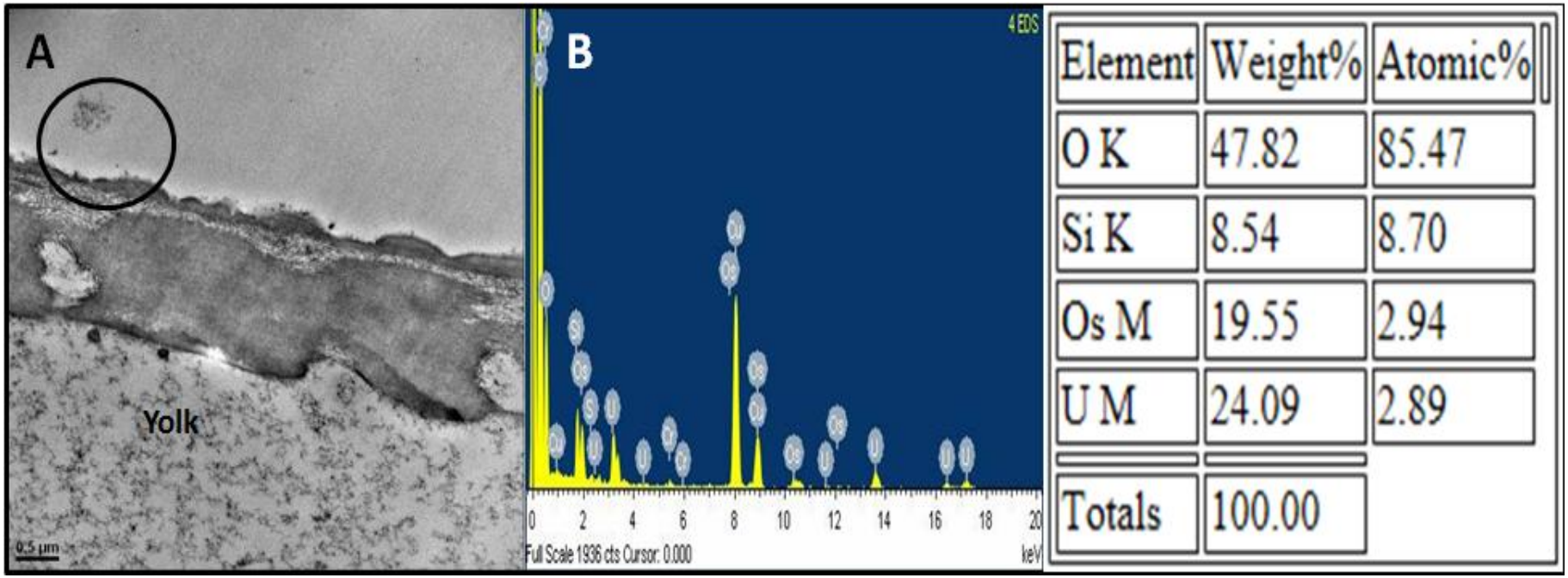

Element	Weight%	Atomic%
O K	47.82	85.47
Si K	8.54	8.70
Os M	19.55	2.94
U M	24.09	2.89
Totals	100.00	

Figure 5.7. TEM and EDS spectra images of *D. rerio* embryo after incubated for 3 hr with 1000 mg/L of TiO_2NPs/PSS/PAH in visible light. (A) TEM image of microtome-sectioned *D. rerio* embryo. (B) EDS spectrum from microtome-sectioned *D. rerio* embryo, no TiO_2NPs was detected in the analytical spectrum of EDS. Table shows weight percent and atomic percent of the elements present in the sample.

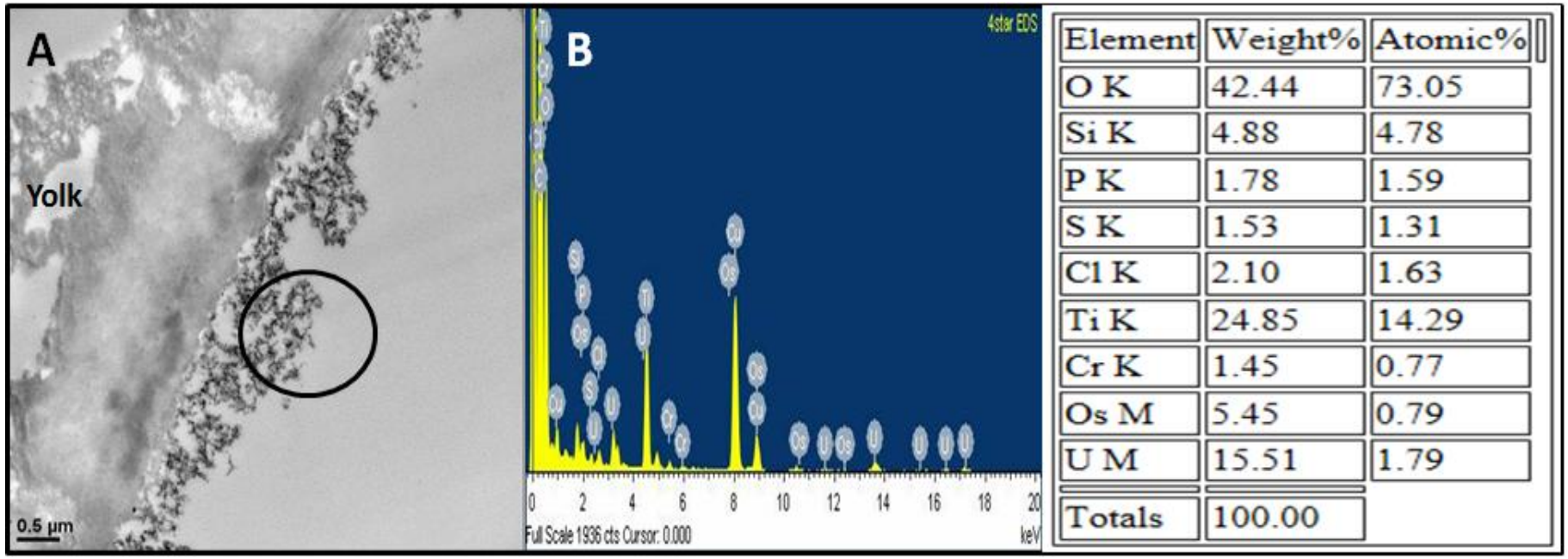

Element	Weight%	Atomic%
O K	42.44	73.05
Si K	4.88	4.78
P K	1.78	1.59
S K	1.53	1.31
Cl K	2.10	1.63
Ti K	24.85	14.29
Cr K	1.45	0.77
Os M	5.45	0.79
U M	15.51	1.79
Totals	100.00	

Figure 5.8. TEM and EDS spectra images of *D. rerio* embryo after incubated for 3 hr with 1000 mg/L of TiO_2NPs/PSS/PAH in dark. (A) TEM image of microtome-sectioned *D. rerio* embryo. (B) EDS spectrum from microtome-sectioned *D. rerio* embryo that included TiO_2NPs and other elements, the peaks on the EDS spectrum validated the presence of TiO_2NPs. Table shows weight percent and atomic percent of the elements present in the sample.

5.3.3 QPCR analysis of target gene expression in *D. rerio* embryos following exposure to TiO_2NPs

The expression levels of *SOD2.1*, *HIF.4*, and *Pxmp2.4* mRNA were analysed in controls and each treatment group of TiO_2NPs with concentrations of 0, 500 and 1000 mg/L in dark and visible light conditions using the optimised qPCR method. Firstly, an overall statistical analysis using the Scheirer-Ray-Hare test (Table 5.2) showed that the TiO_2NP type, concentration, condition, the interaction between the types and concentration; and the interaction between the concentration and condition all significantly affected the relative gene expression levels of *SOD2.1* mRNA (Table 5.2). The mRNA expression level of *Pxmp2.4* and *HIF.*4 was not significantly impacted by any of the types of TiO_2NPs, concentration, nor condition of the exposure regime (Table 5.2).

Using the Kruskal-Wallis test for individual statistical tests it was also possible to highlight further significance within the dataset as follows. Figures 5.8, 9, and 10 show comparative box-and-whisker plots of the relative gene expression for each target gene compared with various coating types, conc entration and exposure conditions. Figure 5.9 shows significant difference in *SOD2.1* expression as a result of TiO_2NP type, concentration, and condition. *HIF.4* and *Pxmp2.4* expression was not affected by any condition (Fig. 5.10 and 5.11). Separate Kruskal-Wallis tests (Table 5.2) for one-way analysis of the individual data between TiO_2NPs types, concentration, and condition, revealed that *SOD2.1* mRNA expression was significantly affected by both types and condition. *HIF.4* mRNA didn't show any significant differences in expression by any factors, and *Pxmp2.4* mRNA expression shows significant difference only by condition effect.

Table 5.2. Summary of statistical analysis on the effect of TiO_2NPs, coated with different number of layers of anionic (PSS) and cationic (PAH) polyelectrolytes, on the mRNA expression level of *SOD2.*1, *HIF.*4, and *Pxmp2.*4 in *D. rerio* embryos. Exposures were conducted at three particle concentrations (0, 500 and 1000 mg/L) for 3 hr exposure time in either dark or visible light.

	Scheirer-Ray-Hare test							Kruskal-Wallis test		
Gene	**Types**	**Conc**	**Cond**	**Int[1]**	**Int[2]**	**Int[3]**	**Int[4]**	**Types**	**Conc**	**Cond**
SOD2.1	*P*<0.05	*P*<0.05	*P*<0.05	*P*<0.05	ns	*P*<0.05	ns	*P*<0.05	*ns*	*P*<0.05
HIF.4	ns	ns	ns	ns	ns	ns	ns	ns	ns	ns
Pxmp2.4	ns	ns	ns	ns	ns	ns	ns	ns	ns	*P*<0.05

Effect of concentration (**Conc**), Exposure condition (**Cond**), [1]Interaction between types of TiO_2NPs and concentration (**Int[1]**), [2]Interaction between types of TiO_2NPs and exposure condition (**Int[2]**), [3]Interaction between concentration and exposure condition (**Int[3]**), [4]Interaction between types of TiO_2NPs, Concentration, and exposure condition (**Int[4]**), **ns**: not significant.

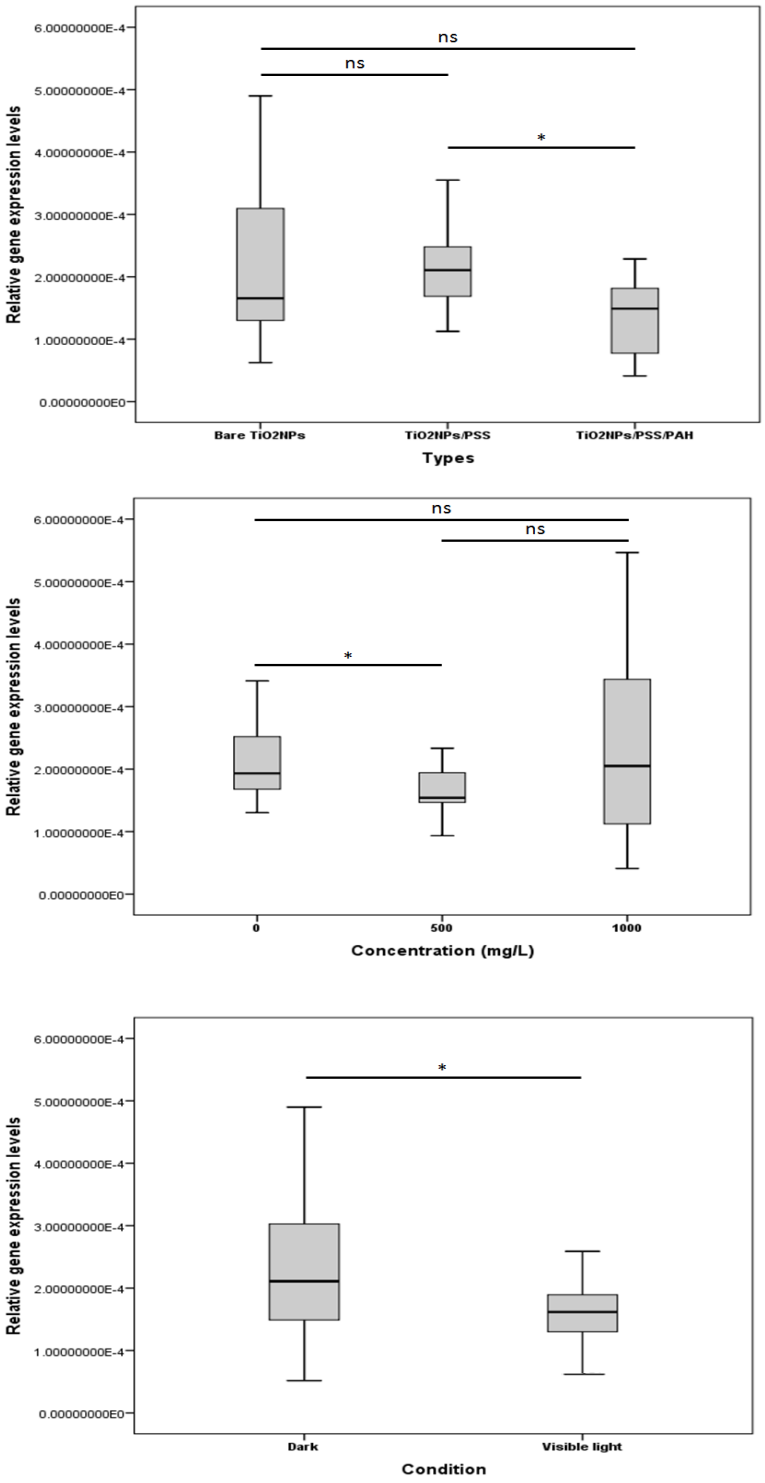

Figure 5.9. Box-and-whisker plots of the gene expression levels of *SOD2.1* gene following exposure to TiO_2NPs with various coatings, concentration and exposure condition (p<0.05). The plots were generated using IBM SPSS Statistics 22 software.

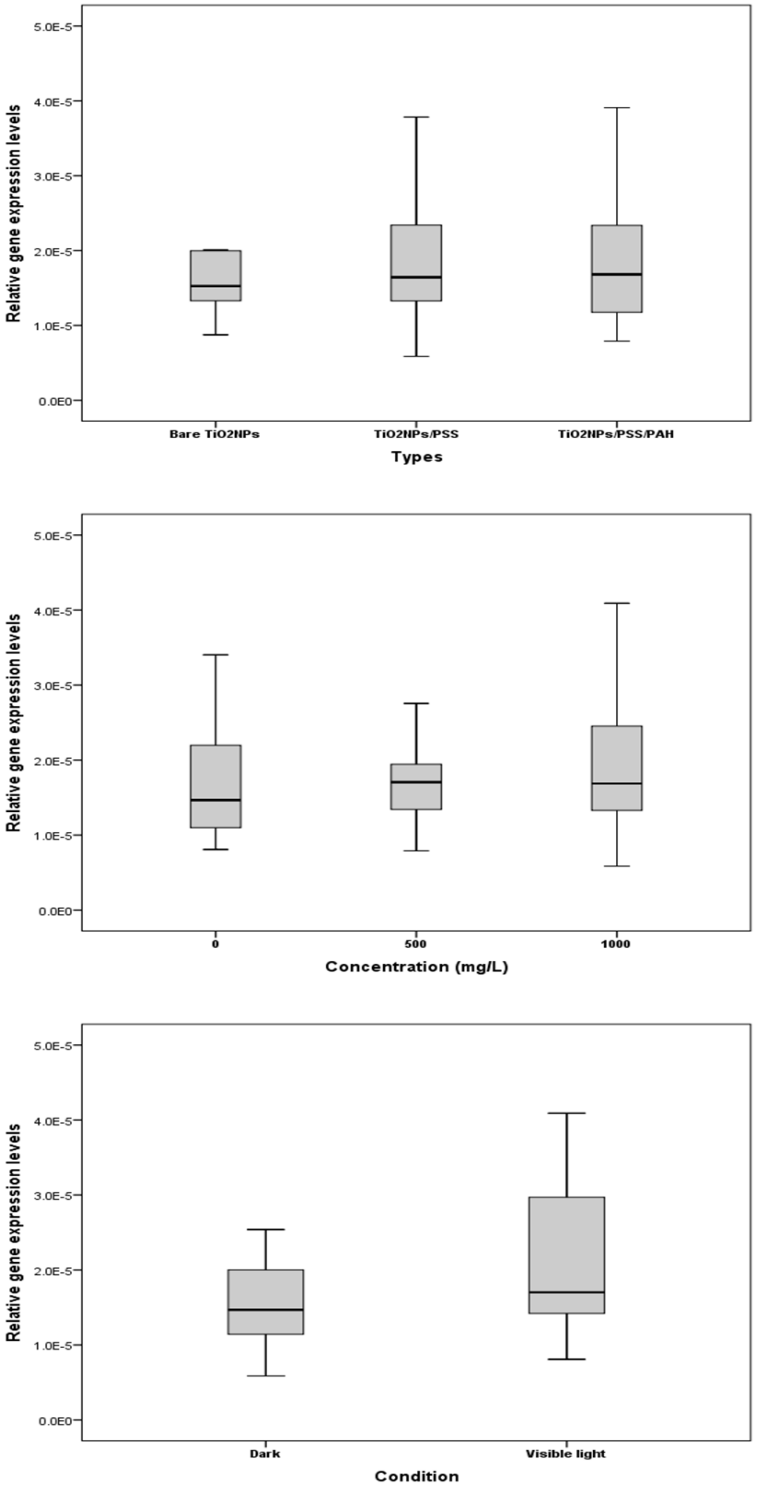

Figure 5.10. Box-and-whisker plots of the gene expression levels of *HIF.4* gene following exposure to TiO_2NPs with various coatings, concentration and exposure condition (p<0.05). The plots were generated using IBM SPSS Statistics 22 software.

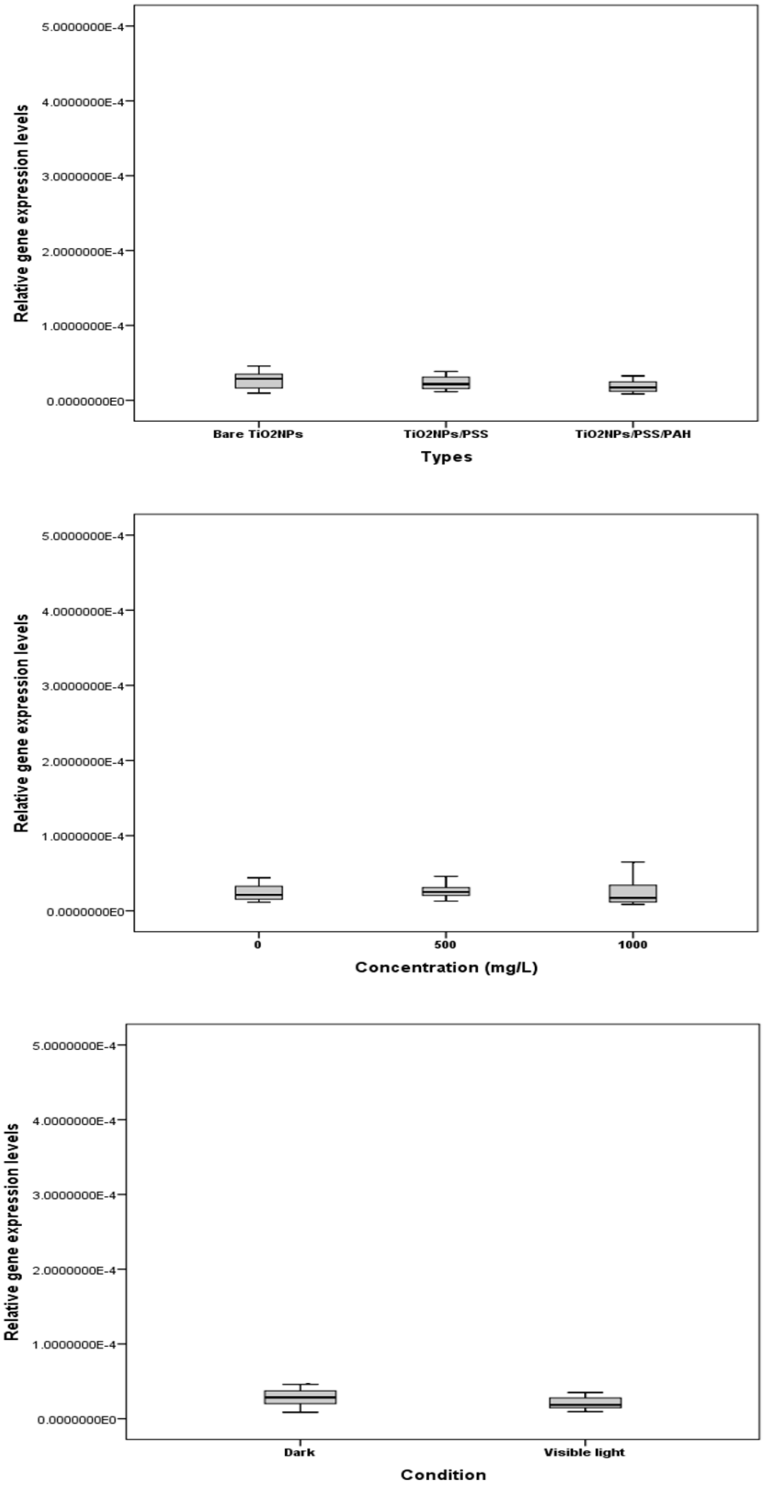

Figure 5.11. Box-and-whisker plots of the gene expression levels of *Pxmp2.4* gene following exposure to TiO_2NPs with various coatings, concentration and exposure condition (p<0.05). The plots were generated using IBM SPSS Statistics 22 software.

5.4 Discussion

In this chapter we examined the effect of TiO_2NPs coated with different layers of anionic (PSS) and cationic (PAH) polyelectrolytes on *D. rerio* embryo viability (which determines which cells are living), morphology (observed under TEM), and the expression level of selected target genes *SOD2.1*, *HIF.*4, and *Pxmp2.*4 mRNA. Different particle concentrations (0, 500 and 1000 mg/L) were used for exposures of 3 hr exposure duration in dark and visible light conditions. Each will be discussed in turn.

Cell viability of *D. rerio* embryos after exposure to TiO_2NPs

The *D. rerio* embryos were assessed for their viability with two types of TiO_2NPs with two concentrations (500 and 1000 mg/L), and an incubation duration of 3 hrs. Embryo viability was tested immediately after removing the excess of TiO_2NPs from the embryo suspension. With the method and conditions used no measurable change in the embryo viabilities were observed after incubation in dark and visible light conditions with exposure concentrations of 500 and 1000 mg/L for all types of TiO_2NPs. From the results of this current study, admittedly only carried out at two concentrations only, it is not clear what conditions/concentrations may cause a change in embryo viability. However, in common with the wider literature, there was little effect reported on goldfish skin cell viability following exposure to 5 nm TiO_2NPs (0.1-1000 g/ml), whereas co-exposure with UVA caused a significant decrease in cell viability at the higher concentration (1000 mg/mL) to ~40% (Reeves et al., 2008). A decrease in cell viability was also reported in transgenic mouse primary embryo fibroblasts exposed to the 40 nm TiO_2NPs at a dose level of 30 mg/L for 24 hr (Xu et al., 2009).

The polyelectrolyte coated TiO_2NPs effect on the cell viability to yeast (*Saccharomyces cerevisiae*) and microalgae (*Chlamydomonas reinhardtii*) has previously been assessed using different concentrations of bare, anionic, and cationic TiO_2NPs coating (0, 100, and 500 mg/L) (Al-Awady et al., 2015). In contrast to our study, a longer incubation time of 6 hrs in both dark conditions or in UV light was used for the microalgae experiment (Al-Awady et al., 2015). Following the yeast experiment by Al-Awady, different particle concentrations (of 0, 1000, and 2500 mg/L) were used

and incubated at (0 hr, 6 hr, 12 hr, and 24 hr) in dark conditions or illuminated with UV light (Al-Awady et al., 2015). The results showed that TiO_2NPs affected the microalgae viability at a concentration above 50 mg/L, while TiO_2NP concentrations higher than 250 mg/L led to loss of viability (Al-Awady et al., 2015). For yeast, no measurable change in viability was observed for anionic or cationic TiO_2NPs even at the higher concentration of 500 mg/L, but a strong effect of bare TiO_2NPs was observed on cells viability upon illumination with UV light at high concentrations (Al-Awady et al., 2015). A possible explanation for this difference in response may relate to yeast cell walls being thicker (~200 nm) than microalgae, which may suggest a reason why a higher concentration is required to impact the yeast cells viability (Al-Awady et al., 2015). Since the *D. rerio* embryo size is ~1.5 mm thick (Sun et al., 2004), a longer exposure time or higher range of TiO_2NPs concentrations may be required to cause similar changes in viability. In another study, the survival of *D. rerio* embryos exposed to two commercial TiO_2NPs preparations at concentrations from 0.01-10,000 ng/mL, over a 23 day period, produced significant mortality compared to the control (Bar-Ilan et al., 2013). However, mortality is a different end point to the cell viability tested in this experiment, so a direct comparison is not possible, Additionally, 1000 mg/L of TiO_2NPs reduced cell viability (measured using MTT assay) of human skin (HaCaT cells) after 7 days of exposure, and were only found in the outermost layer of the epidermis (Crosera et al., 2015). In future work, it would therefore be ideal to assess the embryos viability for a longer range of incubation time periods (6 hr, 12 hr, 24 hr and even up to a longer term on 7 days) for acute and chronic toxicity assessment, in order to compare with previously published studies.

D. rerio embryos morphology after exposure to TiO_2NPs

The EDS attached to TEM method was used to confirm the presence of TiO_2NPs in *D. rerio* embryos exposed to different types of TiO_2NPs for 3 hr in dark and visible light conditions as described in section 5.2.4. The chorion which surrounds the *D. rerio* embryos during the first 72 hpf permits the passage of materials through pores or the passive diffusion (Cunningham et al., 2013). Therefore the NPs could pass through the chorion (Cunningham et al., 2013). *D. rerio* embryo stages with chorion accumulated more silver after exposure to 1000 µg/L of AgNPs and $AgNO_3$ compared to the later

stages without the chrion (Böhme et al., 2015). In the current study, only five embryos were examined, a limitation that makes conclusions difficult to draw. To sample the entire *D. rerio* embryo using TEM that would require thousands of slide images like the one presented in Figures 5.2-7. Yet the sample preparation, imaging and processing image technologies required time and considerable funds, a limiting factor beyond the scope of this project. None-the-less, TiO_2NPs were detected in the outer surface of microtome-sectioned *D. rerio* embryos exposed to 500 mg/L of TiO_2NPs/PSS in both dark and visible light conditions (Fig. 5.4 and Fig. 5.5). Relevantly, TiO_2NPs/PSS were not detected inside the embryos. No TiO_2NPs were detected in microtome-sectioned *D. rerio* embryo exposed to 500 mg/L of TiO_2NPs/PSS/PAH in either dark or visible light conditions (Fig. 5.6 and Fig. 5.7). The positively charged NPs and negatively charged biological membranes are likely to interact (Cunningham et al., 2013; Sharma et al., 2014). We analysed microtome-sectioned *D. rerio* embryo exposed to higher concentration of TiO_2NPs/PSS/PAH (1000 mg/L) in the dark to check for the presence of TiO_2NPs and TiO_2NPs (Fig. 5.8).

Regarding possible mechanisms to understand how such particle build up may occur, the negative charge of the cell membrane has been found to facilitate internalization, and affect the toxicity of positively charged coated NPs such as gold NPs (AuNPs), which are more toxic than negatively and/or neutrally charged AuNPs (Goodman et al., 2004; Lin et al., 2010). Such findings suggest a way of controlling the AuNPs interactions with cells, by manipulating surface charge, to exploit their biomedical applications (Lin et al., 2010).

Targeted gene expression in *D. rerio* embryos after exposure to TiO_2NPs

In the current study, the expression of *SOD2.1* mRNA was analysed in *D. rerio* embryos in control and bare TiO_2NPs and TiO_2NPs coated with anionic and cationic polyelectrolytes at concentrations of 0, 500 and 1000 mg/L in dark and visible light. The expression of *SOD2.1* mRNA was affected by the types of TiO_2NPs, concentration, and condition (Table 5.2, Fig. 5.9). The expression level of *HIF.4* and *Pxmp2.4* mRNA was not affected by any factor (Table 5.2, Fig. 5.10 and 5.11). This pattern of different gene expression can potentially be partly explained by the visible light condition that

can, in the presence of oxygen, activate TiO_2NPs and produce ROS as follows. it also can be size-dependent as 25 nm TiO_2NPs was used in the current study and it has been shown in previous study that oxidative damage is size-dependent where the smaller size of 10 and 20 nm TiO_2NPs produced oxidative DNA damage in BEAS-2B cells, a human bronchial epithelial cell line in the absence of light irradiation, while the treatment with larger size of TiO_2NPs (200 and >200 nm) did not cause oxidative stress in the absence of light irradiation (Gurr et al., 2005).

As mentioned in Chapter 1, the SOD enzyme catalyses the dismutation of the reactive superoxide ion (O_2^-) to yield hydrogen peroxide (H_2O_2) and oxygen molecule during oxidative oxygen processes (Velkova-Jordanoska et al., 2008). In a published study, the exposure of developing *D. rerio* embryos to 0.01-10,000 ng/mL TiO_2NPs, illuminated with a lamp, has been shown to produce toxicity through cumulative ROS (Bar-Ilan et al., 2013). Other studies, using human cells, also showed that covering TiO_2NPs with coating agents could reduce or eliminate ROS generation by TiO_2NPs following UV irradiation (Mills and Le Hunte, 1997; Carlotti et al., 2009; Tran and Salmon, 2011). TiO_2NPs/PSS/PAH are cationic and UV-photoactive which could affect the embryos viability through the positive charge of the cationic TiO_2NPs that can be adsorber and disrupt with the negatively charged cell membrane (Al-Awady et al., 2015), or the NPs could possibly penetrate through the cell membrane and interact with cell organelles (Al-Awady et al., 2015). Further studies are required to fully understand these mechanisms. Ideally, future experiments would also include a titanium metal control to also rule out the possibility of metal-only induced toxicity.

Conclusions

In summary, TiO_2NP size, surface charge, concentration and the presence/absence of light have been shown to determine their potential toxicity measured in this study as specific gene expressions. Polyelectrolytes coatings are used in some NM formulations to enhance dispersion stability (Batley et al., 2013). The polyelectrolyte multilayer films (PAH/PSS) provide a stable nanocomposite thin film which interact with NPs (Cho et al., 2005). The nanotoxicty of polyelectrolyte coated TiO_2NPs have been previously been studied in yeast and microalgae and the results showed that the toxicity of the

coated TiO_2NPs changes with their surface charge where cationic polyelectrolyte coating were more toxic than the anionic polyelectrolyte coating (Al-Awady et al., 2015). The novelty of the current study is that we have now examined the toxicity of different TiO_2NPs coatings on *D. rerio* embryos and find that *D. rerio* embryos remain alive after exposure to 500 and 1000 mg/L of TiO_2NPs coated with anionic and cationic polyelectrolytes for 3 hr. Also, embryos exposed to cationic polyelectrolytes coating showed no TiO_2NPs using EDS while the higher concentration of 1000 mg/L of the same coating start to show NPs residues. Importantly, *SOD2.1* mRNA transcript expression showed significant effect changes related to all factors, indicative of oxidative stress. Only a small concentration range and short exposure regime has been used in this study. Therefore, there is still a lack of information about the potential biological effects of different TiO_2NP concentrations and exposure conditions (dark, visible light, and UV light).

6. Chapter Six: Wider discussion, relevance and future work

Relevance and contribution to the research field

In Chapter 1 the literature was reviewed and it was found that there is an extensive and increasing use of nanomaterials which has caused their consequent release into the environment as manufactured or degraded components (Selck et al., 2016). Quantifying and characterizing nanomaterials in environmental samples and experimental media has been highlighted as challenging as they are time consuming require special equipment, and it is difficult to measure dose and organism response (Petersen et al., 2015). Of particular interest in the research field is the toxicity of nanomaterials and its potential impacts on aquatic organisms as they are yet only partially characterised. A recent literature search was conducted by a group of researchers, using the Web of Science, on 8 June 2015 and that recorded that the number of published studies (hits) fulfilling the terms 'nano-' with 'fish' showed around 2314 hits related (Selck et al., 2016). Repeating that search today, for 'nano-' with 'fish' on 11 September 2016 resulted in 2981 hits. Yet, more studies still need to be done to cover specific areas of toxicity effects of different types of NPs on aquatic species and particularly fish. For comparison, significantly more studies have been carried out for 'nano-' with 'human' (49,963 hits found using the Web of Science on 11 September 2016). Studies must also focus more on the mechanisms of damage and also the development of early indicators of damage that may be developed for future use to monitor such NM-induced impacts in aquatic organisms.

In this dissertation, we have highlighted the biological effects mediated by 4 and 10 nm AgNPs, with silver ion alone in parallel, and TiO_2NPs on *D. rerio* embryos. The *D. rerio* was selected based on its large number of offspring produced, rapid development, the transparancy of its embryos, and the similarity with human genome (Braunbeck and Lammer, 2006; Howe et al., 2013). We considered several endpoints of impacts, such as potential oxidative stress and altered membrane function, as well as specific types of gene expressions. This work also has considered some of the major factors that influence these various AgNP and TiO_2NPs effects *in vitro,* including size (in Chapter 3), concentration (in Chapter 5), condition (in Chapter 5), and surface

chemistry (Chapter 5). This work forms the basis for potential development of AgNP-specific molecular biomarkers (Chapter 3) for use in future environmental monitoring and provides new mechanistic impact details concerning the biological effects of such chemical contaminants in fish (in Chapter 4).

According to the literature (reviewed in Chapter 1), the most frequently reported mechanisms of manufactured NM toxicity in vertebrates are related to oxidative stress (section 1.4.1), oedema (section 1.4.1.3), mucosal inflammation (section 1.4.1.3), and membrane interactions (section 1.4). There may be other uncharacterised mechanisms of NM induced damage while each of these mentioned is already quite late in terms of impact to an organism. Therefore, this investigation concerned the development of possible biomarkers of biological effect that would be available to detect changes at an earlier point before such serious impacts were observed. Therefore the main aims of this dissertation were to identify, isolate, and characterise possible early warning biological effects of AgNP (as described in Chapter 2) and TiO_2NPs (as described in Chapter 5) exposure in *D. rerio* embryos before organisms die (Robinson et al., 2000). Although, by applying both the targeted approach and the global approach of gene expression investigation, it is also possible to provide a better understanding of the molecular events that occur as a response to NPs toxicity. Accordingly, the qPCR-based assay was used to quantify mRNA transcription of the potential biological markers after exposure to AgNPs and silver ion alone (as described in Chapter 3), and TiO_2NPs (as described in Chapter 5). Later the SSH global approach was also used to isolate and identify differently regulated mRNA transcripts from embryos that respond to 4 nm size AgNP exposure to identify any novel indicators of exposure.

Summary and discussion of the main findings

In chapter 2, the main aim was to isolate potential AgNP-induced genes from *D. rerio*. The target mRNA transcripts were selected based on potential biological effects of NMs within various organisms that have been reported in the literature review (chapter 1) and summarised in Table 1.1. All the primers used to isolate these genes were designed based on the conserved domains of similar candidate gene sequences available in closely related species available on the NCBI GenBank database. The

candidate mRNA transcripts initially selected were: *SOD2.1*, *SOD2.2*, *ATP.1*, *HIF.4*, *CRYaa*, *Cat.1*, *Jupa.4*, *Muc2.2*, and *Pxmp2.4* from *D. rerio*. Following their isolation, the deduced amino acid sequences of each of these mRNA transcripts showed a high level of sequence similarity to those for other species available in GenBank. The range of percentage similarity of target mRNA transcript for other species was as high as 94% in some cases. Importantly, the functionally-important conserved domain regions found, were then used as a target for amplification of mRNA expression in response to AgNPs and silver ion exposure using qPCR assays developed and optimised in chapter 3.

Following in chapter 3, five of the candidate mRNA transcripts isolated in chapter 2 were used for the mRNA expression analysis of early *D. rerio* embryos (up to 96 hpf) that had been experimentally exposed to 1.925 mg Ag/L of 4 and 10 nm size of AgNPs and 0.018 mg/L of silver ion alone relative to the corresponding control embryos. These embryos had been kindly supplied by a collaborator Dr Jinping Cheng. The candidate mRNA transcripts selected for gene expression analysis were: *SOD2.1*, *HIF.4*, *Cat.1*, *Muc2.2*, and *Pxmp2.4*, and the remaining mRNA were left for future work if given further time and funds. The results suggested that AgNP toxicity may be size-dependent, with the smaller particles (4 nm) found to show increased expression of *HIF.4* and *Pxmp2.4* mRNA and an increasing trend in *SOD2.*1 compared with the 10 nm size AgNPs, which showed only decrease in *SOD2.*1. In parallel, no significant differences were observed in any mRNA transcript levels upon exposure to silver ion alone. *HIF.4*, *Pxmp2.4* and *SOD2.*1 are correspondingly associated with membrane transport and indicative of oxidative stress. The size of NPs is considered the primary physiochemical property affecting solubility of NPs (Misra et al., 2012). Solubility is the hydrodynamic parameter that controls dissolution process where the dissolving solid molecules move from the surface to the bulk solution through a diffusion layer (Borm et al., 2006). These results suggested that solubility and uptake of 4 nm AgNPs are more than 10 nm AgNPs (at the concentrations used) and both are available for uptake and are causing mRNA transcript level changes, while the silver ions alone did not, in developing embryos. Previous studies have shown that AgNPs (5-20 nm) were able to penetrate through the chorion pore channels and accumulate in the nucleus of the *D. rerio* embryos, which may lead to genomic damage and instability (Asharani et al.,

2008). AgNPs (5-46 nm) was also able to transport in and out of *D. rerio* embryos through chorion pore canals and create specific effects on embryonic development and may form unique response from embryonic neural development pathways (Lee et al., 2007), and using 5 and 28 nm AgNPs induced superoxide within mitochondrial membranes in primary human monocytes given the possibility of cell membrane disturbance through direct invasion of AgNPs into cells (Yang et al., 2012). Patlolla and colleagues (2015) report that 10 nm AgNPs with doses of 50 and 100 mg/kg for five days caused organ toxicity and oxidative stress in rat liver (Potlolla et al., 2015). All previous results are consistent with our results in terms of the cell uptake of NPs is size-dependent.

In chapter 4, the global gene expression profiling (SSH) approach allowed us to isolate differentially expressed genes following exposure to 4 nm sized AgNPs (1.925 mg/L). The SSH technique was used to highlight genes encoding proteins involved in pathways that are changed under AgNPs exposure and may allow a better understanding of the underlying mechanisms of NPs regulation in *D. rerio* embryos. The sequences identified using the SSH, transcripts associated with fertility, membrane transport, and cell mobility, were highlighted as potentially toxic impacts of AgNPs. Similarly to the targeted genes developed for quantitative assays, these candidate genes could also now potentially be developed as possible biomarkers of AgNP exposure and form the basis of further mechanistic toxicology studies. While the SSH technique has not previously been conducted using zebrafish exposed to similar AgNPs, there have been studies using a microarray approach that have been performed with zebrafish (Denslow et al., 2007). SSH and microarray analysis are useful for identifying differentially expressed transcripts between control and experimental groups, and the expression levels of transcripts highlighted can then be validated using qPCR (Hall et al., 2011). The first use of microarray in fish was done to study gene expression in a hypoxia-tolerant burrow-dwelling goby fish, *Gillichthys mirabilis* (Gracey et al., 2001). Differentially expressed genes were identified by microarray analysis of zebrafish gills exposed to nancopper, nanosilver, and nanotitania where each exposure was suggested to produce biological response by a different mechanism (Griffitt et al., 2009). The potential of zebrafish embryo

microarray analysis in nanotoxicology was also examined after exposed the embryos to TiO_2 and hydroxylated fullerenes NPs, and the NPs exposure caused changes in genes related to cell kinase activity, circadian rhythm, intracellular trafficking, and immune response (Jovanovic, 2011).

In terms of the potential molecular mechanisms impacted by 4 nm AgNPs, significant differences in expression levels of both *HIF.4* and *Pxmp2.4* mRNA are good possible candidates for future biomarker development. *HIF.4* is indicative of a hypoxic cellular environment, and its function is mainly regulated by HIF-1α protein stability (Jiang et al., 1997). Where *Pxmp2* was assumed to be playing a role in the transmembrane transport of solutes by selectivity of pore-forming proteins (Van et al., 1987). *Pxmp2* is also known to have a role in the transmembrane transport of solutes by acting as a nonselective pore-forming protein (Van Veldhoven et al., 1987). *Pxmp2* playing a role in the transmembrane transport of solutes by selectivity of pore-forming proteins which expressed in mouse liver (Rokka et al., 2009). However, *Pxmp2* leads to prediction that the mammalian peroxisomal membrane is permeable to small solutes while it required specific transporters to transfer large metabolites, e.g., cofactors (NAD/H, NADP/H, and CoA) and ATP (Rokka et al., 2009). The activation of many oxygen-regulated genes is known to be mediated by HIF (Hu et al., 2003). Many researchers have shown the transcriptional activation of HIF-1α after exposure to NPs (Lim et al., 2009; Pietruska et al., 2011). For example, HIF-1α levels were increased on *P. promelas* after 48 h of 6 nm AgNPs exposure (Jang et al., 2012). Consistent with the present study results, a previous study showed that HIF-1α was significantly up-regulated in *P. promelas* after exposure to 20 nm PVP-AgNP, and citrate-AgNP exposures (50.3 µg/L PVP-AgNP; 56.0 µg/L citrate-AgNP), but not in the $AgNO_3$ (3.81 µg/L) for 96 hr (Garcia-Reyero et al., 2015). Which is slightly different from previously shown result were HIF-1α was up-regulated both $AgNO_3$ and PVP-AgNP exposures, where suggestion have been made that the effects of $AgNO_3$ and AgNP at the transcriptional level may differ by tissue (Garcia-Reyero et al., 2014). Overall, *HIF* and *Pxmp2* could be developed as possible biomarkers of NPs exposure of further mechanistic toxicology studies. Meanwhile, in terms of embryo viability and morphology impacts, the expression of *SOD2.*1, *HIF.*4, and *Pxmp2.*4 mRNA transcripts

following controlled experimental exposure to TiO_2NPs relative to control embryos were also subsequently investigated in chapter 5.

TiO_2NPs can potentially be toxic to aquatic life when released in the environment as they can generate hydroxyl radicals upon exposure to oxygen and sunlight which can initiate oxidations and could damage cells content (Dunford et al., 1997). TiO_2NPs are cationic and UV-photoactive NPs, they could affect the cell viability in the presence of oxygen and sunlight through different pathways: (i) TiO_2NPs can be adsorb and disrupt the cell membrane due to its cationic nature, (ii) TiO_2NPs could penetrate through the cell membrane and interfere with vital cell organelles, (iii) TiO_2NPs can be activated by UV/visible light and produce ROS which may degrade the cell membranes in their vicinity and damage the cell DNA (Al-Awady et al., 2015). In general, the NPs surface are affected by chemical composition, surface functionalization, shape and angle of curvature, porosity, surface charge, crystallinity, heterogeneity, roughness, and hydrophobicity or hydrophilicity (Vertegel et al. 2004; Oberdörster et al. 2005a; Nel et al. 2006). Preliminary results herein showed no measurable change in the embryo viabilities after exposure to 500 and 1000 mg/L concentrations of different types of TiO_2NPs samples (bare TiO_2NPs, TiO_2NPs/PSS, or TiO_2NPs/PSS/PAH) in dark and visible light conditions for 3 hr. Quantitative EDS X-ray microanalysis using TEM images for control, TiO_2NPs/PSS, and TiO_2NPs/PSS/PAH at 500 and 1000 mg/L concentrations for 3 hr showed the formation of a significant build-up of anionic TiO_2NPs (500 mg/L TiO_2NPs/PSS in dark and light conditions) on the embryo surface comparing to the same concentration of cationic TiO_2NPs, where no such accumulation for TiO_2NPs was found. Yet a significant build-up of cationic TiO_2NPs on the embryo surface was clearly observed at 1000 mg/L concentration (Fig. 5.8). In parallel, the *SOD2.1* mRNA expression, which is a biomarker of oxidative stress, was affected by the types of TiO_2NPs, concentration, and condition. The NPs surface are affected by chemical composition, surface functionalization, shape and angle of curvature, porosity, surface charge, crystallinity, heterogeneity, roughness, and hydrophobicity or hydrophilicity (Vertegel et al. 2004; Oberdörster et al. 2005a; Nel et al. 2006). The expression level of *HIF.4* and *Pxmp2.4* mRNA was not affected by any

factor. *SOD2.1* mRNA expression levels may thus be potentially useful in the detection of apparent oxidative stress induced by NP build up on the embryo surface.

The size of particle is an important parameter to determine the mechanism and rate of cell uptake of a NPs and its ability to penetrate through tissue, as well as surface chemistry and charge will affect the uptake of NPs (Lu et al., 2009). Particle size can affect the efficiency and pathway of cellular uptake by influencing the adhesion of the particles and their interaction with cells (Lee et al., 1993). NPs uptake could be checked with TEM and TEM-EDS. For instance, AgNPs uptake into the stratum corneum and the outermost surface of the epidermis were confirmed using TEM (Carlson et al., 2008).

Oxidative stress is a well identified mechanism of NMs induced damage. Estimating oxidative stress in biological systems (section 1.4.1.1) includes the measurement of the increase or decrease in redox-sensitive molecules that respond to oxidative stress (Powers and Jackson, 2008). To protect biomolecules from oxidative stress, the cell produces different antioxidant molecules and enzymes include *superoxide dismutase* (*SOD*), *glutathione reductase* (*GR*), *glutathione peroxidase* (*GPx*), as well as *catalase* (*Cat*). *SOD* gene was up regulated in rats liver treated with AgNPs (Coccini et al., 2014). Increased *SOD* activity has also been observed in medaka fish (*O.latipes*) embryos after exposure to AgNP (Wu and Zhou, 2012). In contrast, *SOD* activities were found to be reduced in rat plasma after they received AgNPs (Ranjbar et al., 2014). Alongside with our findings in the present study, the *SOD* response following AgNP exposure therefore could assessed as biomarker.

Ion release is a critical point, as as AgNPs dispersed in aqueous medium can release Ag ions (Patlolla et al., 2015) and metal NPs can release a significant amount of ions because of their high surface/mass ratio (Filon et al., 2015). AgNPs and the released ions readily bind to proteins and DNA, may cause cell damage. If Ag ions released from AgNPs, it is likely that small size particles are more toxic than larger particles due to a larger surface area per weight unit (Patlolla et al., 2015).

In the present study, results suggest that pathways expressed in response to NP exposure differ among both AgNPs and TiO_2NPs, either due to the size, concentration,

exposure time, exposure conditions, surface chemistry and surface charge of coatings of the NPs. The effects of NPs cannot be explained solely by ions release, and could be dependent on NP size and coating which could affects their solubility. The responses in general indicate that *D. rerio* embryos respond to NPs with not only an oxidative stress response, but with transcripts associated with fertility and metabolic functions such as membrane transport and mitochondrial metabolism. This information may be used to develop early warning tools of NP-induced biological effects to be able to monitor and manage for any possible impacts.

Future work

In the present work, for the targeted approach, we focused on only a selection of potential NP-induced genes according to the biological effects reported previously in the literature (see Table 1.1). The candidate mRNA transcripts selected were: *SOD2.1*, *SOD2.2*, *ATP.1*, *ATPase.1*, *HIF.4*, *CRYaa*, *HSP.2*, *Cat.1*, *Jupa.4*, *Muc2.1*, *Muc2.2*, and *Pxmp2.4*. All were isolated and characterized but only *SOD2.1*, *HIF.4*, *Cat.1*, *Muc2.2*, and *Pxmp2.4* were used to develop further as potential biomarkers of NPs in the current work. The remaining mRNA sequences obtained in the course of this work could also be validated in the future, as additional potential biomarkers of biological impacts of NPs in fish. We also have focused on the gene expression at the mRNA level, which may not actually predict for its actual protein level.

In the literature, previous studies have focused on protein levels analysis in response to NPs. These include studies of protein activities associated with oxidative stress and apoptosis in HaCat cells after exposure to 10 µg/mL of 15 and 30 nm nano-SiO_2 (Yang et al., 2010). Also 20 nm AgNP exposure was found to interfere with protein regulations of mitochondrial translation more than 100 nm AgNPs and silver ions in human colon adenocarcinoma LoVo cells (Verano-Braga et al., 2014). Another study found that exposure to 3-5 nm AgNPs (5, 10, 12.5 µg/mL) increased the protein level of amyloid precursor protein (*APP*) for amyloid-β (Aβ) generation, and reduced low-density lipoprotein receptor (*LDLR*) and neprilysin (*NEP*) for Aβ uptake or transporter and Aβ degradation in mouse brain neural cells (Huang et al., 2015). The authors suggested that AgNPs may cause neurodegenerative disorder progression underlying Aβ deposition (Huang et al., 2015). Moreover, the differentially expressed proteins by

25 nm TiO_2NPs in mouse lung were examined to measure the TiO_2NPs toxicities at the protein level, where 5 proteins showed increased intensities in TiO_2NPs exposed lungs (cytoplasmic aconitase, L-lactate dehydrogenase A chain, carbonic anhydrase 1, pyruvate kinase isoform M2 and peroxiredoxin-6) while 3 proteins (HSP, moesin and apolipoprotein A-1 precursor) showed reduced intensities (Jeon et al., 2011). All these studies using protein level impacts therefore indicate that there is future scope for a similar approach with *SOD2.1*, *HIF.4*, *Cat.1*, *Muc2.2*, and *Pxmp2.4* ptotein/enzyme activies. Perhaps the development of a quantitative method to measure protein levels using enzyme-linked immunosorbent assays (ELISA), Western blots or spectrophotometric enzyme assays could be employed. Focusing on protein expression altered by NPs exposure will help understand the molecular toxicity of NPs at the next level of cellular organisation, relating the genomic level change to a functional level/protein impact.

The literature review has highlighted the chemical and physical structural of NPs that may caused toxicity such as shape, surface area, surface coating, molecular size, solubility, oxidation status, degree of agglomeration and aggregation (Ray et al., 2009; Nel et al., 2006; Xia et al., 2008; Wang et al., 2008; Shaligram et al., 2013; Lu et al., 2010). Only two types of NPs have been used in the current study which was AgNPs and TiO_2NPs. These had been selected based on their wide use (Yang et al., 2007; Trouiller et al., 2009; Dobrzynska et al., 2014) compared with other NPs. It is important to check whether the toxicity observed by AgNPs and TiO_2NPs is due to the novel properties of NPs or as a result of the release of ions, or a combination of both. Further work needs to be done using ion exposure controls. For example, an experiment can be done to distinguish between NPs and released ions after exposure, using the inductively coupled plasma mass spectrometry (ICP-MS) method to confirm the presence of metals in single particle mode to distinguish its form (Reidy et al., 2013). TEM and EDS could offer a particle sizing approach, but are costly and time consuming.

In this work the concentration level was 1.925 mg/L of 4 and 10 nm sizes of AgNPs coated with oleic acid and 500 and 1000 mg/L of 5 nm sizes of TiO_2NPs (Hydrodynamic diameter 25 nm) coated with anionic and cationic polyelectrolytes.

Therefore, it would be interesting to try pre-coating AgNPs with anionic and cationic polyelectrolytes to find potential safer coatings of NPs.

Similarly to concentration levels, the chemical exposure time is another factor that could be further explored. It would be ideal to assess the embryos viability after exposure to TiO_2NPs for a longer range of incubation time periods (6 hr, 12 hr, 24 hr and even up to a longer term on 7 days) for acute and chronic toxicity assessment, in order to compare it with previously published studies.

Aside from contributing factors to toxicity as suggestions for further studies, there was also an interesting observation relating to larvae development and behaviour that would be an interesting lead to follow. During the microscopic observation of viability of *D. rerio* embryos exposed to TiO_2NPs coated with anionic and cationic polyelectrolytes at 1000 mg/L concentration for 3 hr in dark and light conditions, movement of embryos after exposure was visibly different than in control, as there was like continues rapid contractions in the whole body of the embryo. Therefore, it would be useful for future work to analyse the movement closely and accurately for embryos after exposure to NPs. Locomotion in *D. rerio* embryos could be analysed as previously described in Qiang et al., (2016), in which the effects of 1-5 µg/L of carbamazepine in *D. rerio* embryos and larvae development of motor behaviours were analysed by videotaping observation for 35 s under a CCD camera mounted on a fluorescence microscope (Qiang et al., 2016).

Finally, the present study only focused on short-term exposures. It would be interesting to understand how NPs affect *D. rerio* over several generations. As *D. rerio* embryos up to 96 hpf for AgNPs experiments and up to 72 hpf for TiO_2NPs experiment were only used in the current study, different life stages can be predicted to vary in their response towards NP toxicity. Therefore, additional work could be conducted to cover the biological effects of suggested NPs on different life stages of *D. rerio* to investigate the overall effects of NPs.

General conclusion

Molecular biomarker analytical tools may provide important information regarding the early biological effects of NPs and can be used in future environmental monitoring

applications. The results obtained in the present study, combined with the literature in the field, indicates that pathways expressed in response to NP exposure differ among both AgNPs and TiO_2NPs, either due to the size, concentration, exposure time, exposure conditions, surface chemistry and surface charge of coatings of the NPs. The responses across current experiments in this dissertation indicate that *D. rerio* embryos respond to NPs with not only an oxidative stress response but transcripts associated with fertility and metabolic functions like membrane transport and mitochondrial metabolism according to the differential gene expression patterns obtained (In Chapter 3 and 4). Global gene expression profiling has been very useful tool to allow a higher throughput approach towards evaluating the toxicity of NPs. The SSH technique used in the current study is one of the potential global approaches, yet it is much cheaper than other alternative techniques. None-the-less using the technique it was possible to highlight the candidate genes (Table 4.3) which all showed a differential expression in AgNP exposed embryos compared with control embryos. These candidate genes form the basis from which it would now be possible to be further analysed.

6. References

Achard-Joris, M., Gonzalez, P., Marie, V., Baudrimont M., and Bourdineaud, J. (2006) 'Cytochrome c oxydase subunit I gene is up-regulated by cadmium in freshwater and marine bivalves' *BioMetals*, vol. 19, pp. 237-244.

Ackroyd, R., Kelty, C., Brown, N., and Reed, M. (2001) 'The History of photodetection and photodynamic therapy' *Photochemistry and Photobiology*, vol. 74, pp. 656-669.

Aitken, R.J., Chaudhry, M.Q., Boxall, A.B., and Hull, M. (2006) 'Manufacture and use of nanomaterials: current status in the UK and global trends' *Occupational Medicine*, vol. 56, pp. 300-306.

Al-Awady, M.J., Greenway, G.M., and Paunov, V.N. (2015) 'Nanotoxicity of polyelectrolytefunctionalized titania nanoparticles towards microalgae and yeast: role of the particle concentration, size and surface charge' *RSC Advances*, vol. 5, pp. 37044-37059.

Al-Shaeri, M., Ahmed, D., McCluskey, F., Turner, G., Paterson, L., Dyrynda, E.A., and Haertl, M.G. (2013) 'Potentiating toxicological interaction of a single-walled carbon nanotubes with dissolved metals' *Environmental Toxicology and Chemistry*, vol. 32, no. 12, pp. 2701-2710.

Amarnath, S., Hussain, M.A., Nanjundiah, V., and Sood, A.K. (2012) 'Galactosidase leakage from *Escherichia coli* points to mechanical damages likely cause of carbon nanotube toxicity' *Soft Nanoscience Letters*, vol. 2, pp. 41-45.

An, K.H., Jeon, K.K., Kim, W.S., Park, Y.S., Lim, S.C., Bae, D.J., and Lee, Y.H. (2001) 'Characterization of supercapacitors using singlewalled carbon nanotube electrodes' *Korean Physical Society*, vol. 39, pp. S511-S517.

Antonenkov, V.D., Grunau, S., Ohlmeier, S., and Hiltunen, J.K. (2010) 'Peroxisomes are oxidative organelles' *Antioxidants and Redox Signaling*, vol. 13, no. 4, pp. 525-537.

Anway, M.D., and Skinner, M. (2008) 'Epigenetic programming of the germ line: effects of endocrine disruptors on the development of transgenerational disease' *Reproductive Biomedecine Online*, vol. 16, pp. 23-25.

Asada, K. (1999) 'The water-water cycle in chloroplasts: scavenging of active oxygens and dissipation of excess photons' *Annual Review of Plant Biology*, vol. 50, pp. 601-639.

Asakura, M., Sasaki, T., Sugiyama, T., Takaya, M., Koda, S., Nagano, K., Arito, H., and Fukushima, S. (2010) 'Genotoxicity and cytotoxicity of multi-wall carbon nanotubes in cultured Chinese hamster lung cells in comparison with chrysotile a fibers' *Occupational Health*, vol. 52, no. 3, pp. 155-166.

Aschberger, K., Johnston, H.J., Stone, V., Aitken, R.J., Hankin, S.M., Peters, S,A., Tran, C.L., and Christensen, F.M. (2010) 'Review of carbon nanotubes toxicity and exposure-appraisal of human health risk assessment based on open literature' *Critical Reviews in Toxicology*, vol. 40, no. 9, pp. 759-790.

Aschberger, K., Micheletti, C., Sokull-Kluttgen, B., and Christensen, F.M. (2011) 'Analysis of currently available data for characterising the risk of engineered nanomaterials to the environment and human health — Lessons learned from four case studies' *Environment International*, vol. 37, no. 6, pp. 1143-1156.

Asharani, P.V., Wu, YL., Gong, Z., and Valiyaveettil, S. (2008) 'Toxicity of silver nanoparticles in zebrafish models' *Nanotechnology*, vol. 19, no. 25, DOI: 10.1088/0957-4484/19/25/255102.

Augusteyn, R.C. (2004) 'Alpha-crystallin: a review of its structure and function' *Clinical and Experimental Optometry*, vol. 87, no. 6, pp. 356-366.

Avallone, E., Baumeister, T., and Sadegh, A. (2006) '*Marks' standard handbook for mechanical engineers*' 11th ed. New York, US, McGrew-Hill, 1800 pages.

Bai, Y., Zhang, Y., Zhang, J., Mu, Q., Zhang, W., Butch, E.R., Snyder, S.E., and Yan, B. (2010) 'Repeated administrations of carbon nanotubes in male mice cause

reversible testis damage without affecting fertility' *Nature Nanotechnology*, vol. 5, pp.683-689.

Baklouti-Gargouri, S., Ghorbel, M., Mahmoud, A., Mkaouar-Rebai, E., Cherif, M., Chakroun, N., Sellami, A., Fakhfakh, F., and Ammar-Keskes, L. (2013) 'A novel m.6307A>G mutation in the mitochondrial *COXI*gene in asthenozoospermic infertile men' *Molecular Reproduction and Development*, vol. 80, pp. 581-587.

Bar-Ilan, O., Albrecht, R., Fako, V., and Furgeson, D. (2009) 'Toxicity assessments of multisized gold and silver nanoparticles in zebrafish embryos' *Small*, vol. 5, pp. 1897-1910.

Bar-Ilan, O., Chuang, C.C., Schwahn, D.J., Yang, S., Joshi, S., Pedersen, J.A., Hamers, R.J., Peterson, R.E., and Heideman, W. (2013) 'TiO2 Nanoparticle exposure and illumination during zebrafish development: Mortality at parts per billion concentrations' *Environmental Science and Technology*, vol. 47, pp. 4726-4733.

Barker, P.J., and Branch, A. (2008) 'The interaction of modern sunscreen formulations with surface coatings' *Progress in Organic Coatings*, vol. 62, pp. 313-320.

Batley, G.E., Kirby, J.K., and Mclaughlin, M.J. (2013) 'Fate and risks of nanomaterials in aquatic and terrestrial environments' *Accounts of Chemical Research*, vol. 46, no. 3, pp. 854-862.

Baveye, P., and Laba, M. (2008) 'Aggregation and toxicology of titanium dioxide nanoparticles' *Environmental Health Perspective*, vol. 116, no. 4, pp. A152-A155.

Bilberg, K., Hovgaard, M.B., Besenbacher, F., and Baatrup, E. (2012) 'In vivo toxicity of silver nanoparticles and silver ions in zebrafish (*Danio rerio*)' *Journal of Toxicology*, vol. 2012, DOI: 10.1155/2012/293784.

Bobe, J. and Goetz, F.W. (2000) 'A tumor necrosis factor decoy receptor homologue is up-regulated in the brook trout (*Salvelinus fontinalis*) ovary at the completion of ovulation. *Biology of Reproduction*, vol. 62, no. 2, pp. 420-426.

Böhme, S., Stärk, H-J., Reemtsmab, T., and Kühnel, D. (2015) 'Effect propagation after silver nanoparticle exposure in zebrafish (*Danio rerio*) embryos: a correlation to internal concentration and distribution patterns' *Environmental Science: Nano*, vol. 2, pp. 603-614.

Boisen, K., Main, K., Rajpert-De Meyts, E., and Skakkebaek, N. (2001) 'Are male reproductive disorders a common entity? The testicular dysgenesis syndrome' *Annals of the New York Academy of Sciences*, vol. 948, pp. 90-99.

Borm. P., Klaessig, F.C., Landry, T.D., Moudgil, B., Pauluhn, J., Thomas, K. (2006) 'Research stratigies for safety evaluation of nanomaterials, part V: role of dissolution in biological fate and effects of nanoscale particles' *Toxicological Sciences*, nol. 90, no. 1, pp. 23-32.

Bottini, M., Bruckner, S., Nika, K., Bottini, N., Bellucci, S., Magrini, A., Bergamaschi, A and Mustelin, T. (2006) 'Multi-walled carbon nanotubes induce T lymphocyte apoptosis' *Toxicology Letters*, vol. 160, no. 2, pp. 121-126.

Boutet, I., Moraga, D., Marinovic, L., Obreque, J. and Chavez-Crooker, P. (2008) 'Characterization of reproduction-specific genes in a marine bivalve mollusc: Influence of maturation stage and sex on mRNA expression' *Gene*, vol. 407, pp. 130-138.

Braunbeck, T., Lammer, E. (2006) 'Draft detailed review paper on fish embryo toxicity assays' UBA Contract Number 203 85 422. Umweltbundesamt–German Federal Environment Agency, Dessau, Germany.

Brosius, U., Dehmel, T., and Gärtner, J. (2002) 'Two different targeting signals direct human peroxisomal membrane protein 22 to peroxisomes' *The Journal of Biological Chemistry*, vol. 277, no. 1, pp. 774-784.

Bustin, S.A., Benes, V., Garson, J.A., Hellemans, J., Huggett, J., Kubista, M., Mueller, R., Nolan, T., Pfaffl, M.W., Shipley, G.L., Vandesompele, J. and Wittwer, C.T. (2009) 'The MIQE guidelines: minimum information for publication of

quantitative real-time PCR experiments' *Clinical Chemistry*, vol. 55, pp. 611-622.

Buzea, C., Blandino, I.I.P., and Kevin, R. (2007) 'Nanomaterials and nanoparticles: sources and toxicity' *Biointerphase*, vol. 2, pp. MR17-MR172.

Calabrese, V., Scapagnini, G., Ravagna, A., Colombrita, C., Spadaro, F., Butterfield, D.A., and Stella, A.M.G. (2004) 'Increased expression of heat shock proteins in rat brain during aging: relationship with mitochondrial function and glutathione redox state' *Mechanisms of Ageing and Development*, vol. 125, pp. 325-335.

Carabante, I., Grahn, M., Holmgren, A., Kumpiene, J., and Hedlund, J. (2009) 'Adsorption of As (V) on iron oxide nanoparticle films studied by in situ ATR–FTIR spectroscopy' *Colloids and Surfaces A*, vol. 346, pp. 106-13.

Carlotti, M.E., Ugazio, E., Sapino, S., Fenoglio, I., Greco, G., and Fubini, B. (2009) 'Role of particle coating in controlling skin damage photoinduced by titania nanoparticles' *Free Radical Research*, vol. 43, no. 3, pp. 312-322.

Carlson, C., Hussain, S.M., Schrand, A.M., Braydich-Stolle, L.K., Hess, K.L., Jones, R.L., Schlager, J.J. (2008) 'Unique cellular interaction of silver nanoparticles: size dependent generation of reactive oxygen species' *Journal of Physical Chemistry B*, vol. 112, pp. 13608-13619.

Carpena, X., Soriano, M., Klotz, M.G., Duckworth, H.W., Donald, L.J., Melik-Adamyan, W., Fita, I., and Loewen, P.C. (2003) 'Structure of the Clade 1 catalase, CatF of Pseudomonas syringae, at 1.8 a resolution' *Proteins*, vol. 50, no. 3, pp. 423-436.

Chae, Y.J., Pham, C.H., Lee, J., Bae, E., Yi, J., and Gu, M.B. (2009) 'Evaluation of the toxic impact of silver nanoparticles on Japanese medaka (Oryzias latipes)' *Aquatic Toxicology,* vol. 94, no. 4, pp. 320-327.

Chen, J., and Poon, C-S. (2009) 'Photocatalytic construction and building materials: from fundamentals to applications' *Building and Environment*, vol. 44, no. 9, pp. 1899-1906.

Chen, L., Hu, P., Zhang, L., Huang, S., Luo, L., and Huang, C. (2012) 'Toxicity of graphene oxide and multi-walled carbon nanotubes against human cells and zebrafish' *Science China Chemistry*, vol. 55, pp. 2209-2216.

Cheng, J., Chan, C.M., Veca, M.L., Poon, W.L., Chan, P.K., Qu, L., Sun, Y.P., and Cheng, S.H. (2009) 'Acute and long-term effects after single loading of functionalized multi-walled carbon nanotubes into zebrafish (*Danio rerio*). *Toxicology and Applied Pharmacology*, vol. 235, no. 2, pp. 216-225.

Cheng, J., Flahaut, E., and Cheng, S.H. (2007) 'Effect of carbon nanotubes on developing zebrafish (*Danio rerio*) embryos' *Environmental Toxicology and Chemistry*, vol. 26, no. 4, pp. 708-716.

Cheng, J.P, and Cheng, S.H. (2012) 'Influence of carbon nanotube length on toxicity to zebrafish embryos' *International Journal of Nanomedicine*, vol. 7, pp. 3731-3739.

Chevrollier, A., Loiseau, D., Reynier, P., and Stepien, G. (2011). 'Adenine nucleotide translocase 2 is a key mitochondrial protein in cancer metabolism' *Biochimica et Biophysica Acta*, vol. 1807, no. 6, pp. 562-567.

Cho, J., and Caruso, F. (2005) 'Investigation of the Interactions between Ligand-Stabilized Gold Nanoparticles and Polyelectrolyte Multilayer Films' *Chemistry of Materials*, vol. 17, pp. 4547-4553.

Cho, J-G., Kim, K-T.,Ryu, T-K., Lee, J-W., Kim, J-E., Kim, J., Lee, B-C., Jo, E-H., Yoon, J., Eom, I-C., Choi, K., and Kim, P. (2013) 'Stepwise embryonic toxicity of silver nanoparticles on *Oryzias latipes*' *BioMed Research International*, vol. 2013, DOI: 10.1155/2013/494671.

Cho, M., Chung, H., Choi, W., and Yoon, J. (2004) 'Linear correlation between inactivation of E. coli and OH radical concentration in TiO_2 photocatalytic disinfection' *Water Resorces*, vol. 38, pp. 1069-1077.

Choi, H., Stathatos, E., and Dionysiou, D.D. (2006) 'So-lgel preparation of mesoporous photocatalytic TiO_2 films and TiO_2/Al_2O_3 composite membranes for

environmental applications' *Applied Catalysis B: Environmental*, vol. 63, pp. 60-67.

Choi, J.E., Kim, S., Ahn, J.H., Youn, P., Kang, J.S., Park, K., Yi, J., and Ryu, D-Y. (2010) 'Induction of oxidative stress and apoptosis by silver nanoparticles in the liver of adult zebrafish' *Aquatic Toxicology*, vol. 100, pp. 151-159.

Choi, S.J., Oh, J.M., and Choy, J.H. (2009) 'Toxicological effects of inorganic nanoparticles on human lung cancer A549 cells' *Inorganic Biochemistry*, vol. 103, no. 3, pp. 463-471.

Ciocan, C.M., Cubero-Leon, E., Minier, C. and Rotchell, J.M. (2011) 'Identification of reproduction-specific genes associated with maturation and estrogen exposure in a marine bivalve *Mytilus edulis*' *PloS One*, vol. 6, DOI: 10.1371/journal.pone.0022326.

Ciocan, C.M., Cubero-Leon, E., Peck, M.R., Langston, W.J., Pope, N., Minier, C. and Rotchell, J.M. (2012) 'Intersex in *Scrobicularia plana*: Transcriptomic analysis reveals novel genes involved in endocrine disruption' *Environmental Science and Technology*, vol. 46, no. 23, pp. 12936-12942.

Coccini, T., Gornati, R., Rossi, F., Signoretto, E., Vanetti, I., Bernardini, G., and Manzo, L. (2014) 'Gene expression changes in rat liver and testes after lung instillation of a low dose of silver nanoparticles' *Nanomedicine & Nanotechnology*, vol. 5, DOI: 10.4172/2157-7439.1000227.

Craft, J.A., Gilbert, J.A., Temperton, B., Dempsey, K.E., Ashelford, K., Tiwari, B., Hutchinson, T.H. and Chipman, J.K. (2010) 'Pyrosequencing of *Mytilus galloprovincialis* cDNAs: tissue specific expression patterns' *PloS One*, vol. 5, DOI: 10.1371/journal.pone.0008875.

Crosera, M., Prodi, A., Mauro, M., Pelin, M., Florio, C., Bellomo, F., Adami, G., Apostoli, P., De Palma, G., Bovenzi, M., Campanini, M., Filon, F.L. (2015) 'Titanium dioxide nanoparticle penetration into the skin and effects on HaCaT cells'

International Journal of Environmental Research and Public Health, vol. 12, no. 8, pp. 9282-9297.

Cui, D.X., Tian, F.R., Ozkan, C.S., Wang, M., and Gao, H. (2005) 'Effect of single wall carbon nanotubes on human HEK293 cells' *Toxicology Letters*, vol. 155, pp. 73-85.

Cunningham, S., Brennan-Fournet, M.E., Ledwith, D., Byrnes, L., and Joshi, L. (2013) 'Effect of nanoparticle stabilization and physicochemical properties on exposure outcome: acute toxicity of silver nanoparticle preparations in zebrafish (Danio rerio)' *Environmental Science and Technology*, vol. 47, pp. 3883-3892.

Da silva, R.G.T. (2014) 'The effect of silver nanoparticles: a chronic *in vivo* study for the evaluation of hepatic mitochondrial toxicity' MSc Dissertation, University of Coimbra.

Darlington, T.K., Neigh, A.M., Spencer, M.T., Nguyen, O.T., and Oldenburg, S.J. (2009) 'Nanoparticle characteristics affecting environmental fate and transport through soil' *Environmental Toxicology and Chemistry*, vol. 28, pp. 1191-1199.

Dastjerdi, R., and Montazer, M. (2010) 'A review on the application of inorganic nano-structured materials in the modification of textiles: focus on anti-microbial properties'. *Colloids and Surfaces* B, vol. 79, no. 1, pp. 5-18.

Dayeh, V.R., Lynn, D.H., and Bols, N.C. (2005) 'Cytotoxicity of metals common in mining effluent to rainbow trout cell lines and to the ciliated protozoan, Tetrahymena thermophila' *Toxicology in Vitro*, vol. 19, pp. 399-410.

Denslow, N.D., Garcia-Reyerob, N., and Barberc, D.S. (2007) 'Fish 'n' chips: the use of microarrays for aquatic toxicology' *Molecular BioSystems*, vol. 3, pp. 172-177.

Diatchenko, L., Lau, Y.F., Campbell, A.P., Chenchik, A., Moqadam, F., Huang, B., Lukyanov, K., Gurskaya, N., Sverdlov, E.D., and Siebert, P.D. (1996) 'Suppression subtractive hypridization: a method for generating diferentially regulated or tissue-specific cDNA probes and libraries' *Proceedings of the*

National Academy of Sciences of the United States of America, vol. 93, pp. 6025-6030.

Dimitrov, D. (2006) 'Interactions of antibody-conjugated nanoparticles with biological surfaces' *Colloids and Surfaces A*, vol. 282-283, pp. 8-10.

Dobrzynska, M.M., Gajowik, A., Radzikowska, J., Lankoff, A., Dusinská, M., and Kruszewski, M. (2014) 'Genotoxicity of silver and titanium dioxide nanoparticles in bone marrow cells of rats in vivo' *Toxicology*, vol. 315, pp. 86-91.

Dodd, N.J.F., and Jha, A.N. (2011) 'Photoexcitation of aqueous suspensions of titanium dioxide nanoparticles: an electron spin resonance spin trapping study of potentially oxidative reactions' *Photochemistry and Photobiology*, vol. 87, pp. 632-640.

Du, J., Wang, S., You, H., and Zhao, X. (2013) 'Understanding the toxicity of carbon nanotubes in the environment is crucial to the control of nanomaterials in producing and processing and the assessment of health risk for human: A review' Environmental *Toxicology and Pharmacology,* vol. 36, pp. 451-462.

Duan, Y., Liu, J., Ma, L., Li, N., Liu, H., Wang, J., Zheng, L., Liu, C., Wang, X., Zhao, X., Yan, J., Wang, S., Wang, H., Zhang, X., and Hong, F. (2010) 'Toxicological characteristics of nanoparticulate anatase titanium dioxide in *mice'Biomaterials*, vol. 31, pp. 894-899.

Dubińska-Magiera, M., Jablońska, J., Saczko, J., Kulbacka, J., Jagla, T., and Daczewska, M. (2014) 'Contribution of small heat shock proteins to muscle development and function' *Federation of European Biochemical Societies*, vol. 588, no. 4, pp. 517-530.

Dunford, R., Salinaro, A., Cai, L., Serpone, N., Horikoshi, S., Hidaka, H., and Knowland, J. (1997) 'Chemical oxidation and DNA damage catalysed by inorganic sunscreen ingredients' *FEBS letters*, vol. 418, pp. 87-90.

Esteban, M.A. (2012) 'An Overview of the Immunological Defenses in Fish Skin' ISRN Immunology, vol. 2012, Article ID 853470, DOI: 10.5402/2012/853470.

Esterkin, C.R., Negro, A.C., Alfano, O.M., and Cassano, A.E. (2005) 'Air pollution remediation in a fixed bed photocatalytic reactor coated with TiO_2' *AIChE Journal*, vol. 51, pp. 2298-2310.

European Commission. (2005) 'Conclusions recommendations for new research. In: Tomellini, R., De Villepin, C. (Eds.), Proceedings of the Workshop: Research Needs on Nanoparticles' Brussels, pp. 75-79.

European Commission. (2012) 'EU Approach to Resilience: Learning from Food Security Crises' 586 final, available at: http://ec.europa.eu/echo/files/policies/resilience/com_2012_586_resilience_en.pdf

Fan, F.L., Qin, Z., Bai, J., Rong, W.D., Fan, F.Y and Tian, W., Wu, X.L., Wang, Y., and Zhao, L. (2012) 'Rapid removal of uranium from aqueous solutions using magnetic Fe3O4–SiO2 composite particles' *Environmental Radioactivity*, vol. 106, pp. 40-46.

Farkas, J., Christian, P., Gallego-Urrea, J.A., Roos, N., Hassellov, M., Tollefsen, K.E., and Thomas, K.V. (2011) 'Uptake and effects of manufactured silver nanoparticles in rainbow trout (*Oncorhynchus mykiss*) gill cells' *Aquatic Toxicology*, vol. 101, pp. 117-125.

Federici, G., Shaw, B.J., and Handy, R.D. (2007) 'Toxicity of titanium dioxide nanoparticles to rainbow trout (*Oncorhynchus mykiss*): gill injury, oxidative stress, and other physiological effects' *Aquatic Toxicology*, vol. 84, pp. 415-430.

Ferreira, A.J., Cemlyn-Jones, J., and Robalo C.C. (2013) 'Nanoparticles, nanotechnology and pulmonary nanotoxicology' *Revista Portuguesa Pneumologia*, vol. 19, no. 1, pp. 28-37.

Filon, F.L., Mauro, M., Adami, G., Bovenzi, M., and Crosera, M. (2015) 'Nanoparticles skin absorption: New aspects for a safety profile evaluation' *Regulatory Toxicology and Pharmacology*, vol. 72, pp. 310-322.

Foulkes, E.C. (2000) 'Transport of toxic heavy metals across cell membranes' *Proceedings of the Society for Experimental Biology and Medicine*, vol. 223, pp. 234-240.

Frangville, C., Rutkevicius, M., Richter, A.P., Velev, O.D., Stoyanov, S.D., and Paunov, V.N. (2012) 'Fabrication of environmentally biodegradable lignin nanoparticles' *Chemical Physics and Physical Chemistry*, vol. 18, pp. 4235-43.

Freitas, R.A. (2005) 'What is nanomedicine?' *Nanomedicine*, vol. 1, pp. 2-9.

Friedrich, K.A., Henglein, F., Stimming, U., and Unkauf, W. (1998) 'Investigation of Pt particles on gold substrates by IR spectroscopy — particle structure and catalytic activity' *Colloids and Surfaces A*, vol. 134, pp. 193-206.

Galloway, T., Lewis, C., Dolciotti, I., Johnston, B.D., Moger, J and Regoli, F. (2010) 'Sublethal toxicity of nano-titanium dioxide and carbon nanotubes in a sediment dwelling marine polychaete' *Environmental Pollution*, vol. 158, pp. 1748-1755.

Garcia-Reyero, N., Kennedy, A.J., Escalon, B.L., Habib, T., Laird, J.G., Rawat, A., Wiseman, S., Hecker, M., Denslow, N., Steevens, J.A., Perkins, E.J. (2014) 'Differential Effects and Potential Adverse Outcomes of Ionic Silver and Silver Nanoparticles in Vivo and in Vitro' *Environmental Science and Technology*, vol. 48, no. 8, pp. 4546-4555.

Garcia-Reyero, N., Thornton, C., Hawkins, A.D., Escalon, L., Kennedy, A.J., Steevens, J.A., and Willett, K. (2015) 'Assessing the exposure to nanosilver and silver nitrate on fathead minnow gill gene expression and mucus production' *Environmental Nanotechnology, Monitoring and Management*, DOI: http://dx.doi.org/10.1016/j.enmm.2015.06.001

Gärtner, J., Moser, H., and Valle, D. (1992) 'Mutations in the 70K peroxisomal membrane protein gene in Zellweger syndrome' *Nature Genetics*, vol. 1, pp. 16-23.

Gelis, C., Girard, S., Mavon, A., Delverdier, M., Paillous, N., and Vicendo, P. (2003) 'Assessment of the skin photoprotective capacities of an organo-mineral broad-spectrum sunblock on two ex vivo skin models' *Photodermatology Photoimmunology & Photomedicine*, vol. 19, no. 5, pp. 242-253.

Ghafari, P., St-Denis, C.H., Power, M.E., Jin, X., Tsou, V., Mandal, H.S., Niels C. Bols, N.C., and Tang, X. (2008) 'Impact of carbon nanotubes on the ingestion and digestion of bacteria by ciliated protozoa' *Nature Nanotechnology*, vol. 3, pp. 347-351.

Goodman, C.M., McCusker, C.D., Yilmaz, T., and Rotello, V.M. (2004) 'Toxicity of gold nanoparticles functionalized with cationic and anionic side chains' *Bioconjugate chemistry*, vol. 15, pp. 897-900.

Gottschalk, F., and Nowack, B. (2011) 'The release of engineered nanomaterials to the environment' *Journal of Environmental Monitoring*, vol. 13, DOI: 10.1039/c0em00547a.

Gottschalk, F., Sonderer, T., Scholz, R., and Nowack, B. (2009) ,Modeled environmental concentrations of engineered nanomaterials (TiO2, ZnO, Ag, CNT, fullerenes) for different regions' *Environmental Science and Technology*, vol. 43, no. 24, pp. 9216-9222.

Gottschalk, F., Sonderer, T., Scholz, R.W., and Nowack, B. (2010) 'Possibilities and limitations of modeling environmental exposure to engineered nanomaterials by probabilistic material flow analysis' *Environmental Toxicology and Chemistry*, vol. 29, pp. 1036-1048.

Gracey, A.Y., Troll, J.V., and Somero, G.N. (2001) 'Hypoxia-induced gene expression profiling in the euryoxic fish*Gillichthys mirabilis*' *Proceedings of the* National

Academy *of Sciences of the* United States *of America*, vol. 98, no. 4, pp. 1993-1998.

Greenamyre, J.T., MacKenzie, G., Peng, T.I., and Stephans, S.E. (1999) 'Mitochondrial dysfunction in Parkinson's disease' *Biochemical Society Symposium*, vol. 66, pp. 85-97.

Griffitt, R. J., Weil, R., Hyndman, K. A., Denslow, N. D., Powers, K., Taylor, D., and Barber, D. S. (2007) 'Exposure to copper nanoparticles causes gill injury and acute lethality in zebrafish (*Danio rerio*)' *Environmental Science and Technology*, vol. 41, pp. 8178-8186.

Griffitt, R.J., Hyndman, K., Denslow, N., and Barber, D.S. (2009) 'Comparison of molecular and histological changes in zebrafish gills exposed to metallic nanoparticles' *Toxicological Sciences*, vol. 107, pp. 404-415.

Griffitt, R.J., Luo, J., Gao, J., Bonzongo, J.C., and Barber, D.S. (2008) 'Effects of particle composition and species on toxicity of metallic nanomaterials in aquatic organisms' *Environmental Toxicology and Chemistry*, vol. 27, pp. 1972-1978.

Gromadzka-Ostrowska, J., Dziendzikowska, K., Lankoff, A., Dobrzyńska, M., Instanes, C., Brunborg, G., Gajowik, A., Radzikowska, J., Wojewódzka, M., and Kruszewski, M. (2012) 'Silver nanoparticles effects on epididymal sperm in rats' *Toxicology Letters*, vol. 214, pp. 251-258.

Guo, L.L., Liu, X.H., Qin, D.X., Gao, L., Zhang, H.M., Liu, J.Y., and Cui, Y.G. (2009) 'Effects of nanosized titanium dioxide on the reproductive system of male mice' *Zhonghua Nan Ke Xue*, vol. 15, pp. 517-522.

Gurr, J.R., Wang, A.S.S., Chen, C.H., and Jan, K.Y. (2005) 'Ultrafine titanium dioxide particles in the absence of photoactivation can induce oxidative damage to human bronchial epithelial cells' *Toxicology*, vol. 213, pp. 66-73.

Gurskaya, N.G., Diatchenko, L., Chenchik, A., Siebert, P.D., Khaspekov, G.L., Lukyanov, K.A., Vagner, L.L., Ermolaeva, O.D., Lukyanov, S.A., and Sverdlov, E.D. (1996) 'Equalizing cDNA Subtraction Based on Selective Suppression of Polymerase

Chain Reaction: Cloning of Jurkat Cell Transcripts Induced by Phytohemaglutinin and Phorbol 12-Myristate 13-Acetate' *Analytical Biochemistry*, vol. 240, pp. 90-97.

Gusev, A.A., Fedorova, I.A., Tkachev, A.G., Godymchuk, A.Y., Kuznetsov, D.V., and Polyakova, I.A. (2012) 'Acute Toxic and Cytogenetic Effects of Carbon Nanotubes on Aquatic Organisms and Bacteria' *Nanotechnologies in Russia*, vol. 7, no. 9-10, pp. 509-516.

Gustafsson, Å., Lindstedt, E., Elfsmark, L.S., and Bucht, A. (2011) 'Lung exposure of titanium dioxide nanoparticles induces innate immune activation and long-lasting lymphocyte response in the Dark Agouti rat' *Journal of Immunotoxicology*, vol. 8, pp. 111-121.

Gutteridge, J.M. (1995) 'Lipid peroxidation and antioxidants as biomarkers of tissue damage' C*linical Chemistry*, vol. 41, pp. 1819-1828.

Haitina, T., Lindblom, J., Renstrom, T., and Fredriksson, R. (2006) 'Fourteen novel human members of mitochondrial solute carrier family 25 (SLC25) widely expressed in the central nervous system' *Genomics*, vol. 88, pp. 779-790.

Hall, S., Bradley, T., Moore, J.T., Kuykindall, T., and Minella, L. (2009) 'Acute and chronic toxicity of nano-scale TiO2 particles to freshwater fish, cladocerans, and green algae, and effects of organic and inorganic substrate on TiO2 toxicity' *Nanotoxicology*, vol. 3, pp. 91-97.

Hall, J.R., Clow, K.A., Rise, M.L., and Driedzic, W.R. (2011) 'Identification and validation of differentially expressed transcripts in a hepatocyte model of cold-induced glycerol production in rainbow smelt (Osmerus mordax)' *American Journal of Physiology - Regulatory, Integrative and Comparative Physiology*, vol. 301, no. 4, pp. R995-R1010.

Handy, R.D., and Shaw, B.J. (2007) 'Ecotoxicity of nanomaterials to fish: challenges for ecotoxicity testing' *Integrated Environmental Assessment and Management*, vol. 3, pp. 458-60.

Hartl, M.G.J., Gubbins, E., Gutierrez, J., and Fernandes, T.F. (2015) 'Review of existing knowledge – emerging contaminant: Focus on nanomaterials and microplastics in the aquatic environment' CREW - Centre of Expertise for Waters.

Hawkins, A.D., Thornton, C., Steevens, J.A., and Willett, K.L. (2014) 'Alteration in Pimephales promelas mucus production after exposure to nanosilver or silver nitrate' *Environmental Toxicology and Chemistry*, vol. 33, pp. 2869-2872.

Hill, A.J., Teraoka, H., Heidemann, W., and Peterson, R.E. (2005) 'Zebrafish as model vertebrate for investigating chemical toxicity' *Toxicological Sciences*, vol. 86, pp. 6-19.

Hillegass, J.M., Shukla, A., Lathrop, S.A., MacPherson, M.B., Fukagawa, N.K., and Mossman, B.T. (2010) 'Assessing nanotoxicity in cells in vitro. Wires Nanomed' *Nanobiotechnology*, vol. 2, no. 3, pp. 219-231.

Ho, L., Titus, A.S., Banerjee, K.K., George, S., Lin, W., Deota, S., Saha, A.K., Nakamura, K., Gut, P., Verdin, E., and Kolthur-Seetharam, U. (2013) 'SIRT4 regulates ATP homeostasis and mediates a retrograde signaling via AMPK' *Aging,* vol. 5, no. 11, pp. 835-849.

Hoet, P.H.M., Bruske-Hohlfeld, I., and Salata, O.V. (2004) 'Nanoparticles - known and unknown health risks' *Nanobiotechnology,* vol. 2, pp. 12-27.

Hoshino, A., Fujioka, K., Oku, T., Suga, M., Sasaki, Y.F., Ohta, T., Yasuhara, M., Suzuki K., and Yamamoto, K. (2004) 'Physicochemical properties and cellular toxicity of nanocrystal quantum dots depend on their surface modification' *NANO Letters*, vol. 4, no. 11, pp. 2163-2169. Available at:

Howe, K., Clark, M.D., Torroja, C.F., Torrance, J., Berthelot, C., Muffato, M., Collins, J.E., Humphray, S., McLaren, K., et al. (2013) 'The zebrafish reference genomesequence and its relationship to the human genome' *Nature*, vol. 496, pp. 498-503.

Hu, C.J., Wang, L.Y., Chodosh, L.A., Keith, B., and Simon, M.C. (2003) 'Differential roles of hypoxia-inducible factor 1alpha (HIF-1alpha) and HIF-2alpha in hypoxic gene regulation' *Molecular and Cell Biology,* vol. 23, pp. 9361-9374.

Hu, J., Chen, G., and Lo, I. (2005) 'Removal and recovery of Cr (VI) from wastewater by maghemite nanoparticles. *Water Research*, vol. 39, no. 18, pp. 4528-4536.

Huang, C-L., Hsiao, I-L., Lin, H-C., Wang, C-F., Yuh-Jeen and Huang, Y-J. (2015) 'Silver nanoparticles affect on gene expression of inflammatory and neurodegenerative responses in mouse brain neural cells' *Environmental Research*, vol. 136, pp. 253-263.

Huczko, A., Lange, H., Calko, E., Grubek-Jaworska, H and Droszcz, P. (2001) 'Physiological testing of carbon nanotubes: are they asbestos-like?' *Fullerene Science and Technology*, vol. 9, pp. 251-254.

Imanaka, T., Aihara, K., Takano, T., Yamashitai, A., Sato, R., Suzuki, Y., Yokota, S., and Osumi, T. (1999) 'Characterization of the 70-kDa peroxisomal membrane protein, an ATP binding cassette transporter' *Biological Chemistry*, vol. 274, no. 17, pp. 11968-11976.

Jang, S., Park, J.W., Cha, H.R., Jung, S.Y., Lee, J.E., Jung, S.S., Kim, J.O., Kim, S.Y., Lee, C.S., and Park, H.S. (2012) 'Silver nanoparticles modify VEGF signaling pathway and mucus hypersecretion in allergic airway inflammation' *International Journal of Nanomedicine*, vol. 7, pp. 1329-1343.

Jebali, A., Hekmatimoghaddam, S., and Kazemi, B. (2014) 'The cytotoxicity of silver nanoparticles coated with different free fatty acids on the Balb/c macrophages: an*in vitro* study' *Drug and Chemical Toxicology*, vol. 37, pp. 433-439.

Jeon, Y-M., Park, S-K., Kim, W-J., Ham, J-H., and Lee, M-Y. (2011) 'The effects of TiO2 nanoparticles on the protein expression in mouse lung' *Molecular and Cellular Toxicology*, vol. 7, pp. 283-289.

Jevtov, I., Samuelsson, T., Yao, G., Amsterdam, A., and Ribbeck, K., (2014) 'Zebrafish as a model to study live mucus physiology' *Scientific Reports*, vol. 4, e6653. DOI: 10.1038/srep06653.

Jia, G., Wang, H., Yan, L., Wang, X., Pei, R., Yan, T., Zhao, Y., and Guo, X. (2005) 'Cytotoxicity of carbon nanomaterials: single-wall nanotube, multi-wall nanotube, and fullerene' *Environmental Science and Technology*, vol. 39, no. 5, pp. 1378-1383.

Jiang, B.H., Zheng, J.Z., Leung, S.W., Roe, R., and Semenza, G.L. (1997) 'Transactivation and inhibitory domains of hypoxia-inducible factor 1alpha. Modulation of transcriptional activity by oxygen tension' *The Journal of Biological C*hemistry, vol. 272, no. 31, pp. 19253-19260.

Jiang, D., Zhu, X-L., Zhao, J-F., Zhou, Y-K., Zhong, C., Zhang, J., and Huang, X. (2014) 'Subtractive screen of potential limb regeneration related genes from Pachytriton brevipes' *Molecular Biology Reports*, vol. 41, pp. 1015-1026.

Jimeno, C.D. (2008) 'A transcriptomic approach toward understanding PAMP-driven macrophage activation and dietary immunostimulant in fish' PhD Thesis, 222 pages, Departament de Biologia Cellular, Fisiologia i Immunologia, Facultat de Ciències, Universitat Autòmona de Barcelona, Barcelona, Spain.

Johari, S.A., Kalbassi, M.R., Soltani, M., and Yu, I.J. (2013) 'Toxicity comparision of colloidal sliver nanoparticlesin various life stages of rainbow trout (Oncorhynchus mykiss)' *Iranian Journal of Fisheries Sciences*, vol. 12, no. 1, pp. 76-95.

Jovanovic, B. (2011) 'Immunotoxicology of titanium dioxide and hydroxylated fullerenes engineered nanoparticles in fish models' PhD Thesis, Iowa State University. Ames, Iowa. Paper 10134.

Justo-Hanani, R., and Dayan, T. (2014) 'The role of the state in regulatory policy for nanomaterials risk: Analyzing the expansion of state-centric rulemaking in EU and US chemicals policies' *Research Policy*, vol. 43, pp. 169-178.

Kagan, V.E., Tyurina, Y.Y., Tyurin, V.A., Konduru, N.V., Potapovich, A.I., Osipov, A.N., Kisin, E. R., Schwegler-Berry, D., Mercer, R., Castranova, V., and Shvedova, A.A. (2006) 'Direct and indirect effects of single walled carbon nanotubes on RAW 264.7 macrophages: role of iron' *Toxicology Letters*, vol. 165, no. 1, pp. 88-100.

Kaida, T., Kobayashi, K., Adachi, M., and Suzuki, F. (2004) 'Optical characteristics of titanium oxide interference film and the film laminated with oxides and their application for cosmetics' *Journal of Cosmetic Science*, vol. *55*, pp. 219-220.

Kang, S., Pinault, M., Pfefferle, L.D., and Elimelech, M. (2007) 'Single-walled carbon nanotubes exhibit strong antimicrobial activity' *Langmuir*, vol. 23, no. 17, pp. 8670-8673.

Kapralov, A.A., Feng, W.H., Amoscato, A.A., Yanamala, N., Balasubramanian, K., Winnica, D.E., Elena R. Kisin, Kotchey, G.P., Gou, P., Sparvero, L.J., Ray, P., Mallampalli, R.K., Klein-Seetharaman, J., Fadeel, B., Star, A., Shvedova, A.A., and Kagan, V.E. (2012) 'Adsorption of Surfactant Lipids by Single-Walled Carbon Nanotubes in Mouse Lung upon Pharyngeal Aspiration: Role in Uptake by Macrophages' *ACS Nano*, vol. 6, pp. 4147-4156.

Karlsson, H.L. (2010) 'The comet assay in nanotoxicology research' *Analytical and Bioanalytical Chemistry*, vol. 398, no. 2, pp. 651-666.

Kashiwada, S., Ariza, M.E., Kawaguchi, T., Nakagame, Y., Jayasinghe, B.S., Gärtner, K., Nakamura, H., Kagami, Y., Sabo-Attwood, T., Ferguson, P.L., and Chandler, G.T. (2012) 'Silver nanocolloids disrupt medaka embryogenesis through vital gene expressions' *Environmental Science and Technology*, vol. 46, no. 11, pp. 6278-6287.

Kim, B., Park, C.S., Murayama, M., and Hochella, M.F. (2010) 'Discovery and characterization of silver sulfide nanoparticles in final sewage sludge products' *Environmental Science and Technology*, vol. 44, pp. 4509-7514.

Kisin, E.R., Murray, A.R., Keane, M.J., Shi, X.C., Schwegler-Berry, D., Gorelik, O., Arepalli, S., Castranova, V., Wallace, W.E., Kagan, V.E., and Shvedova, A.A. (2007) 'Single-walled carbon nanotubes: geno- and cytotoxic effects in lung fibroblast V79 cells' *Toxicology and Environmental Health, Part A*, vol. 70, no. 24, pp. 2071-2079.

Klaine, S.J., Alvarez, P.J.J., Batley, G.E., Fernandes, T.F., Handy, R.D., Lyon, D.Y., Mahendra, S., Mclaughlin, M.J., and Lead, J.R. (2008) 'Nanomaterials in the environment: behavior, fate, bioavailability and effects' *Environmental Toxicology and Chemistry*, vol. 27, no. 9, pp. 1825-1851.

Koehler, A., Som, C., Helland, A., and Gottschalk, F. (2008) 'Studying the potential release of carbon nanotubes throughout the application life cycle' *Cleaner Production*, vol. 16, pp. 927-937.

Koivisto, A.J., Lyyranen, J., Auvinen, A., Vanhala, E., Hameri, K., Tuomi, T., and Jokiniemi, J. (2012) 'Industrial worker exposure to airborne particles during the packing of pigment and nanoscale titanium dioxide' *Inhalation Toxicology*, vol. 24, pp. 839-849.

Koyama, S., Kim, Y.A., Hayashi, T., Takeuchi, K., Fujii, C., Kuroiwa, N., Koyama, H., Tsukahara, T and Endo, M. (2009) 'In vivo immunological toxicity in mice of carbon nanotubes with impurities' *Carbon*, vol. 47, no. 5, pp. 1365-1372.

Kumar, V., Abbas, A.K., and Fausto, N. (2005) 'Book review: robbins and cotran pathologic basis of disease. Chapter 1, cell injury, cell death, and adaptations, 7th Ed, DOI: 10.1354/vp.42-4-521.

Kwok, K.W., Auffan, M., Badireddy, A.R., Nelson, C.M., Wiesner, M.R., Chilkoti, A., Liu, J., Marinakos, S.M., and Hinton, D.E. (2012) 'Uptake of silver nanoparticles and toxicity to early life stages of Japanese medaka (Oryzias latipes): effect of coating materials' *Aquatic Toxicology*, vol. 120-121, pp. 59-66.

Laban, G., Nies, L.F., Turco, R.F., Bickham, J.W., and Sepulveda, M.S. (2010) 'The effects of silver nanoparticles on fathead minnow (*Pimephales promelas*) embryos' *Ecotoxicology*, vol. 19, pp. 185-195.

Lai, J.C., Ananthakrishnan, G., Jandhyam, S., Dukhande, V.V., Bhushan, A., Gokhale, M., Daniels, C.K., and Leung, S.W. (2010) 'Treatment of human astrocytoma U87 cells with silicon dioxide nanoparticles lowers their survival and alters their expression of mitochondrial and cell signaling proteins' *International Journal of Nanomedicine*, vol. 5, pp. 715-723.

Lam, C.W., James, J.T., McCluskey, R., and Hunter, R.L. (2004) 'Pulmonary toxicity of single-wall carbon nanotubes in mice 7 and 90 days after intratracheal instillation' *Toxicological Sciences*, vol. 77, pp. 126-134.

Lee, B., Duong, C.N., Cho, J., Lee, J., Kim, K., Seo, Y., Kim, P., Choi, K., and Yoon, J. (2012) 'Toxicity of citrate-capped silver nanoparticles in common carp (*Cyprinus carpio*)' *Journal of Biomedicine and Biotechnology*, vol. 2012, DOI: 10.1155/2012/262670.

Lee, B-C., Kim, K.T., Jeong, S.W., Kim, H.L., Lee, S-H., Choi, K., Kim, P., Seo, Y.R., and Yoon, J. (2011) 'Gene expression profiling of silver nanoparticle-exposed *Cyprinus carpio* using DNA microarray' *Cancer Prevention Research*, vol. 16, pp. 147-54.

Lee, J.H., Cha, K.E., Kim, M.S., Hong, H.W., Chung, D.J., Ryu, G., and Myung, H. (2009) 'Nanosized polyamidoamine (PAMAM) dendrimer-induced apoptosis mediated by mitochondrial dysfunction' *Toxicology Letters*, vol. 190, pp. 202-207.

Lee, K.D., Nir, S., and Papahadjopoulos, D. (1993) 'Quantitative analysis of liposome-cell interactions in vitro: Rate constants of binding and endocytosis with suspension and adherent J774 cells and human monocytes' *Biochemistry*, vol. *32*, no. 3, pp. 889-899.

Lee, K.J., Nallathamby, P.D., Browning, L.M., Osgood, C.J., and Xu, X-H.N. (2007) '*In Vivo* Imaging of Transport and Biocompatibility of Single Silver Nanoparticles in Early Development of Zebrafish Embryos' *ACS Nano*, vol. 1, no. 2, pp. 133-143.

Leelatanawit, R., Klinbunga, S., Aoki, T., Hirono, I., Valyasevi, R., and Menasveta, P. (2008) 'Suppression subtractive hybridization (SSH) for isolation and characterization of genes related to testicular development in the giant tiger shrimp Penaeus monodon' *BMB report*, pp. 796-802.

Lele, Z., and Krone, P.H. (1996) 'The zebrafish as a model system in developmental, toxicological and transgenic research' *Biotechnology Advances*, vol. 14, no. 1, pp. 57-72.

Lettieri, T. (2006) 'Recent applications of DNA microarray technology to toxicology and ecotoxicology. *Environmental Health Perspectives*, vol. 114, no. 1, pp. 4-9.

Li, C., Taneda, S., Taya, K., Watanabe, G., Li, X., Fujitani, Y., Nakajima, T., and Suzuki, A. (2009) 'Effects of in utero exposure to nanoparticle-rich diesel exhaust on testicular function in immature male rats' *Toxicology Letters*, vol. 185, pp. 1-8.

Li, L., Fan, M., Brown, R.C., Van Leeuwen, J., Wang, J., Wang, W., Song, Y., and Zhang, P. (2006a) 'Synthesis, properties, and environmental applications of nanoscale iron-based materials: a review' *Critical Reviews in Environmental Science and Technology*, vol. 36, pp. 405-431.

Li, X.Q., Elliott, D.W., and Zhang, W.X. (2006b) 'Zero-valent iron nanoparticles for abatement of environmental pollutants: materials and engineering aspects' *Critical Reviews in Solid State and Materials Sciences*, vol. 31, pp. 111-122.

Lieschke, G.J., and Currie, P.D. (2007) 'Animal models of human disease: zebrafish swim into view' *Nature Reviews Genetics*, vol. 8, pp. 353-367.

Lim, W., Cho, J., Kwon, H.Y., Park, Y., Rhyu, M.R., and Lee, Y. (2009) 'Hypoxia-inducible factor 1 alpha activates and is inhibited by unoccupied estrogen receptor beta' *FEBS Letters*, vol. 583, no. 8, pp. 1314-1318.

Lin, Z., Fernández-Robledo, J-A., Cellier, M.F.M., and Vasta, G.R. (2009) 'Metals and membrane metal transporters in biological systems: the role(s) of nramp in host-parasite interactions' *Argentine Chemical Society*, vol. 97, no. 1, pp. 210-225.

Lin, J., Zhang, H., Chen, Z., and Zheng, Y. (2010) 'Penetration of lipid membranes by gold nanoparticles: insights into cellular uptake, cytotoxicity, and their relationship' *ACS Nano*, vol. 4, no. 9, pp. 5421-5429.

Liu, W.T., (2006) 'Nanoparticles and their biological and environmental applications' *Bioscience and Bioengineering*, vol. 102, pp. 1-7.

Liu, X., and Sun, J. (2010) 'Endothelial cells dysfunction induced by silica nanoparticles through oxidative stress via JNK/P53 and NF-kB pathways' *Biomaterials*, vol. 31, no. 32, pp. 8198-8209.

Livak, K.J., and Schmittgen, T.D. (2001) 'Analysis of relative gene expression data using real-time quantitative PCR and the $2^{-\Delta\Delta C}{}_{T}$ method' *Methods*, vol. 25, pp. 402-408.

Long, Z., Ji, J., Yang, K., Lin, D., and Wu, F. (2012) 'Systematic and quantitative investigation of the mechanism of carbon nanotubes' toxicity toward algae' *Environmental Science and Technology*, vol. 46, no. 15, pp. 8458-8466.

Lu, F., Wu, S-H., Hung, Y., and Mou, C-Y. (2009) 'Size effect on cell uptake in well-suspended, uniform Mesoporous silica nanoparticles' *Small*, vol. 5, no. 12, pp. 1408-1413.

Lu, W., Senapati, D., Wang, S., Tovmachenko, O., Singh, A.K., Yu, H., and Ray, P.C. (2010) 'Effect of surface coating on the toxicity of silver nanomaterials on human skin keratinocytes. *Chemical Physics Letters*, vol. 487, pp. 92-96.

Lushchak, V.I., Lushchak, L.P., Mota, A.A., and Hermes-Lima, M., (2001) 'Oxidative stress and antioxidant defenses in goldfish Carassius auratus during anoxia and reoxygenation' *American Journal of Physiology. Regulatory, Integrative and Comparative Physiology*, vol. 280, pp. 100-107.

Ma-Hock, L., Treumann, S., Strauss, V., Brill, S., Luizi, F., Mertler, M., Wiench, K., Gamer, A.O., Ravenzwaay, B.V., and Landsiedel, R. (2009) 'Inhalation toxicity of multiwall carbon nanotubes in rats exposed for 3 months' *Toxicological Sciences*, vol. 112, pp. 468-481.

Maier, C.M., and Chan, P.H. (2002) ' Role of superoxide dismutases in oxidative damage and neurodegenerative disorders' *Neuroscientist*, vol. 8, pp. 323-334.

Maiorino, F.M., Brigelius-Flohe, R., Aumann, K.D., Roveri, A., Schomburg, D., and Flohe, L. (1995) 'Diversity of glutathione peroxidases' *Methods Enzymology*, vol. 252, pp. 38-48.

Manning, B.B. (2010) 'Mycotoxins in aquaculture feed. In: Nutrition and Fish Health, L. Chhorn & C.D. Webster (Eds.)' The Haworth Press, Inc. Binghamton, New York, USA, pp. 267-287.

Maran, C., Tassone, E., Masola, V., and Onisto, M. (2009) 'The story of SPATA2 (Spermatogenesis-Associated Protein 2): From Sertoli Cells to Pancreatic Beta-Cells' *Current Genomics*, vol. 10, no. 5, pp. 361-363.

Martin, E.D., Moriarty, M.A., Byrnes, L., and Grealy, M. (2009) 'Plakoglobin has both structural and signalling roles in zebrafish development' *Developmental Biology*, vol. 327, pp. 83-96.

Martins, I.M., López, M.C., Dominguez, A., and Choupina, A. (2013) 'Isolation and Sequencing of Actin1, Actin2 and Tubulin1 Genes Involved in Cytoskeleton Formation in Phytophthora cinnamomi' *Plant Pathology and Microbiology*, vol. 4, DOI: 10.4172/2157-7471.1000194.

Mattos, J.J., Siebert, M.N., Luchmann, K.H., Granucci, N., Dorrington, T., Stoco, P.H., Grisard, E.C., and Bainy, A.C.D. (2010) 'Differential gene expression in *Poecilia vivipara* exposed to diesel oil water accommodated fraction' *Marine Environmental Research*, vol. 69, no. 1, pp. S31-S33.

McGrath, P, Li C. (2008) 'Zebrafish: a predictive model for assessing drug-induced toxicity' *Drug Discovery Today,* vol. 13, no. 9-10, pp. 394-401.

Mills, A., and Le Hunte, S. (1997) 'An overview of semiconductor photocatalysis' *Journal of Photochemistry and Photobiology A: Chemistry*, vol. 108, pp. 1-35.

Misra, S.K., Dybowska, A., Berhanu, D., Luoma, S.N., and Valsami-Jones, E. (2012) 'The complexity of nanoparticle dissolution and its importance in nanotoxicological studies' *Science of the Total Environment*, vol. 438, pp. 225-232.

Moghimi, S.M., Hunter, A.C., and Murray, J.C. (2001) 'Long-circulating and targetspecific nanoparticles: theory to practice' *Pharmacological Reviews*, vol. 53, pp. 283-318.

Morita, M., and Imanaka, T. (2012) 'Peroxisomal ABC transporters: structure, function and role in disease' *Biochemica et Biophsica Acta*, vol. 1822, no. 9, pp. 1387-1396.

Moro, E., Claudio Maran, C., Slongo, M.L., Argenton, F., Toppo, S., and Onisto, M. (2007) 'Zebrafish spata2 is expressed at early developmental stages' *The International Journal of Developmental Biology*, vol. 51, pp. 241-246.

Mouchet, F., Landois, P., Flahaut, E., Pinelli, E., and Gauthier, L. (2007) 'Assessment of the potential in vivo ecotoxicity of double-walled carbon nanotubes (DWNTs) in water, using the amphibian ambystoma mexicanum' *Nanotoxicology*, vol. 1, no. 2, pp. 149-156.

Mueller, N.C., and Nowack, B. (2008) 'Exposure modeling of engineered nanoparticles in the environment' *Environmental Science and Technology*, vol. 42, no. 12, pp. 4447-4453.

Muller, J., Huaux, F., and Lison, D. (2006) 'Respiratory toxicity of carbon nanotubes: how worried should we be?' *Carbon*, vol. 44, pp. 1048-1056.

Murphy, L.D., Herzog, C.E., Rudick, J.B., Fojo, A.T., and Bates, S.E. (1990) 'Use of the polymerase chain reaction in the quantitation of mdr-1 gene expression' *Biochemistry*, vol. 29, no. 45, pp. 10351-10356.

Murre, C., Bain, G., Van Dijk, M.A., Engel, I., Furnari, B.A., Massari, M.E., Matthews, J.R., Quong, M.W., Rivera, R.R., and Stuiver, M.H. (1994) 'Review: structure and function of helix-loop-helix proteins' *Biochimica et Biophsica Acta*, vol. 1218, no. 2, pp. 129-135.

Mwangi, J.N., Wang, N., Ingersoll, C.G., Hardesty, D.K., Brunson, E.L., Li, H., and Baolin D.B. (2012) 'Toxicity of carbon nanotubes to freshwater aquatic invertebrates' *Environmental Toxicology and Chemistry*, vol. 31, no. 8, pp. 1823-1830.

Nel, A., Xia, T., Mädler, L., and Li, N. (2006) 'Toxic potential of materials at the nanolevel' *Science*, vol. 311, pp. 622-627.

Nguyen, B., Bowers, R.M., Wahlund, T.M., and Read, B.A. (2005) 'Suppressive subtractive hybridization of and differences in gene expression content of calcifying and noncalcifying cultures of emiliania huxleyi Strain 1516' *Applied and Environmental Microbiology*, vol. 71, no. 5, pp. 2564–2575.

Noori, A., Parivar, K., Modaresi, M., Messripour, M., Yousefi, M.H., and Amiri, G.R. (2011) 'Effect of magnetic iron oxide nanoparticles on pregnancy and testicular development of mice' *African Journal of Biotechnology*, vol. 10, pp. 1221-1227.

Novais, S.C., Arrais, J., Lopes, P., Vandenbrouck, T., De Coen, W., Roelofs, D., Soares, A.M.V.M., and Amorim, M.J.B. (2012) 'Enchytraeus albidus microarray: enrichment, design, annotation and database (EnchyBASE)' *PLoS ONE,* vol. 7, DOI: 10.1371/journal.pone.0034266.

Novoa, B., and Figueras, A. (2012) 'Zebrafish: model for the study of inflammation and the innate immune response to infectious diseases' *Advances in Experimental Medicine and Biology*, vol. 946, pp. 253-275.

Oberdörster, E. (2004) 'Manufactured nanomaterials (fullerenes, C60) induce oxidative stress in the brain of juvenile largemouth bass' *Environmental Health Perspectives*, vol. 112, pp. 1058-1062.

Oberdörster, E., Zhu, S., Blickley, T.M., McClellan-Green, P., and Haasch, M.L. (2006) 'Ecotoxicology of carbon-based engineered nanoparticles: effects of fullerene (C60*)* on aquatic organisms' *Carbon*, *vol.* 44, pp. 1112-1120.

Oberdörster, G., Maynard, A., Donaldson, K., Castranova, V., Fitzpatrick, J., Ausman, K., Carter, J., Karn, B., Kreyling, W., Lai, D., Olin, S., Monteiro-Riviere, N., Warheit, D., Yang, H., and a report from the ILSI Research Foundation/Risk Science Institute Nanomaterial Toxicity Screening Working Group. (2005b) 'Principles for characterizing the potential human health effects from exposure to nanomaterials: elements of a screening strategy' *Particle and Fiber Toxicology*, vol. 2, DOI: 10.1186/1743-8977-2-8.

Oberdörster, G., Oberdörster, E., and Oberdörster, J. (2005a) 'Nanotoxicology: an emerging discipline evolving from studies of ultrafine particles' *Environmental Health Perspectives*, vol. 113, no. 7, pp. 823-839.

Okuda-Shimazaki, J., Takaku, S., Kanehira, K., Sonezaki, S., and Taniguchi, A. (2010) 'Effects of titanium dioxide nanoparticle aggregate size on gene expression' *International Journal of Molecular Sciences,* vol. 11, pp. 2383-2392.

Olasagasti, M., Gatti, A.M., Capitani, F., Barranco, A., Pardo, M.A., Escuredo, K., and Rainieri, S. (2014) 'Toxic effects of colloidal nanosilver in zebrafish embryos' *Journal of Applied Toxicology*, vol. 34, pp. 562-575.

Onisto, M., Slongo, M.L., Graziotto, R., Zotti, L., Negro, A., Merico, M., Moro, E. and Foresta, C. (2001) 'Evidence for fsh-dependent Upregulation of spata2 (spermatogenesis-associated protein 2)' *Biochemical and Biophysical Research Communications,* vol. 283, pp. 86-92.

Oparka, K.J. and Read, N.D. (1994) 'The use of fluorescent probes for studies on living plant cells. In Plant Cell Biology' *A Practical Approach*, (N. Harris and K. J. Oparka, eds), pp. 27-50.

Park, H-G and Yeo, M-K. (2014) 'Metabolic gene expression profiling of Zebrafish embryos exposed to silver nanocolloids and nanotubes' *Molecular and Cellular Toxicology*, vol. 10, pp. 401-409.

Park, H-G., and Yeo, M-K. (2013) 'Comparison of gene expression changes induced by exposure to Ag, Cu-TiO2, and TiO2 nanoparticles in zebrafish embryos' *Molecular and cellular Toxicology*, vol. 9, pp. 129-139.

Pasquini, L.M., Hashmi, S.M., Sommer, T.J., Elimelech, M., and Zimmerman, J.B. (2012) 'Impact of surface functionalization on bacterial cytotoxicity of single-walled carbon nanotubes' *Environmental Science and Technology*, vol. 46, no. 11, pp. 6297-6305.

Patlolla, A.K., Hackett, D., and Tchounwou, P.B. (2015) 'Silver nanoparticle-induced oxidative stress-dependent toxicity in Sprague-Dawley rats' *Molecular and Cellular Biochemistry*, vol. 399, pp. 257-268.

Patnaik, S.C., Sahoo, D.K., and Chainy, G.B. (2013) 'A Comparative Study of Catalase Activities in Different Vertebrates' *WebmedCentral ZOOLOGY*, vol. 4, no. 6, available at: http://www.webmedcentral.com/article_view/4270

Pauluhn, J. (2010) 'Subchronic 13-week inhalation exposure of rats to multi walled carbon nanotubes: toxic effects are determined by density of agglomerate structures, not fibrillar structures' *Toxicological Sci*ences, vol. 113 pp. 226-242.

Peters, A., Veronesi, B., Calderon-Garciduenas, L., Gehr, P., Chen, L.C, Geiser, M., Reed, W., Rothen-Rutishauer, B., Schurch, S., and Schultz, H. (2006) 'Translocation and potential neurological effects of fine and ultrafine particles A critical update *Part*' *Fibre Toxicology*, vol. 3, DOI: 10.1186/1743-8977-3-13.

Petersen, E.J., Diamond, S.A., Kennedy, A.J., Goss, G.G., Ho, K., Lead, J., Hanna, S.K., Hartmann, N.B., Hund-Rinke, K., Mader, B., Manier, N., Pandard, P., Salinas, E.R., and Sayre, P. (2015) 'Adapting oecd aquatic toxicity tests for use with

manufactured nanomaterials: key issues and consensus recommendations' *Environmental and Science Technology'* vol. 49, no. 16, pp. 9532-9547.

Petersen, E.J., Reipa, V., Watson, S.S., Stanley, D.L., Rabb, S.A., and Nelson, B.C. (2014) 'DNA damaging potential of photoactivated P25 titanium dioxide nanoparticles' *Chemical research in toxicology*, vol. 27, no. 10, pp. 1877-1884.

Petersen, E.J., Zhang, L., Mattison, N.T., O'Carroll, D.M., Whelton, A.J., Uddin, N., Nguyen, T., Huang, Q., Henry, T.B., Holbrook, R.D., and Chen, K.L. (2011) 'Potential release pathways, environmental fate, and ecological risks of carbon nanotubes' *Environmental Science and Technology*, vol. 45, pp. 9837-9856.

Petersen, E.J., Huang, Q., and Weber, W.J. (2008) 'Ecological uptake and depuration of carbon nanotubes by Lumbriculus variegatus' *Environmental Health Perspectives*, vol. 116, no. 4, pp. 496-500.

Pickering, K.D., and Wiesner, M.R. (2005) 'Fullerol-sensitized production of reactive oxygen species in aqueous solution' *Environmental Science and Technology*, vol. 39, pp. 1359-1365.

Pietruska, J.R., Liu, X., Smith, A., McNeil, K., Weston, P., Zhitkovich, A., Hurt, R., and Kane, A.B. (2011) 'Bioavailability, intracellular mobilization of nickel, and HIF-1α activation in human lung epithelial cells exposed to metallic nickel and nickel oxide nanoparticles' *Toxicology Sciences*, vol. 124, no. 1, pp. 138-148.

Poland, C.A., Duffin, R., Kinloch, I., Maynard, A., Wallace, W.A.H., Seaton, A., Stone, V., Brown, S., MacNee, W., and Donaldson, K. (2008) 'Carbon nanotubes introduced into the abdominal cavity of mice show asbestos-like pathogenicity in a pilot study' *Nature Nanotechnology,* vol. 3, pp. 423-428.

Powers, S.K., and Jackson, M.J. (2008) 'Exercise-induced oxidative stress: cellular mechanisms and impact on muscle force production' *Physiology Review*, vol. 88, no. 4, pp. 1243-1276.

Pryor, J., Hughes, C., Foster, W., Hales, B., and Robaire, B. (2000) 'Critical windows of exposure for children's health: the reproductive system in animals and humans' *Environmental Health Perspectives*, vol. 108, no. 3, pp. 491-503.

Pulskamp, K., Diabat'e, S., and Krug, H. F. (2007) 'Carbon nanotubes show no sign of acute toxicity but induce intracellular reactive oxygen species in dependence on contaminants' *Toxicology Letters*, vol. 168, no. 1, pp. 58-74.

Qiang, L., Cheng, J., Yi, J., Rotchell, J.M., Zhu, X., and Zhou, J. (2016) 'Environmental concentration of carbamazepine accelerates fish embryonic development and disturbs larvae behavior' *Ecotoxicology*, vol. 25, pp. 1426-1437.

Ranjbar, A., Ataie, Z., Khajavi, F., and Ghasemi, H. (2014) 'Effects of silver nanoparticle (Ag NP) on oxidative stress biomarkers in rat' *Spring*, vol. 1, no. 3, pp. 2015-211.

Ray, P.C., Yu, H., and Fu, P.P. (2009) 'Toxicity and environmental risks of nanomaterials: challenges and future needs' *Journal of Environmental Science and Health*, vol. 27, pp. 1-35.

Reeves, J.F., Davies, S.J., Dodd, N.J.F., and Jha, A.N. (2008) 'Hydroxyl radicals (·OH) are associated with titanium dioxide (TiO2) nanoparticle-induced cytotoxicity and oxidative DNA damage in fish cells' *Mutation Research/Fundamental and Molecular Mechanisms of Mutagenesis*, vol. 640, pp. 113-122.

Reidy, B., Haase, A., Luch, A., Dawson, K.A., and Lynch, I. (2013) 'Mechanisms of Silver Nanoparticle Release, Transformation and Toxicity: A Critical Review of Current Knowledge and Recommendations for Future Studies and Applications: A review' *Materials*, vol. 6, pp. 2295-2350.

Roberts, A.P., Mount, A.S., Seda, B., Souther, J., Qiao, R., Lin, S., Chun Ke, P., Rao, A.M., and Klaine, S.J. (2007) 'In vivo modification of lipid-coated nanotubes by Daphnia magna' *Environmental Science and Technology*, vol. 41, no. 8, pp. 3025-3029.

Roberts, R.J., Aqius, C., Saliba, C., Bossier, P., and Sung, Y.Y. (2010) 'Heat shock proteins (chaperones) in fish and shellfish and their potential role in relation to fish health: a review' *Journal of Fish Diseases*, vol. 33, no. 10, pp. 789-801.

Robinson, B. W., Erle, D. J., Jones, D. A., Shapiro, S., Metzger, W. J., Albelda, S. M., Parks, W. C. and Boylan, A. (2000) 'Recent advances in molecular biological techniques and their relevance to pulmonary research' *Thorax* , vol. 55, pp. 329-339.

Roco, M.C. (2003) 'Nanotechnology: convergence with modern biology and medicine' *Current Opinion in Biotechnology*, vol. 14, pp. 337-346.

Roco, M.C. (2007) *National nanotechnology initiative– past, present, future*, Taylor and Francis. In Handbook on Nanoscience, Engineering and Technology, 2nd ed., *Taylor and Francis*, pp. 3.1-3.26.

Rodrigues, D.F., and Elimelech, M. (2010) 'Toxic effects of single-walled carbon nanotubes in the development of *E. coli* biofilm.' *Environmental Science and Technology*, vol. 44, no. 12, pp. 4583-4589.

Rokka, A., Antonenkov, V.D., Soininen, R., Immonen, H.L., Pirila, P.L., Bergmann, U., Sormunen, R.T., Weckström, M., and Benz, R. (2009) 'Pxmp2 Is a Channel-Forming Protein in Mammalian Peroxisomal Membrane' *PLoS ONE*, vol. 4, no. 4, DOI: 10.1371/journal.pone.0005090.

Rollerova, E., Tulinska, J., Liskova, A., Kuricova, M., Kovriznych, J., Mlynarcikova, A., Kiss, A., and Scsukova, S. (2015) 'Titanium dioxide nanoparticles: some aspects of toxicity/focus on the development' *Endocrine Regulations*, vol. 49, no. 2, pp. 97-112.

Rothschild, A., Cohen, S.R., and Tenne, R. (1999) 'WS2 nanotubes as tips in scanning probe microscopy' *Applied Physics*, vol. 75, no. 25, DOI: 10.1063/1.125526.

Safe work Australia (SWA). (2010) 'An evaluation of MSDS and labels associated with the use of engineered nanomaterials, commonwealth of Australia' Available at:

http://www.safeworkaustralia.gov.au/sites/swa/about/publications/Documents/374/AnEvaluationofMSDSandLabelsassociatedwiththeuseofengineerednanomaterials_June_2010.pdf

Safekordi, A.K., Attar, H., and Binaeian, E. (2012) 'Study on toxicity of manufactured nanoparticles to bacteria *Vibrio fischeri* using homemade luminometer'. 2nd International Conference on Chemical, Ecology and Environmental Sciences (ICCEES'2012) Singapore, pp. 60–65.

Saha, J.C., Dikshit, A.K., Bandyopadhyay, M., and Saha, K.C. (1999) 'A Review of Arsenic Poisoning and its Effects on Human Health' *Critical Reviews in Environmental Science and Technology*, vol. 29, pp. 281-313.

Saier, M.H. (2002) 'Families of Transporters and Their Classification, in Transmembrane Transporters' (ed M. W. Quick), John Wiley and Sons, Inc., Hoboken, NJ, USA. DOI: 10.1002/0471434043.ch1.

Sang, X., Zheng, L., Sun, Q., Li, N., Cui, Y., Hu, R., Gao, G., Cheng, Z., Cheng, J., Gui, S., Liu, H., Zhang, Z., and Hong, F. (2012) 'The chronic spleen injury of mice following long-term exposure to titanium dioxide nanoparticles' *Journal of Biomedical Materials Research Part A*, vol. 100A, pp. 894-902.

Schilling, K., Bradford, B., Castelli, D., Dufour, E., Nash, J.F., Pape W, Schulte, S., Tooley, I., van den Bosch, J., and Schellauf, F. (2010) 'Human safety review of "nano" titanium dioxide and zinc oxide' *Photochemical and Photobiological Sciences*, vol. 9, no. 4, pp. 495-509.

Scott, J. L., Gabrielides, C., Davidson, R. K., Swingler, T. E., Clark, I. M., Wallis, G. A., Boot-Handford, R.P., Kirkwood, T.B.L., Talyor, R.W., and Young, D.A. (2010) 'Superoxide dismutase down regulation in osteoarthritis progression and end-stage disease' *Annals of the Rheumatic Diseases*, vol. 69, no. 8, pp. 1502–1510.

Scown, T.M., Santos, E.M., Johnston, B.D., Gaiser, B., Baalousha, M., Mitov, S., Lead, J.R., Stone, V., Fernandes, T.F., Jepson, M., Aerle, R.V., and Tyler, C.R. (2010)

'Effects of aqueous exposure to silver nanoparticles of different sizes in Rainbow Trout' *Toxicological Sciences*, vol. 115, no. 2, pp. 521-534.

Selck, H., Handy, R.D., Fernandes, T.F., Klaine, S.J., and Petersen, E.J. (2016) 'Nanomaterials in the aquatic environment: a european union-united states perspective on the status of ecotoxicity testing, research priorities, and challenges ahead' *Environmrntal Toxicology and Chemistry*, vol. 35, no. 5, pp. 1055-1067.

Shaligram, S., and Campbell, A. (2013) 'Toxicity of copper salts is dependent on solubility profile and cell type tested' *Toxicology in Vitro*, vol. 27, pp. 844-851.

Sharma, V., Shukla, R.K., Saxena, N., Parmar, D., Das, M., and Dhawan, A. (2009) 'DNA damaging potential of zinc oxide nanoparticles in human epidermal cells' *Toxicology Letters*, vol. 185, pp. 211-218.

Sharma, V.K., Siskova, K.M., Zboril, R., and Gardea-Torresdey, J.L. (2014) 'Organic-coated silver nanoparticles in biological and environmental conditions: fate, stability and toxicity' *Advances in Colloid and Interface Science*, vol. 204, pp. 15-34.

Shaw, B.J., Al-Bairuty, G., and Handy, R.D. (2012) 'Effects of waterborne copper nanoparticles and copper sulphate on rainbow trout, (*Oncorhynchus mykiss*): Physiology and accumulation' *Aquatic Toxicology*, vol. 116– 117, pp. 90-101.

Shaw, B.J., and Handy, R.D. (2011) 'Physiological effects of nanoparticles on fish: a comparison of nanometals versus metal ions' *Environment International*, vol. 37, pp. 1083-1097.

Shen, Y.F., Tang, J., Nie, Z.H., Wang, Y.D., Ren, Y., and Zuo, L. (2009) 'Tailoring size and structural distortion of Fe3O4 nanoparticles for the purification of contaminated water' *Bioresource Technology*, vol. 100, pp. 4139-4146.

Shephard, K.L. (1994) 'Functions for fish mucus' *Reviews in Fish Biology and Fisheries*, vol. 4, pp. 401-429.

Shoemaker, C.A., Klesius, H.P., and Lim C. (2001) 'Immunity and disease resistance in fish, Chapter 7, In: Nutrition and Fish Health, L. Chhorn and C.D. Webster (Eds.), Binghamton, New York, USA, pp. 149-162.

Shvedova, A.A., Castranova, V., Kisin, E.R., Schwegler-Berry, D., Murray, A.R., Gandelsman, V.Z., Maynard, A., and Baron, P. (2003) 'Exposure to carbon nanotube material: Assessment of nanotube cytotoxicity using human keratinocyte cells. *Journal of Toxicology and Environmental Health, Part A,* vol. 66, pp. 1909-1926.

Shvedova, A.A., Kisin, E.R., Mercer, R., Murray, A.R., Johnson, V.J., Potapovich, A.I., Tyurina, Y.Y., Gorelik, O., Arepalli, S., Schwegler-Berry, D., Hubbs, A.F., Antonini, J., Evans, D.E., Ku, B-K., Ramsey, D., Maynard, A., Kagan, V.E., Castranova, V., and Baron, P. (2005) 'Unusual inflammatory and fibrogenic pulmonary responses to single-walled carbon nanotubes in mice' *American Journal of Physiology, Lung Cellular and Molecular Physiology Published*, vol. 289, no. 5, pp. L698-L708.

Simon-Deckers, A., Gouget, B., Mayne-L'Hermite, M., Herlin-Boime, N., Reynaud, C., and Carriere, M. (2008) 'In vitro investigation of oxide nanoparticle and carbon nanotube toxicity and intracellular accumulation in A549 human pneumocytes' *Toxicology*, vol. 253, no. 1-3, pp. 137-146.

Smith, C.J., Shaw, B.J., and Handy, R.D. (2007) 'Toxicity of single walled carbon nanotubes to rainbow trout, (*Oncorhynchus mykiss*): respiratory toxicity, organ pathologies, and other physiological effects' *Aquatic Toxicology*, vol. 82, no. 2, pp. 94-109.

Sun, C.K., Chu, S.W., Chen, S.Y., Tsai, T.H., Liu, T.M., Lin, C.Y., and Tsai, H.J. (2004) 'Higher harmonic generation microscopy for developmental biology' *Journal of Structural Biology*, vol. 147, no. 1, pp. 19-30.

Taylor, B.L., and Zhulin, I.B. (1999) 'PAS domains: internal sensors of oxygen, redox potential, and light' *Microbiology and Molecular Biology Reviews*, vol. 63, no. 2, pp. 479-506.

Templeton, R.C., Ferguson, P.L., Washburn, K.M., Scrivens, W.A., and Chandler, G.T. (2006) 'Life-cycle effects of single-walled carbon nanotubes (SWNTs) on an estuarine meiobenthic copepod' *Environmental Science and Technology*, vol. 40, no. 23, pp. 7387-7393.

Terlecky, S.R., Terlecky, L.J., and Giordano, C.R. (2012) 'Peroxisomes, oxidative stress, and inflammation' *The World Journal of Biological Chemistry*, vol. 3, no. 5, pp. 93-97.

Terzuoli, G., Iacoponi, F., Moretti, E., Renieri, T., Baldi, G., and Collodel, G. (2011) '*In vitro* effect of silver engineered nanoparticles on human spermatozoa' *Journal of Siena Academy of Science*, vol. 3, pp. 27-29.

Therapeutics Good Administration. (2013) 'Literature review on the safety of titanium dioxide and zinc oxide nanoparticles in sunscreens' Symonston, ACT: TGA.

Thomas, K.V., Farkas, J., Farmen, E., Christian, P., Langford, K., Wu, Q., and Tollefsen, K.E. (2011) 'Effects of dispersed aggregates of carbon and titanium dioxide engineered nanoparticles on rainbow trout hepatocytes. *Toxicology and Environmental Health, Part A*, vol. 74, pp. 466-477.

Tian, F., Cui, D., Schwarz, H., Estrada, G.G., and Kobayashi, H. (2006) ,Cytotoxicity of single-wall carbon nanotubes on human fibroblasts' *Toxicology In Vitro*, vol. 20, no. 7, pp. 1202-1212.

Tiedke, J., Cubuk, C., and Burmester, T. (2013) 'Environmental acidification triggers oxidative stress and enhances globin expression in zebrafish gills' *Biochemical and Biophysical Research Communications*, vol. 441, pp. 624-629.

Towe, K.M., and Moench, T.T. (1981) 'Electron optical characterization of bacterial magnetite' *Earth and Planetary Science Letters*, vol. 52, pp. 213-220.

Tran, D.T., and Salmon, R. (2010) 'Potential photocarcinogenic effects of nanoparticle sunscreens' *Australasian Journal of Dermatology*, vol. 52, pp. 1-6.

Trouiller, B., Reliene, R., Westbrook, A., Solaimani, P., and Schiestl, H. (2009) 'Titanium dioxide nanoparticles induce DNAdamage and genetic instability in vivo in mice' *Cancer Research*, vol. 69, pp. 8784-8789.

Tsoi, S.C.M., Ewart, K.V., Penny, S., Melville, K., Liebscher, R.S., Brown, L.L., and Douglas, S.E. (2004) 'Identification of immune-relevant genes from atlantic salmon using suppression subtractive hybridization' *Marine Biotechnology*, vol. 6, pp. 199-214.

Tsuji, J.S., Maynard, A.D., Howard, P.C., James, J.T., Lam, C., Warheit, D.B., and Santamariak. (2006) 'Reasearch strategies for safety evaluation of nanomaterials, part IV: risk assessment of nanoparticles' *Toxicological Sciences*, vol. 89, no. 1, pp. 42-50.

U.S. Environmental Protection Agency. (2007) 'Nanotechnology white paper' EPA 100/B-07/001. Available at: www.epa.gov/osa

Uchino, T., Tokunaga, H., Ando, M., and Utsumi, H. (2002) 'Quantitative determination of OH radical generation and its cytotoxicity induced by TiO(2)-UVA treatment' *Toxicology In Vitro*, vol. 16, no. 5, pp. 629-635.

Uribe, C., Folch, H., Enriquez, R., and Moran, G. (2011) 'Innate and adaptive immunity in teleost fish: a review' *Veterinarni Medicina,* vol. 56, no. 10, pp. 486-503.

Usenko, C. Y., Harper, S.L., and Tanguay, R.L (2007) '*In vivo* evaluation of carbon fullerene toxicity using embryonic zebrafish' *Carbon,* vol. 45, pp. 1891-1898.

Usenko, C.Y., Harper, S.L., and Tanguay, R.L. (2008) 'Fullerene C60 exposure elicits an oxidative stress response in embryonic zebrafish' *Toxicology and Applied Pharmacology,* vol. 229, pp. 44-55.

Van den Bosch, H., Schutgens, R.B.H., Wanders, R.J.A., and Tager, J.M. (1992) 'Biochemistry of peroxisomes' *Annual Review in Biochemistry,* vol. 61, pp. 157-197.

Van der Meer, D.L., van den Thillart, G.E., Witte, F., de Bakker, M.A., Besser, J., Richardson, M.K., Spaink, H.P., Leito, J.T., and Bagowski, C.P. (2005) 'Gene expression profiling of the long-term adaptive response to hypoxia in the gills of adult zebrafish' *The American Journal of Physiology, Regulatory, Integrative and Comparative Physiology,* vol. 289, pp. 1512-1519.

Van Veldhoven, P.P., Just, W.W., and Mannaerts, G.P. (1987) 'Permeability of the peroxisomal membrane to cofactors of beta-oxidation. Evidence for the presence of a pore-forming protein' *The Journal of Biological Chemistry*, vol. 262, no. 9, pp. 4310-4318.

Vandewalle, J., Bauters, M., Van Esch, H., Belet, S., Verbeeck, J., Fieremans, N., Holvoet, M., Vento, J., Spreiz, A., Kotzot, D., Haberlandt, E., Rosenfeld, J., Andrieux, J., Delobel, B., Dehouck, M-B., Devriendt, K., Fryns, J-P., Marynen, P., Goldstein, A., and Froyen, G. (2013) 'The mitochondorial solute carrier *SLC25A5* at Xq24 is a novel candidate gene for non-syndromic intellectual disability' *Human Genetics*, vol. 132, no. 10, pp. 1177-1185.

Velkova-Jordanoska, L., Kostoski, G., and Jordanoska, B. (2008) 'Antioxidative enzymes in fish as biochemical indicators of aquatic pollution' *Bulgarian Journal of Agricultural Science*, vol. 14, no. 2, pp. 235-237.

Verano-Braga, T., Miethling-Graff, R., Wojdyla, K., Rogowska-Wrzesinska, A., Brewer, J.R., Erdmann, H., and Kjeldsen, F. (2014) 'Insights into the cellular response triggered by silver nanoparticles using quantitative proteomics' *ACS Nano*, vol. 8, pp. 2161-2175.

Vertegel, A.A., Siegel, R.W., and Dordick, J.S. (2004) 'Silica nanoparticle size influences the structure and enzymatic activity of adsorbed lysozyme' *Langmuir*, vol. 20, no. 16, pp. 6800-6807.

Wäge, J., Lerebours, A., Hardege, J.D., and Rotchell, J.M. (2015) 'Exposure to low pH induces molecular level changes in the marine worm, Platynereis dumerilii' *Ecotoxicology and Environmental Safety,* vol. 124, pp. 105-110.

Wanders, R.J., and Waterham, H.R. (2006) 'Biochemistry of mammalian peroxisomes revisited' *Annual Review of Biochemistry*, vol. 75, pp. 295-332.

Wang, J., Zhou, G., Chen, C., Yu, H., Wang, T., Ma, Y., Jia, G., Gao, Y., Li, B., and Sun, J. (2007) 'Acute toxicity and biodistribution of different sized titanium dioxide particles in mice after oral administration' *Toxicology Letters*, vol. 168, no. 2, pp. 176-185.

Wang, S., Lu, W., Tovmachenko, O., Rai, U.S., Yu, H., and Ray, P.C. (2008) 'Challenge in understanding size and shape dependent toxicity of gold nanomaterials in human skin keratinocytes' *Chemical Physics Letters*, vol. 463, pp. 145-149.

Wang, Y., Zhou, J., Liu, L., Huang, C., Zhou, D., and Fu, L. (2016) 'Characterization and toxicology evaluation of chitosan nanoparticleson the embryonic development of zebrafish, Danio rerio' *Carbohydrate Polymers*, vol. 141, pp. 204-210.

Warheit, D.B., Laurence, B.R., Reed, K.L., Roach, D.H., Reynolds, G.A.M., and Webb, T.R. (2004) 'Comparative pulmonary toxicity assessment of single-wall carbon nanotubes in rats' *Toxicological Sciences*, vol. 77, pp. 117-125.

Welch, W.J. (1993) 'Heat shock proteins functioning as molecular chaperones: their roles in normal and stressed cells' *Philosophical transactions of the Royal Society of* London*. Series* B*, Biological sciences*, vol. 339, pp. 327-333.

Weydert, C.J., and Cullen, J.J. (2010) 'Measurement of superoxide dismutase, catalase and glutathione peroxidase in cultured cells and tissue' *Nature Protocols*, vol. 5, pp. 51-66.

Wiesener, M.S., Jürgensen, J.S., Rosenberger, C., Scholze, C.K., Hörstrup, J.H., Warnecke, C., Mandriota, S., Bechmann, I., Frei, U.A., Pugh, C.W., Ratcliffe, P.J., Bachmann, S., Maxwell, P.H., and Eckardt, K.U. (2003)

'Widespread hypoxia-inducible expression of HIF-2alpha in distinct cell populations of different organs' *The Journal of the Federation of American Societies for Experimental Biology*, vol. 17, no. 2, DOI: 10.1096/fj.02-0445fje.

Wiesenthal, A., Hunter, L., Wang, S., Wickliffe, J., and Wilkerson, M. (2011) 'Nanoparticles: small and mighty' *International Journal of Dermatology,* vol. 50, pp. 247-254.

Wijnhoven, S.W.P., Peijnenburg, W.J.G.M., Herberts, C.A., Hagens, W.I., Oomen, A.G., Heugens, E.H.W., Roszek, B., Bisschops, J., Gosens, I., Meent, D.V.D., Dekkers, S., De Jong, W.H., Zijverden, M.V., Sips, A.J.A.M., and Geertsma, R.E. (2009) 'Nano-silver - a review of available data and knowledge gaps in human and environmental risk assessment' *Nanotoxicology*, vol. 3, no. 2, pp. 109-138.

Wong, M.L., and Medrano, J.F. (2005) 'Real-time PCR for mRNA quantitation' *BioTechniques*, vol. 39, no. 1, pp. 75-85.

Wu, J., Liu, W., Xue, C., Zhou, S., Lan, F., Bi, L., Xu, H., Yang, X., and Zeng, F-D. (2009) 'Toxicity and penetration of TiO2 nanoparticles in hairless mice and porcine skin after subchronic dermal exposure' *Toxicology Letters*, vol. 191, pp. 1-8.

Wu, Y., and Zhou, Q., (2012) 'Dose- and time-related changes in aerobic metabolism, chorionic disruption, and oxidative stress in embryonic medaka (*Oryzias latipes*): underlying mechanisms for silver nanoparticle developmental toxicity' *Aquatic Toxicology*, vol. 124-125, pp. 238-246.

Xia, T., Kovochich, M., Brant, J., Hotze, M., Sempf, J., Oberley, T., Sioutas, C., Yeh, J.I., Wiesner, M. R., and Nel, A.E. (2006) 'Comparison of the abilities of ambient and manufactured nanoparticles to induce cellular toxicity according to an oxidative stress paradigm' *Nano Letters*, vol. 6, pp. 1794-1807.

Xia, T., Kovochich, M., Liong, M., Mädler, L., Gilbert, B., Shi, H., Yeh, J.I., Zink, J.I., and Nel, A.E. (2008) 'Comparison of the mechanism of toxicity of zinc oxide and cerium oxide nanoparticles based on dissolution and oxidative stress properties' *American Chemical Society* nano, vol. 2, pp. 2121-2134.

Xin, Q., Rotchell, J.M., Cheng, J., Yi, J., and Zhang, Q. (2015) 'Silver nanoparticles affect the neural development of zebrafish embryos' *Journal of Applied Toxicology*, vol. 35, pp. 1481-1492.

Xiong, D., Fang, T., Yu, L., Sima, X., and Zhu, W. (2011) 'Effects of nano-scale TiO2, ZnO and their bulk counterparts on zebrafish: acute toxicity, oxidative stress and oxidative damage' *Science of the Total Environment*, vol. 409, pp. 1444-1452.

Xiu, Z.M., Ma, J., and Alvarez, P.J.J. (2011) 'Differential effect of common ligands and molecular oxygen on antimicrobial activity of silver nanoparticles versus silver ions' *Environmental Science and Technology*, vol. 45, pp. 9003-9008.

Xu , P., Zeng, G.M., Huang, D.L., Feng, C.L., Hu, S., Zhao, M.H., Lai, C., Wei, Z., Huang, C., Xie, G.X and Liu, Z.F. (2012) 'Use of iron oxide nanomaterials in wastewater treatment: a review' *Science of the Total Environment*, vol. 424, pp. 1-10.

Xu, A., Chai, Y.F., Nohmi, T., and Hei, T.K. (2009) 'Genotoxic responses to titanium dioxide nanoparticles and fullerene in gpt delta transgenic MEF cells' *Particle and Fibre Toxicology*, vol. 6, DOI: 10.1186/1743-8977-6-3.

Xu, F., Piett, C., Farkas, S., Qazzaz, M., and Syed, N.I. (2013) 'Silver nanoparticles (AgNPs) cause degeneration of cytoskeleton and disrupt synaptic machinery of cultured cortical neurons' *Mplecular Brain*, vol. 6, no. 29, DOI: 10.1186/1756-6606-6-29.

Yamaguchi, S., Miura, C., Ito, A., Agusa, T., Iwata, H., Tanabe, S., Tuyen, B.C., and Miura, T., (2007) 'Effects of lead, molybdenum, rubidium, arsenic and organochlorines on spermatogenesis in fish: Monitoring at Mekong Delta area and *in vitro* experiment' *Aquatic Toxicology*, vol. 83, pp. 43-51.

Yang, E-J., Kim, S., Kim, J.S., and Choi, I-H. (2012) 'Inflammasome formation and IL-1b release by human blood monocytes in response to silver nanoparticles' *Biomaterials*, vol. 33, pp. 6858-6867.

Yang, X., Liu, J., He, H., Zhou, L., Gong, C., Wang, X., Yang, L., Yuan, J., Huang, H., He, L., Zhang, B., and Zhuang, Z. (2010) 'SiO2 nanoparticles induce cytotoxicity and

protein expression alteration in HaCaT cells' *Particle and Fibre Toxicology*, vol. 7, DOI: 10.1186/1743-8977-7-1.

Yang, Y., Gupta, M.C., and Dudley, K.L. (2007) 'Studies on electromagnetic interference shielding characteristics of metal nanoparticle- and carbon nanostructure-filled polymer composites in the ku-band frequency' *Micro and Nano Letters*, vol. 2, pp. 85-89.

Yantasee, W., Warner, C.L., Sangvanich, T., Addleman, R.S., Carter, T.G., Wiacek, R.J., Fryxell, G.E., Timchalk, C and Warner, M.G. (2007) 'Removal of heavy metals from aqueous systems with thiol functionalized superparamagnetic nanoparticles' *Environmental Science and Technology*, vol. 41, pp. 5114-5119.

Yauk, C., Polyzos, A., Rowan-Carroll, A., Somers, C., Godschalk, R., Van Schooten, F. J., Berndt, M., Pogribny, I., Koturbash, I., Williams, A., Douglas, G.R., and Kovalchuk, O. (2008) 'Germ-line mutations, DNA damage, and global hypermethylation in mice exposed to particulate air pollution in an urban/industrial location' *Proceedings of the National Academy of Sciences of the United States of America*, vol. 105, pp. 605-610.

Yu, T., Malugin, A., and Ghandehari, H. (2011) 'Impact of silica nanoparticle design on cellular toxicity and haemolytic activity' *ACS Nano*, vol. 5, no. 7, pp. 5717-5728.

Zámocký, M., and Koller, F. (1999) 'Understanding the structure and function of catalases: clues from molecular evolution and in vitro mutagenesis' *Progress in Biophysics and Molecular Biology*, vol. 72, no. 1, pp. 19-66.

Zhang, L., Jiang, Y., Ding, Y., Daskalakis, N., Jeuken, L., Povey, M., O'neill, A.J., and York, D.W. (2010) 'Mechanistic investigation into antibacterial behavior of suspensions of ZnO nanoparticles against *E.coli*' *Nanoparticle Research*, vol. 12, pp. 1625-1636.

Zhou, Y.F., Eng, E.T., Zhu, J., Lu, C., Walz, T., and Springer, T.A. (2012) 'Sequence and structure relationships within von Willebrand factor' *Blood*, vol. 120, no. 2, pp. 449-458.

Zhu, S.Q., Oberdörster, E and Haasch, M.L. (2006). 'Toxicity of an engineered nanoparticle (fullerene, C-60) in two aquatic species, *Daphnia* and fathead minnow' *Marine Environmental Research*, vol. 62, pp. S5-S9.

Zhu, X., Zhu, L., Li, Y., Chen, Y., and Tian, S. (2009) 'Acute toxicities of six manufactured nanomaterial suspensions to *Daphnia magna*' *Nanoparticle Research*, vol. 11, pp. 67-75.

Zhu, X., Zhu, L., Li, Y., Duan, Z., Chen, W., and Alvarez, P.J. (2007) 'Developmental toxicity in zebrafish (*Danio rerio*) embryos after exposure to manufactured nanomaterials: Buckminsterfullerene aggregates (nC60) and fullerol' *Environmental Toxicology and Chemistry*, vol. 26, pp. 976-979.

Zhu, X.S., Zhu, L., Lang, Y.P., and Chen, Y.S. (2008) 'Oxidative stress and growth inhibition in the freshwater fish *Carassius auratus* induced by chronic exposure to sublethal fullerene aggregates' *Environmental Toxicology and Chemistry*, vol. 27, no. 9, pp. 1979-1985.

Zolnik, B.S., González-Fernández, Á., Sadrieh, N., and Dobrovolskaia, M.A. (2010) 'Nanoparticles and the immune system' *Endocrinology*, vol. 151, no. 2, pp. 458-465.